The role of *Desmozoon lepeophtherii* in complex gill disorder of Atlantic salmon (*Salmo salar*)

Thesis presented for the degree of

Doctor of Philosophy in

Aquatic Veterinary Studies

by

Ana Herrero-Fernández

September 2019

Declaration

The research presented in this thesis is entirely my own work unless otherwise stated in the text. The material contained in this thesis has not been submitted for any other degree or professional qualification.

CANDIDATE NAME: Ana Herrero-Fernández

SIGNATURE: ……

DATE: ……

Acknowledgments

I would like to express my deepest gratitude to all those that made this research possible. Most of all I would like to thank my supervisors at the Moredun Research Institute (MRI), Dr. Kim Thompson and Dr. Mark Dagleish, for their mentoring, knowledge and continual support throughout the whole period of my study. Many thanks to my supervisors at the University of Stirling, Professor James Bron, Professor Alexandra Adams and Professor Giuseppe Paladini, for their help and advice during this project. I would also like to express my sincere gratitude to Dr. Hamish Rodger, for his help during this project and for sharing his limitless knowledge about gill disease.

My gratitude extents to all the staff and students at the MRI for their advice, technical assistance and good memories, especially to Dr. Janina Costa, for her patience helping me with the cell culture experiments. I am especially thankful to my friends Maria and Anna, for their encouragement and friendship throughout my study period.

Many thanks to all the staff at the Fish Vet Group for always offering their help when needed, and for their advice in various aspects of fish health.

I would like to thank the MRI and the University of Stirling for providing the opportunity for this project. This thesis was funded by the Moredun Research Institute and partially financed by the Fish Vet Group. I would also like to thank all the fish farming companies that allowed and helped me to collect the samples and data used in the thesis. None of the results presented could have been achieved without their support.

I sincerely thank my family, for their ongoing support over the years. Lastly, I am especially thankful to Carlota, for all her love and endless patience through this period.

Abstract

Gill disease is an important challenge for Atlantic salmon (*Salmo salar* L.) aquaculture worldwide. Complex gill disorder (CGD) is a multifactorial and multiaetiological condition that tends to occur from late summer to early winter in salmon. The microsporidian *Desmozoon lepeophtherii* has been associated with CGD, but the interaction between the pathogen and its host remains to be understood. This thesis examines different aspects of *D. lepeophtherii* in an attempt to clarify the role and significance of *D. lepeophtherii* in CGD. Spores from *D. lepeophtherii*, derived from the sea lice (*Lepeophtheirus salmonis*) were used to infect different fish cell lines (rainbow trout gill cells and salmon head kindey cells) and primary macrophage cultures from Atlantic salmon head kidney *in vitro*. However, there was no evidence of *D. lepeophtherii* replication in any of the cultures. A one-year longitudinal study was carried out at two marine salmon farms to determine the correlation between gill pathology and the putative pathogens associated with CGD (*D. lepeophtherii*, *Candidatus* Branchiomonas cysticola and salmon gill pox virus (SGPV)), as well as *Paramoeba perurans*, the aetiological agent of amoebic gill disease (AGD). The two farms were positive for the four pathogens, with *Ca.* B. cysticola and *D. lepeophtherii* being the most frequently detected agents, and SGPV detected sporadically throughout the study. *Paramoeba perurans* was detected in the two farms but an outbreak of AGD only occurred in one of the farms. Statistical analysis of the data from the two farms showed that variations in SGPV and *Ca.* B. cysticola loads were not associated with an increase in the gill score ($p>0.05$), while *D. lepeophtherii* and *P. perurans* were ($p< 0.001$), although obvious pathology associated with *D. lepeophtherii* infection was not evident. An *in situ* hybridisation (ISH) method was developed to detect the developmental and spore stages of the parasite, the sensitivity (92%) of which was higher than other staining methods currently used to detect the microsporidian. There was a significant association between high loads of *D. lepeophtherii* by ISH and gill pathology ($p< 0.001$). In conclusion, it would seem that chronic infection with *D. lepeophtherii* is common in farmed salmon gills, but does not appear to cause any clinical manifestation in healthy fish. Gill pathology is present when parasite burdens are high, however.

Potential reactivation of latent microsporidiosis is a risk, but the factors to trigger this are still unknown.

Contents

List of abbreviations

µg	microgram
µl	microlitre
µm	micrometre
µM	micromolar
AGD	amoebic gill disease
ANOVA	analysis of variance
BLAST	basic alignment search tool
bp	base pairs
cDNA	complementary DNA
CGD	complex gill disorder
CI	confidence interval
Ct	threshold cycle
CW	Calcofluor White
d.p.e	days post exposure
DNA	deoxyribonucleic acid
DPBS	Dulbecco's phosphate buffered saline without Ca and Mg
E	efficiency of PCR
et al.	*et alia* (and others)
FBS	foetal bovine serum
FCS	foetal calf serum
g	Gram
GAM	generalised additive model
h	Hours
h.p.1	hours post infection
H&E	haematoxylin and eosin
H_2O_2	hydrogen peroxide
ITS	internal transcribed spacer
L	Litre
L-15	Leibovitz-15

M	Molar
MEM	minimum essential media
mg	milligrams
min	Minute
ml	Millilitre
mm	millimetre
nm	nanometre
MRI	Moredun Research Institute
PBS	phosphate buffered saline
PCR	polymerase chain reaction
PGD	proliferative gill disease
PI	propidium iodine
Pk	proteinase K
R^2	correlation co-efficiency
RNA	ribonucleic acid
RT	reverse transcription
RTgill-W1	rainbow trout gill cell line
RT-rtPCR	reverse transcription polymerase chain reaction
sd	standard deviation
SE	standard error
SHK-1	salmon head kidney -1 cells
SGPV	salmon gill poxvirus
SSC	saline-sodium citrate buffer
SSU	small subunit
TAE	tris acetate EDTA
TBS	tris buffered saline
TEM	transmission electron microscopy
U	Units
v	Volt
v/v	volume/volume percent

List of Figures

List of Tables

Chapter 1 Literature Review

1.1 Structure, function of fish gills and gill pathology

1.1.1 Structure and function

The fish gill is a structurally complex organ, vital for many physiological functions including respiration, ionoregulation, osmoregulation, acid–base balance, nitrogenous waste excretion (reviewed by Evans *et al.*, 2005), immune function (Dos Santos *et al.*, 2001; Haugarvoll *et al.*, 2008) and hormone metabolism (Okabe & Graham, 2004; Olson, 1998). Gills are located bilaterally on either side of the pharynx and contain four bony (cartilaginous in early life) respiratory gill arches that bear a series of paired caudolaterally oriented filaments (also called primary lamellae) on each arch, which are free at their distal ends but supported by an interbranchial septum at their base (Wilson & Laurent, 2002). One row of filaments is termed a hemibranch, while both constitute the holobranch. These filaments project an array of lamellae (also called secondary lamellae) that are critical for gaseous exchange (Evans *et al.*, 2005). The gills are protected by an operculum, a bony external cover that participates in the buccal pumping mechanism that provides a continuous flow of water across the gills. Briefly, water enters through the pharynx into the buccal pump when the opercular valves are closed, then it moves through the inter-lamellar spaces until the mouth closes and the opercular valves open caudally forcing the water out (Hughes, 1960). The pseudobranch, found anteriodorsally under the operculum, is a gill arch remnant present in many teleost fish and is thought to be involved in respiration, osmoregulation and sensory functions amongst others (reviewed by Bridges *et al.*, 1998), although its exact physiological role still remains unclear (Mölich *et al*., 2009).

To efficiently extract oxygen dissolved in water, which has low solubility and diffusion gradient compared with atmospheric oxygen fish use a counter-current flow system (blood flow in lamellae is opposite to water flow) that increases the diffusion gradients of gases and metabolites (reviewed by Randall, 2014). Other factors aiding respiration include the large surface area of the gill and the interlamellar distance

which is optimal for oxygen uptake (Park *et al.*, 2014). Three circulation circuits have been described in the gills, the interlamellar, the nutrient and the arterio-arterial pathway (Olson, 2002). Exchange of gases between the blood and the environment occurs in the arterio-arterial vasculature, also known as the "respiratory pathway" (reviewed by Evans *et al.*, 2005). From the heart and the ventral aorta, blood enters the gills via afferent branchial arteries (ABAs), which feed the two hemibranchs of each arch via afferent filament arteries (AFAs) and these feed the afferent lamellar arterioles (ALAs). Blood flow in the lamellae occurs through the lamellar sinusoids created by the pillar cells, which have contractile proteins and are thought to regulate perfusion. Oxygenated blood from ALAs are fed into efferent lamellar arterioles (ELAs), which direct the blood to the efferent filament arterioles (EFAs) that feeds the efferent branchial arterioles (EBA). EBA continue into the dorsal aorta that feeds the subsequent systemic circulation to other tissues. The interlamellar and nutrient circulation are part of the arteriovenous vasculature supplied by the post-lamellar blood and are thought to provide nutrients to the filaments (Olson, 2002). The most important part of the arteriovenous vasculature is the central venous sinus, which runs along the filaments, and has been suggested to be vital in the ionoregulation of the fish (Laurent & Dunel, 1980).

The majority of the filament and lamellar surface is covered by squamous cell epithelium, while the basal and intermediate layers of the epithelium contain undifferentiated cells (Wilson & Laurent, 2002). Two thin layers of epithelial cells are present in the lamellae. The surface of the outer lamellar epithelium is composed of microridge-like structures, rich in glycocalyx, thought to increase the respiratory surface area and aid in the interaction between the secreted mucus and host cell surface (Speare & Ferguson, 2006). The inner layer of the epithelium surrounds the vasculature. Lamellar blood spaces are supported by modified endothelial cells termed pillar cells that hold the epithelial layers together and create pillar channels for blood flow (Wilson & Laurent, 2002). Mucus cells are present more frequently on the edges of the filament but occur also within the lamellae. These cells play a role in ionoregulation, and mechanical and immunological protection (Wilson & Laurent, 2002). Chloride cells are mainly located in the base of the lamellae regions and are mitochondria rich-cells essential for the intensive energy processes

associated with osmotic regulation mediating ion exchange (i.e. sodium chloride secretion in marine fish) (Claiborne *et al.*, 2002). Eosinophilic granular cells, that appear to have similar functions to mast cells in mammals (Reite, 1997), are located along the length of the filament. Other cells present in filament interstitium include rodlet cells, thought to participate in host defence (Koppang *et al.*, 2015), neuroepithelial cells, macrophages, neutrophils and lymphocytes (Speare & Ferguson, 2006).

1.1.2 Response of gills to damage

The gill is covered by a thin (10 μm) epithelium (Eddy & Handy, 2012) (Figure 1.1) and is estimated to have the largest organ-specific surface in direct contact with the environment (0.1–0.4 m^2/kg body weight) (Koppang *et al.*, 2015), which makes the gill vulnerable to waterborne irritants and infectious agents (Bell, 1961). Importantly, restrictions on elective behaviour imposed by intensive farming reduces the options for fish to avoid harmful organisms (i.e. phytoplankton blooms) and can favour the selection of infections agents with high virulence (Pulkkinen *et al.*, 2009). In addition, under high demand situations like energetic swimming, when ventilation increases from 50 min^{-1} at rest to 1000 min^{-1} (Eddy & Handy, 2012), or hypoxia (Davis & Cameron, 1971; reviewed by Perry *et al.*, 2009; Yang & Albright, 1992;), exposure to water borne irritants and pathogens increases greatly. Uptake of larger water volumes favours oxygen uptake but this will also increase the gills exposure to solids or organisms in the environment. For instance, infection trials of rainbow trout (*Oncorhynchus mykiss*) with the trematode *Diplostomum pseudospathaceum* demonstrated increased infestation of gills for those fish exposed to lower levels of oxygen and a consequent higher ventilation volume (Mikheev *et al.*, 2014).

Figure 1.1. Gills of Atlantic salmon macroscopically (left) and microscopically stained with haematoxylin and eosin (H&E) (right). The histological sagittal section of the gill shows (1) the filament, (2) mucus cells, (3) chloride cells, (4) the (pavement) lamellar epithelial cells, (5) pillar cells, and (6) erythrocytes within the capillaries. The photomicrograph was kindly provided by the Fish Vet Group.

The response of gills to damage is generally relatively limited (Roberts, 2012) and similarities can be seen in non-specific host responses resulting from different types of gill assaults (Mallat, 1985). The latter author, who reviewed studies on the main alterations induced mainly by toxic substances, divided the type of changes seen in gill pathology into (1) those caused by the direct and early exposure of the fish to a stressor, and (2) changes found under continuous exposure to a stressor at non-lethal levels that correspond to the defence mechanism of fishes, and which were sometimes found during acute exposure to some irritants (Rodrigues *et al.*, 2019). These two categories are very similar to the current descriptions of acute and chronic responses for gill pathology (Speare & Ferguson, 2006). Histopathological changes in an acute response include cell degeneration, cell death, and vascular changes such as congestion, oedema and haemorrhages; while chronic responses include cell hyperplasia, lamellar fusion or formation of thrombi. The infiltration of inflammatory cells can be seen in both, acute and chronic responses. Pathological changes seen in gills are summarised below and in Table 1.1.

1.1.3 Gill pathology

1.1.3.1 Cell swelling

Cell swelling: This is sometimes referred as hypertrophy because it involves an enlargement of individual cells. However, contrary to the increase in the number of organelles seen within the cells as occurs during true hypertrophy, cell swelling results from alterations in membrane permeability (Kumar *et al.*, 2017), due to damage of the sodium pump, resulting in an increase of intracellular fluid (Rodger & Roberts, 2012). It is an early occurrence associated with acute cell damage and, although reversible, can lead to necrosis if the initiating cause persists (Wallig & Janovitz, 2013). Cell swelling can be difficult to recognise under light microscopy, but cells appear pallid, due to lower protein concentration and therefore stain affinity when subjected to haematoxylin and eosin (H&E) (Matthew *et al.*, 2013). Also, they are enlarged, and the cytoplasm appears vacuolated as a result of altered segments of endoplasmic reticulum (ER) (hydropic or vacuolar degeneration) (Kumar *et al.*, 2017). Cell swelling can occur due acute exposure to toxic substances (Roberts & Rodger, 2012). Under acute exposure to toxins from *Karlodinium micrum*, zebrafish (*Danio rerio*) suffered swelling of different cells, due to an increase in membrane permeability, followed by lysis and necrosis of the epithelial surfaces (Deeds *et al.*, 2006).

1.1.3.2 Cell death

There are two broad types of cell death, apoptosis and necrosis, although other classifications exist (Kroemer *et al.*, 2009). Necrosis is an energy-independent, passive process of cell death caused by external agents. The event is characterised by the disruption of the plasma membrane, swelling of organelles, and lysis of the cell contents. Because of the leaking of the cell contents, necrosis often stimulates a potentially damaging inflammatory response (AnvariFar *et al.*, 2017). Cytomorphological changes in the nucleus during cell necrosis include karyolysis, which is the dissolution of the chromatin and fading of basophilia (less affinity for the basophilic dye in the H&E stain) secondary to the degradation by endonucleases, pyknosis (condensation of chromatin and the nucleus) and karyorrhexis (fragmentation of the nucleus) (Kumar *et al.*, 2017). Necrosis of the gill epithelium

has previously been associated with heavy metal exposure (Mallat, 1985), high concentrations of silver nanoparticles (Farmen *et al.*, 2012), insecticides (Cengiz & Unlu, 2006), irritant phytoplankton or zooplankton (Rodger 2007; Rodger *et al.*, 2011), and infectious agents (Granzow *et al.*, 2014; Nylund *et al.*, 2010; Powell *et al.*, 2004).

Apoptosis, also known as "programmed cell death", is essential for metazoan organisms to eliminate altered or unwanted cells (Edinger & Thompson, 2004). The process is highly regulated by cellular signalling pathways and although reports on apoptosis in fish are limited (AnvariFar *et al.*, 2017), equivalent pathways of apoptosis to those present in mammals are believed to be occur (Dos Santos *et al.*, 2008). Apoptosis is largely regulated by the Bcl2 family of proteins and is associated with loss of mitochondrial function and caspase enzyme activation; cleavage of endonucleases and fragmentation of DNA; destruction of the cytoskeleton and shrinkage of structures including pyknotic (condensed with increased basophilia) and karyorrhectic (fragmented) nuclei; and plasma membrane changes such as blebbing; phagocytic removal of material induced by phospholipids in apoptotic bodies (a result of shrinkage, fragmentation and budding of the cells) (Miller & Zachary, 2017). Unlike necrosis, apoptotic cells do not release their cellular contents into the surrounding interstitial tissue and therefore the inflammatory response, if present, is very mild (Elmore, 2007).

Apoptosis can be initiated by toxins, radiation or infectious organisms. For example, structural damage and enzyme impairment causing necrosis or apoptosis of chloride cells was observed in gills of tilapia exposed to copper (Dang *et al.*, 2000) and salmon gill poxvirus (SGPV) has also been associated with apoptosis in epithelial and chloride cells of Atlantic salmon (Gjessing *et al.*, 2015).

1.1.3.3 Circulatory disturbances

Vascular disturbances in fish gills include congestion, oedema, haemorrhages, aneurysms and thrombosis. Oedema will be explained in detail in a separate section due to the frequency of this condition in many gill disease studies. In gill pathology, congestion is understood to be an excess of blood in the capillaries (Speare & Ferguson, 2006) without distinction or if it is an active (hyperaemia) or a passive

(congestion) process, as defined for mammal pathology (Kumar *et al.*, 2017). Haemorrhage is defined as the extravasation of blood from vessels (Kumar *et al.*, 2017). Aneurysms (or telangiectasias) are the result of collapsed pillar cells and weakness of vascular integrity (Rodrigues *et al.*, 2019) and can be identified as blood-filled ovoid expansions of individual lamellae (Wolf *et al.*, 2015), that eventually fibrose and repair with the formation of thrombi (Poppe & Ferguson, 2006)

Circulatory disturbances are normally caused by toxins, chemical irritants or mechanical damage of the lamellar epithelium. Causes of haemorrhage include chemical irritants (Rosety-Rodrıguez, *et al.*, 2002), heavy metals, parasitic infections (Dezfuli *et al.*, 2007), and physical abrasion such as the mechanical irritation from setae-bearing diatom algae (Roberts & Rodger, 2012) or contact with cnidocysts of gelatinous zooplankton (Baxter *et al.*, 2011). Aneurysms can be due to exposure to pollutants (Rodrigues *et al.*, 2019) or mechanical damage (e.g. fish pumping during boat treatments), but this change is a common gill artefact associated with head concussion and some euthanasia-related procedures, whereas the formation of thrombi indicates that true aneurysms have occurred (Wolf *et al.*, 2015).

1.1.3.4 Lamellar oedema

Oedema is the accumulation of fluid resulting from a net outward movement of water into extravascular spaces due to an alteration in the permeability of the vascular wall and by Starling forces – an upset in the balance of hydrostatic and osmotic pressures (Mosier, 2017). The oedematous fluid that accumulates owing to an imbalance of the Starling forces typically is a low-protein containing transudate, in contrast with the more eosinophilic, protein-rich oedema fluid due to increased vascular permeability (Kumar *et al.*, 2017). In fish, lamellar oedema is associated with the presence of sub-epithelial proteinaceous material (Mitchell *et al.*, 2012; Wolf *et al.*, 2015), and therefore most of the cases of oedema detected are likely due to increases in vascular permeability. Epithelial lifting is the detachment of the outer epithelial layer of the lamellae (pavement cells), very similar to oedema, but without any content in the sub-epithelial gap. It was suggested that lifting of the lamellar epithelium does not necessarily represent true oedema because the sub-epithelial fluid might come

primarily from the water passing over the gills rather than originating as a blood exudate (Mallat, 1985). Conversely, after assessment by electron microscopy it has been suggested that epithelial lifting is due to interstitial oedema present in the space between the two layers of lamellar epithelium (Speare & Ferguson, 2006). However, the direct effect of toxicants, both in terms of oedema and epithelial lifting, have been suggested to have a protective effect on the fish by increasing the distance that waterborne irritants must diffuse to reach the fish's bloodstream (Mallat, 1985). Epithelial lifting and lamellar oedema often appear as an acute response to direct contact with pollutants such as heavy metals (Figueiredo-Fernandes *et al.,* 2007), biocides (Bruno & Ellis, 1988), hydrogen peroxide over-exposure (Kiemer & Black, 1997; Tort *et al*., 2002), algae toxins (Rodger *et al.*, 1994) or physical irritation (i.e. contact with the siliceous setae of algae) (Kent *et al.*, 1995).

1.1.3.5 Lamellar synechiae

Lamellar synechiae is the adhesion between adjacent lamellae (often the tips) and is a more specific indicator of pavement cell necrosis (Wolf *et al.*, 2015). The exact mechanism by which lamellar synechiae develop is unknown but the most likely causes have been reviewed by Speare & Ferguson (2006). One proposed mechanism involves an alteration in the mucus glycoprotein covering epithelium which modulates the negative charge causing adhesion to neighbouring lamellae. Another hypothesis involves loss of the outer layer of the mature epithelium and resultant increase in less mature cells that form junctional complexes as they migrate to the damaged site. Therefore, if fish are "gasping" (opening the mouth in the water column), the lamellae collapse, and this promotes the fusion of adjacent lamellae through the immature cells.

Lamellar adhesions are common after exposure to heavy metals, algal toxins (Roberts & Rodger, 2012) or infectious agents, such as SGPV infections (as a result of extensive apoptosis and detachment of the epithelial cells) (Gjessing *et al.,* 2015), parasitic infections (e.g. sparicoltilosis or costiasis) (Sitjà-Bobadilla & Alvarez-Pellitero, 2009; Speare & Ferguson, 2006) or sequestration of bacteria (Ostland *et al.,* 1999).

1.1.3.6 Cell hypertrophy

Cell hypertrophy is an increase in cell size resulting from an increase in the number and size of organelles (Miller & Zachary, 2017). It occurs due to either an increase of functional demand (i.e. chronic pressure or volume overload can cause the hearts of vertebrates to remodel) (Keen *et al.*, 2016) or from growth factor or hormonal stimulation (Kumar *et al.*, 2017) and is a more energy-efficient method of increasing the size of an organ than hyperplasia because it does not involve cell duplication (Ong *et al.*, 2007). As mentioned previously, cell hypertrophy in the gill epithelium has been recorded repeatedly as a direct result of contact with toxins, although only as a term to indicate an increase in cell size rather than any inference as to the mechanism of the increase.

Examples of increased cell size to compensate for reduction in function without signs of degeneration or intracellular infection are most frequently associated with mucus or chloride cells (Jagoe *et al.*, 1997). Mucus cell hypertrophy was observed in rainbow trout (*Oncorhynchus mykiss*) exposed to low levels of erythromycin (Rodrigues *et al.*, 2019). The authors suggested it was an adaptation to increase mucus secretion by the gills to help protect their surface and to stimulate the rate of operculum movements to increase ventilation. The enlargement of epithelial cells (not true hypertrophy) can be caused by the development of intracellular infectious agents such as epitheliocysts-associated bacteria (Guevara-Soto *et al.*, 2016) or microsporidian parasites such as *Loma salmonae* (Kent & Speare, 2005).

1.1.3.7 Cell hyperplasia

Hyperplasia is an increase in the number of individual cells in a cell population capable of mitosis, such as the epithelial cells of the gills (Temmink *et al.*, 1983). Many epithelial cells are able to undergo hyperplasia in response to hormonal stimulation, inflammation, or physical trauma (Miller & Zachary, 2017). In gills, epithelial cell division occurs normally from the progenitor compartment at the base of the lamellae (Speare & Ferguson, 2006). Hyperplasia of gill epithelial cells is a very common non-specific host response to sub-acute to chronic gill damage (Wolf *et al.*, 2015) and is thought to be an attempt to reduce the respiratory surface available for pathogens (Roberts & Rodger, 2012). Progressive hyperplasia leads to

fusion of adjacent gill lamellae. However, an increase in lamellar thickness will reduce the functional area of the lamellae and also the efficiency of gaseous exchange (Speare & Ferguson, 2006). Despite gill epithelial cell hyperplasia being one of the most common host responses to gill disease, the molecular mechanisms underlying these pathological changes are not well understood (Marcos-López *et al.*, 2018).

Marked gill epithelial proliferation can be seen after direct exposure to toxic chemicals and heavy metals (Mallat, 1985). Amoebic gill disease is characterised by a hyper-proliferation of the gill epithelial tissue and has been suggested to be mediated by the down-regulation of the p53 tumour suppressor protein mRNA (Morrison *et al.*, 2006), although further studies failed to find consistent modulation of this gene (Marcos-López *et al.*, 2018). Other infectious diseases in salmon associated with marked lamellar epithelial proliferation include microsporidiosis (Matthews *et al.*, 2013) and SGPV infections (Gjessing *et al.*, 2015). Non-infectious waterborne insults such as contact with harmful algal blooms (HABs), are also associated with epithelial hyperplasia (Rodger *et al.*, 2011). Nutritional deficiencies can also cause a proliferative pattern, such as pantothenic acid deficiency, which has been a notable problem for salmonid aquaculture in the past (Wood & Yasutake, 1957), and causes a characteristic hyperplasia that starts from the distal part of the filament and progresses in a proximal direction (Karges & Woodward, 1983).

Mucus and chloride cell hyperplasia can be seen as a response to mild, chronic gill irritation (Speare & Ferguson, 2006). Mucus cells secrete mucin glycoproteins, which have a critical role, including limiting infectious diseases (Linden *et al.*, 2008). Both hyperplasia and increased mucin secretion can be stimulated by several conditions (e.g. AGD) (Marcos-López *et al.*, 2018), although overproduction of mucus will increase the lamellar thickness and hinder the diffusion of gases (Laurent & Perry, 1991). Lamellar chloride cell proliferation results in the multiplication of these cells along the length of the lamellae (Wolf *et al.*, 2015), which in turn enhances the ion transporting capacity of the gill under situations that disturb ionic homeostasis. During experimental transmission of *Sparicotyle* spp. to gilthead seabream (*Sparus aurata*), chloride cells were abundant in infected fish, and seemed

to be a response to the ionoregulatory disturbance induced by the epithelial injuries caused by the parasite (Sitjà-Bobadilla & Alvarez-Pellitero, 2009).

1.1.3.8 Inflammatory infiltration

Inflammation is a complex host response aimed at eliminating the cause of cell injury, necrotic cells, and to initiate the process of repair (Kumar *et al.*, 2017), although it can also exacerbate the disease process (Roberts & Rodger, 2012). Initiation of an inflammatory response involves soluble mediators and recruitment of inflammatory cells to the area (Kumar et al., 2017). Acute inflammation and occurs in a short time (from hours to a few days). Chronic inflammation occurs when the origin of the pathology persists, and the immune and inflammatory response is sustained. It is characterised by the infiltration of mononuclear cells, tissue destruction and repair (Kumar *et al.*, 2017).

Different immune cell types are present in fish, although these can be difficult to recognise in gill tissue (Speare & Ferguson, 2006). In addition, salmonids possess a dense population of resident lymphocytes at the caudal rim of each of the interbranchial septa (Haugarvoll *et al.*, 2008) that should not be confused with branchitis when present additionally in the distal two-third of the filaments (Wolf *et al.*, 2015). Immune cells seen in gills include neutrophils, macrophages, melanomacrophages, multinucleated giant cells, lymphocytes and eosinophilic granular cells, among others (Koppang *et al.*, 2015).

Some of the gill injuries frequently seen in marine-net pen salmonids induce an acute inflammatory response, such as spine silica diatom-induced branchitis (foreign body response) (Ferguson, 2006) or when in contact with gelatinous zooplankton, such as *Aurelia aurita* (response to trauma and toxic component) (Baxter *et al.*, 2011). Sub-acute inflammation has been described in rainbow trout gills 3 days after showing clinical signs of bacterial gill disease (BGD) infections and were characterised by the influx of monocytes after an initial infiltration of neutrophils (Speare *et al.*, 1991). Experimentally, chronic inflammation was seen after naïve salmon co-habited with fish infected with the betaproteobacteria *Candidatus* Branchiomonas cysticola and was characterised by mononuclear cell infiltration into the sub-epithelial tissues 30 days after the start of the trial (Wiik-Nielsen *et al.*,

2017). Events of gill tissue repair are not frequently reported. Evidence of neovascularization and vascular remodelling were present in the gills of chinook salmon *Oncorhynchus tshawytsch* following an acute inflammatory response and tissue damage caused by the rupture of the xenoma (cyst containing different developmental stages of a microsporidian) filled by the parasite *Loma salmonae* (Lovy *et al.*, 2007).

Examples of inflammation caused by common gill injury, explained briefly above, are based solely on the histological presentation using routine staining techniques such as H&E. More complex immune responses of the gills, usually based on transcription analysis of various immune genes, have been described for certain gill diseases (reviewed by Koppang *et al.*, 2015).

1.1.3.9 Artefacts

Gill tissue is prone to artefacts and interpretation on histopathology, especially acute changes, can be hindered if care is not taken during tissue sampling and processing (Speare & Ferguson, 2006). Lifting of the lamellae and epithelial swelling can occur within five minutes after death if the tissue it is not immediately placed into fixative because of the absence of compensatory water pressure within the branchial cavity (Ferguson, 2006). In addition, the gills are a technically complicated organ to prepare for routine histology as the fixative used or the orientation of sectioning can interfere with the final morphology of the section (Wolf *et al.*, 2015). The technique used to kill fish can also induce artefacts in the gill vasculature (Wolf *et al.*, 2015).

1.1.4 Clinical signs of respiratory disease

The typical clinical signs of gill disease observed in fish result from the animal attempting to compensate for a reduction in the functional area of the organ to fulfil its required physiological functions. This has a high energy cost and routine activities, like swimming or feeding, will be affected as a consequence. Hvas *et al.* (2017) showed a reduced swimming capacity and limited maximum rate of oxygen uptake during exercise in fish suffering from AGD compared with a healthy group (203 mg O_2 kg^{-1} h^{-1} compared to 406 mg O_2 kg^{-1} h^{-1}, respectively). Inappetence is

common in fish with gill disease and reduces productivity if the disease persists (Weli *et al.*, 2017).

Table 1.1. Summary of the pathological changes in gill diseases and microscopic appearance with H&E stain.

Change	**Description**	**Microscopic appearance (H&E)**
Cell swelling	Alteration in the membrane permeability.	Enlarged and cloudy cells (lack of eosinophilia), with clear vacuoles within the cytoplasm.
Cell necrosis	Disruption of the plasma membrane, swelling of organelles, and lysis of the cell content.	Karyolysis, pyknosis and karyorrhexis of the nucleus. Increased eosinophilia of the cytoplasm. Accompanied by influx of inflammatory cells.
Cell apoptosis	Regulated programmed cell death that does not elicit an inflammatory response.	Pyknosis and karyorrhexis. Formation of apoptotic bodies. Absence or very mild inflammatory reaction.
Circulatory disturbances	- Congestion: due to increase in vascular permeability - Haemorrhage: caused by the rupture of the vascular wall. - Aneurysms: result of the collapse of pillar cells. It can be an artefact. - Thrombosis: resolved aneurysms.	- Congestion: excess of blood in the capillaries. - Haemorrhage: extravasation of erythrocytes from vessels. - Aneurysms: blood-filled, ovoid expansions of vessels. - Thrombosis: fibrin-rich material within the blood vessel after disruption of blood vessel endothelial cells.
Lamellar oedema /Epithelial lifting	Alterations in the walls of blood vessels and impairment of hydrostatic and oncotic pressure gradients across the capillary resulting in accumulation of fluid within the extravascular spaces. Epithelial lifting can be an artefact of this.	Epithelial lifting: detachment of the outer lamellar epithelial layer with a space between the vasculature and the pavement cells. Oedema: the same but with proteinaceous material in the space.
Lamellar synechiae	Suggested to be caused by an alteration in the glycoproteins of the mucus that covers the epithelium, and the loss and regeneration of the pavement cells.	Adhesion between adjacent lamellae (typically the tips) not caused by epithelial proliferation.
Cell hypertrophy	Increase in the cell size resulting from increased number and size of organelles due to an increase of functional demand, a growth factor effect or hormonal stimulation.	Enlargement of cell without obvious signs of cell degeneration.
Cellular hyperplasia	Suggested that this reduces the respiratory surface available for pathogens and/or enhances cell function.	Increased number of cells leading to fusion of adjacent gill lamellae.
Branchitis	Inflammation is the host response to eliminate the cause of cell injury, necrotic cells, or initiate cellular repair.	Extravasation of immune cells.

Signs of gill dysfunction include swimming close to the water surface or crowding together facing into the oncoming current at the side of the pen and an increased respiratory rate.

Gross lesions are variable but include variable degrees of swollen and/or shortened gill filaments, pallor, mucus accumulation and petechial haemorrhages (Kvellestad *et al.*, 2005). Lesions can be focal or diffuse and may be limited to a single gill arch or, more commonly, affect several or all gill arches in affected individuals. Haemorrhage can also be caused by waterborne irritants or trauma during events such as mechanical removal lice (e.g. hydrolyser) (Hjeltnes *et al.*, 2018).

1.2 Gill diseases in Atlantic salmon

1.2.1 Relevance of gill disease to the Atlantic salmon aquaculture industry

1.2.2 Atlantic salmon aquaculture in the UK and globally

According to the Food and Agriculture Organization of the United Nations (FAO), aquaculture is "*the farming of aquatic organisms, including fish, molluscs, crustaceans and aquatic plants*". Aquaculture is an ancient practice, with details of carp aquaculture production as early as the fifth century B.C. in the writings of Fan Li in China, while the Romans documented coastal aquaculture practices before the end of the second century B.C. in Europe (Carter, 2002). In the last few decades, globally, aquaculture has expanded rapidly and has achieved annual growth rates of approximately 10% in the 1980s and 1990s. Although this growth has slowed to 5.8% per year during 2000-2016, aquaculture remains the fastest growing food-producing sector (FAO, 2018).

Atlantic salmon (*Salmo salar*) production represents 4% of the total finfish production worldwide (FAO, 2018), with Scotland being the third largest producer of Atlantic salmon after Norway and Chile. In 2016, Scotland produced 162,817 tonnes of salmon, which was worth approximately £800 million by value (Kenyon & Davies, 2018). With the predicted rise in the world's population to 8.5 billion by

2030, an increase in aquaculture production has been suggested as one of the main solutions to meet future demands for animal protein (Béné *et al.*, 2015). The Scottish aquaculture industry has an ambition to produce up to 400,000 tonnes of salmon annually by 2030 (Gatward *et al.*, 2017), but for this, constraints resulting from different challenges, including health issues, need to be addressed (Gatward *et al.*, 2017).

1.2.3 Impact of gill diseases to the salmon industry

The most widely recognised, and therefore the best studied gill pathogen in Atlantic salmon is *Paramoeba perurans* (syn *Neoparamoeba perurans*) (Murray *et al.*, 2016), the causative agent of amoebic gill disease (AGD) (Munday *et al.*, 2001). In Tasmania, AGD has been estimated to be responsible for 10-20% of the total production costs (Munday *et al.* 2001) and is still considered to be the most serious health problem during the marine stage of salmon farming (Oldham *et al.*, 2016). The estimated cost of AGD-associated mortality outbreaks to the salmon industry globally has been reported to be over one million in certain production years (USD 1-81 million) (Shinn *et al.*, 2015). The term "gill disease" groups various conditions of different aetiologies. Overall, estimating the true cost of these to the industry is difficult because gill disease is wide-ranging and not notifiable. Gill disease has been recorded in Europe since the 1980s (Kvellestad *et al.*, 2005; Rodger & McArdle, 1996). In Norway, gill disease of a proliferative nature affected 18.8% of Atlantic salmon production during 1998/1999 and this increased to 35.3% by 2002/2003 (Nygaard, 2004, cited in Nylund *et al.*, 2008). However, according to the literature, it was not until 2003/2005 that gill conditions were considered an emerging problem (Kvellestad *et al*., 2005; Rodger, 2007). At the time of writing, gill diseases are one of the most important health problem in all major Atlantic salmon producing countries, including Australia (Oldham *et al*., 2016), Canada (Laurin *et al.*, 2019; McPhee *et al.*, 2017), Chile (Santana, 2018), Norway (Hjeltnes *et al.*, 2018), Ireland (Downes *et al.* 2018; Marcos-López, 2018) and Scotland (Matthews *et al.*, 2013). Data from Mowi's report for 2018, the world's largest farmed salmon producer, highlighted gill infections as the second major cause of loss in 2018, just after

cardiomyopathy syndrome in term of biomass and the third in terms of total fish numbers (Mowi, 2019) (Table 1.2).

Table 1.2. Main causes of reduced survival in salmon farming 2018 (Modified from Mowi, 2019-Integrated Annual Report 2018).

	Infectious		**Non-infectious**	
	Fish numbers	Biomass	Fish numbers	Biomass
1	Cardiomyopathy syndrome	Cardiomyopathy syndrome	Treatment	Treatment
2	Wounds (bacterial skin diseases)	Gill infections	Poor performers	Physical damage
3	Gill infections	Wounds (bacterial skin diseases)	Physical damage	Poor performers
4	Pancreas disease	Pancreas disease	Transport	Handling

1.2.4 Multifactorial gill diseases

Infectious and non-infectious aetiologies have been associated with gill disease (Mitchell & Rodger 2011; reviewed by Rodger *et al.*, 2011). Therefore, even though gill disease can be caused by a single agent, it is frequently multifactorial making it difficult to establish one definitive aetiology (Kvellestad *et al.*, 2005). A peak in gill disease incidence occurs in Northern Europe from summer to early winter (Steinum *et al.*, 2010). However, the difficulty in establishing the cause of this multi-pathogen and multifactorial disease has resulted in inconsistent classification and, as such, no specific case definition exists currently.

The term “proliferative gill inflammation” (PGI) has been used to describe recurrent gill disease outbreaks occurring in autumn in salmon farms on the southwest coast of Norway. These primarily affect smolts that have been transferred to the sea the previous spring (S1) (Kvellestad *et al.*, 2005), although outbreaks have also been reported at other times of the year (Steinum *et al.*, 2009). Histological changes in the gills of affected fish included epithelial cell proliferation and necrosis,

inflammation and vascular changes, such as lamellar haemorrhage and/or lamellar thrombosis (Kvellestad *et al.*, 2005). However, the changes seen are relatively non-specific and can be found at a level insufficient to consistently cause disease. Moreover, gill disease pathology can vary depending on the agent or physical event responsible. In Scotland, the seasonality and pattern of gill disease appears similar to that described for PGI in Norway, but the vascular changes were inconsistent (Matthews *et al.*, 2013) and this has limited the use of the term PGI. Proliferative gill disease (PGD) has been used as a non-specific term derived from examination and scoring of gross lesions in salmon gills. The term PGD could have been used by researchers in the past to refer to histological proliferation (lamellar epithelial cell hyperplasia and fusion of adjacent lamellas, e.g. Nylund *et al.*, 2008) or by pathologists in Scotland to refer to gill diseases with histological proliferative element of uncertain aetiology (Matthews *et al.*, 2013). However, PGD is also a non-specific term that describes neither a syndrome or a specific disease aetiology in salmon. Additionally, there is already a gill disease termed proliferative gill disease or "Hamburger Disease" that affects channel catfish (*Ictalurus punctatus*) and creates confusions with the term PGD used in Europe for salmonids. Chance *et al.* (2018) discussed the occurrence of emergent gill diseases in Europe, such as AGD, waterborne irritants and PGD but the reference cited for PGD referred to the disease in catfish caused by the myxosporean *Henneguya ictaluri* (Pote *et al.*, 2000). Other terms, such as "chronic gill disease" or "autumn gill disease" (Hjeltnes *et al.*, 2017), have also been used but due to variability in the clinical presentation no case definition has been established.

Complex gill disorder, also known as complex gill disease (CGD) is the preferred term being used by those working in the field of fish health to refer to this varied syndrome of probable multifactorial aetiology and variable histopathology and this encompasses the syndromes referred to as PGI or PGD in articles published previously. Although a complete case definition for CGD has not yet been established, efforts are focused on identifying knowledge gaps to address this (SRUC, 2017). The following section will focus in the latest knowledge available related to CGD and putative causes associated with the disease.

1.2.5 Putative pathogens associated with complex gill disorder

The aetiological agents involved in CGD are uncertain due to the inability to culture and grow several of the suspected organisms *in vitro* (e.g. epitheliocyst-forming bacteria) (Kvellestad *et al.*, 2003) and because some are present frequently in clinically normal animals (Steinum *et al.*, 2010) The putative causes associated with the disease are summarised in Table 1.3.

Table 1.3. Putative pathogens associated with CGD and other contributing causes (Rodger, 2016).

Viruses	Bacteria	Parasites	Non-infectious	Others
Atlantic Salmon Paramyxovirus Salmon Gill Poxvirus	*Ca*. B. cysticola *Ca.* Piscichlamydia salmonis *Ca*. Syngnamydia salmonis *Tenacibaculum* spp.	*Paramoeba perurans* *Desmozoon lepeophtherii* *Trichodina* spp. *Ichthyobod*o spp. *Parvicapsula pseudobanchiocola*	Harmful algae blooms Harmful zooplankton	Hydrogen peroxide Mechanical damage (handling or treatments) Water quality

1.2.5.1 Atlantic salmon paramyxovirus

A total of nine paramyxoviruses have been described in fish, although not always associated with disease (reviewed by Meyers & Batts, 2016). The complete sequence of Atlantic salmon paramyxovirus has been determined and phylogenetic analysis suggests that the virus is a novel member of the sub-family Paramyxovirinae, most closely related to the respiroviruses (Falk *et al.*, 2008). It was first isolated in 1995, from a population of Atlantic salmon post-smolts suffering from gill disease in Norway, using cultures of rainbow trout gill cells (RTgill-W1) and CHSE-214 cells infected with diseased gills (Kvellestad *et al.*, 2003). The mortality in this population of fish reached 40% and the gills of infected salmon had epithelial necrosis, vascular changes, branchitis, lamellar epithelial proliferation (these four changes represent the

description of PGI) and presence of epitheliocyst organisms. While attempting to culture the epitheliocysts *in vitro* the authors observed the growth of ASPV as a cytopathic effect in the tissue cultures 9 weeks post-infection with a growth range between 6-21ºC (Kvellestad *et al.*, 2003). Infection trials with the virus in salmon post-smolts successfully transmitted infection to naïve salmon, but did not produce pathology (Fridell 2003, cited in Meyers & Batts, 2016) or mortalities (Fridell 2003, cited in Fridell *et al.*, 2004). The authors did not discard the possibility that the virus was somehow associated with the disease and in later studies immunohistochemistry (IHC) was used to detect ASPV and subsequently to screen the gills of post-smolts from three farms with gill disease problems and with a history of PGI (Kvellestad *et al.*, 2005). Abundant positive labelling was seen in the epithelial and endothelial cells of the affected gills, although not all gills with PGI were positive. However, it was suggested that the agent was contributing to the pathology observed. Nylund *et al.*, (2008) failed to detect ASPV in two marine farms examined despite mortalities close to 80% in salmon suffering from gill disease of a proliferative nature. Additionally, Steinum *et al.* (2010) detected ASPV in only one of six farms examined with fish suffering from PGI. This suggests that the presence of the virus is not always associated with the disease and it was not involved in the PGI that occurred on these farms (Steinum *et al.*, 2010). The role of ASPV in gill disease is still controversial but it is highly unlikely to be a primary pathogen.

1.2.5.2 Salmon Gill Poxvirus

Poxviruses have been associated with gill disease in fish including koi and common carp (*Cyprinus carpio*) and ayu (*Plecoglossus altivelis*) (reviewed by Gjessing *et al.*, 2016). Proliferative gill diseases have been present in Norway during both the freshwater and seawater stages of Atlantic salmon production since the 1990s (Nylund *et al.*, 2008) and it was suspected that a poxvirus was associated with this since the 1990s, especially in the freshwater stage. However, it was not until 2008 that salmon gill poxvirus (SGPV) was first described using transmission electron microscopy (TEM) (Nylund *et al.*, 2008). Later, next-generation sequencing provided the whole genome of SGPV placing the virus in the sub-family Chordopoxvirinae (Gjessing *et al.*, 2018) and the presence of the virus was confirmed in samples of diseased salmon gills dating back to 1995.

SGPV has been reported recently in Ireland (Downes *et al.*, 2018), the Faroe Islands and Scotland (Gjessing *et al.*, 2018), and a recent variant has been detected in Atlantic salmon in North America which, unlike the Norwegian variant, is permissive to cell culture (LeBlanc *et al.*, 2019). However, unlike the European variant, fish infected with the North American SGPV variant did not show any pathology (LeBlanc *et al.*, 2019). Horizontal transmission from infected to naïve fish has been demonstrated including indirectly via water coming from infected fish pens (Wiik-Nielsen *et al.*, 2017). SGPV is found in salmon hatcheries that do not receive any incoming seawater (Gjessing *et al.*, 2017) and it is in the freshwater phase of salmon rearing where SGPV shows its most typical manifestation of clinical disease (Gjessing *et al.*, 2016). However, studies suggest that the virus may have a marine origin because the prevalence of SGPV is relative high in wild Atlantic salmon in Norway returning from marine migration and it has not been found in (non-anadromous) landlocked salmon that have never had contact with the marine environment (Garseth *et al.*, 2018).

In fry, the course of the disease occurs synchronously in all fish within the tank. Clinical signs associated with the disease have been described mainly for salmon fry, pre- and post-smolts and include loss of appetite, lethargy and crowding in the bottom of the tank. On gross examination the gills appear pale and the filaments swollen. In addition, redness of the abdomen has been described (Gjessing *et al.*, 2018).

Using TEM, Nylund *et al.* (2008) observed that gills of fish suffering from SGPV presented a severe proliferative reaction with inflammation and the complete absence of interlamellar spaces in some gill arches. Cells infected with poxvirus particles protrude from the surface of the outer lamellae due to being enlarged and have condensed nuclear chromatin. An IHC method was used to study the course of the infection in pre-smolts infected with the virus in three different freshwater farms in Norway at different stages of the disease: before, during and after mortalities occurred (Gjessing *et al.*, 2015). Before mortalities, histopathology of affected fish revealed the presence of apoptotic cells, denoted by TUNEL stain, in the lamellar epithelium and hypertrophy of the squamous epithelium, hyperplasia of the chloride

cells and fusion of the adjacent lamellae. During the peak mortality stage detachment of the apoptotic epithelial cells was present together with abundant SGPV, as denoted by IHC labelling, widespread adherence of neighbouring lamellae, severe epithelial cell proliferation and apoptosis of chloride cells. The changes to chloride cells suggest that SGPV could affect the smoltification process and predispose the fish to secondary infections by causing direct damage to the respiratory epithelium (Gjessing *et al.*, 2017). Hemophagocytosis in the kidney and spleen by scavenger endothelial cells and macrophages in the absence of SGPV IHC positive labelling was also present (Gjessing *et al.*, 2015; Gjessing *et al.*, 2018), although the mechanisms for this is not well understood. One week after mortalities stopped, most fish had mild clinical signs of disease and less severe pathology.

Similar pathology to that observed in freshwater fish has been described for fish infected with SGPV in the marine stage (Gjessing *et al.*, 2017; Nylund *et al.*, 2008). However, gill disease in the marine environment is often multifactorial and associated with proliferation of the epithelial cells and fusion of the lamellae, which can mask the presence of the protruding apoptotic cells suggestive of SGPV (Gjessing *et al.*, 2017). Gjessing *et al.*, (2017) showed widespread presence of SGPV in salmon in the marine environment using improved detection methods for the virus, including quantitative polymerase chain reaction (qPCR) and IHC. Archived samples from the first case of amoebic gill disease, which caused approximately 80% mortality in the affected site in Norway (Steinum *et al.*, 2008), tested positive for SGPV (Gjessing *et al.*, 2015). Conversely, detection of SGPV was variable in the longitudinal study carried out by Downes *et al.* (2018) in Ireland and no pathology was observed in infected fish. Although it appears infected fish can overcome the disease and eliminate the virus (Wiik-Nielsen *et al.*, 2017), it might be that the virus becomes latent and can be re-activated at a later stage, for example during episodes of immunosuppression (Downes *et al.*, 2018). While the pathogenesis of SGPV still needs to be fully elucidated, it has been suggested that it could evade the innate immunity of the host, allowing it to replicate (Gjessing *et al.*, 2018), and the resulting apoptosis and shedding of infected cells may be caused by the virus itself to allow it to spread to other hosts (Garseth *et al.*, 2017).

1.2.5.3 Epitheliocyst-forming bacteria

The term epitheliocyst has been used widely to describes the presence of cysts in the epithelial cells (Blandford *et al.*, 2018), and are found primarily in the epithelial cells of the gills and skin (Nowak & LaPatra, 2006). These inclusions were first detected in 1920 in common carp (*Cyprinus carpio*) and reported as "mucophilosis" (cited in Nowak & LaPatra, 2006) and later described by Hoffman *et al.*, (1969) in the gills of bluegill (*Lepomus macrochirus*). The presence of epitheliocysts has been recorded in at least 90 species of fish (Blandford *et al.*, 2018) and often in the presence of disease and mortalities (Katharios *et al.*, 2008). However, the difficulty in culturing the causative agents and lack of experimental models hinders the study of these cyst-forming organisms (Nowak & LaPatra, 2006). Initially, the origin of the epitheliocysts were thought to be Gram-negative, Chlamydia-like and rickettsial intracellular bacteria (Nowak & LaPatra, 2006) but recent understanding is that they are caused by a wide range of different bacteria (Blandford *et al.*, 2018). Since the start of salmon farming in Norway, there have been reports of epitheliocysts associated with mortalities (Nylund *et al.* 1998). Epitheliocysts are a common finding in the gills of seawater farmed Atlantic salmon during gill disease outbreaks (Kvellestad *et al.*, 2005; Steinum *et al.*, 2009) and have been associated with various putative pathogens including the bacteria *Ca.* Branchiomonas cysticola (Toenshoff *et al.*, 2012), *Candidatus* Piscichlamydia salmonis (Draghi *et al.*, 2004), *Candidatus* Clavichlamydia salmonicola (Mitchell *et al.*, 2010) and *Candidatus* Sygnamidia salmonis (Nylund *et al.*, 2015). A moderate positive association has been found between the loads of *Ca*. P. salmonis, estimated by real-time PCR targeting 16S rRNA, and the severity of PGI in fish (Steinum *et al.*, 2010). However, the presence of *Ca*. P. salmonis did not correlate with the prevalence of epitheliocysts in gill tissue, suggesting that another organism was responsible. It was later discovered that the betaproteobacteria *Ca. B. cysticola* (Toenshoff *et al.*, 2012) was linked with the presence of epitheliocysts and with an increased severity of PGI, suggesting it may have a significant role in the disease (Mitchell *et al.*, 2013). *Ca. B. cysticola* infection can also be detected in the fresh-water stage of salmon production (Wiik-Nielsen *et al.*, 2017). During infection trials, in which the water of infected fish was used as a source of waterborne infection for a population of naïve juvenile Atlantic salmon,

Ca. B. cysticola infections were associated with gill epithelial cell proliferation and subepithelial inflammation (Wiik-Nielsen *et al.*, 2017). These findings suggest that other histological lesions, not only the formation of cysts in the epithelial cells, can occur in gills infected by the bacteria. Unfortunately, the high prevalence of *Ca*. B. cysticola in healthy fish (Downes *et al.*, 2018) has hindered our understanding of its role in gill diseases.

1.2.5.4 Desmozoon lepeophtherii

The microsporidian parasite *Desmozoon lepeophtherii* (syn. *Paranucleospora theridion*) is highly prevalent in both healthy fish and those affected by gill disease (Steinum *et al.*, 2010, Nylund *et al.*, 2011). However, parasite loads have been shown to be considerably greater in fish with PGI by real-time reverse transcriptase PCR (RT-rtPCR) (Steinum *et al.*, 2010). Infections with *D. lepeophtherii* have been associated with fish with lower condition factor (Gunnarson *et al.*, 2017) and stunted growth (Weli *et al.*, 2017). Histologically, *D. lepeophtherii* spores have been observed in clusters within lesions which are typically comprised of widespread hypertrophied and necrotic inter-lamellar epithelial cells in the gills (Matthews *et al.*, 2013). More information about *D. lepeophtherii*-associated pathology can be found in Section 1.4.8.

1.2.5.5 Paramoeba perurans

The protozoan *Paramoeba perurans* (= *Neoparamoeba perurans*), which causes a specific proliferative gill pathology known as amoebic gill disease (AGD), represents an aetiologically important gill disease (Munday *et al.*, 2001). *Paramoeba perurans* has also been reported in some multifactorial outbreaks of autumn gill disease and if PGI and AGD appear together, the mortality rate can reach 80% (Nylund *et al.*, 2011; Steinum *et al.*, 2008). In recent years, a complex scenario, comprising several different types of gill pathology in association with AGD, has been frequently reported in Scotland (Rodger, 2014) and Norway (Gjessing *et al.*, 2017). This increase in disease occurrence could be due to increased prevalence of concomitant pathogens. The role of *P. perurans* in gill disease is well-known and has been reviewed by various authors (e.g. Oldham *et al.*, 2016; Rodger 2014).

1.2.5.6 Other pathogens

Tenacibaculosis is caused by *Tenacibaculum* spp., a Gram-negative, filamentous, marine bacterium, and is an important disease in aquaculture worldwide (Avendaño-Herrera *et al.*, 2006; Toranzo *et al.*, 2005). Three different species have been recovered from Atlantic salmon populations: *Tenacibaculum maritimum*, *Tenacibaculum finnmarkense* (Småge *et al.*, 2016) and *Tenacibaculum dicentrarchi* (Avendano-Herrera *et al.*, 2015). These different bacterial species include a variety of strains that are associated with different levels of pathogenicity (Småge *et al.*, 2018). The bacterium can be detected in healthy gills, but the bacterial load increases in presence of clinical disease (Fringuelli *et al.*, 2012).

Other parasites reported during CGD, but not consistently present, include *Parvicapsula pseudobranchiola*, *Ichthyobodo* spp., and *Trichodina* spp. (Kvellestad *et al.*, 2005; Nylund *et al.*, 2011) and the presence of opportunistic gill pathogens can aggravate gill disease.

1.2.5.7 Other factors involved in CGD

The factors associated with CGD have yet to be determined. Some environmental conditions and handling procedures have been proposed to play a key role in the disease. Harmful algal blooms can precede CGD outbreaks, presumably by causing physical damage or irritation to the gill epithelium and facilitating the ingress of infectious agents (Rodger *et al.*, 2011). HABs can induce excess mucus production, multiple small foci of thickening along the gill filaments and haemorrhages (Rodger *et al.*, 2011). Histologically, the gill pathology associated with HABs can include oedema causing severe separation of the lamellar epithelium and congestion of branchial vessels, epithelial cell necrosis and epithelial cell sloughing (Speare & Ferguson, 2006). Some gelatinous zooplankton represent important environmental challenges to gills, such as relatively large jellyfish, and are carried onto outer surfaces of fish cages by tides and currents causing them to break up and pass through the mesh (Delannoy *et al.*, 2011). After being inhaled by the fish during respiration, the jellyfish can pass directly over the gills causing mechanical/toxin-related damage via the release of stinging cells (Mariottini & Pane 2010).

Phytoplankton blooms may increase stress in affected fish populations resulting in secondary bacterial infection due to damaged gill epithelium (Rodger *et al.*, 2011).

Net cleaning is a necessary procedure in salmon farming to avoid the overgrowth of biofouling and waste accumulation and facilitate oxygenation of the pen. However, certain routine handling procedures contribute to gill disease, for example *in situ* net-pen cleaning with high-pressure jets can cause gill lesions similar to those that occur in a jellyfish bloom. This is due to the physical disruption of fouling organisms, such as hydroids and anemones which also possess nematocysts (Baxter *et al.*, 2012), and may also facilitate the exposure to infectious organisms accumulated in the waste trapped in the nets (Floerl et al., 2016).

A rapid change in delousing methodologies has occurred in recent years in salmon farming. In Norway, there has been a considerable increase in the use of mechanical (based on flushing the lice from the skin of salmon) and thermal (exposure of the infected fish to warm water temperatures) de-lousing systems and a reduction in the use of chemical treatments from 2017 to 2018 (Hjeltnes et al., 2019). According to the Fish Health Norwegian Veterinary Institute, in surveys undertaken during 2017, fish farmers reported that gill haemorrhage was detected especially during the developmental phase of the mechanical treatments (Hjeltnes et al. 2018), and it was commonly observed after the thermal treatment during the surveys of 2018 (Hjeltnes et al., 2019). However, the effect that these types of treatment have on gill health is poorly documented and more studies are necessary to elucidate their role in gill disease (Overton et al., 2018). Exposure to hydrogen peroxide (H_2O_2) in bath treatments has been associated with gill pathology, especially when the water temperature is above 13˚C (Rodger *et al.*, 2011). The roles that these and various other factors (treatments, host genetics, concurrent disease, salmon year class, *etc*.) play in CGD pathogenesis have only been hypothesized and further epidemiological and experimental studies are required to determine the actual risk factors.

1.2.6 Histopathology of CGD

Recently, a workshop at the Scottish Aquaculture Innovation Centre (SAIC) was held for experienced fish pathologists to agree on the histological diagnostic criteria

for CGD to enable its use in future diagnostic and research projects (Noguera *et al.*, 2019). The hallmark to diagnose CGD, recently described by (Nogeura et al., in press), consists in ssignificant, non-specific, proliferative branchitis which cannot be attributed to a known single aetiology and is characterised by:

- Moderate to severe hyperplasia and fusion of the lamellar epithelium, with variable amounts of mucus cell hyperplasia and occasional lacunae (pseudocysts).
- Acute, subacute and/or chronic lamellar inflammation (may include either or both granulocytic to lymphohistiocytic cellular infiltration)
- Variable amounts of cellular degeneration and necrosis
- Variable amounts of haemorrhage, hyperaemia and thrombosis
- Variable amounts of filament infiltration by inflammatory cells
- Variable amounts of hypertrophy and hyperplasia of highly eosinophilic cells
- Rarely, proliferation/dysplasia of gill cartilage
- Variable numbers of the following agents or evidence of their presence may be associated with the above changes: Amoebae, epitheliocysts (Branchiomonas-type, less than 10 µm in diameter and densely basophilic), Gram-positive microsporidian spores within degenerate cells or microvesicles, salmon gill pox virus (apoptotic cells with clearing of central nuclear chromatin), other pathogens (e.g. *Ichthyobodo* sp., *Tenacibaculum spp*) or damaged by harmful planktonic organisms (e.g. jellyfish).

1.3 Current knowledge of the microsporidian *Desmozoon lepeophtherii*

1.3.1 General characteristics of Microsporidia

Microsporidia are single cell, eukaryotic, obligate intracellular organisms related to fungi (James *et al.*, 2006; Vávra & Lukeš, 2013). The earliest report of these organisms was given by Gulge in 1838, who observed the presence of a microsporidian (later known as *Glugea anomala*) in skin tumours present in three-spined stickleback fish (*Gasterosteus aculeatus*). However, the first identification of microsporidiosis is considered to be in 1857 with the detection of *Nosema bombycis* as the causative agent of an important disease in the European silkworm (*Bombyx mori*) (Nägeli, 1857), later referred as "pebrine disease", which almost destroyed the production of silk in France and Italy in the 19th century (Franzen, 2008). The study of Microsporidia gained momentum during the AIDS pandemic after *Enterocytozoon bieneusi* was detected in the enterocytes of an affected person as it was causing life-threating diarrhoea (Desportes *et al.*, 1985). Currently, there are over 1400 species of microsporidian described, and new species are discovered regularly (Szumowski & Troemel, 2015). Most species infect arthropods and fish but all five classes of vertebrates and nearly all invertebrates, including protists such as ciliates and gregarines, have been reported to be infected by microsporidians (Wittner, 1999).

The classification of Microsporidia has been controversial due to some of their unique features, leading to repeated changes in phylogenetic position over the years (Figure 1.2) (reviewed by Keeling, 2014). The first microsporidian to be named, *N. bombycis*, was thought to be a yeast-like organism and was placed in the Schizomycete clade (Nageli 1857). Based on their intracellular parasitic nature, the Microsporidia were later reclassified as Sporozoa, where it remained for many years with other unrelated groups. Their position within Sporozoa was narrowed to the Cnidosporidia, together with the Helicosporidia and Myxosporidia, because of their similar mechanisms of infection (Balbiani 1882, cited in Keeling 2014). Due to the absence of mitochondria in microscopy studies, microsporidians were suggested to be of an ancient lineage that had evolved before the origin of mitochondria, and their

cellular simplicity was interpreted as an ancestral primitive state (Cavalier-Smith 1983, cited in Keeling 2014). Microsporidia were then classified with other "amitochondriate" eukaryotes as Archezoa, and further analysis of their SSUr RNA supported their position as the deepest branch of eukaryotes (Vossbrink et al., 1987). Analysis of protein coding genes suggested that microsporidians are, in fact, related to fungi (Edlind et al., 1996) and phylogenomic analyses place them as the earliest diverging fungi (Capella-Gutiérrez et al., 2012). Studies of their HSP70 and other mitochondrial-like genes demonstrated that microsporidia were not ancestrally amitochondriate, but instead they have reduced mitochondrial remnants known as mitosomes (Williams et al., 2002). However, not all mitochondrial-derived proteins are functional, and microsporidians use nucleotide transport proteins to acquire ATP from their hosts (Dean et al., 2018).

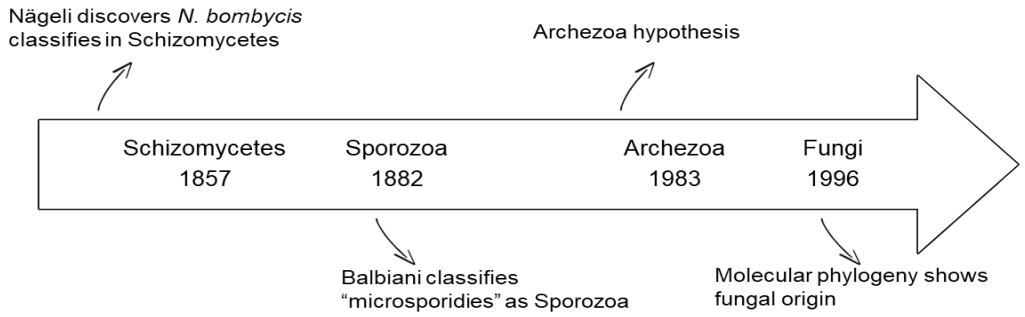

Figure 1.2. Timeline of the changing taxonomic position of Microsporidia (modified from Keeling, 2009).

Microsporidia possess two distinct life stages, a vegetative or multiplicative stage and a productive or infective stage (Vávra & Larsson, 2014) (Figure 1.3). Germination occurs when the contents of the microsporidian spore (sporoplasm) are injected on to or into the host cell, through a specialised extension called the polar tube (Keohane & Weiss, 1999). . After piercing the target, the sporoplasm passes through the tube and is either delivered on to the surface of the host cell or into the host cytoplasm, the latter avoids the extracellular defences of the host (Keeling, 2009). Two developmental stages are recognised within the host cell cytoplasm: the merogonic, or proliferative, and the sporogonic, or spore developing, phases (Cali & Takvorian, 2014). During merogony the sporoplasm develops into a meront which can be transported to other sites within the body of the host and starts multiplying

within the infected cell creating a primary infection. Sporogony involves the conversion of meronts into sporonts, cells that produce the sporoblasts and subsequently mature spores. Microsporidia lyse cells to exit their host, but another mechanism has been proposed for certain species that does not cause the cells to burst. Instead, they exit through a non-damaging mechanism that involves restructuring the host-cell's cytoskeleton with the mobilization of actin and reorganization of the terminal web, a structure that may be a barrier to the parasite's exit (Estes *et al.*, 2011). Mature spores are released from the host into the environment or to other hosts but can survive outside a host for several years (Vávra & Larsson, 2014).

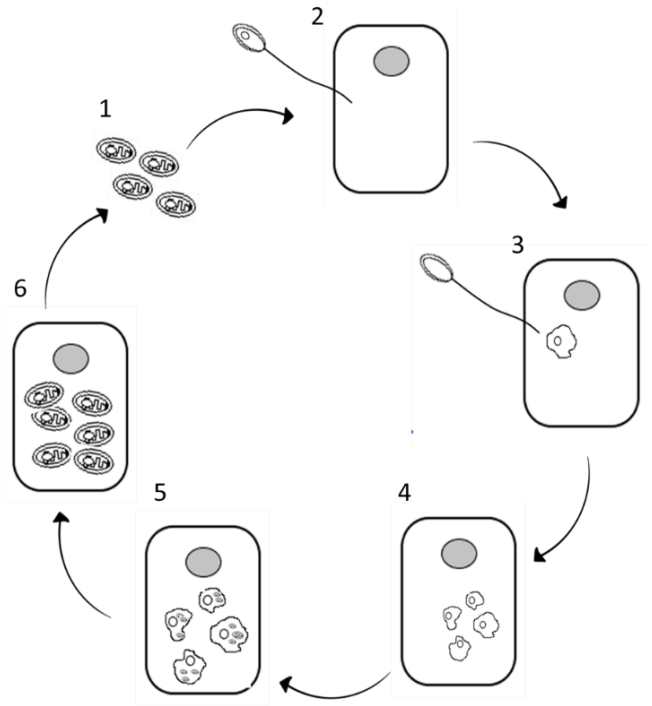

Figure 1.3. Diagram of the general life cycle of microsporidia. (1) Spores are free in the environment in an "inactive" stage. (2) When a suitable host is present and conditions are optimal, the living spore ejects the polar tube and pierces the target host cell. (3) The sporoplasm passes through the polar tube to the host cell. (4) Inside the host cell the sporoplasm undergoes extensive multiplication either by merogony (binary fission) or schizogony (multiple fission). (5) After merogony, sporogony occurs and new spores are produced. (6) Once the spores mature, these leave the cell, mostly through the lysis of the host cell, and new spores are free to infect again.

1.3.2 The structure of microsporidians

1.3.2.1 The spore

The microsporida life cycle starts and ends with the spore (Vàvra & Larsson, 2014) (Figure 1.3). These are highly compact structures that range in size from 1 to 40 µm in length (Williams, 2009). Typically, spores from the same microsporidian species have a similar size range but there are some genera (e.g. *Pleistophora* or *Heterosporis*) that produce macro- and microspores which differ in size and the numbers of polar tubule turns in the spore wall (Lom & Nielsen, 2003). In addition, a single species can produce more than one spore type that are distinct physiologically and structurally and can be the result different developmental cycles occurring in a single host or various host species (Vávra & Lukeš, 2013). For instance, some species produce auto-infective spores that germinate immediately to infect the same host to spread the infection within an individual. Alternatively, other spores created in the same host are released into the environment where they can infect other individuals and other species.

The spore consists of a spore wall, cytoplasm, nucleus and an extrusion apparatus (Vávra & Lukeš, 2013; Williams, 2009) (Figure 1.4). An important feature of the spore for the resistance to the environment is the wall, which is composed of a protein-rich exospore and an inner endospore layer rich in α-chitin (Vàvra & Larsson, 2014). At the apex of the spore the endospore layer is thinner, and ejection of the polar tubule during germination occurs through rupture of this area (Bigliardi & Sacchi, 2001). Beneath the endospore the plasma membrane surrounds the sporoplasm (Bigliardi & Sacchi, 2001). The sporoplasm contains the nucleus, which can be single or binucleate (diplokaryon) (Vàvra & Larsson, 2014), and the cell cytoplasm (Williams, 2009). Within the cytoplasm is the ER and analogues of the Golgi apparatus (Williams, 2009). The secretory products, that ultimately will be part of the injection apparatus, and the spore case are processed through the classical endoplasmic reticulum-Golgi synthesis pathway (Vávra & Lukeš, 2013). However, mature microsporidia spores do not have the typical Golgi complex but instead have tubular networks of varicose appearance that display histochemical features equivalent to the Golgi apparatus (Beznoussenko *et al.*, 2007). More recently,

Takvorian *et al.* (2013) demonstrated evidence of Golgi-like activity in the sporoplasm in an organelle called the multi-layered interlaced network (MIN) and this is likely to maintain its integrity. Furthermore, the MIN is pulled through the everting polar tube and appears to deposit its dense contents on the surface of the sporoplasm within minutes of spore discharge thickening the parasite's plasma membrane. The ER is seen as strands of polyribosomes that are especially prominent around the nucleus in young spores (Vàvra & Larsson, 2014).

The infectious apparatus is the defining characteristic of all microsporidia and comprises the polar tube or polar filament, polar sac-anchoring disk complex, the polaroplast and posterior vacuole (Vávra & Larsson, 2014). The polar filament is a hollow, multi-layered structure, with a very narrow diameter (0.1 to 0.2 μm) (Franzen, 2004; Yang *et al.*, 2018). It is tightly coiled around the periphery of the sporoplasm and is attached to the inside of the anchoring dish at the anterior pole of the spores (Weiss, 2001). The polaroplast is a system of membrane-limited cavities divided into an anterior (lamellar) and posterior (vesicular) part (Bigliardi & Sacchi, 2001). The posterior vacuole is a membrane-bound organelle that occupies the posterior pole of the spore and takes up more than one half of its volume (Vávra & Larsson, 2014). It is included in the infectious apparatus components because it swells before germination and creates the necessary pressure for the polar tubule to be extruded (Xu & Weiss, 2005). Triggers of spore germination vary widely as a result of the organisms' adaptations to their host but regardless of the stimulus that promotes germination, all respond to an increase in intrasporal osmotic pressure. By increasing the osmotic pressure there is an influx of water together with the swelling of the polaroplast and posterior vacuole that results in polar tube ejection (Xu & Weiss, 2005).

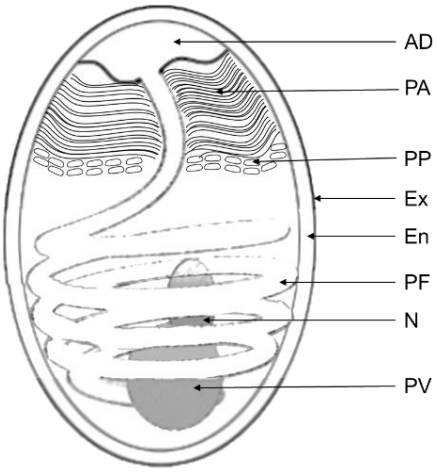

Figure 1.4. Schematic representation of microsporidian spore. The spore wall is composed of an electron-dense exospore (Ex), a thick electron-lucent endospore (En), and a plasma membrane between the endospore and the cytoplasm. The infectious apparatus consists of the coiled polar tube (PF) (the number of coils depends on the particular species) terminating at the apical part of the spore in an anchoring disk (AD), the posterior vacuole (PV), the posterior polaroplast (PP) and anterior polaroplast (PA). Other contents of the sporoplasm include the ribosomes and the nucleus (N).

1.3.2.2 Meront

In permissive host cells the sporoplasms become meronts and a stage of growth and division begins that varies between microsporidian species. Most microsporidian develop in direct contact with the host cell cytoplasm, not within a host phagocytic vacuole as many other intracellular parasites do, but some species induce the formation of a surrounding membrane at an early stage of infection known as the parasitophorous vacuole (Franzen, 2004). At this stage microsporidia often induce significant changes to the host, although they may be not obviously detrimental (Keeling & Fast, 2002). Meronts proliferate by repeated binary or multiple fission or by plasmotomy. They may contain one or more nuclei, and when more nuclei are present, they may be separate or in a diplokaryotic arrangement.

1.3.2.3 Sporont

Transition between merogony and sporogony is characterised by the spore wall material deposits in the plasma membrane, which are only detectable by TEM (Vàvra & Larsson, 2014). The onset of sporogony is marked in some species by the separation of diplokaryotic nuclei and in others by meiosis, although synaptonemal

complexes have been observed in all life stages of some microsporidian. Morphological features are more consistent indicators of sporogony and include a thickening of the plasma membrane (due to the accumulation of electron-dense material) and increased amounts of ER and ribosomes. Both the ER and ribosomes change morphology throughout sporogony; the ER becomes highly ordered and the ribosomes increasingly form arrays attached to the ER, known as polyribosomes. Although sporogony can occur in direct contact with the host cytoplasm, some species produce a sporophorous vesicle in which the sporonts develop. In most species, this stage of the life cycle is also accompanied by some degree of division, although the number of sporoblasts (presporal cells) produced varies among species from two (bisporous) to many (polysporous). Following division, the extrusion apparatus (including the polar filament, polaroplast, and posterior vacuole) begins to develop. As the extrusion apparatus nears complete formation and the sporoblasts approach maturity, the cells decrease in size and the chitinous endospore layer develops. Once complete, the mature spores are released (Vàvra & Larsson, 2014).

1.3.3 The importance of Microsporidia in fish and the aquaculture industry

Currently, there are over 200 known genera of Microsporidia (Becnel *et al.*, 2014) and they are one of the most frequently observed parasites of both invertebrates and vertebrates, with about 1300 to 1500 species described. (Vávra & Lukeš, 2013). Over 80 genera of microsporidian are known to infect aquatic organisms (Stentiford *et al.*, 2013) and the second most common host, after arthropods, are fish (Lom, 2002).

In fish, about 120 species of microsporidian have been described and several of these are known to have a negative impact on fish health (Kent *et al.*, 2014). Microsporidia are considered to be secondary opportunistic agents. However, this is not always true for microsporidian infecting aquatic species as there are various examples of them acting as primary pathogens. For instance, the decline in wild populations of the American smelt (*Osmerus mordax*) (Haley, 1954) was attributed to microsporidia. In commercial aquaculture, microsporidia have been reported as serious, economically important pathogens. Marine shrimp (*Penaeus monodon*) farms in Southeast Asia are affected by *Enterocytozoon hepatopenaei* and associated

with considerable reduction in growth and increased mortality (Tang *et al.*, 2015). *Enterospora nucleophila* has been associated with significant mortalities and decreased growth in gilthead sea bream (*Sparus aurata*) (Palenzuela *et al.*, 2014). *Nucleospora cyclopteri* has been linked with severe systemic infections and high mortalities (65%) in affected farmed lumpsucker (*Cyclopterus lumpus*) (Alarcón *et al.*, 2016). In cultured salmonids, four microsporidian species have been associated with mortalities and disease: *Loma salmonae* causing severe gill damage in coho salmon (*Oncorhynchus kisutch*) (Kent *et al.*, 1989) and chinook salmon (*Oncorhynchus tshawytscha*) (Kent *et al.*, 1995); *Nucleospora salmonis* infecting hematopoietic cells leading to a leukaemia-like condition (Hedrick *et al.*, 1990) in multiple salmonid species (El Alaoui *et al.*, 2006); *Desmozoon lepeophtherii* (syn. *Paranucleospora theridion*) (Nylund *et al.*, 2010) and one unnamed microsporidian associated with encephalitis in Atlantic salmon (Brocklebank *et al.*, 1999) and the other forming xenomas (hypertrophic host cells with the accumulation of different microsporidian developmental stages) within the cytoplasm of cells in the internal organs (Drinan *et al.*, 1992). Among the species mentioned above, *L. salmonae* has been the most studied and problematic pathogen with associated mortalities in farmed chinook salmon between 3-13% to more than 30% in some farm sites (Beaman *et al.*, 1999; Becker & Speare, 2007), and infections being more severe in fish close to market size (Beaman *et al.*, 1999). Even though microsporidian infections are known to cause important losses for the aquaculture industry, there are considerable knowledge gaps relating to the host's immune response to the parasite, the parasite's biology, the pathogenesis and how to control it (Rodriguez-Tovar *et al.*, 2011).

1.3.4 *Desmozoon lepeophtherii* as a fish pathogen

The microsporidian *D. lepeophtherii* was first discovered and described in the salmon louse (*Lepeophtheirus salmonis*) while looking for potential biological controls (Freeman, 2002). Sea lice are ectoparasitic copepod crustaceans (*Caligidae, Siphonostomatoida*) that are one of the key disease challenges for Atlantic salmon aquaculture worldwide. The microsporidian's gene sequence was closely related to other fish microsporidian and it was presumed that this microsporidian could

possibly infect Atlantic salmon. Sea lice, infected with *D. lepeophtherii* ,were collected from six salmon originating from salmon farms in Scotland anddifferent salmon organs, including the kidney, liver, heart, gill and peripheral blood, were subject to a nested PCR for *D. lepeophtherii* and five out of six fish were found to be positive for the microsporidian. The PCR product sequences had a 99.4% similarity to that of the microsporidian within the sea lice. The molecular identity of the partial ribosomal DNA sequence obtained from microsporidia within the sea lice was later published (Freeman *et al.,* 2003) (GenBank AJ431366) and molecular phylogeny placed it within the clade containing the family *Enterocytozoonidae*.

A description of the parasite's ultrastructure, together with the name *Desmozoon lepeophtherii,* was later given by Freeman and Sommerville in 2009. Differences in the original sequences between the salmon and louse microsporidian (Freeman, 2002) made the authors re-sequence the microsporidian from the sea louse (Freeman & Sommerville, 2011). The new sequence differed in 9 of the 1411 bases stated for the original sea louse microsporidian sequence (Freeman & Sommerville, 2009). Conversely, sequences obtained for the microsporidian infecting Atlantic salmon aligned 100% with the new sequence from the sea lice derived microsporidian. Again in 2009, but prior to the first naming of *D. lepeophtherii* in a scientific journal, there was a non-peer reviewed publication referring to a microsporidian parasite infecting both sea lice and Atlantic salmon named *Paranucleospora theridion* (Nylund *et al.*, 2009). However, this name was published with no associated description of the parasite or intention to name a novel species (Freeman & Sommerville, 2011). Later, Nylund *et al.* (2010) published a detailed description of the microsporidian found in Atlantic salmon and sea louse. In addition, the authors stated in their publication that *P. theridion* was the correct name for the parasite.

Controversy concerning the parasite's name remains. According to the Code of Zoology "Criteria of Publication", the rules of priority would consider *P. theridion* as the appropriate term for the microsporidian (Kent *et al,* 2014). However, the paper published by Nylund *et al.* (2009) was not peer-reviewed (Freeman & Sommerville, 2011) and provided no formal description of the microsporidian (absence of diagnosis or indication of type of material used) (Kent *et al,* 2014). Therefore,

Desmozoon lepeophtherii is the generic name that met the criteria defined by the Code of Zoological Nomenclature (Becnel *et al.*, 2014) and is registered as the senior name on the World Register of Marine Species (WoRMS) with *Paranucleospora theridion* referred as a junior synonymised taxon (Freeman & Sommerville, 2011).

1.3.5 Transmission of *D. lepeophtherii*

How sea lice become infected with *D. lepeophtherii* is not known. Økland (2012) studied the intensity and prevalence of *D. lepeophtherii* in different life stages of the sea louse using samples collected from salmon farms in Norway with real-time RT-PCR and light and electron microscopy. The microsporidian was detected in salmon-feeding stages (chalimus 1 onwards) only and not in the planktonic stages (nauplii and copepodid) stages, suggesting that sea lice only become infected when feeding on infected salmon. Sveen *et al.* (2012) studied the infection dynamics of *D. lepeophtherii* using real-time RT-PCR to screen two populations of salmon transferred to sea water during different seasons and found the microsporidian in the gills and kidney of the salmon and also the sea lice infecting the salmon. The gills of the population transferred to sea in spring became infected with *D. lepeophtherii* early after transfer, and this infection was also detected in kidney several weeks later. When sea lice started to settle on the salmon population, they became infected with the parasite. The population transferred to sea in the autumn only had detectable levels of the parasite in the gills, but not in the kidneys. The sea lice on these fish had no detectable *D. lepeophtherii*. The authors suggested that cold temperatures in autumn and winter (≤ 10C°) would arrest the parasite's development and therefore auto-infective spores did not infect other tissues. Furthermore, the lack of the auto-infective spores would impede the development of the environmental spores, which infect the nucleus of the epithelial cells of the skin, and therefore the fish were not infectious to feeding sea lice.

Vertical transmission of *D. lepeophtherii* on sea lice was considered by Nylund *et al.* (2010) after finding the egg strings of *L. salmonis* to be highly positive for *P. theridion* by real time PCR. However, it was not possible to detect the parasite in the sea louse by TEM or light microscopy. Although vertical transmission of

Microsporidia is the main route of infection in various aquatic arthropods hosts, it is often the case that the targeted cell type may actually be connective tissue cells supporting the ovary rather than the cytoplasm of the oocytes (Stentiford & Dunn, 2014). Later studies have found *D. lepeophtherii* in the gonadal segment of lice, but infections occurred in the connective tissue of gonad whilst the oocytes were free of infection (Økland, 2012).

The route of infection in salmon is similarly still unknown. *Desmozoon lepeophtherii* is the first microsporidian that has been demonstrated to occur in a vertebrate and invertebrate host from the family Enterocytozoonidae (Nylund *et al.*, 2010). It is not known if the parasite can be transmitted directly fish to fish, fish to louse, louse to louse or louse to fish. Presence of lice in the salmon population does not seem to be a requisite for the parasite to infect fish (Sveen *et al.*, 2012), but this does not exclude the possibility that waterborne spores previously released by the lice could infect salmon. Sveen *et al.* (2012) demonstrated that *D. lepeophtherii* infects the gills first and then infections spread to the kidney (Sveen *et al.*, 2012). The presence of *D. lepeophtherii* spores within polymorphonuclear leucocytes and macrophages has been confirmed (Nylund *et al.*, 2010; Nylund *et al.*, 2011; Weli *et al.*, 2017) and these phagocytic cells might be a mechanism for transporting auto-infective spores of the microsporidian to different tissues (Sveen *et al.*, 2012). In addition, developmental stages within polymorphonuclear leucocytes have been observed by Nylund *et al.* (2011) using TEM, and within macrophages using ISH (Weli *et al.*, 2017). Therefore, these immune cells could have an essential role in spore development, rather than just acting as a transport system. Release of microsporidian spores into the environment seems to occur mainly through gills but other tissues such as skin and gut epithelium can also be heavily infected with *D. lepeophtherii* spores and are potential locations for microsporidian release (Nylund *et al.*, 2010; Weli *et al.*, 2017).

1.3.6 Life cycle of *Desmozoon lepeophtherii*

1.3.6.1 Life cycle in Atlantic salmon

In Atlantic salmon, Nylund *et al.* (2010) described the presence of two developmental cycles that lead to two different types of spores: (1) autoinfective and (2) environmental (Figure 1.5a & b).

Developmental cycle I occurs in direct contact with the cytoplasm of polymorphonuclear leucocytes, macrophages, epithelial cells of the gills and skin, and endothelial cells of blood vessels within most tissues. The first merogonial stages are surrounded by a unit membrane and are small (0.8-1.8 μm in diameter). These contain a diplokaryotic nucleus, abundant ribosomes and a single prominent ER. Multiplication of dyplokaria results in plasmodia (1.9-4.6 μm in length) with up to 12 dyplokaria observed and up to three different plasmodia in each infected cell. The development of the plasmodia is surrounded by host mitochondria and occurs juxtanuclear, sometimes in an invagination. Transition from merogony to sporogony is not accompanied by the deposition of dense material on its surface, as commonly seen in other microsporidian (Cali & Takvorian, 2014). Instead, sporonts can be distinguished by the presence of dense disks associated with the formation of the polar tube (Nylund *et al.*, 2010). Sporonts are 1.7-5.5 μm in length and the diplokaryotic nuclei can be surrounded by short zones of nuclear apposition. The precursors of the polar tubule mainly develop in the centre of the sporonts. Up to 14 sporoblasts can be observed within a sporogonial plasmodium. Schizogonic division produces diplokaryotic sporoblasts, which will develop into small (0.9–1.2 μm in diameter) spherical/oval shaped spores. Up to 30 spores and sporoblasts are present in a single cell. These have a thin-wall and short polar tube and are thought to spread the infection through host and are therefore termed auto-infective spores (Nylund *et al.*, 2010).

Developmental cycle II takes place in the nucleus of epithelial cells of the gills and skin, although spores have been seen in the chloride cells of the gills (Nylund *et al.*, 2010) and within the nuclei of gut epithelial cells (Weli *et al.*, 2017). Similar to the previous developmental cycle, the first observed structure is a meront in direct contact with the cell nucleoplasm that contains a single diplokaryotic nucleus and is

surrounded by a unit membrane. The meront contains abundant ribosomes and a single ER. A maximum of two dyplokaria are present in a single meront. Sporogonic stages are characterised by the presence of dense barrel shaped elements measuring about 80 nm in diameter and a polar sac primordium. Again, no deposition in the surface of the plasmalemma is observed in the transition from meronts. Sporogonic stages with polar tube precursors develop two sets of extrusion apparatus before division, giving rise to two sporoblasts. The resultant ellipsoidal spores from the sporoblasts mostly appear in singles or pairs. These products are thought to be environmental spores because they are larger (2.4-2.7μm long x 2.0-2.17 μm wide), possess a thicker wall (exospore of 28 nm and endospore of 130 nm) and contain a longer polar tube.

1.3.6.2 Life cycle in sea lice

Desmozoon lepeophtherii was first discovered forming xenomas in the basal lamina of the epidermal layer of the sea louse copepod *L. salmonis* (Freeman, 2002). This basal portion of the epidermal layer is composed of a glycocalyx that contains various epidermal cells including epithelial cells and desmocytes. Due to the extreme hypertrophy of the cells containing xenomas the authors were unable to discern the exact type of cells infected but based on TEM they hypothesized that desmocytes were the primary cell type infected. Therefore, the genus name *Desmozoon* refers to the type of cell infected, the desmocytes, which encompasses any elongated interstitial cell (i.e. fibrocyte), whilst the specific name *lepeophtherii* refers to the parasite's host, *L. salmonis*. Further studies have demonstrated the presence of the parasite in desmocytes (fibroblasts/fibrocytes), epithelial cells, gonadal cells, satellite cells, haemocytes and tegmental gland cells of the sea louse (Nylund *et al.*, 2010; Økland, 2012). Xenomas seem to be more pronounced in the cephalothorax of the louse but can also be seen in the gonadal segment (near the gut), mouth tubule, lumen of the gut and other extremities (Økland, 2012), and these contain abundant spores at different stages of developmental (Freeman & Sommerville, 2009).

The development of *D. lepeophtherii* in sea lice has been described by Freeman *et al*. (2003), Nylund *et al.* (2010) and Økland (2012) (Figure 1.5c). The earliest stage detected in the louse are diplokaryotic meronts within the cytoplasm of

haemocytes. Although meronts can be observed alone in infected cells, they are normally associated with the presence of all other developmental stages within the xenoma. Merogonial stages are spherical and have one or two dyplokaria. The diplokaryotic nuclei are rounded and contain a small amount of ER and a moderate number of ribosomes. The merogonial stages divide through schizogony and form a multilobed merogonial plasmodium (9 μm in diameter) with several dyplokaria. There is fission of dyplokaria during the merogonial stage and early sporonts stages can contain diplokaryotic nuclei or two closely arranged monokarya. Transition between merogony and sporogony is recognised by the presence of electron dense material in the surface of the plasma membrane. Sporonts are round or multi-lobed (2.7-5.7 μm in length) and are actively dividing during the first stage of their development. In later stages sporonts are unicellular cells with a single monokaryon, appearing smaller in size (2.0-2.7 μm length) and with prominent ER, together with early elements of developing extrusion apparatus. Sporonts stop dividing in advanced stages with the formation of the polar tubule, anchoring disk and polar cap, which are considered sporoblasts.

The spores that develop in sea lice are round to ovoid with a single nucleus (Freeman & Sommerville, 2009). In fresh smears the spores are 2.4 μm in diameter but can appear slightly smaller in ultrathin sections (1.6-2 μm) (Nylund *et al.*, 2010). The endospore is relatively thick, 150-250 nm, and surrounded by a thinner, electron dense exospore measuring 35-40 nm (Freeman & Sommerville, 2009). The polar tube has 5-8 turns, normally in a double coil, and a diameter of 65-85 nm. An anomalous, different type of spores of 5 μm in diameter, containing several disorganized extrusion apparatuses, are seen occasionally and are thought to be the result of anomalous development (Nylund *et al.*, 2010).

In salmon all developmental stages of *D. lepeophtherii* are diplokaryotic, whereas in the sea lice they vary between mono- and diplokaryotic suggesting that sexual processes such as meiosis and karyogamy may occur (Økland, 2012). For this reason, Nylund *et al.* (2010) considered sea lice to be the definitive host of *D. lepeophtherii* and salmon an alternate host but the true identity of the sea louse or salmon as definitive or intermediate hosts still needs to be elucidated. Økland, (2012)

suggested that several spores would infect the sea lice cells concurrently, transferring their diploid monokaryon sporpoplasm to the host-cell cytoplasm. During merogony, fusion of sporoplasm would occur with the formation of meronts with two haploid diplokarya. The diplokarya proliferate through mitotic division. In early sporonts, when the diplokarya dissociate and the nuclear membrane disappears, diploid monokarya are produced during the formation of a new nuclear membrane. Schizogony will then result in late sporonts containing diploid monokarya and then the development of diploid monokaryotic sporoblasts and spores completes the cycle. However, sexual reproduction in the sea louse still needs to be demonstrated.

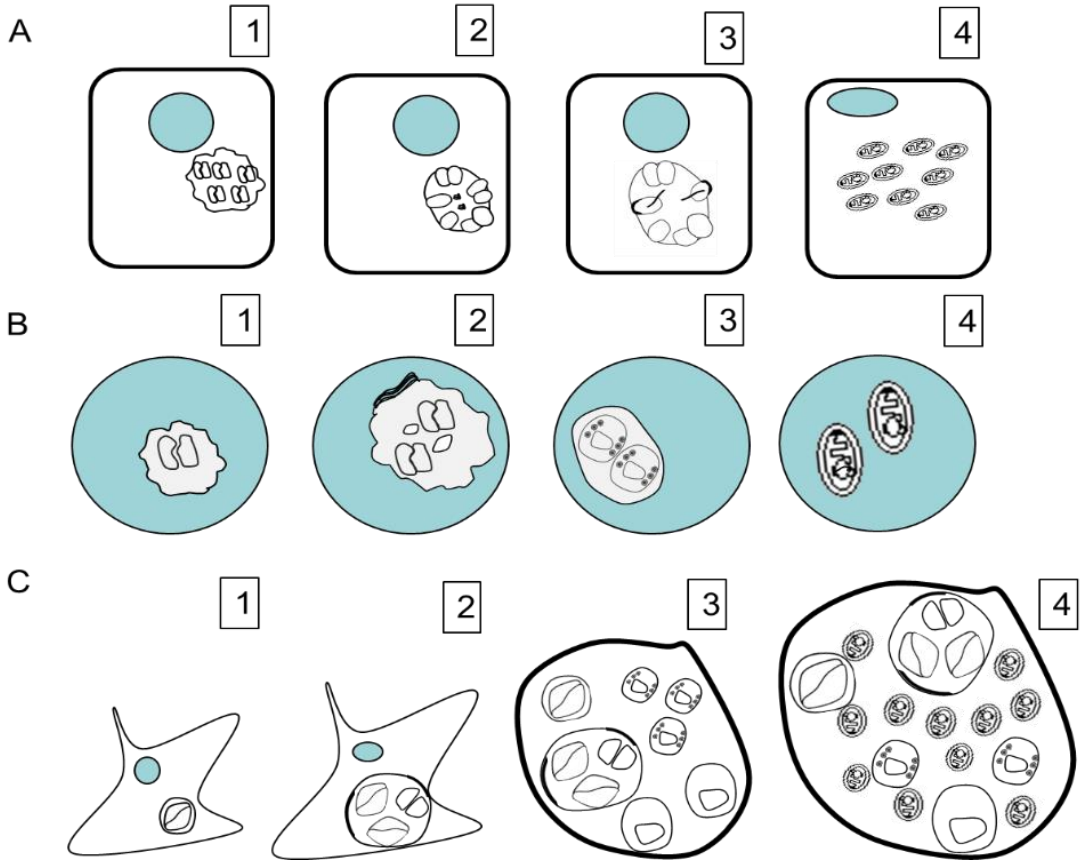

Figure 1.5. Developmental cycles of *Desmozoon lepeophtherii* in Atlantic salmon and sea lice. Host cell nucleus stained blue. (A) Developmental cycle I in salmon cells. (1) Merogonial plasmodium after multiplication of the diplokaryotic nuclei. (2) Sporogonial plasmodium with three diplokarya and dense disks in the centre associated with the formation with the polar tube. (3) Late sporonts before schizogony showing peripheral anchoring discs in polar caps. (4) Schizogonic division produces diplokaryotic sporoblasts, which will result in small spherical/oval spores. (B) Developmental cycle II in salmon nucleus of epithelial cells of gill, skin and gastrointestinal tract. (1) Meront containing a single diplokaryotic nucleus and surrounded by a unit membrane. (2) Sporogonic stages with rough endoplasmic reticulum and with the presence of dense barrel shaped elements (3) Sporobolast with two sets of extrusion apparatus before division. (4) The resultant ellipsoidal spores from the sporoblasts mostly appear in singles or pairs. (C) Developmental cycle in sea lice (1) Presence of diplokaryotic meronts in direct contact within the cell cytoplasm. (2) The merogonial stages divide through schizogony and form a multilobed merogonial plasmodia. Transition between merogony and sporogony is recognised by the presence of the dense material in the surface of the plasma membrane. There is fission of dyplokaria during the merogonial stage and early sporonts stages can contain diplokaryotic nuclei or two closely arranged monokarya. (3) Various developmental stages present together in a hypertrophied cell (formation of xenoma). Early monokaryotic sporonts and more advance stages containing polar tube primordium. (4) Various developmental stages including newly formed spores with a single nucleus.

1.3.7 Study of host-pathogen interactions of *D. lepeophtherii*

Knowledge of the interaction between a pathogen and its host is key to understanding the disease process and to develop treatment strategies to control the infectious agent (Welch, 2015). Studies *in vivo*, using animal-based infection models are frequently used to study host-pathogen interactions in more detail, such as routes of infection by the pathogen and pathogenesis of the disease. An *in vivo* experimental infection with *D. lepeophtherii* and its hosts (sea lice and Atlantic salmon) was documented by Freeman in 2002. The author found that *D. lepeophtherii* spores injected into the midgut of naïve *L. salmonis* did not result in infection of the lice. Similarly, Atlantic salmon challenged with *D. lepeophtherii* spores isolated from lice, placed into the water tank with the fish did not cause infection or disease in the fish. An unsuitable route of infection, the use of potentially non-viable spores, or the fact that the louse needed an alternate host to become infected were the reasons given by the author why the experimental infections were unsuccessful. Conversely, Sveen et al. (2012) claimed that a few Atlantic salmon that received infected sea lice in an experiment were infected by *D. lepeophtherii*. However, no further information relating to this is available in the literature.

Another approach to studying host-pathogen interactions involves the use of cell cultures derived from animal and insect tissues. Even though the use of *in vivo* experiments is still essential for understanding certain aspects of the host-pathogen interaction of microsporidia, *in vitro* studies are preferred over the use of live fish wherever possible (Schaeck et al., 2013). There are two types of cell cultures: primary and secondary. Primary cell cultures consist in short-lived cell types whilst secondary cultures are long-term cell lines. The use of tissue and cell cultures has been key in the study of intracellular parasites such as microsporidia (Gisder et al., 2011). Different applications of *in-vitro* cell systems in the research of microsporidia include the study of the life cycle, infectivity, evaluation of possible treatments or propagation of the spores in cell cultures for diagnostic purposes or further pathogenesis studies (Lallo et al., 2016; Monaghan et al., 2009). No reports of experimental infections with *D. lepeophtherii* within cell culture systems have been published.

1.3.8 Epidemiology of *D. lepeophtherii*

Desmozoon lepeophtherii is one of the most prevalent putative disease-associated agents detected by molecular methods in the gills of farmed populations of Atlantic salmon in Europe (Downes *et al.*, 2018; Steinum *et al.*, 2010). In addition, the parasite has been detected in sea lice (*Lepeophtheirus salmonis* and *Caligus elongatus*) (Nylund *et al.*, 2010), various species of wrasse (Steigen *et al.*, 2018) and in brown trout and rainbow trout (*Salmo trutta* and *Oncorhynchus mykiss*) (Nylund *et al.*, 2010).

A different genotype of *D. lepeophtherii* has been detected from lice *(L. salmonis*) infecting farmed Atlantic salmon in the Pacific Ocean with a partial ribosomal DNA sequence differing by 0.4% (Jones *et al.*, 2012) from the genotype obtained in Europe. Even though the latter studies did not detect the presence of *D. lepeophtherii* in the farmed salmon, more recent studies have demonstrated that the microsporidian is also highly prevalent in gills of Atlantic salmon and Pacific salmon farmed in the northeast Pacific (Laurin *et al.*, 2019) and different species of wild Pacific salmon (ICES Working Group, 2018; Thakur *et al.*, 2019).

Desmozoon lepeophtherii has been mostly associated with salmon in the marine stage of the cycle, whereas detection of the parasite in freshwater has been anecdotal. In Norway, Nylund *et al.* (2011) detected the parasite in the tissues of salmon in a smolt hatchery to which sea water was added but no pathology was associated. Results of a questionnaire produced by Hjeltnes *et al.* (2017) stated that *Desmozoon lepeophtherii* was ranked “the most important cause of health problems” in recirculation and flow-through hatcheries. However, no further studies regarding the potential importance of *D. lepeophtherii* in freshwater stages are available in the literature.

In Norway, *D. lepeophtherii* is present in all areas of salmon production but higher prevalence and densities of the parasite are seen in southern Norway (Nylund *et al.*, 2011). Sea temperatures above 10°C have been suggested to be necessary for the parasite to develop (Sveen *et al.*, 2012), and higher temperatures are normally

achieved in south and western Norway. This, and other risk factors for the development of *D. lepeophtherii* still need to be elucidated.

1.3.9 *Desmozoon lepeophtherii* and CGD

Desmozoon lepeophtherii was first detected in salmon tissue by conventional PCR in the kidney, liver, heart, gills and circulating blood cells from (clinically normal) farmed Atlantic salmon in Scotland (Freeman, 2002). On histological examination of the kidney there was moderate hyperplasia of the renal interstitium and numerous mitotic figures in immature leucocytes. The heart showed hyperplasia of myocardiocytes with occasional hypertrophy of myocardial nuclei. However, special stains failed to reveal any structure suggestive of microsporidian infection in the tissues examined under light microscopy. Furthermore, TEM of the PCR positive tissue did not reveal the presence of the microsporidian.

Nylund *et al.* (2010) were the first authors to implicate *D. lepeophtherii* as a gill pathogen. The authors detected the microsporidian using TEM in farmed Atlantic salmon suffering from gill disease. On gross examination, some of the fish used for the study had skin haemorrhages, loss of scales and slightly pale gills. According to the authors, the gill epithelium was hypertrophic, hyperplastic, necrotic and inflammatory cells were present. In other organs (kidney, heart, spleen, gut, and exocrine pancreas), inflammatory cells were also observed, and the presence of the microsporidian was confirmed by TEM, light microscopy and molecular methods. These authors also suggested that the parasite was associated with disease causing up to 80% mortality in certain marine salmon farms, but no further information was given about this. Later studies considered the possibile role of *D. lepeophtherii* in various diseases with a marked inflammatory cell response in salmon such as PGI, pancreas disease, heart and skeletal muscle inflammation and cardiomyopathy syndrome (Nylund *et al.*, 2011). However, high loads of the microsporidian were only associated with an increase in severity in PGI but no other diseases. Fish showed similar gross and histological changes to those described by Nylund *et al.* (2010). Darkening of the somatic muscle was noted for fish displaying high levels of *D. lepeophtherii* in other organs, but the presence of the microsporidian in muscle

was not reported. Developmental stages of the parasite were detected in blood vessel endothelial cells and the cytoplasm of leukocytes by TEM and the latter suggests the possibility of immunosuppression. Steinum at al. (2010) showed similar findings when studying the role of several organisms in PGI. *Desmozoon lepeophtherii* was highly prevalent in salmon farms in Norway but a considerable increase in the parasite load was noted when fish were suffering from clinical PGI. A significant correlation was also found between high loads of *D. lepeophtherii* and gill pathology (Pflaum, 2012).

In Scotland, *Desmozoon lepeophtherii* was associated with an outbreak of gill disease in farmed salmon with necrotic and proliferative pathology in the basal lamellar epithelial cells (referred as Malpighian cells in the study) (Matthews *et al.*, 2013). Similar pathology has been found in Ireland (Rodger *et al.*, 2011). However, the high prevalence of the microsporidian in healthy individuals and the, often, complex presentation of gill disease (Mitchell & Rodger, 2011) hinders the determination of the exact role of *D. lepeophtherii* with respect to a primary or secondary pathogen and further studies are necessary to elucidate this.

1.4 Conclusion

Gill disease is one of the most important causes of morbidity and mortality in the marine stage of Atlantic salmon. Complex gill disorder (CGD) is still being characterised but is a multifactorial and multi-aetiological disease that occurs mainly from late summer to early winter in Scotland. *Desmozoon lepeophtherii* is a microsporidian parasite that has been associated with CGD, however, the significance of *D. lepeophtherii* in CGD is still uncertain. Further studies are therefore required to elucidate the exact role and significance of *D. lepeophtherii* in gill disorders of farmed Atlantic salmon.

1.5 Aims and objectives

The central hypothesis underlying the research conducted for this PhD is that *D. lepeophtherii* contributes to the pathology associated with CGD.

The aim of this study was to gain a better understanding of the parasite *D. lepeophtherii* and its role in gill disease in farmed Atlantic salmon (*Salmo salar*) in Scotland. To achieve this, the following objectives were proposed:

- Culture the parasite *in vitro* using different cell lines to provide a tool for research and to allow study of different aspects of the parasite infection, such as its biology and the nature of host cell immune responses targeting the parasite.

- Perform a longitudinal study to 1) gain a better understanding of the prevalence status of *D. lepeophtherii* in Scotland, and that of other key agents thought to be involved in complex gill disorder such as *Ca.* B. cysticola and SGPV in Scottish salmon farms 2) elucidate the dynamics of *D. lepeophtherii* infection and its relationship with the presence gill pathology.

- Develop a sensitive and specific technique to detect the parasite in tissue sections under light microscopy.

Chapter 2 Culture of *Desmozoon lepeophtherii in-vitro*

2.1 Introduction

2.1.1 Use of cell lines for the study of microsporidia

The culture of microsporidia *in vitro* is an ideal method for the isolation, large-scale production and study of different aspects of these intracellular parasites, such as their life cycle (Couzinet *et al.*, 2000; Franzen *et al.*, 2005), kinetics of infection (Panek *et al.*, 2018), host cell immune response to the infection (Fischer *et al.*, 2008) or drug screening (Santiana *et al.*, 2016).

The first microsporidian to be cultured *in vitro* was *Nosema bombycis* in ovarian tube lining cells of silkworm (Trager, 1937). Subsequent work tended to focus on microsporidian species that infected economically important insects, such as *Nosema apis*, a microsporidium of the honeybee (Visvesvara, 2002). Interest in animal cell cultures started once microsporidia were found to be clinically important to humans (Desportes *et al.*, 1985). Until the 1990s, *Encephalocytozoon cuniculi* was the only microsporidium of mammalian origin that was culturable (Visvesvara, 2002), however various microsporidian species have since been successfully cultured in different laboratories (Lallo *et al.*, 2016; Visvesvara, 2002). Continuous cultures of microsporidian species are now available from research laboratories and the American Type Culture Collection (ATCC) repository, facilitating the obtention and study of these parasites (Molestina *et al.*, 2014).

The host specificity of microsporidia varies, and some species have been demonstrated to infect a wide range of hosts (reviewed by Monaghan *et al.*, 2009), including zoological groups different to that of their natural host. The lack of host specificity of some microsporidia seems to be more obvious using *in vitro* infection challenges (Monaghan *et al.*, 2011), as demonstrated from work on the well-studied microsporidium *Ancaliia algerae*, a microsporidian of mosquitoes (e.g. *Anopheles stephensi*) that has been successfully gown in mammal, insect and fish cell lines (Belkorchia *et al.*, 2008; Monaghan *et al.*, 2011).

2.1.2 Study of fish microsporidia *in vitro*

Research on fish microsporidia is less extensive than that existing for mammals or insect microsporidia, and this is reflected in the number of reports available relating to the culture of fish microsporidia *in vitro* (Monaghan *et al.*, 2009) (Table 2.1). Short-term primary cultures have been used to study the interaction of microsporidia spores with cells associated with the innate immune system of their host. These cultures tend to have been used within 48 h of isolation, with the aim of studying phagocytic and respiratory burst activities of isolated phagocytes (Leiro *et al.*, 1996). For example, Shaw *et al.* (2001) demonstrated that the phagocytic index of macrophages ingesting spores of *Loma salmonae,* an important microsporidian of pacific salmon, was higher in the macrophages of chinook salmon than those from Atlantic salmon, and suggested that the higher clearance of the parasite in Atlantic salmon was one reason why this species is less susceptible to infections with this microsporidia than chinook salmon.

Complete replication of the life cycle of certain economically important microsporidian species has been achieved in culture. For instance, when chinook salmon leucocytes infected with *Nucleospora salmonis* were incubated with uninfected leucocytes, the naïve cells became infected and continual passage of these onto new cultures of naïve leukocytes supported the growth of the microsporidium for almost a year *in vitro* (Wongtavatchai *et al.*, 1994; Wongtavatchai *et al.*, 1995). *Loma salmonae* has been shown to replicate *in vitro* in rainbow trout gill cells (RTG-1), with spores being produced after one week of infection through the formation of xenomas (McConnachie *et al.*, 2015). The microsporidian *Loma morhua* has also been grown *in vitro* in larval cod cells (GML-5), when culture conditions of the medium were modified using a pH shift from neutral to alkaline during the infection process (MacLeod *et al.*, 2018) Developmental stages of *Heterospora anguillarum* were observed using immunohistochemistry in the eel kidney epithelial cell (EK-1), but the formation of spores were not observed (Kou *et al.*, 1995 For most of the fish microsporidians successfully cultured *in vitro,* germination of the spores have occurred during the experimental process while in contact with the cell cultures, and without the previous artificial stimulation of the polar tube extrusion. However, a pH

shift from neutral to alkaline was necessary for the microsporidian *Loma morhua* to cause infection in larval cod cells (GML-5). Conditions to activate spores seem to be related to the adaptation of the microsporidian species with its host and environment, (reviewed by Weiss et al., 2014). According to MacLeod et al. (2018), the pH change represented a means of detecting passage acidic stomach to the alkaline small intestine for the microsporidian.

Table 2.1. Fish- associated microsporidia successfully cultured *in vitro.*

Microsporidia	**Infected host**	**Cell type used**	**Authors**
Heterosporis anguillarum	Japanese eel (*Anguilla japonica*)	EP-I (epithelial cell line persistently infected with *H. anguillarum* of elves of Japanese eel)	Kou *et al.* (1995)
Nucleospora salmonis	Chinook salmon	Primary culture of leukocytes from peripheral blood of chinook salmon and primary culture of epithelial-like cell from kidney of rainbow trout	Desportes-Livage *et al.* (1996); Wongtavatchai *et al.* (1994); Wongtavatchai *et al.* (1995)
Glugea sp.	Greater sand eel (*Hyperoplus lanceolatus*)	Derived cells from pooled newly hatched *Aedes albopictus* larvae and CHSE-214 (chinook salmon embryo)	Lores *et al.* (2003)
Pseudoloma neurophilia	Zebrafish	CCO (channel Catfish Ovary); SJD.1 (zebrafish caudal fin fibroblast); EPC (carp epithelioma); FHM (fathead minnow)	Watral *et al.* (2006) cited in Monaghan *et al.* (2009)
Heterosporis saurida	Lizardfish (*Saurida undosquamis*)	EK-1 (eel kidney epithelial cell); RK-13 (Rabbit kidney epithelial cell)	Kumar *et al.* (2014); Saleh *et al.* (2014)
Loma salmonae	Chinook salmon	RTgill-W1 (rainbow trout epithelial cells)	McConnachie *et al.* (2015)
Loma morhua	Atlantic cod (*Gadus morhua*)	GML-5 (larval cod cell lines)	MacLeod *et al.* (2018)

2.1.3 Aims and objectives

2.1.3.1 Aims

The life cycle of *D. lepeophtherii* has previously been described by Nylund *et al.* (2010). However, the routes and processes of infection have not been detailed either *in vitro* or *in vivo*, and all proposed pathways of infection are hypothetical. It has not been established whether the parasite is transmitted from the water column to fish, from the sea louse to fish, fish to fish, sea louse to sea louse, or sea louse to fish, as hypothesised.

An important step in understanding the biology of this parasite is the development of models for its propagation. Currently, no *in vitro* or *in vivo* model supporting *D. lepeophtherii* development is available. *Desmozoon lepeophtherii* has been detected in the gills of rainbow trout by PCR. Considering this, and the apparent lack of host-specificity exhibited by other microsporidian parasites (Monaghan *et al.*, 2011), the purpose of this study was to infect a rainbow trout gill epithelial cell line (RTgill-W1), a salmon head kidney 1 cell line (SHK-1), and a primary culture of salmon-isolated macrophages, with *D. lepeophtherii* spores isolated from sea lice collected from salmon farms.

Successful culture of the parasite *in vitro*, would enable crucial experiments to be performed to study different aspects of *D. lepeophtherii* biology and reproduction (*e.g.* temperature dependence, cell response studies, possible treatment effect, etc.) important for understanding the role of this parasite in gill disease.

2.2 Material and methods

2.2.1 Collection of sea louse derived microsporidian spores

Sea lice were isolated from infected Atlantic salmon collected from different salmon farms on the west coast of Scotland. Initial batches of sea lice were kindly provided by the health staff at a salmon production site and transported in sea water to Moredun Research Institute. Samples subsequent to 2017 were either sent by health staff by post or collected directly from the farm sites, but sea lice were placed in 0.85% sterile saline containing antibiotics (100 mg of penicillin/streptomycin and 2

μg gentamicin per mL^{-1}) (Sigma-Aldrich, Dorset, UK) as recommended by MacConechie *et al*. (2015) for transporting gills infected with *L. salmonae*. In addition, 5 μg mL^{-1} of Amphotericin B were added to the saline (Gibco, Invitrogen, Paisley, UK). The sea lice obtained prior to 2017 were rinsed twice with sterile saline, while batches of sea lice received after 2017 were also dipped into 0.5% Virkon® for 1 sec and then rinsed with sterile saline. Individual sea lice were then homogenised using a mortar and pestle, and spores were isolated following the technique described by McConnachie *et al.* (2015) (Figure 2.1). The homogenate was passed through a cell sieve with a 20 μM mesh (Pluriselect, Cambridge Bioscience, Cambridge, UK), the material was centrifuged at 350 x g for 10 min at 4°C and the pellet resuspended in 10 ml ultrapure water mixed with 10 ml of Percoll® (GE Healthcare, Little Chalfont, UK). The mixture was vortexed and then centrifuged at 1000 x g for 10 min at 4°C and the microsporidian spores in the homogenate formed a pellet at the bottom of the tube, while the cellular debris remaining in the supernatant was discarded. The pellet was resuspended in 2 ml of saline and centrifuged at 1000 x g for 10 min at 4°C. This step was repeated three times. The efficacy of the spore purification procedure was assessed by making smears on glass microscope slides, which were then stained with Giemsa. This was performed on the spore smears using a freshly prepared Giemsa solution (Sigma-Aldrich), by diluting 1:10 (v/v) in double distilled water and staining for 10 min. Smears were air-dried and slides were evaluated under the microscope.

An estimation of the spore obtained was made by counting the spores in a haemocytometer, making duplicate counts for each batch of spores prepared. Spore were kept at 4°C in sterile saline. Spores collected after 2017, were kept in sterile saline containing 100 mg of penicillin/streptomycin, 2 μg gentamicin, and 5 μg of Amphotericin B per mL^{-1}. Spores were used within 4 weeks of isolation to infect the cell cultures.

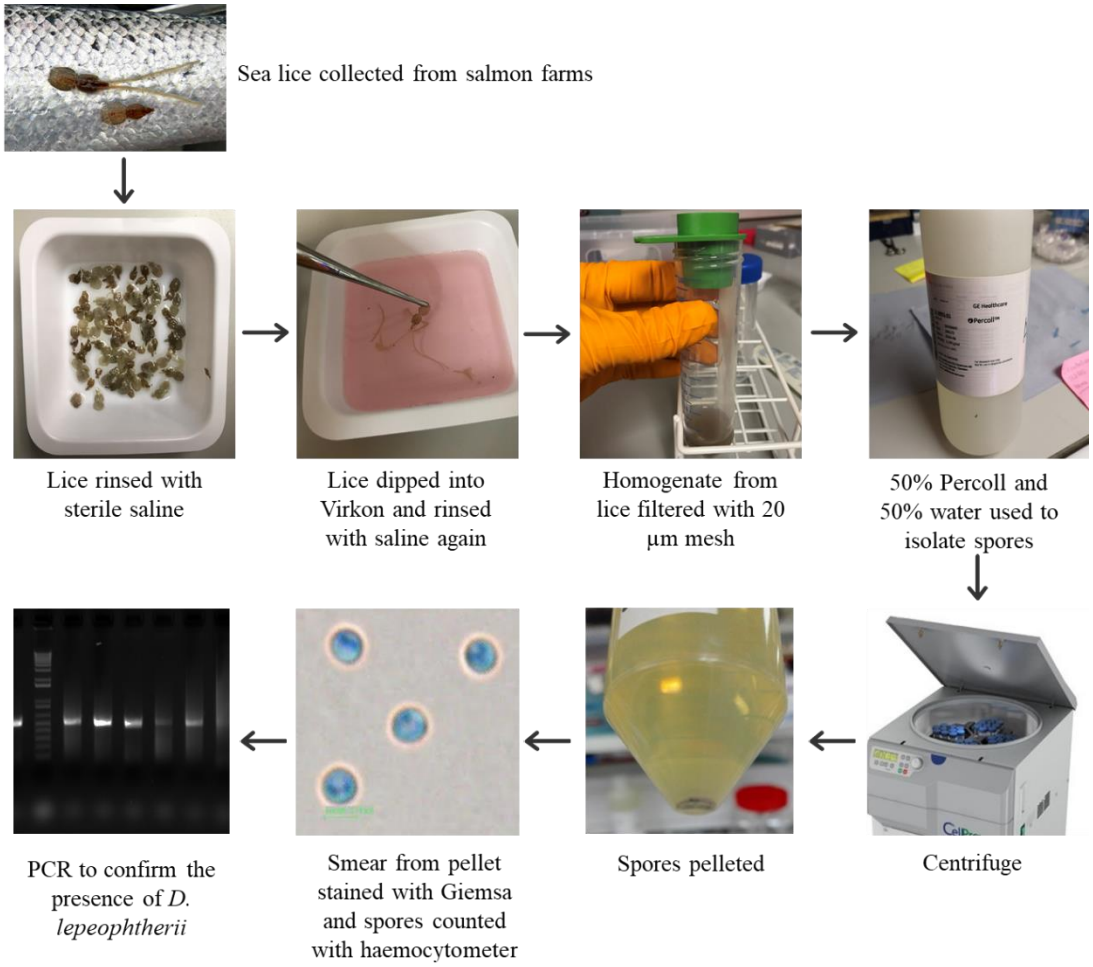

Figure 2.1. Flow diagram of spore extraction method based on Monaghan (2011) with modifications.

2.2.2 Transmission electron microscopy to detect *D. lepeophtherii*

Spores from the first two batches prepared were fixed in 3% glutaraldehyde in 0.1M sodium cacodylate buffer, pH 7.3, for 2 h, then washed 3 times in 0.1M sodium cacodylate buffer for 10 min. Preparations were post-fixed in 1% osmium tetroxide in 0.1M sodium cacodylate for 45 min, then washed as before. Samples were dehydrated sequentially in 50%, 70%, 90% and 100% ethanol (x3) for 15 min each, then twice in propylene oxide for 10-min each. Samples were subsequently embedded in TAAB 812 resin. Sections, 1 µm thick, were cut on a Leica Ultracut ultramicrotome (Leica Microsystems Ltd, Milton Keynes, UK), stained with toluidine blue, and viewed with a light microscope to select suitable areas for investigation. Ultrathin sections, 60 nm thick, were prepared from selected areas,

stained with uranyl acetate and lead citrate and viewed in a Jeol JEM-1400 transmission electron microscopy (Jeol Ltd., Welwyn, UK). Images were taken on a Gatan Orius CCD (Gatan Inc, Pleasanton, CA).

2.2.3 DNA extraction of spores

Extraction of DNA from the microsporidian spores was necessary to perform subsequent experiments in other chapters, such as molecular-based techniques for diagnosis and species differentiation. However, the presence of some of the components in the spore wall (e.g. chitin) increases the difficulty of successfully extracting parasite DNA. In this study, different methodologies to extract the microsporidian DNA using enzymatic and mechanical disruption of the spores were tested based on previous studies by Reabel (2012) with modifications. For Method 1 (enzymatic disruption), approximately 10^6 *D. lepeophtherii* spores, previously frozen at -20°C for 24h, were used and incubated with 80 µl filter-sterilized PBS, 100 µl of lysis buffer Qiagen tissue extraction kit (Qiagen, Hilden, Germany), 20 µl of Proteinase K (20 mg/ml) (Qiagen) and 0.4 U chitinase (Sigma-Aldrich, C6137) at 56°C for 5 h. Method 2 (enzymatic and mechanical disruption) involved the addition of glass beads (200 mg; 0.4 mm diameter, 40 mesh) to the mixture, which was then vortexed every 15 min for 1 min during the 2 first h. After performing Methods 1 or 2, the DNA was extracted following the manufacturer's instructions for the DNA Blood and tissue Kit (Qiagen). Method 3 involved DNA extraction from 10^6 *Desmozoon lepeophtherii* frozen spores, following manufacturer's instructions for the DNA Blood and tissue Kit (Qiagen).

The DNA concentration in each sample was determined using a Nanodrop 1000 Spectrophotometer (Thermo Scientific, Loughborough, UK). Spore identity was then verified by conventional PCR with the primers and conditions described below (Section 2.3.4). The quality of DNA was determined by calculating the A260/A280 ratio. A PCR was performed with all DNA extractions, plus the use of 10^6 *Desmozoon lepeophtherii* spores in order to corroborate if the boiling step in the PCR process was sufficient to extract genetic material from the spores as described by Nylund *et al.* (2011).

2.2.4 Polymerase chain reaction (PCR)

DNA from purified spores was used for the amplification of the 16S ribosomal small subunit rRNA gene (16S rRNA), partial sequence of *D. lepeophtherii* using primers Nuc-F1 (5'-GCG ATG ATC TGC TCT AGT TGT G-3') and Nuc-R2 (5'-GCT AAT CCT ACT CAT CCG TAA GC-3') (Sigma-Aldrich, Dorset, UK), which yielded a 969 base pair fragment from position 100 to 1091 (GenBank accession no. FJ594981) as described previously (Nylund *et al.*, 2010; Nylund *et al.*, 2011). Each PCR mixture consisted in 25 µl of GoTaq G2 Green Master Mix (Promega, Southampton, UK), (contains 400 µmol l^{-1} of each dATP, dGTP, dCTP and dTTP 3 mM $MgCl_2$), 5 µl of each primer (concentration 1 µmol l^{-1}), 5 µl of template and 10 µl of nuclease-free water. An additional negative control was used in each run. Amplification was performed at 95°C for 5 min; 35 cycles of 94°C for 30 s, 50°C for 45 s, 72°C for 2 min; followed by extension at 72°C for 10 min and a short storage at 4°C.

The PCR product obtained was visualized in a 1% agarose (Bioline, London, UK) gel stained with GelRed (Biotium, Fremont, CA) using 5 µl of PCR product per lane and a 100–1000 bp ladder (Promega) to determine the product size. The gel was run at 80 v for 70 min in 1 x TAE buffer (Sigma-Aldrich) and the obtained products were visualised with ultraviolet irradiation using a UV Transilluminator (Alpha imager 2200; Alpha Innotech, Exeter, UK).

2.2.5 Testing spore viability

The spores used for the various experiments performed in this chapter, were always used within 4 weeks of isolation. The viability of the spores was confirmed prior to performing each experiment by measuring the artificial extrusion of the polar tubule and testing the membrane integrity of the spore. To stimulate the extrusion of the polar tube, spores were incubated for 45 min at 21°C with 30% H_2O_2 (Sigma-Aldrich). A total of 100 spores were randomly counted under the microscope at 600x magnification and were categorized as extruded (visible polar filaments) or not extruded. To determine the membrane integrity, the uptake of dyes across the cell membrane was tested using the LIVE/DEAD BacLight Bacterial Viability Kit

(Invitrogen), which combines the SYTO® 9 green-fluorescent nucleic acid stain with the red-fluorescent nucleic acid stain, propidium iodide (PI). PI cannot cross plasma membranes and only damaged (non-viable) cells take up the dye and fluorescence red (Amigó *et al.*, 1995). An equal volume of SYTO® 9 and PI was combined in a microcentrifuge tube. Then, 3 µl of this mixture was added to 1 ml of the spore suspension (maximum 10^6 spores per mL^{-1}) and incubated for 15 min in the dark. A total of 5 µl of the stained spores were added to a slide and samples were immediately examined at 40× objective lens using an Olympus BX51 Fluorescence Microscope (KeyMed, Southend-on-Sea, UK) with a fluorescein isothiocyanate (FITC) filter (excitation range 480 to 490 nm) and a PI red filter (excitation range 493 to 636 nm), photomicrographs taken with an Olympus DP70 Digital Camera System (KeyMed) and analysed using analySiS® software (Soft Imaging System GmbH, Munster, Germany). Viability of two batches of spores was measured 4 weeks after isolation and subsequently after 12 weeks.

To compare the success of the techniques, a negative control of heat inactivated spores (95˚C in a water bath for 30 min) (Green *et al.*, 2000) or 2-year old frozen spores were used.

2.2.6 Fish and macrophage isolation

Atlantic salmon (50 g), obtained from Institute of Aquaculture, University of Stirling of were euthanized with an overdose of tricaine methanesulfonate (MS 222) (Pharmaq, Hampshire, UK). Head kidney macrophages was isolated according to Secombes (1990) with modifications. The head kidney of salmon was dissected aseptically and teased through a 100 µm nylon mesh into Leibovitz's medium (L-15) supplemented with 2% foetal bovine serum (FBS) and heparin (10 u/mL) and the suspension layered slowly onto a 34% 51% v/v Percoll gradient using a sterile Pasteur pipette. The gradient was then centrifuged at 400g for 25 min at 4˚C, the supernatant carefully removed and the band of cells at the 34-51% interface (~1 cm of space with the interface) collected with a sterile pipette. The cells were centrifuged for 7 min at 400g. The supernatant was removed, and the cell pellet gently resuspended in 50 mL of L-15 medium and centrifuged again 7 min at 400 g.

The supernatant was removed, and the pellet resuspended in L-15 (5 ml). An aliquot of the suspension was taken for macrophages enumeration, using 0.1% trypan blue (Gibco) to assess the viability of the macrophages.

2.2.7 Maintenance of fish cell lines

Rainbow trout epithelial cell (RTgill-W1) was obtained from the American Type Culture Collection (ATCC) and, the Atlantic salmon head kidney (SHK-1), was obtained from the European Collection of Authenticated Cell Cultures (ECACC). RTgill-W1 were grown in Leibovitz (L-15) medium with GlutaMax, supplemented with 10% FBS and SHK-1 cells were grown in L-15 medium with GlutaMax, supplemented with 2 μM L-glutamine and 40 μM mercaptoethanol and with 10% FBS. Cells were incubated in a 4% CO2 incubator at 18°C.

All the cells lines were cultured at 18°C in 75-cm^2 cell culture in non-vented flasks (Corning, Tewksburym, MA, USA). Cells were checked daily to assure they were healthy and not contaminated. All the chemicals and media were obtained from Gibco (UK). Propagation of cells was carried out as follows. Briefly, ~8-day old cells (when 80% of confluence was achieved) were washed x2 with Dulbecco's phosphate buffered saline (DPBS) and trypsinised for 2 min using x1 Trypsin / ethylenediaminetetraacetic acid (EDTA). The flasks were then tapped to remove the cells from the flask and mixed with aliquots of RTgill-W1 to split cells into a 1:3 ratio for RTgill-W1 and 1:2 for SHK-1.

2.2.8 Preliminary infections with *D. lepeophtherii* spores

Preliminary experiments were performed using the initial batches of spores isolated from sea lice obtained from fish farms between 2015 and 2016. In these experiments, spores were used within a week of isolation. The RTgill-W1 and SHK-1 cells were split 1:3 into 25-cm^2 non-vented flasks and maintained until a confluence of 70% was achieved. The spores were re-counted with a haemocytometer prior to use and an aliquot of spores at the desired concentration collected. The aliquot was centrifuged at 200 x g for 10 min, the supernatant removed, and the spores re-suspended in L-15/FBS. One flask of each cell line was used for infections and one

was used as a control. A ratio of at least 10:1 spore to cells was used in this experiment (Monaghan *et al*., 2011). The cells grew until a confluence of 70% was achieved, then approximately 2.5 x 10^7 spore were seeded into each of the flasks. In addition, 100 mg of penicillin/streptomycin, 2 µg gentamicin, and 2.5 µg of Amphotericin B per mL^{-1} were added to the L-15/FBS media of the infected flasks and controls. Flask were maintained for 2 weeks.

2.2.9 Control of bacteria in cell cultures

Due to the contamination of yeast and bacteria experienced during the preliminary trials in the flasks exposed to the microsporidia, more aseptic techniques were used in subsequent trials to transport lice, and for spore isolation (see Section 2.2.1). Experiments in which different concentrations of antibiotics were used, were performed to ensure that contamination could be controlled in future experiments. For this, RTgill-W1 and SHK-1 cells were grown in flasks until 80% cell confluence was obtained, after which the cells were harvested, counted using a haemocytometer and seeded onto 24-well plates (Corning). Three different concentration of antibiotics were tested in triplicates: 1x concentration (100 mg of penicillin/streptomycin, 2 µg gentamicin, and 2.5 µg of Amphotericin B per mL^{-1} of L15/FBS medium), 3x concentration and 5x concentration. The microsporidian spores (10^5) were then added into each well. Control wells contained the same quantity of antibiotics but no spores. Plates were maintained for 2 weeks at 12°C and without CO_2.

2.2.10 Infecting cell lines with *D. lepeophtherii* spores

RTgill-W1 and SHK-1 cell lines were grown in flasks until 80% cell confluence was obtained, after which the cells were harvested, counted using a haemocytometer to achieve an ideal concentration of cells and split onto 6-well plates. Cells were then left to acclimate for 2-3 days, until the cells reached the required degree of confluence (60-70%) before inoculating them with spores. A desired concentration of spores was prepared as in descried in Section 2.3.8, and spores were added at different cell:spore ratios (1:1, 1:10, and 1:20) to each well. Infections were carried out in duplicates and a mock control without spores was also included. Two different incubation temperatures were also tested (12°C and 16°C).

After 7 days post exposure (p.e.), the medium was removed from each plate, and wells were rinsed three times and re-fed with fresh medium and antibiotics. The medium was then replaced weekly. Cells were kept for 21 days and then split into new 6-well plates and maintained for another week.

2.2.11 Testing effect of pH shift on *D. lepeophtherii* germination

Experiments were performed following the same procedure as described in Section 2.3.8, but in order to stimulate germination of spores, a shift in pH was induced by following the protocol of MacLeod *et al*. (2018). Briefly, 10^7 spores were suspended in 0.5 ml of Minimal Essential Medium (MEM) containing 10% FBS and then inoculated onto 6-well plates of RTgill-W1 and SHK-1 while incubated at 12°C. The pH of the MEM was raised to 7.8 in the presence of RTgill-W1 and SHK-1 cells for 120 min and the spores were therefore in contact with the cells while the pH shift from neutral to alkaline occurred. After 120 min, each well was made up to 2 ml of L-15/FBS and cells were maintained as described above.

2.2.12 Infecting macrophages with *D. lepeophtherii* spores

A total of 10^6 viable macrophages were added to each well of 8-well chambers-slides (Thermo-Fisher Scientific, Leicestershire, UK) and these were filled with 200 µl of L-15 media and 5% FBS. Macrophages were left to adhere for 2 h at 18˚C and then cultures were washed twice with L-15 medium, removing unattached cells. The monolayer of adherent cells was then supplemented with 200 µl of fresh L-15 medium containing 5% FBS and 100 mg of penicillin/streptomycin, 2 µg gentamicin, and 2.5 µg of Amphotericin B per mL^{-1}. Cells were maintained at 18˚C. Spores at different concentrations were seeded in the wells of the chambers-slides in duplicate wells at different concentrations (1:5 and 1:10 cell to spore ratio). Cultures were maintained for 5 days. A control well, without spores, was also included. Cultures were examined after 24 h.p.e, 3 d.p.e and 5d.p.e. Cells in the chambers-slides were fixed with 100% absolute methanol at 1 d.p.e, 2 d.p.e and 4 d.p.e. For fixation, 0.2 ml of methanol were added to each well and left for 1 min. The chambers-slides were then rinsed with phosphate-buffered saline (PBS), left air dried, and stained with 10% Giemsa and subsequently with Calcofluor White (CW) (Fluka, Buchs,

Switzerland). Calcofluor White staining was performed according to the manufacturer's instructions. Briefly, one drop of KOH (15% w/v) and one drop of CW reagent was added to the slides. After 1 min, the slides were mounted and examined under ultraviolet light (excitation range 300 to 440 nm).

2.2.13 Monitoring cell cultures infected with *D. lepeophtherii* spores

Cells exposed to microsporidia and control cells were monitored daily using an Olympus CK40 phase-contrast inverted microscope (KeyMed) for signs of spore germination, infected cells, and the appearance of developmental stages comparable to other microsporidian cultures (e.g. MacLeod, 2012; Monaghan *et al.*, 2011). Micrographs were taken using a Canon EOS 60D (Canon, Saitama, Japan).

2.3 Results

2.3.1 Lice collection and spore isolation

2.3.1 Lice collection and spore isolation

Sea lice were collected from a number of salmon farms in Scotland at different times of the year. Some of the sites where these were collected are unknown, since the sea lice were sent by the health staff at the salmon production sites, who provided no details of the farm sites where lice were collected. The use of Percoll gradients, as described in Section 2.2.1, proved suitable for the isolation of *D. lepeophtherii* spores. A high number of spores were isolated from sea lice collected on 26.10.2017 and 28.11.2018. The final concentration of spores isolated from each sampling point is summarised in Table 2.2.

Table 2.2. Details of *D. lepeophtherii* isolation from sea lice. The number of spores and weight of the sea lice (g) from which the spores were collected are provided. The number of spores/g sea lice is also shown.

Date of collection	Spores no.	Weight of sea lice (g)	Number of spores/g sea lice	Collection point
10.11.2015	7×10^7	1.34	5.22×10^7	Ardnish
22.01.2016	1.5×10^8	1.8	8.33×10^7	Invasion Bay
12.02.2016	4.6×10^7	1	4.6×10^7	Camas Glas
21.04.2016	1.3×10^7	10.33	1.2×10^6	Loch Alsh and Poll na Gille
26.10.2017	4.9×10^8	10.55	4.6×10^7	Unknown
12.12.2017	4×10^6	4	10^6	Unknown
13.01.2018	3×10^7	0.74	4×10^7	Unknown
26.01.2018	0	1.78	0	Poll Na Gille
05.02.2018	2.3×10^7	1.1	2.1×10^7	Unknown
04.05.2018	0	1.5	0	Skye
21.05.2018	0	0.6	0	Shetland
12.09.2018	0	1.8	0	Loch Kishorn
15.11.2018	0	2	0	Loch Kishorn
27.11.2018	6×10^7	7.58	8.0×10^6	Appin
28.11.2018	1.5×10^9	14.7	1.0×10^8	Loch Fyne
06.12.2018	4×10^8	11	3.6×10^7	Quorry Point
05.03.2019	0	9	0	Loch Creran

When smears of spores were stained with Giemsa, spherical structures approximate 2.5 µm in diameter consistent with microsporidian spores were observed (Figure 2.2). Very low levels of bacterial rods could be seen in some of the spore suspensions.

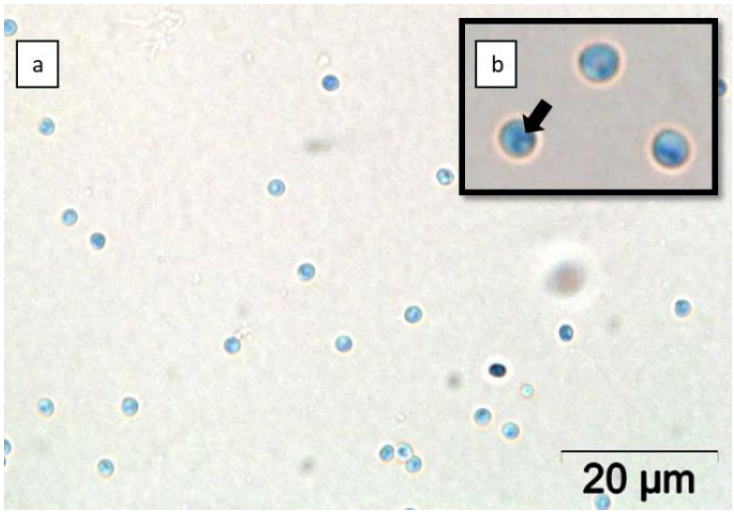

Figure 2.2. (a) Smear of *Desmozoon lepeophtherii* spores after isolation on Percoll gradients stain, blue in colour from Giemsa staining; (b) Note the birefringence of the spore wall and the darker belt-like stripe (arrow) previously described for other microsporidia (Garcia, 2002).

2.3.2 TEM results

The appearance of spores isolated from sea lice collected on 10.11.2015, were typical of microsporidian spores (Figure 2.3) and the description previously give for *D. lepeophtherii* (Figure 2.4) (Freeman & Sommerville, 2009; Nylund *et al.*, 2010) when viewed by TEM. They had a single nucleus and were 1.5-2 µm in length. The spore wall had a thickness of approximately 50 nm. The polar tubule had 4-8 coils and was of an isofilar type, with a diameter of 60-90 nm (Freeman & Sommerville, 2009). Occasional larger spores of 2.5-3 µm in diameter were seen. These possessed a thicker polar wall (~130 nm) and 13-22 coils in the polar tubule (Figure 2.5).

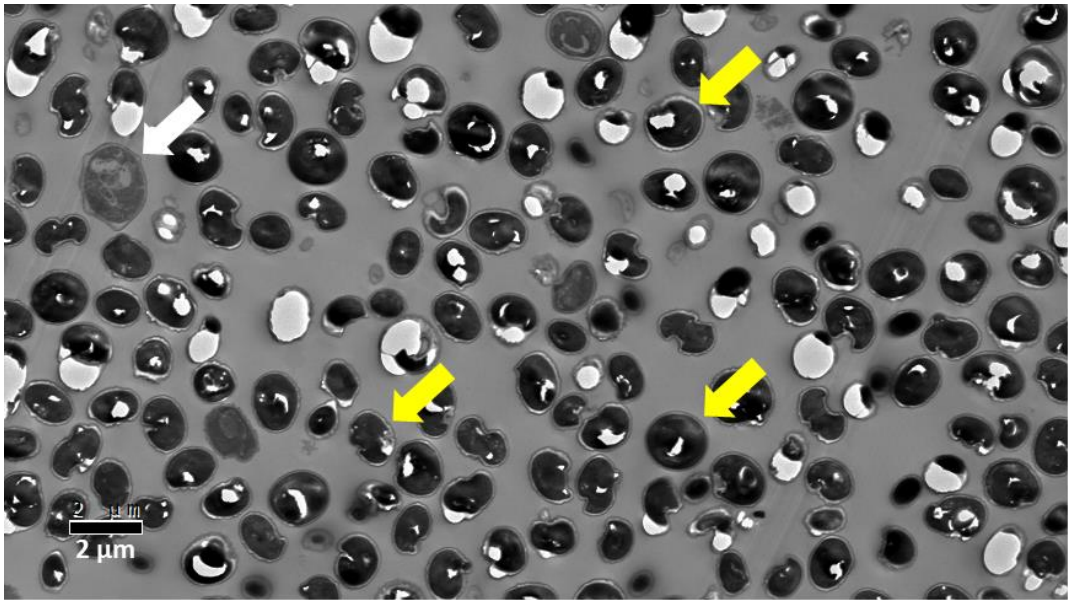

Figure 2.3. TEM micrographs of mature spores of *Desmozoon lepeophtherii* obtained from sea lice after isolation on a Percoll gradient. Two type of spores were noted, smaller spores of 1.5-2µm in length (yellow arrows), and bigger spores of 3-4µm in diameter (white arrow)

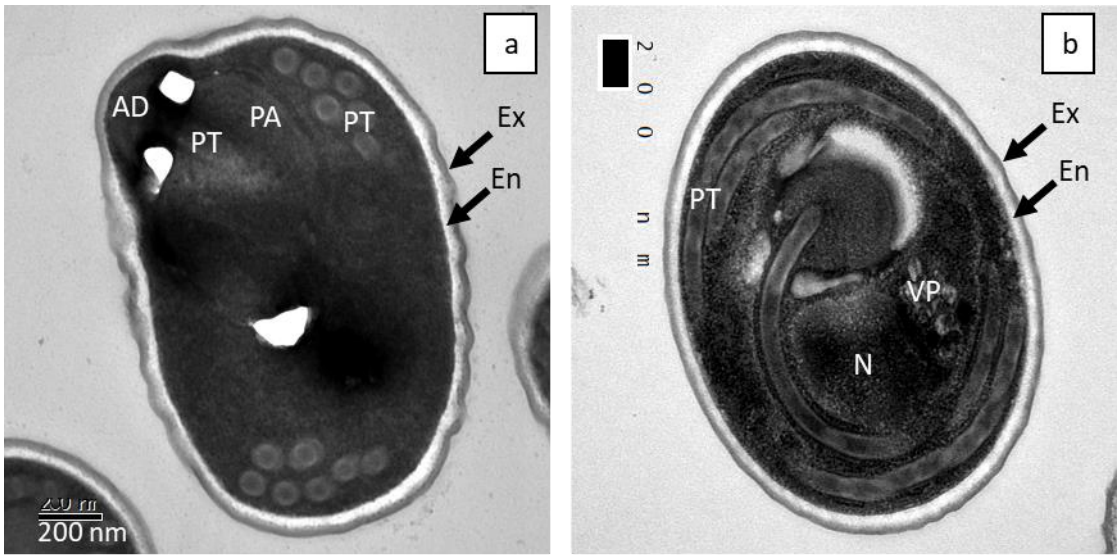

Figure 2.4. TEM micrographs of *Desmozoon lepeophtherii* spores: (a) Sagittal section of spore detailing an electron-dense exospore (Ex), and a thicker electron-lucent endospore (En). The polar tube has an electron dense core (PT) and terminates at the apical part of the spore in an anchoring disk (AD), near the lamellar polaroplast (PA). (b) Transverse section of mature spore with the single nucleus visible (N). The vesicular polaroplast is also present (VP)

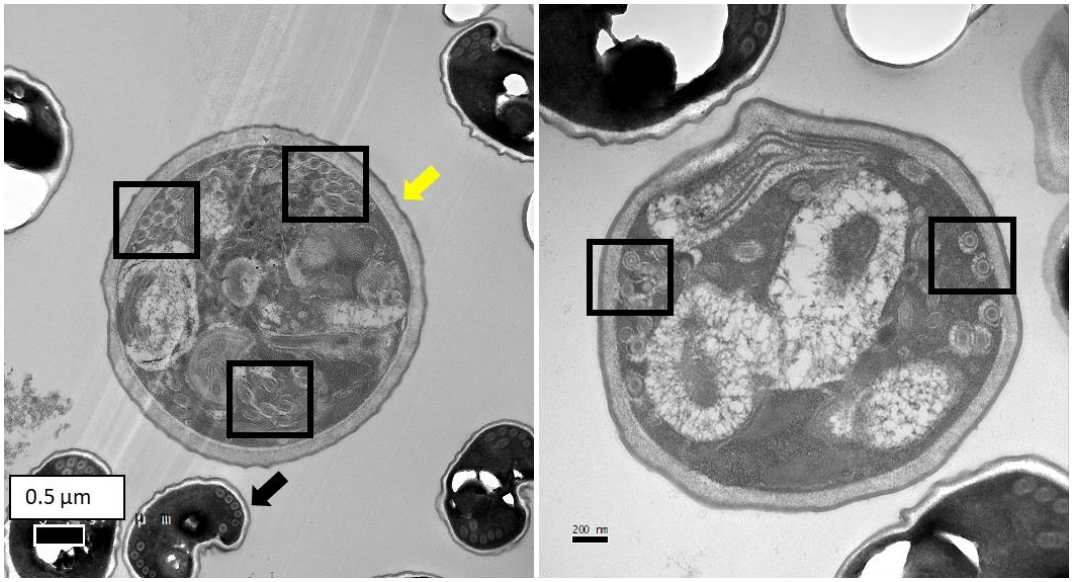

Figure 2.5. TEM micrographs of isolated spores of *D. lepeophtherii*. Two different sizes of spores were noted. Smaller spores were 1.5-2µm in length (arrow), and larger spores were 3-4µm in diameter (yellow arrows). Larger spores (2.5-3 µm in length), were seen occasionally that contained non-regularly arranged coils of the polar tubule.

2.3.3 DNA isolation and PCR

Overall, the extraction methods used yielded low concentrations of parasite DNA (Table 2.3). Chitinase (Method 1), chitinase and glass beads (Method 2) or DNA extraction Kit alone (Method 3) were all used to disrupt the spores, however Method 1 was slightly more effective than treating with either chitinase or Proteinase K alone. DNA from all three methods gave positive results in the PCR (Figure 2.6). The DNA from spores without treatment was sufficient to yield a positive result in a conventional PCR (Figure 2.6). Examples of positive results from spores collected at different sampling points (22.01.2016, 12.02.2016, 13.04.2016) are given in Figure 2.7.

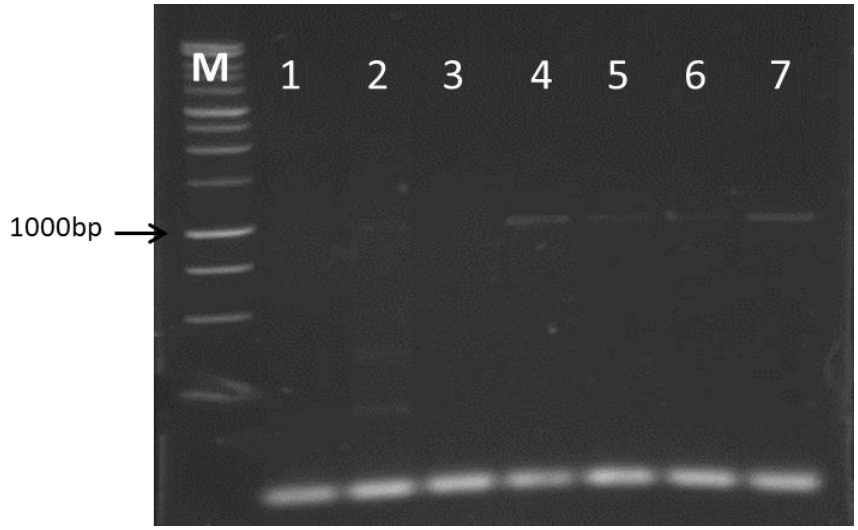

Figure 2.6. Agarose gels showing of PCR products from the various DNA extraction methods tried. Lanes M (marker pointing the fragment size of 1000 in basepairs (bp) with an arrow); lanes 1 and 3 - negative control; lane 2 – kidney from infected fish; lane 4 - DNA extraction using Method 1; lane 5 - DNA extraction method 2; lane 6 - DNA extraction Method 3; and lane 7 results DNA from untreated spores.

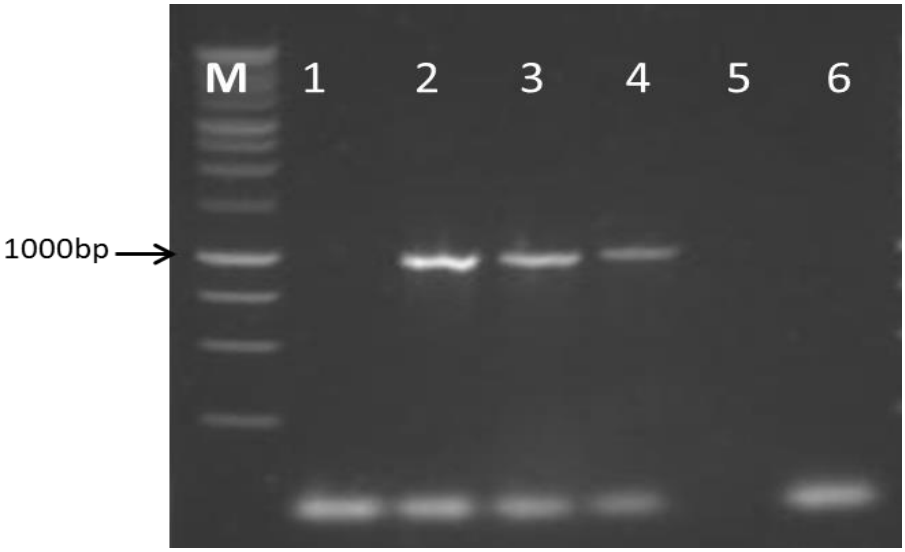

Figure 2.7. Example PCR products from spores isolated at different sampling points. M (marker pointing the fragment size of 1000 in base pairs (bp) with an arrow), lanes 1 and 6 (negative controls), lanes 2-4 (positive results of spores isolated at different sampling points: 22.01.2016; 12.02.2016; 13.04.2016).

Table 2.3. Yields of DNA extracted from spores using different extraction protocols: Method 1 (enzymatic disruption and DNA extraction Kit); Method 2 (enzymatic and mechanical disruption and DNA extraction Kit) and Method 3 (DNA extraction Kit only)

Method	DNA concentration (ng/µl)	A260/280	A260/230
Method 1	6.12	1.93	0.33
Method 2	4.13	2.27	0.18
Method 3	3.64	1.83	0.14

2.3.4 Viability of spores

Spores that were collected on 22.11.2018 and 06.12.2019, and stored at 4°C for 4 weeks in sterile saline, had a polar tubule extrusion rate of 14% and 9% respectively, when exposed to 30% of H_2O_2 (Figure 2.8). The polar tubule length was approximately 8 µm, but this appeared coiled in some spores. Discharge was observed using a 60x objective lens. Negative controls did not show extrusion of the polar tube (boiled spores and 2-years old frozen spores). Using a LIVE/DEAD Kit, the same spores preparations were shown to contain 18.5% and 18.5% of dead spores respectively after 4 weeks of isolation, and 17.3% and 42.6% after 12 weeks of being kept at 4°C. Under the FITC filter, dead spores presented with a slight red fluorescence and the viable cells a green florescence. Under the red PI filter, dead spores had a strong red fluorescence and viable spores could not be seen (Figure 2.9a & b), while 100% of the control spores had red fluorescence, indicating that they were not viable (Figure 2.9c & d).

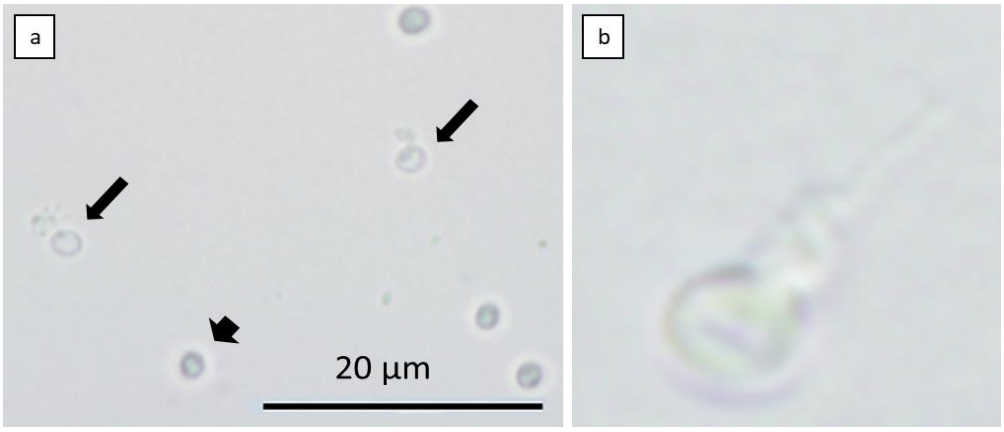

Figure 2.8. Spores of *D. lepeophtherii* exposed to 30% of H_2O_2. (a) Note the presence of the polar tubule after being extruded (arrows) and the absence of it in those spores in which the ejection did not occur (small arrow). (b) a *D. lepeophtherii* spore with the polar tube extruded.

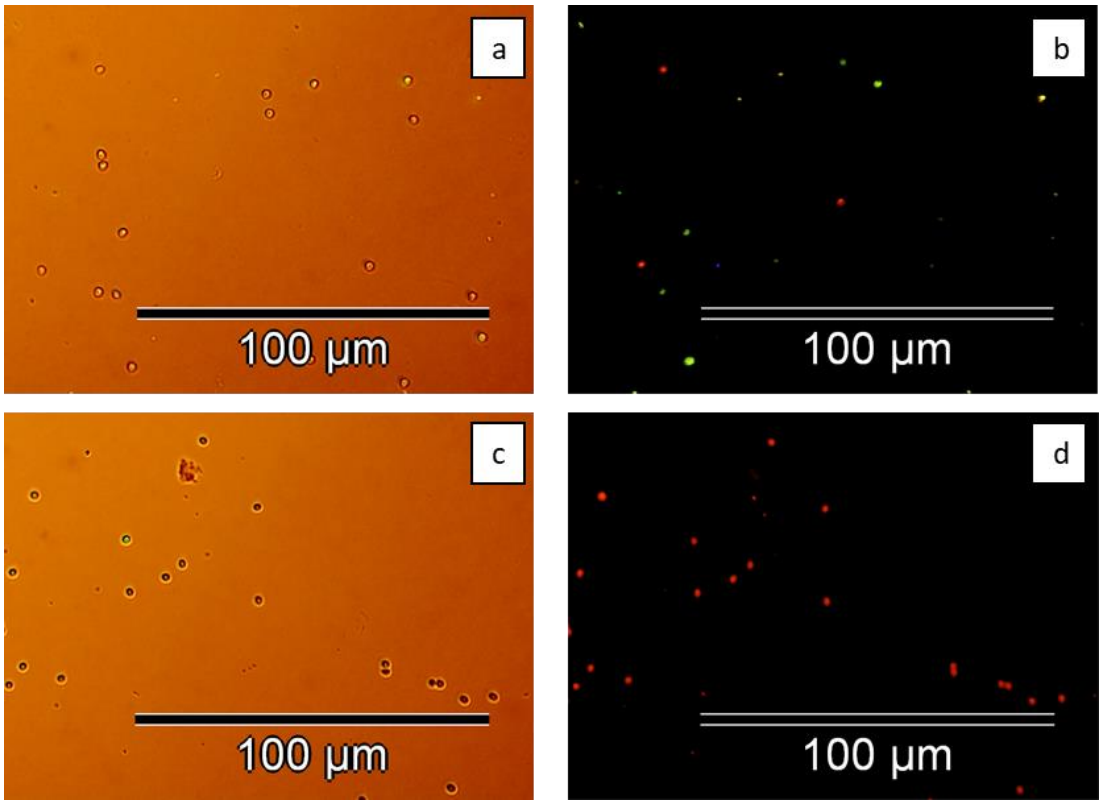

Figure 2.9. Spores stain with the viability kit. (a) Spores examined with light microscopy and (b) under the fluorescence microscope. Note that viable spores have a green fluorescence and non-viable are have a red fluorescence, which indicates that the spore plasma membrane is damage and the PI has been absorbed. (c) Negative

control spores that were previously boiled examined with light microscopy (d) Negative spores all showed a red fluorescence and were therefore non-viable.

2.3.5 Preliminary culture experiments *in vitro*

In the preliminary trials culturing *D. lepeophtherii* in the fish cell lines, spores were used within a week of isolation without any previous treatment with antibiotics or antimycotics. In these experiments, extensive contamination with both yeast and bacteria were obvious 4 d.p.e. in both flasks of RTgill-W1 and SHK-1 cells infected with the spores. Despite continuous cleaning of the flasks by washing and medium changes, it was not possible to control the contamination that resulted, and it was decided to discard the cultures 21d.p.e. Negative control preparations (mock cultures) were not contaminated, indicating that the source of the contamination had come from the spores.

2.3.6 Optimal concentration of antibiotics

To control contamination, the sea lice was transported in a solution of antibiotics and antimycotics from the farm site, and spores were cleaned for two weeks after isolation before being used in the cell culture experiments. Subsequent experiments with different concentrations of antibiotics, revealed that 1x concentration of antibiotics and antimycotics was sufficient to control secondary contamination in the cultures. Very low levels of bacteria were seen throughout the 14 day period of the study, but yeast was not present.

2.3.7 Cell line experiments with *D. lepeophtherii*

Fish cell cultures were examined daily by phase contrast microscopy throughout the experiment after the addition of *D. lepeophtherii* spores to the cells. Immediately after infecting the cells with the spores all the spores appeared bright under phase microscopy, but this changed 24 h.p.e. with some of the spores becoming less bright, suggesting that possible germination of the spores had occurred. Fourty eight h.p.e., spores appeared to form clusters between the cells. Early life cycle stages, developmental stages or spores of *D. lepeophtherii* were not definitively detected in either the RTgill-WI (Figure 2.10) or the SHK-1 cells (Figure 2.11). Similar results

were obtained when these cell lines were incubated with spores at different temperatures (12°C and 16°C) and after the incubating the spores in MEM for 120 min with a pH shift (from 7 to 7.8) to stimulate the germination of the spores through a change in pH. When the medium was removed from the wells and the cells rinsed 7 d.p.e., not all of the spores were removed from the cultures and a large quantity of spores remained in the plates. Spores were not completely removed from the cultures until 21 d.p.e., after the infected cells were washed for a third time, and the cells split (1:2) into new plates. After the infected cells were split, very low number of spores remained and could be seen in the new plates.

When different cell to spore ratios were used, spores at a 1:1 cell spore ratio were considered too low to observe. Only a few spores were present and changes in their birefringence could not be detected. Concentrations of 1:20 completely covered the cell monolayer and did not allow any early events of infection that may have occurred to be visualised. A concentration of 1:10 was considered optimal to see possible changes in the cells and appropriate to allow a sufficient number of spores to potentially infect the cultures.

2.3.8 Experiments with macrophages

Macrophage cultures were examined by phase contrast microscopy daily. Phagocytosis of spores was noted 24 h.p.e. (Figure 2.12). The number of spores within the macrophages increased over time and decreased in the medium. Macrophages were notably enlarged 4 d.p.e. However, developmental stages within the macrophages were not detected. Spores could be clearly seen in the cytoplasm of macrophages with Giemsa staining, but infectious or developmental stages were not observed. Calcofluor White stain confirmed the presence of the spores within the macrophages (Figure 2.13).

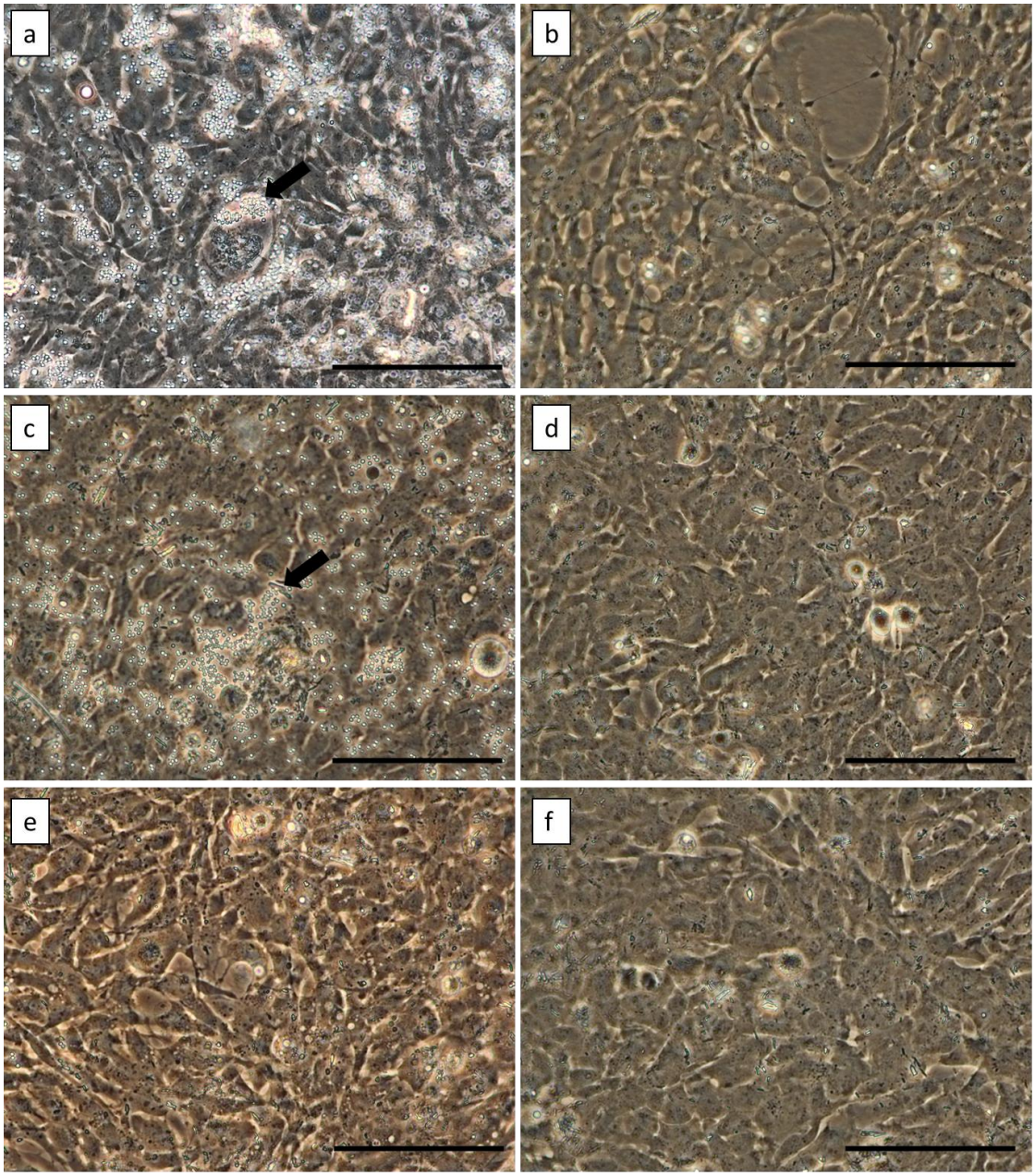

Figure 2.10. RTgill-W1 cells. Exposed cells with *D. lepeophtherii* spores (a) and negative controls cells (b) 24 h.p.e. Note the spores (arrow) present in the infected cultures as singles and in groups; (c) exposed cells and (d) negative control cells 7 d.p.e. After removing the old media and cleaning the cultures with fresh media for 3 times, some spores remained in the cultures (arrow). (e) Exposed cells with *D. lepeophtherii* spores and (f) negative controls 21 d.p.e before cells were split. Cultures had been cleaned twice since the beginning of the experiments and the number of spores decreased. Cells post-exposure did not show obvious changes compared with the cells uninfected. Scale bars 100 µm.

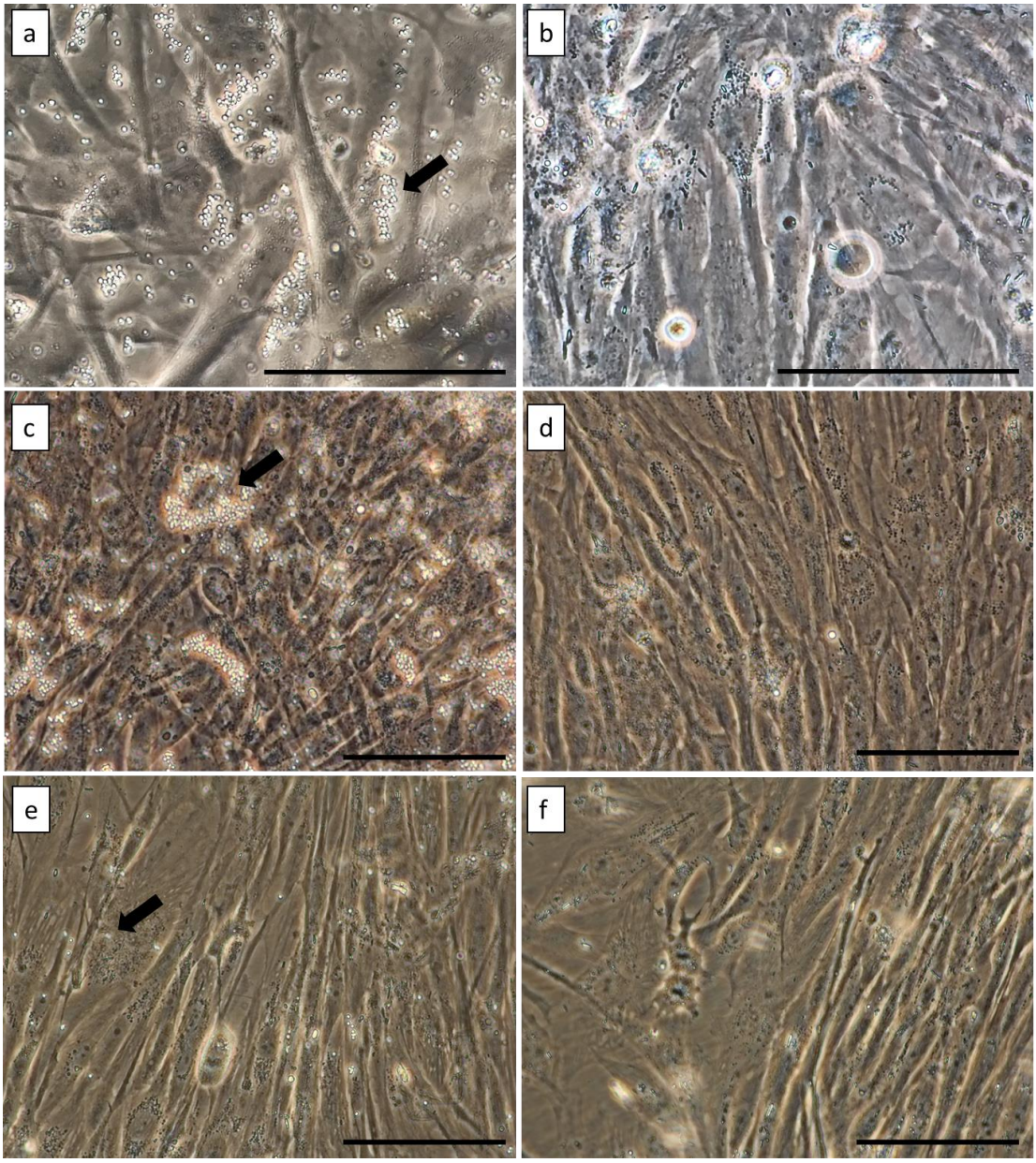

Figure 2.11. Images of the SHK-1 cells. (a) Exposed cells with *D. lepeophtherii* spores and (b) negative control cells after 24 h.p.e. Note the spores (arrow) present in the infected cultures as singles and in groups; (c) Exposed cells and (d) negative control cells after 7 d.p.e. After removing the old media and cleaning the cultures with fresh media for 3 times, some spores remained in the cultures (arrow). (e) Exposed cells and (f) negative control cells after 21 d.p.e before cells were split. Cultures had been cleaned twice since the beginning of the experiments and the number of spores decreased. Infected cells did not show obvious changes compared with the cells uninfected. Scale bars 100 µm.

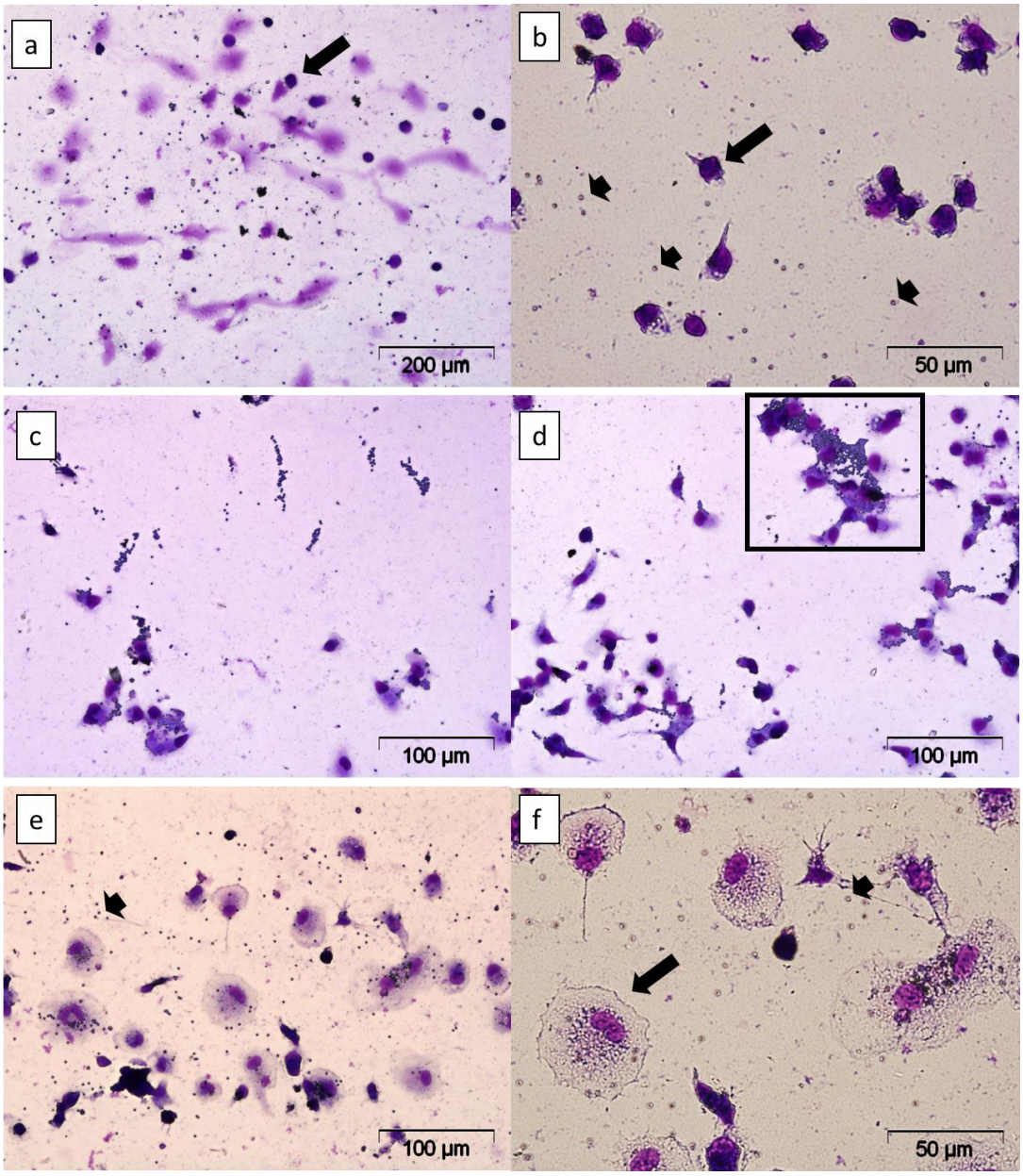

Figure 2.12. Micrographs of macrophages of Atlantic salmon (arrows). Macrophages (a & b) after 3 h. p. e. with *D. lepeophtherii* spores. Note the spores (short arrow) present in the media but not yet internalized by the macrophages; (c & d) after 24 h.p.e. some macrophages contained large amounts of microsporidian spores in their cytoplasm (box); (e & f) after 4 d.p.e. macrophages were enlarged (arrow) and spores were visible associated with the cytoplasm of the macrophages or in the media (short arrow).

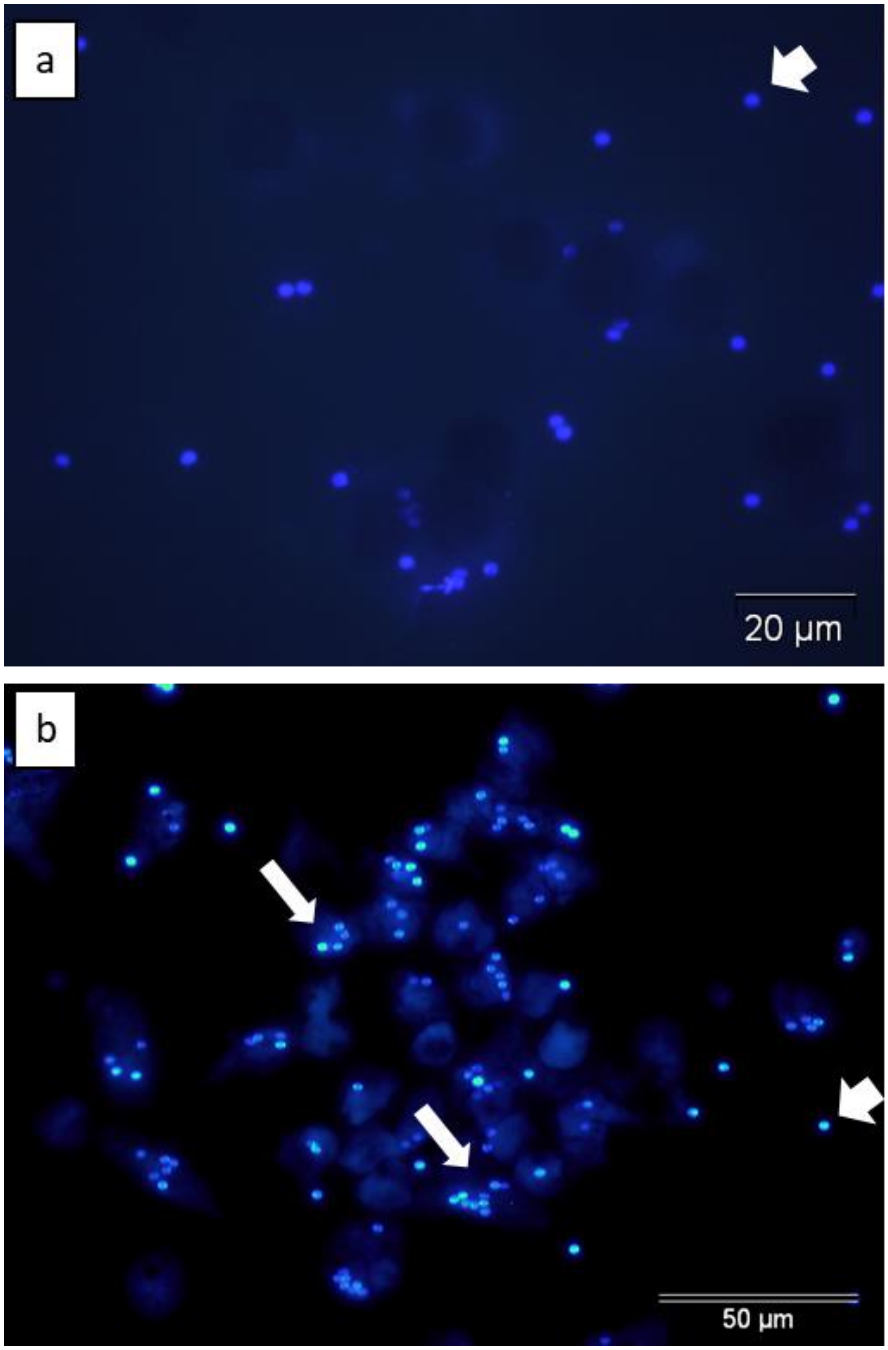

Figure 2.13. Micrographs of macrophages (a) 3 h.p.e with *D. lepeophtherii* stained with Calcofluor White. Note how most of the spores (short arrow) are not associated with the macrophages; (b) 24 h.p.e spores were mostly seen within the macrophages (arrow) and not free in the medium (white arrows).

2.4 Discussion

This study represents the first report of attempts to grow the microsporidian *D. lepeophtherii in vitro*. The results obtained in this study suggest that spores derived from sea lice cannot be propagated in RTgill-W1 cells, SHK-1 cells or short-term primary cultures of macrophages under the conditions used. It was not determined if low grade infections with *D. lepeophtherii* were present in the cells however, and further studies should address the use of more specific methods to identify early stages of the microsporidian in the cell cultures.

Spores of *D. lepeophtherii* were successfully isolated from the sea lice at different sampling points and from different Atlantic salmon farms. Infections of *D. lepeophtherii* in the sea lice has previously been reported in Scotland. Freeman (2002) studied the prevalence of *D. lepeophtherii* infections in sea lice in one salmon farm in Scotland over the course of approximately two years. The study examined the gross appearance of the sea lice and did not focus on the salmon host. Individual sea lice were recorded as infected when presenting obvious opaque areas on their body. These opaque areas had previously been associated with the presence of xenomas caused by the microsporidian. The highest prevalence of infection was noted during the months of October to January. In more sophisticated studies, Sveen *et al*. (2012) measured the levels of *D. lepeophtherii* in two salmon farms in Norway by RT-rtPCR. In one of the farms, the prevalence and loads of *D. lepeophtherii* increased significantly from the months of November to January, whilst in the other farm levels of *D. lepeophtherii* were very low throughout the year. This was possibly related to the low loads of *D. lepeophtherii* that were present in the salmon at that farm and therefore the lice were unable to become infected by feeding on the blood and skin of these salmon. The availability of sea lice from which the spores had been collected, depended on the salmon farming companies to provide these. As a result, the location of where the sea lice had been obtained varied, and this meant it was impossible to carry out a detailed study examining the prevalence and burdens of *D. lepeophtherii* in the sea lice. However, the greatest number of spores were collected during the months of October to February, whilst low numbers or even no spores were isolated from sea lice in February, April, May and September. These findings

are in agreement with the observations of Freeman (2002) and Sveen *et al*. (2012), in which the levels of *D. lepeophtherii* seem to increase during the winter months. However, no spores could be isolated from sea lice collected in November from a salmon farm in the north of Scotland (sampling point 15.11.2018), showing inter-farm variability for infections with the microsporidian.

TEM and PCR results showed that the spores collected belonged to *D. lepeophtherii*. Until now, the only another microsporidian apart from *D. lepeophtherii* that has been isolated from *L. salmonis* is *Facilospora margolisi.* This was isolated from sea lice collected from Atlantic salmon in Canada (Jones *et al*., 2012), but has not been detected in sea lice from Europe. The ovoid spores of *F. margolisi* are larger under TEM (2.6 µm in length) and have between 3-4 coils in their polar tube, compared with the smaller and rounded spores of *D. lepeophtherii* (1.5-2 µm in diameter in length), which has 4-8 coils in their polar tube. Larger and rounded spores were seen in the TEM studies in this study (2.5-3 µm in diameter) that had a bizarre arrangement of the polar tube, but these have been described previously in the development of *D. lepeophtherii* (Freeman, 2002; Nylund *et al*., 2010). The formation of two populations of spores, autoinfective and environmental, has been described for some microsporidians, including *D. lepeophtherii* during its development in salmon (Nylund et al., 2010). Additionally, another type of spores termed macrospores (spores about two times the size of the typical spores and with a higher number of polar tubule coils), have been described for some *Pleistophora* spp. (Canning & Hazard, 1982). According to Freeman (2002), the larger spores found in *D. lepeophtherii* could be similar to the macrospores found in *Pleistophora* spp. However, due to the abnormal arrangement of the internal spore structures (not seen in macrospores), Nylund et al. (2010) suggested that these are thought to be the result of anomalous development but its role in the development of *D. lepeophtherii* remains unknown.

Only spores collected from the first two batches of sea lice were processed for TEM analysis, while Giemsa staining was performed on all other batches of spores to confirm that the morphology of the spores isolated was consistent with those for *D. lepeophtherii*. Additionally, conventional PCR was used to confirm the presence of

D. lepeophtherii in all batches of spores used for the cell culture experiments. Attempts made to extract DNA from the spores resulted in very low yields of genetic material. Similar results were obtained with spores from other microsporidia. Reabel (2012) extracted the DNA from spores of the microsporidian *Encephalitozoon cuniculi* using different combinations of enzymatic and mechanical disruption, and also testing different commercial DNA extraction kits, including the one used here (DNAeasy kit). The results from these extractions gave very low yields of DNA (1.9-3.2 ng/µl) overall and were similar to the yields obtained in the present study, when different methods were used together with the DNAeasy kit to extract DNA from the spores. In contrast, other commercial kits, in particular PrepGEM™ (Zygem, Hamilton, NZ) provided much higher concentrations of DNA. The author suggested that the simplicity of the extraction process with this kit reduced the loss of DNA that results in kits based on multiple step extractions. In the present study, spores used directly in the PCR gave positive results and this method was therefore chosen over other extraction methods due to its simplicity. Freezing and thawing the spores prior to the PCR and the denaturation step at 95 ˚C for 5 min during PCR amplification, was thought to disrupt the spore wall and allow the DNA to be released.

Spores kept under laboratory conditions for long periods of time may be detrimental to the integrity of the spore and affect the outcome of future experiments (Shaw *et al*., 2000). The most effective method to assess spore viability is to use the spores to perform infection trials *in vivo* or *in vitro* (Shaw *et al*., 2000). When these kinds of experimental models are not available, as is the case for *D. lepeophtherii*, other methods can be used to confirm spore viability. Two experiments were used to confirm the viability of the spores: the artificial germination of the polar tube and the capacity of the spore to permit the entrance of dyes. Extrusion of the polar tube occurs when optimal environmental stimulation is present. The necessary stimuli vary between different microsporidian species and the use of various mechanical and chemical stimuli have been investigated. Several hypotheses for germination are presented in the review by Williams *et al*. (2014). One recurrent theory is that activation starts with an influx of ions that results in the displacement of calcium from the intracellular compartments. This may be associated with the loss of spore structure, but also to the activation of the enzyme trehelase, as suggested by Undeen

(1990). Terhalase breaks down trehalose into glucose and smaller molecules metabolites that could increase osmotic pressure within the spore and stimulate the entrance of water. Subsequently, an increase of intrasporal pressure and swelling of organelles may result, causing the polar tube to extrude. Hydrogen peroxide might disturb the inter-membranous compartments in a similar manner, creating an influx of monovalent ions and stimulating the changes previously described. In the present study, the extrusion rate of the polar tube through exposure to a high concentration of H_2O_2 resulted in a very low percentage of germination (9-12%) of *D. lepeophtherii* spores which had been kept at 4°C in 0.85% sterile saline for 4 weeks. It is possible that H_2O_2 concentration used was not strong enough to stimulate the germination of the *D. lepeophtherii* or it could be that after 4 weeks in the laboratory, the capacity of the microsporidian to germinate artificially was reduced. An experiment carried out using *L. salmonae* spores found that the capacity to extrude the polar tube under the exposure to H_2O_2 decreased over time (Shaw *et al*., 2000). After 100 days, the extrusion rate of spores kept in freshwater and seawater at 4°C was 0%. However, even when spore extrusion was only ~ 10% after 95 d, these spores were still able to cause gill xenomas when used to challenge coho salmon.

The membrane integrity of the *D. lepeophtherii* spores used in the present study was also assessed based on membrane's ability to take up dyes, for which a LIVE/DEAD kit that combined SYTO 9® and propidium iodine was used. The use of vitality dyes to confirm the viability of microsporidia has been used previously prior to performing infection trials *in vivo* (Collado *et al*., 2014). The viability of microsporidia varies with species and the conditions in which the spores are kept. The results in this study showed that 18.5% of spores had lost viability after 4 weeks kept at 4°C in saline, and that up to 42.6% of the spores were no longer viable after 12 weeks. Despite the results of the H_2O_2 challenges to assess the polar tube extrusion rate, 80% of spores were viable with the LIVE/DEAD kit when used to perform the infection experiments in the cell lines, with spores always used within 4 weeks of isolation.

Control of contamination in microsporidia spores obtained directly from their host has posed a challenge for other cell cultures studies and has proved to be a limiting

factor for the culture of some microsporidia *in vitro* (e.g. Monaghan *et al*., 2011). The transport of lice and then maintenance of the *D. lepeophtherii* spores in a solution of antibiotics and antimycotics for two weeks prior to use was performed as described by McConnachie *et al.* (2015), and this drastically reduced the levels of yeast and bacteria in the cultures. This should be regarded as a necessary step in future experiments using spores obtained from the sea lice for *in vitro* or *in vivo* experiments.

During this experiment, a few spores with less birefringence were noted in the cultures 24 h.p.e. This has been associated with the germination of microsporidia and subsequent emptiness of spores (Monaghan *et al*., 2011), and it was also noticed after the experimental trials with H_2O_2 after the extrusion of the polar tube. However, it is not clear if these changes were due to germination or to the dead spores (up to 20%) in the suspension used to infect the cultures. No subsequent changes, suggestive that the cells were infections with *D. lepeophtherii* were observed. Culture of *Loma salmonae in vitro* in RTgill-1 cells had the presence of hypertrophic cells that contained intracellular spores that developed 5 d.p.e, and some of the newly produced spores were free in the media 7 d.p.e. Exposure of RTgill-W1 cell with spores from the microsporidian *Loma morhua* did not cause any signs of infections during the 30 days of the trial (MacLeod, 2012), but when cells derived from cod larvae were infected with spores and incubated at 8°C, developmental stages of the spores could be seen by 15 d.p.e (MacLeod *et al*., 2012). A shift in the pH from neutral to alkaline seem to be necessary for some microsporidia to sporulate. Dall (1983) proposed that an alkaline environment establishes a proton gradient and activation of cation/proton exchange in the sporoplasm and other organelles of the spore creates an osmotic imbalance, leading to swelling of the organelles and an increase in intraspore water pressure that leads to the extrusion of the polar tube. However, an increase in alkalinity it is not a requirement for microsporidians to germinate (Williams *et al*., 2014), and conditions required for this seems to depend on individual microsporidian species. A shift in medium pH from neutral to alkaline did not cause any appreciable changes in the *D. lepeophtherii*'s ability to germinate, as seen to occur with other microsporidian species.

The sea louse was chosen as the host to isolate spores of *D. lepeophtherii* because of its readily available and easy to isolates spores compared to isolation from Atlantic salmon gills, and because according to the hypothesised life cycle of *D. lepeophtherii*, spores of lice are able to infect the gills of salmon (Sveen *et al*., 2012). Additionally, the microsporidian has been reported in the gills of rainbow trout by sequencing of the RT-rtPCR product (GenBank accession number FJ594989) and other salmonids (Nylund *et al*., 2010; Thakur *et al.*, 2019) and fish species (Steigen *et al.*, 2018), which suggested that the specificity of the parasite was low, and it could potentially infect a wide range of cells in cell culture. Specificity of the microsporidia *in vitro* varies widely among species, as demonstrated from *A. algerae*, which is able to successfully gown in mammal, insect and fish cell lines (Belkorchia *et al.*, 2008; Monaghan *et al.*, 2011). From the seven fish microsporidia cultured in cell lines, three have been reported to infect non-host derived cell lines (see Table 2.1). Lores *et al.* (2003) showed how the *Glugea* spp. microsporidian, obtained from the greater sand eel, was able to infect and grow in the larval cells of the mosquitoe *A. albopictus* and to infect cells of the chinook salmon embryo (CHSE-214), although development in the latter cell line ceased after 48 h in culture. *Pseudoloma neurophila* isolated from zebrafish, was able to infect a range of cell lines derived from the zebrafish and fish other species (Watral *et al*. (2006) cited in Monaghan *et al*. (2009)). Finally, the microsporidian *H. saurida* grew in kidney cells of rabbit, and spores were obvious in the cytoplasm of the cells 1 week after exposure. However, trials with other fish and mammalian cell lines did not support the development of this species of microsporidian. Despite the range of species from which *D. lepeophtherii* has been detected, the parasite is seems unable to cause obvious infections in cell cultures used derived from trout or salmon.

The life cycle of *D. lepeophtherii* is complex: one type of sporogony occurs in the sea lice and two different stages occur in salmon. This leads to a total of three different spore stages for the microsporidian. Infection of salmon kidney with autoinfective spores of *D. lepeophtherii* have been confirmed by TEM and light microscopy (Nylund *et al*., 2010; Matthews *et al*., 2013), although these seem to occur subsequently to the initial infection seen in the Atlantic salmon gills, and formation of the characteristic autoinfective spores, different to the ones obtained

from the sea lice, probably spread from the gills to other organs of the fish. Developmental stages of *D. lepeophtherii* and autoinfective spores have been also observed in polymorphonuclear leucocytes and macrophages of salmon by TEM and ISH (Nylund *et al*., 2011; Weli *et al*., 2017), but again, this has been suggested to occur secondary to the initial infection of salmon gills and development of autoinfective spores, not by infections by the primary spores of sea lice. Future studies should include the use of a recently developed gill cell line of Atlantic salmon (Gjessing *et al*., 2018) in order to elucidate if spores of sea lice can infect these cells and if the transmission of the microsporidian from sea lice to salmon occurs as hypothesised for its life cycle. Additionally, the inclusion of insect cell lines *in vitro* studies could provide a better environment for the growth of the spores derived from the sea lice. Other approach would be to collect spores from the infected Atlantic salmon. Due to the lack of *in vivo* infection models with *D. lepeophtherii*, collection of gills from farmed salmon infected with *D. lepeophtherii* carries some difficulties. Even though the presence of the microsporidia in salmon farms is common (Steinum *et al*., 2010), intense production of spores seems to occur asynchronously in the farm and in a short time window (Matthews *et al*., 2013). For this, a close monitoring of the health status of one or various populations of farmed salmon and knowledge of the continuous status of the level of infection with *D. lepeophtherii* in the farm is necessary. Furthermore, various isolation attempts could be necessary before collecting a considerable number of spores to perform *in vitro* experiments, as carried out with spores from sea lice.

In conclusion, isolation of *D. lepeophtherii* from sea lice is relatively easy and can be used to gather relatively high loads of spores for future culture experiments. However, *in vit*ro culture of the parasite could not be accomplished in this experiment. *Desmozoon lepeophtherii* has a complex life cycle and how its transmission to fish occurs is unknown. The use of cell lines is an excellent way to study the basic biology and other aspects of the organism and the culture of *D. lepeophtherii in vitro* deserves further research. Future cell culture experiments should include insect cell lines and Atlantic salmon epithelial gill and gut cell lines, as well as the trial of different methods to favour the germination of the microsporidian. *In vivo* trials using different routes of infection in the fish such as

pipetting on gills and skin or gavage would also help to study the biology and development of the parasite at different time points. Importantly, more sophisticated methods to detect *D. lepeophtherii* such as TEM or *in situ* hybridization (ISH) will help to distinguish if infections occur at low level in the cell cultures.

2.4.1 Acknowledgments

I would like to thank Dr. Janina Costa (MRI) for her continuous help during the cell cultures experiments. The health staff at the salmon production companies are thanked for their valuable aid in the collection of the sea lice used in this chapter.

Chapter 3 Prospective longitudinal study of putative agents involved in complex gill disorder in Scotland

3.1 Introduction

3.1.1 Infection dynamics of *Desmozoon lepeophtherii*

A peak in gill disease has been observed in marine farmed salmon in Scotland during autumn months (Matthews *et al*., 2013). Gill disease can be caused by a single or multiple pathogen, environmental challenges and in association with various husbandry practices (Mitchell & Rodger, 2011). Complex gill disorder in farmed Atlantic salmon has not yet been fully characterised but it encompasses the previously described gill conditions of PGI and PGD. The main agents that have been associated with CGD include *D. lepeophtherii* (Steinum *et al*., 2010), *Ca*. B. cysticola (Mitchell *et al*., 2013) and SGPV (Gjessien *et al*., 2017). However, the exact role of each of these pathogens in gill disease remains unknown.

No data is publicly available in Scotland relating to the patterns of infection with these CGD-associated pathogens, including *D. lepeophtherii*. Freeman (2002) recorded that *D. lepeophtherii* was present in sea lice (*L. salmonis*) on farmed salmon in Scottish coastal waters over the course of a year. However, the detection of the microsporidian in the sea lice relied solely on macroscopic observation of the lice, whereby opaque lice were presumed to be infected, but the author did not screen the lice for *D. lepeophtherii* by any definitive method in the study. The microsporidian appears to be very prevalent in salmon farms around Scotland (pers. communications FVG) and has been reported as associated with gill disease (Matthews *et al*., 2013) but the prevalence and infection dynamics of *D. lepeophtherii* in Scottish salmon aquaculture remains unknown.

The prevalence of *D. lepeophtherii* appears to be temperature-dependant and temperatures above 10ºC are associated with increased prevalence of the parasite in salmon. Sveen *et al*. (2012) demonstrated how two groups of salmon smolts transferred to sea at different times of the year (April and November) showed

different patterns of infection dynamics when assessed using RT-rtPCR. Salmon transferred to the sea in April had a higher prevalence and incidence of *D. lepeophtherii* infection during April to September in both the gills and the head kidney. Smolts transferred to sea in November showed *D. lepeophtherii* infection in the gills after 3 weeks (first sampling point) but samples from head kidney showed a low prevalence and incidence of the parasite and no significant variation from November to March. The authors suggested that water temperature might be a limiting factor for the microsporidian to complete its development and that this might explain why salmon transferred to the sea in November failed to develop a systemic infection (low or absent parasite load in kidney tissue) and dissemination of auto-infective spores was not observed. However, the gill pathology associated with the increase or decrease of the parasite loads in the salmon gills was not recorded in this study. To better understand and model co-occurrence of *D. lepeophtherii* with other putative agents involved in CGD (Chapter 1), SGPV, *Ca.* B. cysticola and *P. perurans* were included in the screening during the longitudinal study.

3.1.2 Semi-quantitative gill scoring

Semi-quantitative scoring systems are a useful tool to assess the severity of one or more lesions in the tissues and are widely used in biomedical research (Klopfleisch, 2013). Multiple parameters are usually assessed and quantified separately and then combined to give a total score (Klopfleisch, 2013). Results can then be analysed statistically comparing the presence/absence of a stressor or other variable (Rašković *et al*., 2013). In fish, various scoring systems have been used for different organs, including the gills (Bloecher *et al*., 2018; Knudsen *et al*., 2008). A reliable gill score system was developed by Mitchell *et al*. (2012) to assess gill health. In the latter study, the variability between observers was tested using a weighted kappa coefficient with a result of 0.68 (1 is considered to be a perfect agreement). The score system includes the most relevant histo-morphological changes that can be observed in gill sections, but also maintains enough simplicity and reproducibility to allow other researchers to apply it easily to their studies (e.g. Baxter *et al*., 2012; Bosch-Belmar *et al*., 2016; Downes *et al*., 2018). Briefly, the index criteria included lamellar hyperplasia, lamellar fusion, cellular necrosis, and

lamellar oedema, which were scored from 0 to 3, depending of the severity of the gill lesion (0 was the absence of the lesion, 1 was a small area of the lesion, 2 was a medium amount of the lesion, and 3 was a large amount of the lesion). Other ancillary criteria such as cell hypertrophy, vascular disturbances (haemorrhages, thrombi, congestion), and the presence of pathogens were scored as 0 (absent) or 1 (present).

3.1.3 Aims and objectives

At the time this experiment was designed, the data available on the putative pathogens associated with CGD pathogens was scarce. The aim of this study was to gain a better understanding of the dynamics of *D. lepeophtherii* infection in Scottish salmon farms using prospective longitudinal sampling starting from the freshwater stage of the production cycle and continuing through the marine stage for a whole year. The relative quantities of the parasite, estimated using specific RT-rtPCR Ct values, were correlated with the semi-quantitative histological gill scoring system derived from the samples. The presence or absence of other agents thought to be involved in CGD, such as *Ca.* B. cysticola and SGPV, were also assessed using specific RT-rtPCR methodologies. The presence or absence of *P. perurans*, the cause of amoebic gill disease (Adams *et al*., 2004), was also determined by RT-rtPCR because of its impact and prevalence in Atlantic salmon gill disorders.

3.2 Materials and methods

3.2.1 Study design

A prospective longitudinal study was designed to investigate the infectious dynamics of the putative pathogens of CDG and the disease severity in two production units. A productive unit was defined as a population of Atlantic salmon stocked in the same cage at a specific point in time. The timeframe was February 2016 to March 2017.

Farm A was located in the west of Scotland and had regularly experienced outbreaks of gill pathology of unknown aetiology in previous years but had not experienced significant gill problems in the last two years. Fish were transferred

from a freshwater loch on the Scottish west coast to this marine site during February and March 2016. Samples described in Section 3.3.2 were collected from the freshwater fish in February 2016 before being transferred to sea cages.

Farm B was located in the north west of Scotland. This farm had experienced regular outbreaks of gill disease due to multiple pathogens in previous production cycles. The studied population consisted of S1s that were transferred, from a different Scottish freshwater loch to that of Farm A, to this marine site during March of the same year.

Farm A and Farm B salmon populations were both positive for *D. lepeophtherii* in random samples taken in the previous production cycle.

Both farm sites agreed to participate in the study based on confidential handling of the data collected and farm identity. One pen from each farm was selected as the sentinel unit and studied through the year. The pen sampled at Farm A was stocked in February 2016 and the pen at Farm B in March 2016. The pens were sampled monthly until July, then every two weeks until the end of the study. The timeframe and sampling frequencies were selected to reflect the time of year when gill disease outbreaks occur (summer-early winter). A minimum of 6 fish were collected randomly per sampling after attracting the fish to the surface with feed.

Table 3.1. Farms details.

Farm	Location	Transfer to sea and first sampling point	Background details
A	West	February 2016	Farm had regular occurances of gill pathology of unknown aetiology in previous years, but no significant gill problems had occurred in the preceeding two years.
B	North- west	March 2016	Outbreaks of gill disease reported in previous production cycles.

3.2.2 Sample collection

Sampling commenced on 5 February 2016 and continued until 1 March 2017. All fish were euthanized with an overdose of tricaine methanesulfonate and tissue

sampling conducted on-site using aseptic techniques. At each sample point the second arch of the left side of the gill was collected from each fish and placed in 10% neutral buffered formalin for subsequent histological examination. A piece of the second left gill arch was also placed in RNAlater (Ambion, Paisley, UK), stored at 4˚C overnight and then at -80˚C until homogenization, nucleic acid extraction and RT-rtPCR. Storage time for all gill samples used in this study for RT-rtPCR was less than seven months.

3.2.3 Weeks, months and seasons

Time in the graphs is represented in weeks and seasons. Week 1 represents the first sampling point in the freshwater stage of Farm A (05.02.2016) and week 57 is the last sampling point of the study (01.03.2017). All weeks, sampling dates and season are displayed in Table 3.2.

3.2.4 Data collection from farms

Mortality, growth rates, feeding rate, sea lice counts, macroscopic gill lesion scores (AGD and PGD, see below) and environmental parameters, such as temperature, oxygen levels and salinity, were monitored daily and the data was made available for this study. Averages of the environmental parameter's values from the 14 days prior the sampling points were calculated for each site. Details of pen type and frequency and method of net cleaning were collected. At each sampling time point macroscopic gill lesion scoring was performed, including PGD (proliferative gill disease) (Table 3.3) and amoebic gill disease (AGD) (Table 3.4) scores according to the scoring cards kindly provided by the FVG. From July 2016, fish weight and length were recorded, and condition factor calculated (weight (g) × 100/[body length (cm)]^3).

Table 3.2. Week numbers with their respective sampling dates and seasons.

Week Number	Sampling Dates		Season
	Farm A	Farm B	
1	05/02/2016	-	Winter-1
6	10/03/2016	-	Winter-1
10	05/04/2016	06/04/2016	Spring
14	03/05/2016	04/05/2016	Spring
19	06/06/2016	07/06/2016	Spring
23	07/07/2016	08/07/2016	Summer
28	10/08/2016	11/08/2016	Summer
30	25/08/2016	26/08/2016	Summer
32	06/09/2016	07/09/2016	Summer
34	20/09/2016	21/09/2016	Autumn
36	04/10/2016	05/10/2016	Autumn
38	18/10/2016	19/10/2016	Autumn
40	01/11/2016	02/11/2016	Autumn
43	22/11/2016	23/11/2016	Autumn
45	07/12/2016	06/12/2016	Autumn
47	20/12/2016	19/12/2016	Autumn
49	06/01/2017	05/01/2017	Winter-2
52	25/01/2017	24/01/2017	Winter-2
54	08/02/2017	09/02/2017	Winter-2
57	28/02/2017	01/03/2017	Winter-2

3.2.5 Histopathology

Gill tissue samples fixed in formalin were processed routinely through graded alcohols prior to being embedded in paraffin-wax. Sections (5µm) were mounted on glass microscope slides and stained with H&E (Bancroft & Stevens, 1977). All sections were examined with an Olympus BX51 microscope, photomicrographs taken with an Olympus DP70 Digital Camera System and analysed using analySiS® software. A scoring system proposed by Mitchell *et al*. (2012) for the assessment of pathological changes resulting from gill disease was applied, with slight modifications. Once the collection and production of stained histological sections of tissue was complete, the coding of each slide was covered so that pathology scoring could be performed blinded. The scoring system used has an index criterion which

includes the primary parameters scored in the gill with each given a score from 0 to3 based on the severity and extent of the lesions. Additional ancillary criteria, based on the absence or presence of a parameter, was scored either 0 or 1. Further details about this gill scoring criteria can be found in Table 3.5. The maximum histological gill lesion score was 24. Total gill scores between 0-3 were considered non-significant or indicative of minimal gill changes, scores between 4-6 were considered to be indicative of mild changes, scores of 7-9 reflected moderate pathology and scores over 9 indicated severe pathology. Examples of common lesions present in gill disease are illustrated in Figures 3.1 and 3.2.

Table 3.3. Proliferative gill disease (PGD) field score values (kindly provided by FVG).

Score	Description
0	No sign of proliferative changes, red and healthy colour
1	Very slight thickening or very few filaments affected
2	Frequent thickening but only affecting filament tips
3	Most filaments have thickened tips, with some affected to more than 50% of filament length
4	Most filaments thickened progressing to more than 50% of filament length
5	Almost all filaments affected along the entire length

Table 3.4. Amoebic gill disease (AGD) field score values (kindly provided by FVG).

Score	Description
0	No sign of infection and healthy red colour
1	1 white spot, light, scarring or undefined necrotic streaking
2	2-3 spots/small mucus patch
3	Established thickened mucus patch or spot grouping up to 20% of gill area
4	Established lesions covering up to 50% of gill area
5	Extensive lesions covering most of the gill surface (≥50%)

Table 3.5. Criteria for the histological gill scoring system used in this study. Modified from Mitchell et al. (2012).

		Histo-morphological change				
	Score	**Lamellar Hyperplasia**	**Lamellar Fusion**	**Cellular Death**	**Circulatory Disturbances**	**Inflammation**
Index criteria	None (0)	None or very minor	None or very minor	None or very minor	None or very minor	None or very minor
	Mild (1)	Mild increase in lamellar epithelial cell (<10% of gill tissue affected)	Occasional focal fusion of filaments (<10% of gill tissue affected)	Scattered, occasional, degenerating necrotic or apoptotic cells and/or cell sloughing (<10% of gill tissue affected)	Scattered, occasional vascular changes (<10% of gill tissue affected)	Scattered, occasional inflammatory cells (<10% of gill tissue affected)
	Moderate (2)	Moderate multifocal or widespread increase in lamellar epithelial cells, affecting 10–50% of the tissue	Multifocal areas of fusion, affecting 10–50% of gill tissue interspersed with normal gill tissue	Multifocal, degenerating necrotic or apoptotic cells and/or cell sloughing affecting 10–50% of the tissue	Vascular changes in multifocal areas, affecting 10–50% of the tissue	Inflammatory cells in multifocal areas, affecting 10–50% of the tissue
	Severe (3)	Extensive multifocal or widespread increase in lamellar epithelial cells, affecting >50% of the tissue	Extensive fusion and loss of normal architecture, affecting >50% of the tissue	Extensive, degenerating necrotic or apoptotic cells and/or cell sloughing affecting >50% of the tissue	Multifocal to widespread vascular changes, affecting >50% of the tissue	Multifocal to widespread inflammatory cells, affecting >50% of the tissue
Ancillary criteria	Absence (0) or presence (1)	- Lamellar tissue disruption (disruption of a group of lamellae, associated with haemorrhages and cell death) - Lamellar oedema (≥10% of gill tissue affected) - Eosinophilic Granular Cells (increase of EGCs numbers within the filaments) - Bacteria- Epitheliocysts (variable sized basophilic inclusion bodies found mainly in the branchial epithelium) - Bacteria- *Tenacibaculum* spp. - Protists parasites- *Neoparamoeba* spp. - Protists parasites- *Costia* - Protists parasites- Trichodina - Unidentified metazoan organisms (i.e. filamental metacercaria)				

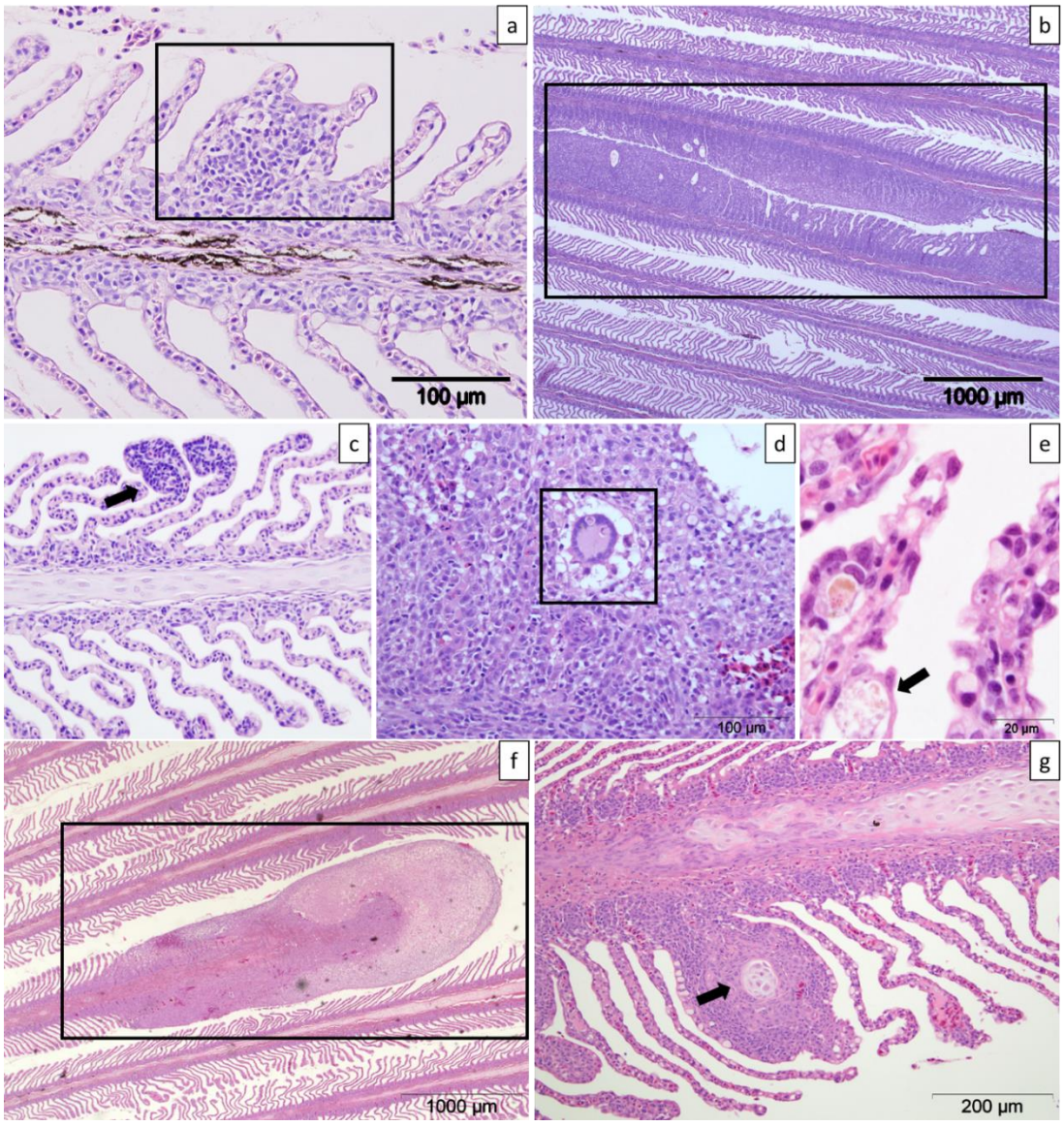

Figure 3.1. Histologic sections of gills from farmed Atlantic salmon stained with haematoxylin and eosin (H&E). (a) Mild focal lamellar epithelial hyperplasia and fusion (box). (b) Two foci of moderate AGD lesions (box). (c) Mild focal lamellar epithelial lymphocytic branchitis (arrow). (d) Presence of a multinucleated cell among the proliferated lamellar tissue (box). (e) Lamellar sub-epithelial infiltration of macrophages (arrow). (f) Proliferation of the distal part of a single shortened filament, PGD-like lesion (box). (g) Cartilage dysplasia of the filament (arrow).

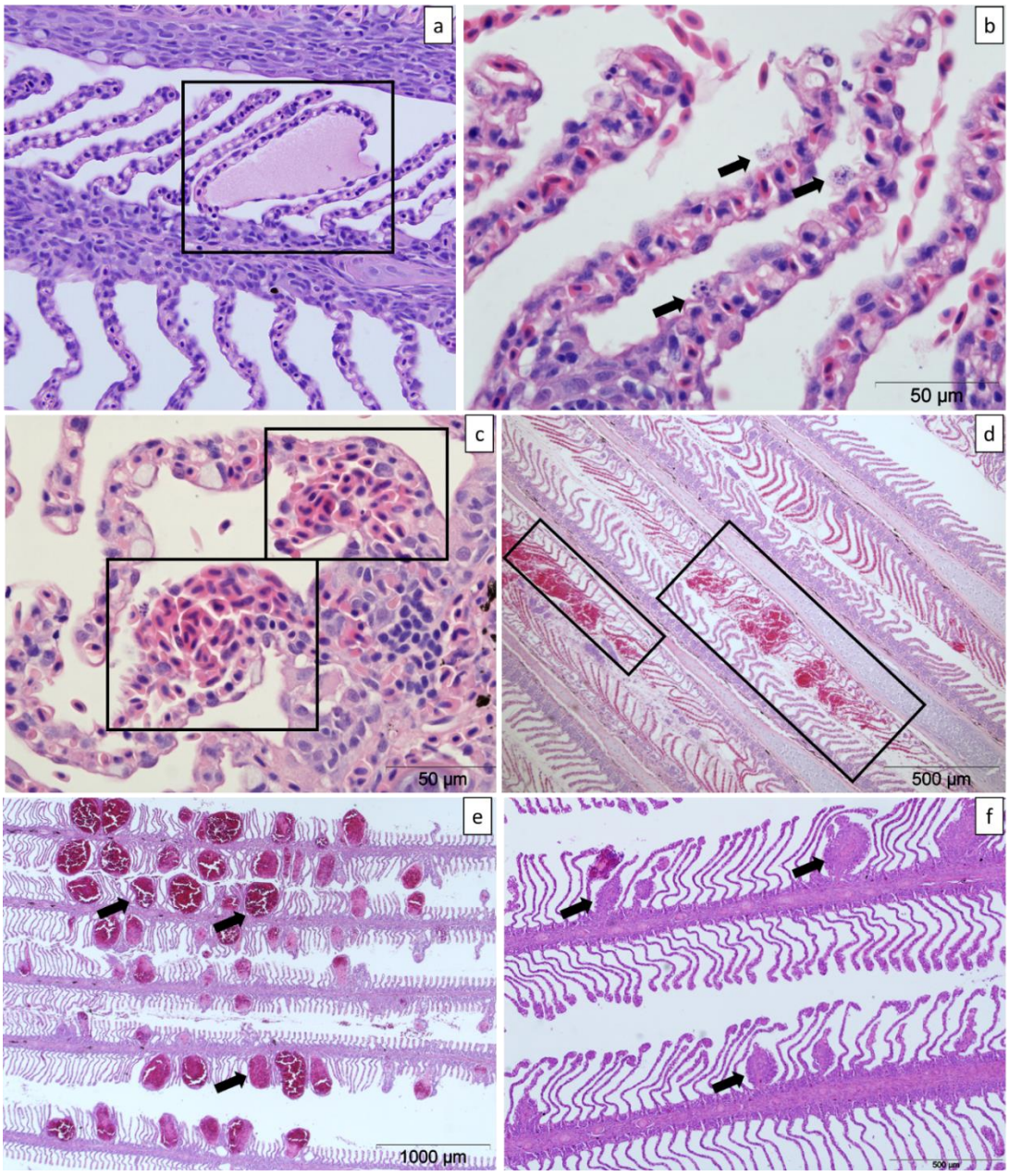

Figure 3.2. Histologic sections of gills from farmed Atlantic salmon stained with haematoxylin and eosin (H&E). (a) Focal lamellar oedema (box). (b) Epithelial cell necrosis of the lamellar outer margins (arrows). (c) Mild focal lamellar haemorrhages (boxes). (d) Two foci of lamellar tissue disruption and haemorrhage (boxes). (e) Moderate multifocal lamellar telangiectasia (arrows). (f) Mild multifocal lamellar thrombi with variable hyperplasia of the surrounding epithelium and lamellar shortening (arrows).

3.2.6 RNA extraction

RNA was extracted from gill and head kidney tissue samples stored frozen in RNAlater using an RNeasy Mini Kit (Qiagen, Hilden, Germany) with slight modification from the manufacturer's instructions. Briefly, tissues stabilized in RNAlater were removed from the reagent and placed in a sterile Eppendorf tube to determine the weight of tissue present. Approximately 30 mg of tissue were used for each extraction. Tissues were placed in separate 2 ml Lysing Matrix B tubes (Thermo Fisher Scientific, Leicestershire, UK) containing specialized beads to which 600 µl of RLT buffer with 1% beta-mercaptoethanol (Sigma-Aldrich, UK) was added. Tubes were vortexed for 15s and placed into a tissue homogeniser (Percellys24, Bertin Instruments, France) for 3 × 23 second cycles at 5,800 revolutions per minute (rpm). Tubes were placed on ice for 2 min between cycles. Samples were then centrifuged for 5 min at 9,000 x g. The resulting supernatant was removed carefully by pipetting, transferred to a new DNase-free microtube (Thermo Fisher Scientific) and 70% ethanol was added in the same volume as the contents of the tube. A total of 700 µl of the previous mixture was collected and transferred to an RNeasy spin column in a 1 ml collection tube and centrifuged for 15 s at 9,000 x g. The resultant flow-through was discarded and any residual DNA was digested on the RNeasy Plus mini kit column with DNase I (Qiagen) by adding 350 µl Buffer RW1 to the RNeasy spin column and the tube centrifuged for 15 s at 9,000 x g to wash the spin column before adding 10 µl DNase I stock solution to 70 µl Buffer RDD. The DNase mix (80 µl made up of 10 µl DNase I stock solution and 70 µl Buffer RDD) was applied directly to the RNeasy spin column membrane and incubated for 15 min at 20-30ºC before adding 350 µl of Buffer RW1 to the RNase spin column and centrifugation for 15 sec at 9,000 x g. The flow-through was discarded, 500 µl of Buffer RPE was added to the RNeasy spin column and the tube centrifuged for 2 min at 9,000 x g. This step was repeated twice more. Finally, the RNeasy spin column was placed in a new 1.5 ml Eppendorf tube, 35 µl of RNase-free water was added directly to the spin column and tubes were centrifuged for 1 min at 9,000 x g. A total of 5 µl was collected in a micro-centrifuge tube and the RNA content quantified spectrophotometrically (see below). The rest of the RNA was stored at -80°C or used in RT-rtPCR assays.

RNA yield was determined using a Nanodrop ND1000 spectrophotometer (Thermo Scientific, Waltham, USA). The ratio of absorbance at 260 nm: 280 nm and the 260 nm:230 nm absorbance was used to assess the purity of RNA; RNA was only used if both ratios were > 2. A few samples with a lower ratio were cleaned by a second RNeasy Plus mini column (Qiagen) as per manufacturer's instructions. Assessment of the RNA integrity was analysed in one in every twenty samples using an RNA 6000 Nano total RNA kit and 2100 Bioanalyzer (Agilent Technologies, Wokingham, UK) which provides quantitative information about the general state of the RNA sample. An RNA integrity number (RIN) above 7.0 was considered optimal.

3.2.7 cDNA synthesis

Synthesis of cDNA was performed using the Maxima First Strand cDNA Synthesis Kit (Thermo Fisher Scientific). Each reverse transcription (RT) master mix used to synthesise cDNA contained a total of 2µg of DNase-treated isolated RNA, 4 µl of 5X Reaction Mix and 2µl of Maxima Enzyme Mix. Nuclease-free water was added to a total volume of 20 µl per reaction. The sample was then mixed gently and centrifuged at 9,000 x g for 2 min. For cDNA synthesis, the reaction was incubated for 10 min at 25°C followed by 30 min at 50°C, followed by heating at 85°C for 5 min. The cDNA was aliquoted and used immediately. For longer storage, RNA samples were kept at -80°C. A negative control lacking reverse transcriptase (RT- control) was prepared by excluding Maxima Enzyme in the RT master mix in order to check for contamination of genomic DNA in the RNA samples. No template control (NTC), which contained all reagents for the RT reaction except for the RNA template, was used to check for contamination of the reagents.

3.2.8 Reverse-transcription real-time polymerase chain reaction assay validation

Two step RT-rtPCR was conducted in duplicate in 96 well PCR plates (Thermo Fisher Scientific, UK) using Path-ID™ qPCR Master Mix (Thermo Fisher Scientific, UK) as per manufacturer's instructions. The reaction volume was 25 µl. The RT-rtPCR reaction was run in a 7500 Fast Real-Time PCR System Cycler (Applied Biosystems, Paisley, UK) using the following conditions: 95°C initial denaturing for

10 min followed by 40 cycles of 15s denaturing at 95°C, and 60s annealing/extension at 60°C. Positive and negative control samples for each run consisted of a known positive cDNA and water only samples, respectively, subjected to the same RNA extraction process as the rest of the tissues. Results were accepted when the Ct value of the positive control fell within a defined range (Ct ≤ 40) and all negative controls failed to amplify.

For the RT-rtPCR, published primers and probes were purchased from Eurofins genomics (Acton, UK; see Table 3.6 for primer and probe sequences) for *Ca*. B. cysticola (Mitchell *et al*., 2013), *D. lepeophtherii* (Nylund *et al*., 2010), SGPV (Gjessing *et al*., 2015) and *P. perurans* (Fringuelli *et al*., 2012). A house-keeping gene, elongation factor 1 α (ELF) was used as an endogenous control (Bruno *et al*., 2007) and detection was carried out duplexing (targeting both the housekeeping and target genes). Probes for target genes were labelled with 5′ 6FAM, fluorescent dye 6-carboxyfluorescein, and 3′BH1, black hole quencher; and probes for the housekeeping and probes were labelled with 5′ 6VIC, fluorescent dye 2'-chloro-7'-phenyl-1, 4-dichloro-6-carboxyfluorescein.

3.2.8.1 *In-silico* evaluation of primers and probes

The validation of primers and probes included theoretical evaluation using the basic local alignment search tool BLAST to search for sequences similarities.

3.2.8.2 Optimization of primer concentration and effects of multiplexing

Field samples previously tested and shown to be RT-rtPCR positive in other laboratories (FVG Norway, Oslo) were used to optimise the primer concentration for the RT-rtPCR for all the target agents. Concentrations of primers tested were 100, 300 and 600 nM, with a probe concentration of 200 nM, and differences in Ct-values were compared. When ideal concentrations of primers were chosen for the target pathogens, results were compared between singleplexing and multiplexing the assays with 20 nM and 40 nM of ELF primers and probe respectively. Each reaction was run in duplicate.

3.2.8.3 Standard curve, efficiency, linearity and correlation coefficient

Five-fold serial dilutions of cDNA in which the genes of interest were known to be present were analysed by RT-rtPCR. Standard curves were obtained by plotting the threshold cycle (Ct) values of the dilutions of the target nucleic acid and efficiency (E) was calculated using the formula $E = 10^{(-1/slope)}-1$. The correlation coefficient of regression (R^2) indicated the linearity of the standard curve. Each reaction was tested in duplicate.

Table 3.6. Sequence of primers and probes used for quantitative RT-rtPCR in the present study.

Primers and probes	Sequence	Tm	GC	Accession Number	Target Gene	Position (base)	Amplicon Size (bp)	Reference
Fwd_Desmo	CGGACAGGGAGCATGGTATAG	58ºC	57%	FJ59481	16S rRNA	522-542	59	Nylund *et al*. (2010)
Rev_Desmo	GGTCCAGGTTGGGTCTTGAG	60ºC	60%			580-561		
Probe_Desmo	TTGGCGAAGAATGAAA	60ºC	38%			544-559		
Fwd_SGPV	ATCCAAAATACGGAACATAAGCAAT	56ºC	32%	KT159937	D13L ORF	99130-99154	101	Gjessing *et al*. (2015)
Rev_SGPV	CAACGACAAGGAGATCAACGC	59ºC	52%			99230-99210		
Probe_SGPV	CTCAGAAACTTCAAAGGA	46ºC	39%			99173-99190		
Fwd_Branch	AATACATCGGAACGTGTCTAGTG	56ºC	43%	JQ723599	16S rRNA	98-120	122	Mitchell *et al*. (2013)
Rev_Branch	GCCATCAGCCGCTCATGTG	60ºC	63%			201-219		
Probe_Branch	CTCGGTCCCAGGCTTTCCTCTCCCA	67ºC	64%			165-189		
Fwd_Neop	GTTCTTTCGGGAGCTGGGAG	59ºC	60%	EF216905	18S rRNA	191-210	139	Fringuelli *et al*. (2012)
Rev_Neop	GAACTATCGCCGGCACAAAAG	60ºC	54%			307-327		
Probe_Neop	CAATGCCATTCTTTTCGGA	52ºC	42%			236-254		
Fwd_ELF	GGCCAGATCTCCCAGGGCTAT	63 ºC	62%	AF321836	ELF	1106-1126	66	Bruno *et al*. (2007)
Rev_ELF	TGAACTTGCAGGCGATGTGA	58 ºC	50%			1153-1172		
Probe_ELF	CCTGTGCTGGATTGCCATACTG	60 ºC	55%			1130-1151		

Note: 16S ribosomal small subunit rRNA gene (16S rRNA), 18S ribosomal small subunit rRNA gene (18S rRNA), vaccinia virus D13L open reading frame (D13L ORF), elongation factor a 1 gene of Atlantic salmon and rainbow trout (ELF) and melting temperature of the probes (Tm)

3.2.9 Statistical analysis

Statistical analyses were performed using R (R software, v. 3.5.3; https://www.r-project.org/). Different seasons were divided as follows: Winter was considered to occur from the 21stDecember, January, February and until 19th March (Winter-1 and Winter-2 occurred in 2016 and 2017 respectively); Spring was considered to be from 20th March, April, May and until 19th June; Summer included 20th June, July, August and until 21st; Autumn included 22nd September, October, November and until 20th December.

Generalised additive models (GAMs) were used to represent changes over time of the RNA loads (expressed as Ct values) of the different infectious agents in the gills of salmon at the various sampling points in the two farms, and to represent the variation of the gill score across time and farms. GAMs fit non-parametric "smooth" functions to the data. Four different GAMs, which each seek to explain the data, were tested to predict the changes over time for each pathogen, and the changes of the histological gill score over time. Model 0 used only Farm ID as a predictor, without smoothing functions. For model 1, Farm ID plus the non-parametric smooth of week was used. In model 2, the interaction between smoothed week and Farm ID was used, but the two farms had the same intercept. Finally, model 3 used the interaction between smoothed week and Farm ID, and also fitted different intercepts in the two farms. The best-fitting model was determined by selecting the model with the lowest Akaike information criterion (AIC) value .

Linear regression models were used to study the possible associations between gill score and different explanatory parameters. The data fitted the assumption of a general model. In general, analyses started with an initial 'full' model and were then simplified by a stepwise fashion to remove non-significant predictors. The deletion stopped when all the present predictors in the model were significant. Statistical significance was inferred when $p \leq 0.05$. Initial models were simplified by removing nonsignificant terms in the order of least significance as determined by p-values calculated from Wald F-tests. Linear model 1 (LM1) of gill score included the following explanatory variables: the presence or absence each pathogen (with the exception of *Ca*. B. cysticola), together with the effect of oxygen, salinity, season

and farm identity (FarmID). *Candidatus* B. cysticola was excluded from the analysis because of the high percentage of positive samples found in the gills analysed, and therefore, effect of presence or absence of the pathogen in the score could not be calculated.

In model 2 (LM2), we used the same structure as LM1, except that the analysis included the Ct value results from the different pathogens, including Ct values for Ca. B. cysticola, instead of its presence/absence. Negative results were transformed to 40s (established limit of detection for all the pathogens). All the other predictors remained the same as in LM1. Some of the predictors, such as the type of net cleaning or use of treatments, differed vastly between farms and therefore it was not possible to account for these factors in models in which scores from both farms were used. Normalization of the obtained Ct values for the target genes with the housekeeping gene (ELF) in form of ΔCt (ΔCt = Ct (gene of interest) – Ct (housekeeping gene)) was not considered necessary due to the consistency of the ELF gene throughout the study (further information in section 3.3.1.6). The word "load" of pathogen is always used to refer to the relative RNA loads detected by RT-rtPCR and expressed as Ct values.

Models 3, 4, 5 & 6 (LM3, LM4, LM5, LM6, respectively) studied the potential effects of the days since the last peroxide treatments, non-medicinal mechanical de-lousing treatments, and net cleaning with high pressure methods on the gill score of fish at Farm B only, which suffered an outbreak of gill disease during the study. In addition, LM3 studied the potential effect of the presence of the pathogens in the gill score, whilst LM4 included the Ct values of the pathogens in the model. For LM5 and LM6 the same parameters as in LM3 and LM4 were used but the potential effect of season was substituted by temperature.

Binomial generalised linear models were used to study the relationship between farms and season with the percentage of fish positive for the pathogens, and also to test the association between the variation of the Ct values of *Ca*. B. cysticola and the presence of epitheliocysts in the gill score. A quadratic effect of temperature was fitted for associations with the variation of the Ct values of each pathogen. If the

quadratic term was not supported, then linear terms were tested for associations between temperature and variations in the Ct variations.

3.3 Results

3.3.1 Assay validation

3.3.1.1 RNA extractions

All RNA extracted from chosen samples had a RIN (RNA integrity number) value above 7.0.

3.3.1.2 *In silico* evaluation of the probes

Desmozoon lepeophtherii primers and probe showed a 100% alignment with the fish parasites *N. cyclopteri* and *N. salmonis*, which are microsporidian parasites of the lumpsucker (*Cyclopterus lumpus*) and different salmon species, including Atlantic salmon, respectively. The parasite *N. cyclopteri* has not been reported in Atlantic salmon and no cross reactivity was expected. Whilst potential cross reaction could occur with *N. salmonis*, the parasite has not been reported in Scotland or Norway and therefore the risk of false positives due to this cross-reaction was considered to be very low.

Separate BLAST searches for the forward primer, reverse primer or probe sequences of SGPV, *P. perurans* and *Ca*. B. cysticola showed similarities with other sequences unrelated to fish. However, none of the three sequences matched the sequence of any organism known to be associated with fish.

3.3.1.3 Effect of primer concentration in assays

Differences between 300 and 500 nM of primers resulted in a variation of <1 Ct value when compared in all the assays. This variation was considered acceptable, and therefore a primer concentration of 300 nM was used in all the RT-rtPCR assays.

3.3.1.4 Effect of multiplexing

The RT-rtPCR results from runs on field cDNA dilution series showed mostly less than one Ct difference between singleplexing and duplexing when run in all assays (see table 3.7. for example).

Table 3.7. Example of effect on assay performance comparing the effect of singleplexing and duplexing for *D. lepeophtherii.* SD (Standard deviation).

Positive sample	Singleplexing	SD	Duplexing	SD
Sample	21.54	0.02	21.52	0.19
Sample 5^{-1}	24.65	0.28	25.02	1.57
Sample 5^{-2}	27.47	0.09	28.26	0.18
Sample 5^{-3}	29.65	0.38	30.13	1.30
Sample 5^{-4}	31.62	0.22	31.81	0.45

3.3.1.5 Standard curves

The slope of the standard curve for *D. lepeophtherii* was -3.60, indicating an amplification efficiency of 89.57%, with a correlation coefficient of 0.99. The slope for *P. perurans* was -3.23, which represented an amplification efficiency of 103.98% and a correlation coefficient of 0.99. For SGPV, the slope was -3.17, with an amplification efficiency of 106.76% and a correlation coefficient of 0.98. Finally, for *B. cysticola* the slope was -2.66, the amplification efficiency 137.65% and the correlation coefficient was 0.97. Details of the standard curves are in Figure 3.3.

3.3.1.6 Consistency of the house keeping gene values

A total of 237 gills were analysed by RT-rtPCR for the detection of the four pathogens investigated in this study. Each RT-rtPCR reaction was carried out in duplicate and by duplexing with the primers and probes of the house keeping gene ELFα. Therefore, a total of 1896 RT-rtPCR reactions were run in this study, from which the consistency of the ELFα could be tested. From the total 1896 reactions, the mean and standard deviation of the ELFα Ct values were 14.83 and 0.39, respectively. For the 472 reactions run targeting *D. lepeophtherii*, the mean and standard deviation of the ELFα Ct values were 14.91 and 0.44, respectively. For the 472 reactions run targeting *Ca*. B. cysticola, the mean and standard deviation of the ELFα Ct values were 14.83 and 0.36, respectively. For the 472 reactions run targeting SGPV, the mean and standard deviation of the ELFα Ct values were 14.82

and 0.37, respectively, and for the 472 reactions run targeting *P. perurans*, the mean and standard deviation of the ELFα Ct values were 14.90 and 0.38, respectively.

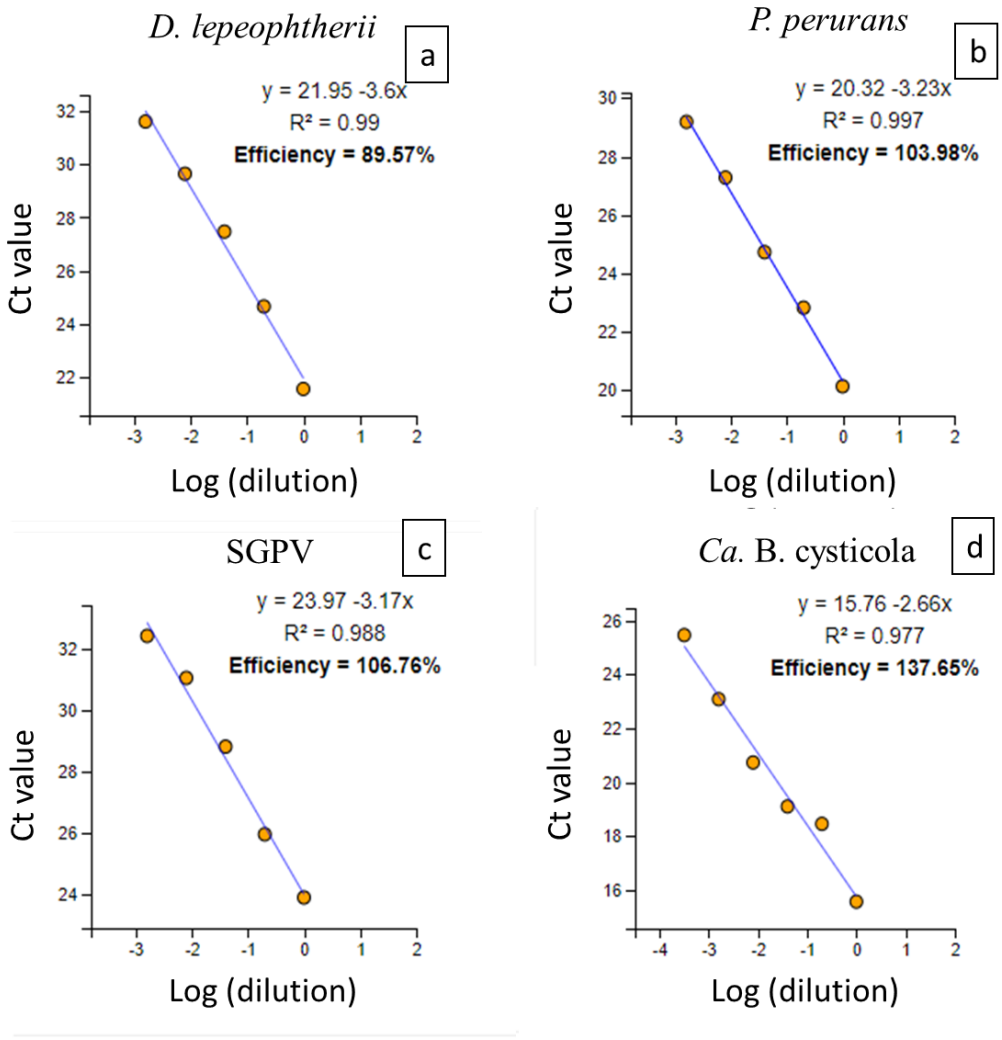

Figure 3.3. Standard curves for (a) *D. lepeophtherii* (b) *P. perurans*, (c) SGPV and (d) *Ca.* B. cysticola (d). Each figure shows the slope, correlation coefficient (R^2) and amplification efficiency.

3.3.1.7 Detection of pathogens in farms

All the putative pathogens were detected in Farm A and B. These findings are further explained in Section 3.3.5. The RT-rtPCR results are summarised in Tables 3.8 and 3.9.

Table 3.8. Farm A qRT-PCR results for the tested pathogens and % of positive fish at different sampling points. ND= Non-detected.

	D. lepeophtherii		*Ca*. B. cysticola		*P. perurans*		SGPV	
Week	% positive	Ct average (range)	% positive	Ct average (range)	% positive	Ct average (range)	% positive	Ct average (range)
1	0%	-	100%	31 (28-34)	0%	-	100%	24 (21-29)
6	17%	32 (32-ND)	100%	25 (23-29)	0%	-	0%	-
10	67%	31 (28-ND)	100%	24 (20-26)	0%	-	0%	-
14	100%	31 (26-39)	100%	24 (22-25)	0%	-	0%	-
19	100%	29 (26-32)	100%	19 (17-23)	0%	-	0%	-
23	100%	29 (24-35)	100%	20 (18-23)	0%	-	0%	-
28	100%	25 (22-31)	100%	24 (23-25)	0%	-	100%	33 (32-34)
30	100%	25 (23-26)	100%	25 (23-29)	0%	-	100%	33 (28-39)
32	100%	24 (20-33)	100%	25 (22-29)	0%	-	0%	-
34	100%	26 (21-31)	100%	26 (21-34)	0%	-	0%	-
36	100%	24 (20-27)	100%	25 (21-31)	0%	-	17%	34 (34-ND)
38	100%	24 (21-27)	100%	25 (22-28)	0%	-	33%	36 (35-ND)
40	100%	25 (22-28)	100%	26 (22-29)	17%	31 (31-ND)	0%	-
43	100%	23 (20-25)	100%	24 (23-25)	42%	31 (25-ND)	0%	-
45	100%	25 (23-26)	100%	25 (22-26)	17%	36 (36-ND)	0%	-
47	100%	26 (23-28)	100%	27 (24-30)	17%	23 (23-ND)	0%	-
49	100%	26 (24-29)	100%	28 (23-32)	0%	-	17%	36 (36-ND)
52	100%	27 (22-31)	100%	30 (25-35)	0%	-	17%	32 (32-ND)
54	100%	28 (25-31)	100%	27 (24-32)	0%	-	0%	-
57	100%	24 (21-27)	100%	28 (23-32)	0%	-	0%	-

Table 3.9. Farm B qRT-PCR results to the tested pathogens and % of fish positive at different sampling points. ND= Non-detected.

	D. lepeophtherii		*Ca*. B. cysticola		*P. perurans*		SGPV	
Week	% positive	Ct average (range)	% positive	Ct average (range)	% positive	Ct average (range)	% positive	Ct average (range)
6	0%	-	83%	29 (24-ND)	0%	-	67%	34 (32-ND)
10	0%	-	83%	26 (25-ND)	0%	-	0%	-
14	0%	-	100%	25 (22-26)	0%	-	0%	-
19	0%	-	100%	20 (18-23)	0%	-	0%	-
23	0%	-	100%	19 (16-24)	33%	32 (30-ND)	0%	-
28	17%	34 (34-ND)	100%	24 (22-27)	100%	30 (24-36)	17%	26 (26-ND)
30	17%	32 (32-ND)	100%	25 (24-27)	100%	25 (17-29)	0%	-
32	86%	29 (24-ND)	100%	23 (22-25)	100%	21 (19-26)	86%	33 (31-ND)
34	100%	27 (22-31)	100%	24 (21-26)	100%	21 (18-24)	100%	34 (28-31)
36	100%	25 (21-31)	100%	25 (22-28)	100%	24 (21-27)	17%	36 (36-ND)
38	100%	26 (24-29)	100%	23 (22-25)	100%	20 (13-24)	0%	-
40	100%	25 (24-26)	100%	23 (19-27)	100%	19 (15-24)	0%	-
43	100%	23 (20-25)	100%	23 (22-24)	100%	25 (13-35)	83%	35 (33-ND)
45	100%	23 (21-27)	100%	23 (20-25)	100%	25 (21-32)	67%	34 (31-ND)
47	100%	24 (20-28)	100%	24 (22-26)	100%	22 (16-34)	17%	28 (28-ND)
49	100%	24 (21-24)	100%	28 (25-30)	100%	26 (19-37)	33%	37 (37-ND)
52	100%	23 (20-25)	100%	24 (21-26)	100%	27 (23-33)	0%	-
54	100%	23 (21-26)	100%	25 (20-34)	100%	31 (22-36)	0%	-
57	100%	24 (21-27)	100%	28 (23-32)	0%	-	0%	-

3.3.2 Environmental data

No extreme environmental fluctuations were observed during the study in terms of oxygen levels or temperature. In both farms, similar temperatures were recorded at the different sampling points, although these were slightly higher in Farm A during the summer months and the beginning of autumn. In Farm A, sea temperatures were between 7.6 ℃ and 8.3 ℃ between March until the beginning of May 2016. From June, temperatures were over 10 ℃, with a maximum of 13.7 ℃ recorded in September. Temperatures decreased to below 10 ℃ after January 2017. Farm B experienced temperatures between 7.4-7.9 ℃ in the months of April and May 2016, but these increased to over 10 ℃ after June. A peak in water temperatures was recorded by the end of September at 12.9 ℃, and then decreased to below 10 ℃ in January 2017. Average monthly oxygen saturation levels varied but were within optimal ranges in both farms (range of 80-110%), with slightly lower levels always recorded in Farm A. Salinity of farm A was from 27.2-33.4 ppt, whilst in farm B average salinity was recorded as 34 ppt throughout the study. Nets were cleaned *in-situ* by water high pressure in farm B every two weeks from June and May and every three weeks in Farm A using an "environmental net cleaning" method (removal of the used net and replacing with a clean one while drying the dirty one in the sun). Environmental parameters collected in Farm A and Farm B are summarised in Table 3.10.

3.4 Descriptive epidemiology

Farm A

The pen chosen as a sentinel unit from Farm A was fully stocked by February 2016. There were no major health issues encountered through the cycle in the freshwater stage and most of the mortalities were attributed to *Saprolegnia* spp. infections. Sampled fish at this stage appeared healthy and had good body condition. No major problems were reported during or immediately after transfer to sea. In February and March, a total of 0.5% cumulative mortalities were attributed to *Saprolegnia* spp. infections. From mid-May until the beginning of June, sporadic increases in numbers of *Chaetoceros socialis* and *Chaetoceros debilis* were recorded at the farm, with a

peak in the levels of algae recorded during the last week of May (180,000 cells L^{-1}) (Figure 3.4a). Fish were swimming deeper at this point and staff at the site stopped feeding the fish when the levels of algae were at the highest. No significant mortalities were reported despite the high algae densities in the water. In June, some the gills of some of the fish examined (3/6) had occasional hyperaemia of the filaments and most had an increase in mucus (Figure 3.4b). During the beginning of July, a slight reduction in feed intake was noticed and fish were only eating very deep in the water column but the cause of this was unknown and nearby farms reported similar problems. One fish at that point had haemorrhagic gills after being placed into a bucket of anaesthetic. For August and September, no major concerns were raised by the staff at the farm. Gill PGD scores were between 1-2 (Figure 3.5a) in a few fish, as assessed by the staff at the farm, with a few fish having petechial haemorrhages (Figure 3.5b) and/or shortening and occasional necrotic filaments. In September, fish from the observational cage were split and only half of the population remained within the pen. During for the rest of the cycle, fish gills remained in good condition with PGD scores between 1-2 (occasionally 3). However, shortening of filaments or areas of petechiae were still seen occasionally. In November a single fish was noticed to have a focal lesion suggestive of AGD (raised patch of mucus). Average AGD and PGD scores in each sampling point are summarised in Table 3.11.

PGD scores in January and February 2017 were 2-3 and fish were harvested after February when they reached a desirable weight of 5-6kg. Cumulative mortality of the total cycle in the observational unit was 5%, with monthly mortality rates always below 1% and most of these were without a diagnosis. No H_2O_2 bath or non-medicinal de-lousing treatments were used in this observation unit.

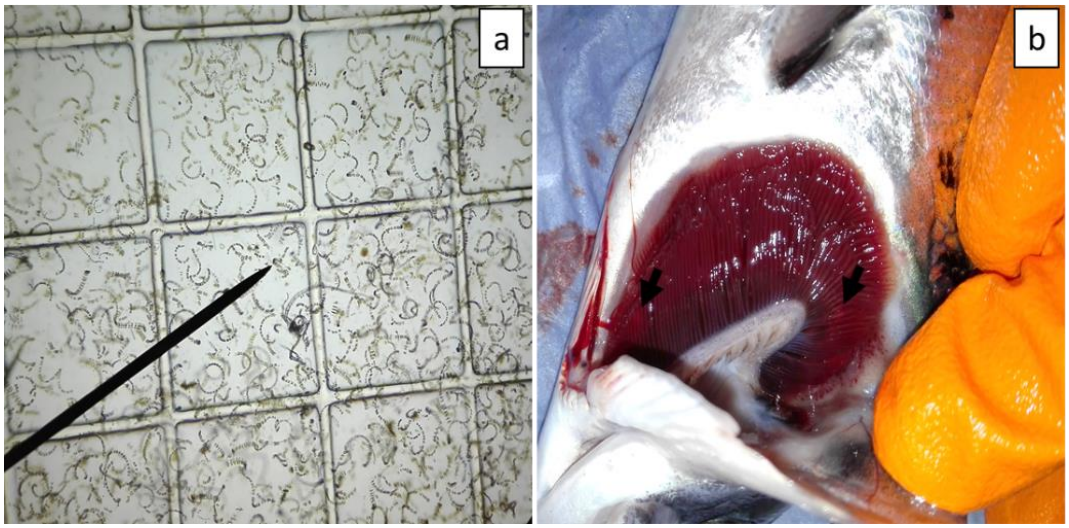

Figure 3.4. (a) Presence of abundant *Chaetoceros spp.* from a water sample at Farm A (b) Gill with hyperaemic areas (arrows) along the filamentsFarm B.

Figure 3.5. Fish from Farm A. (a) Gill with PGD of score 2, note the frequent thickening of the filaments mostly affecting the tips (white arrows). (b) Multifocal petechiae in the tips of the filaments (white arrows).

Farm B

The pen chosen as a sentinel unit from Farm B was fully stocked by March 2016. There were no major health issues encountered through the cycle in the freshwater stage and most of the mortalities were attributed to *Saprolegnia* spp. infections. No major findings were noticed during the first visits to the farm after transfer to sea

water. By the end of May an algae bloom of *C. socialis* (approximately 100,000 cells L^{-1}) that lasted approximately 5 days was recorded and staff at the site stopped feeding the fish when the levels of algae were at the highest. Gross examination of the gills at the end of May did not show any significant changes. By June, gills of most fish had very mild, focal areas of swelling along the filaments and one fish had petechial haemorrhages in the gills. In July, all fish had PGD scores of 1 and small multifocal spots of swelling along the filaments also. At the end of July, a single fish had haemorrhaging gills when placed in the bucket with anaesthetic. Gill health deteriorated by the end of August and lesions typical of AGD were present in the fish sampled. At this point gill haemorrhage was present in two of the six fish sampled when placed in a bucket with the anaesthetic (Figure 3.6a) and one fish showed frank haemorrhages (3.6b). Fish sampled also had raised patches, comprised of mucus, in the gills suggestive of amoebic gill disease (AGD scores 2-4) (Figure 3.7a) and amoebae were identified in gill scrapes. At the beginning of September AGD scores of examined fish remained high (2-3) and PGD levels were between 1-2. One of the fish had haemorrhagic gills and shortening of filaments. Similar findings were seen in the second half of September. At the beginning of October high AGD (2-3) and low PGD scores (1-2) were still present in all fish, one fish showed filament petechiae and necrotic and shortened filaments. By late October one fish had petechiae along the filaments and PGD scores were between 1-3. Small active AGD mucus patches were still observed and flat lesions, suggestive of chronic AGD, were observed also (Figure 3.7b). At the beginning of November PGD scores were between 1-3 and petechiae were seen in the tip of the filaments of two fish. Scores for AGD were 1 for all fish examined. By late November two of the fish examined had slightly pale gills and petechiae were seen within the tips of the filaments. Scores for PGD were 2-3. Lesions suggestive of AGD were still present but milder in severity appearing as flattened patches. From December until February PGD scores were between 2-4 and AGD severity had decreased (scores between 0 and 1) but it was still present, and amoebae were still observed in fresh gill smear preparations. In March no AGD patches were seen but PGD scores remained between 2-4 with multiple foci of swelling along the filaments (Figure 3.7c). At the last sampling, the average weight of the sampled fish was 3.6 kg.

The cumulative mortality of the total cycle had reached 10%, with the highest mortality occurring between September 2016 and January 2017 (monthly cumulative mortalities were between 1-1.8%). Most of the causes of deaths were referred as unknown and gill disease was never recorded as a cause in the spreadsheets. A total of three boat non-medicinal de-lousing treatments and three H_2O_2 bath treatments (normal dosage levels range from 1000 to 1400mg/l in Scotland), were performed in the sentinel net-pen. Average AGD and PGD scores in each sampling point are summarised in Table 3.11.

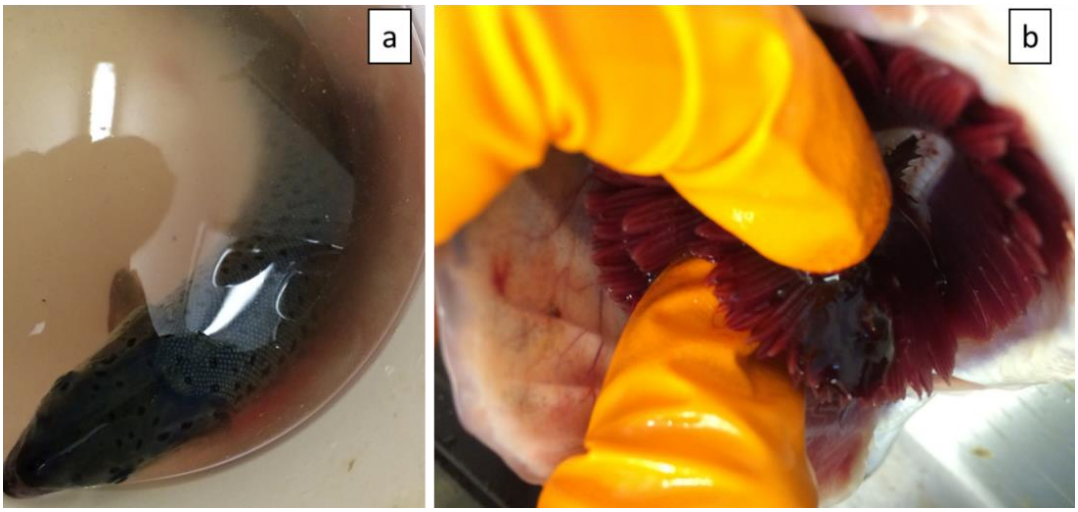

Figure 3.6. Fish from Farm B. (a) Atlantic salmon with gill haemorrhage when placed in a bucket with anaesthetic. (b) Haemorrhage in the gills.

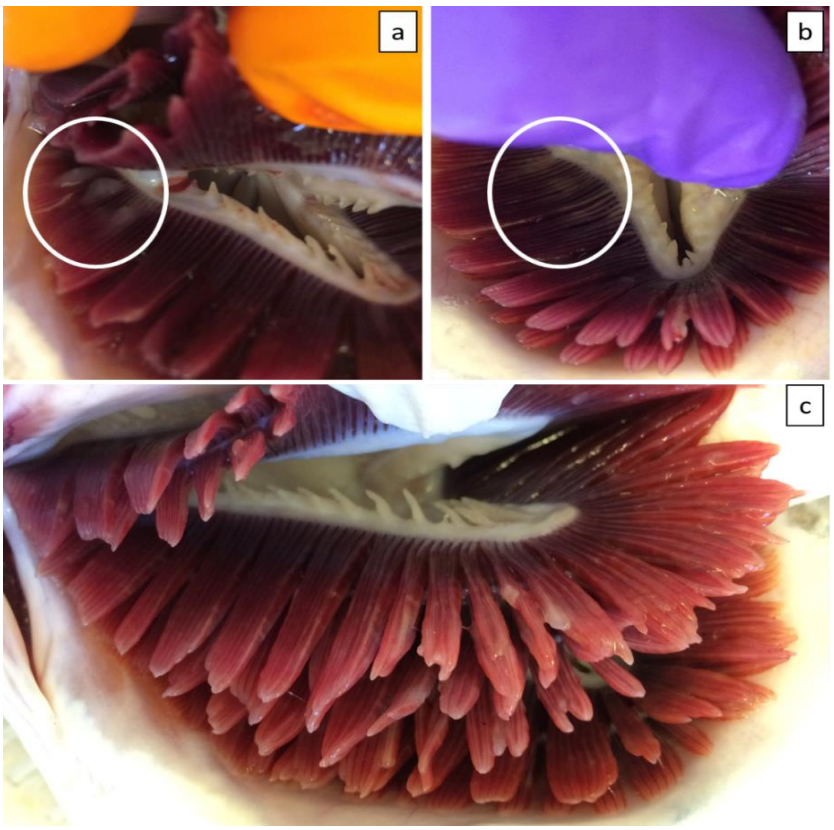

Figure 3.7. Fish from Farm B. (a) Lesions consistent with amoebic gill disease (AGD) (circle). (b) Foci of filaments swollen at the base, indicative of chronic AGD. (c) Presentation of the gills at the end of sampling in Farm B; note the slight gill pallor, multifocal swelling along the gill filaments, shortened filaments and PGD score of 2. By March 2017 fish were negative for AGD.

3.4.1 Histology

Farm A

Fish from Farm A were sampled initially in their freshwater stage before being transferred to the sea pen in February 2016. Most of the fish sampled had mild, occasionally moderate, multifocal lamellar epithelial hyperplasia and fusion, and mild to moderate multifocal changes suggestive of SGPV infection (pyknosis and karyorrhexis of the nuclei, cell blebbing and chromatin margination; Gjessing *et al*. (2015). Mild hyperplasia of the chloride cells was present also. After the fish were transferred to the sea pen in February no significant pathology was seen in the gills during the first few months. In March, low numbers of epitheliocyst structures were seen in the base of the lamellae in all of the fish sampled, consistent with descriptions of *Ca.* Clavochlamydia salmonicola infection (Karlsen *et al*., 2008) (Figure 3.8a). Minimal gill proliferative and low levels of epitheliocysts consistent with *Ca*. B. cysticola (Toenshoff *et al*., 2012) (Figure 3.8b) were seen in all fish sampled in April. In May, the presence of cysts suggestive of *Ca*. B. cysticola were still seen in all of the fish sampled, and in medium numbers in some fish (2/6) but severity of the pathology in the gills remained minimal. Most of the fish sampled (4/6) at the beginning of June had foci of necrosis in the lamellar epithelial cells, tissue sloughing and occasionally congestion, but overall the pathology remained minimal and was not considered clinically significant. In July, mild multifocal lamellar epithelial hyperplasia, mild lamellar branchitis, lamellar thrombi and epitheliocysts, consistent with descriptions of *Ca*. B. cysticola, were present in most of the fish (4/6). Fish examined in the subsequent sampling points to the end of the period of study showed minimal to mild gill pathology with non-specific lamellar epithelium proliferation and/or inflammation and occasional circulatory disturbances such as thrombi and haemorrhages probably caused by environmental or mechanical damage. A total of 7 fish, which represented 6% of the fish sampled in Farm A, had unidentified metazoan organisms 0.1-0.2 mm in length and resembling copepods (present in single to low numbers) between lamellae and were associated with mild foci of sloughed tissue (Figure 3.8c & 3.8d). Low numbers of cysts suggestive of *Ca*. B. cysticola were seen sporadically. Throughout the sampling period only two fish

had moderate gill pathology, both showed moderate thickening of the lamellar epithelium present in the distal part of some filaments (Figure 3.1f). A summary of the histology scores in each of the sampling points is shown in Table 3.11.

Farm B

The first sampling was on a freshwater site on 3 March 2016. Low numbers of *Trichodina* spp. parasites were seen in most of the fish sampled in this period (5/6) but, overall, changes seen in the gill were not considered of clinical significance. The first sampling of fish in the sea water stage was on 4 April; no significant gill lesions were noted. By the beginning of May (, some fish showed minimal gill lesions, with two out of six fish showing foci of sloughing of lamellar tissue, epithelial cell necrosis and oedema. Pathology in the gills remained minimal at the end of June, with only the presence of scattered non-specific lamellar epithelial hyperplasia, occasional lamellar branchitis and lamellar thrombi. A single epitheliocyst organism, suggestive of *Ca*. B. cysticola, was identified in one fish. During July, most of the fish sampled had mild, non-specific, lamellar proliferation and/or branchitis, indicative of low-grade irritation. Fish also had minimal to mild vascular and necrotic/disruptive lamellar lesions, most likely caused by exposure to a water-borne irritant. Similar mild changes were found in gill samples taken in August but, in addition, lesions suggestive of AGD were detected in three of the twelve fish examined, with low to moderate numbers of amoeba present in two fish. Moderate, acute pathology of multifocal areas of lamellar tissue sloughing, epithelial cell necrosis and multifocal telangiectasia and haemorrhages, was present in one fish sampled in early August. Overall, pathology found in samples collected during September was mild in most fish examined (9/13) and characterised by mild multifocal AGD lesions in association with low numbers of amoebae and mild multifocal lamellar circulatory disturbances with occasional lamellar tissue sloughing. Three fish (3/13) had mild to moderate AGD lesions. Metazoan parasites resembling copepods, as described in Farm A, were identified for the first time in 4/13 fish in September and were then present sporadically throughout the rest of the year in the gills sampled. These were usually associated with foci of tissue sloughing and occasional hyperplasia of the surrounding epithelium (Figure 3.8c & 3.9d). From

October to December lesions in the gills were mostly moderate (22/37 fish) with a few fish (3/37 fish) having severe lesions. Pathology in this period was characterised by a combination of AGD lesions (mild to moderate), presence of amoebae and multifocal lamellar thrombi, with variable hyperplasia of the surrounding epithelium, occasional sloughing of lamellar tissue, lamellar haemorrhages and necrosis. Some of the gills in this period had shortened filaments and lesions resembling PGD (proliferation of the distal part of the filaments). AGD lesions were still visible until the beginning of January 2017 but not present in the following months (late January and February 2017). Mostly minimal to mild, chronic gill pathology consisting of lamellar epithelial hyperplasia with occasional fusion and adhesions, and multiple thrombi were present at the end of January (20/24 fish) with a few fish (4/24) still showing moderate gill lesions. Overall, no clinically significant gill pathology was present at the end of February. A summary of the histology scores in each of the sampling points is shown in Table 3.11.

Unidentified metazoan organisms resembling copepods (present singly or in low numbers), similar to the ones found in farm A, were present in 24 gill samples over the investigation representing 18% of the gills examined from the marine phase. Low numbers of epitheliocysts, suggestive of *Ca*. B. cysticola infection, were identified sporadically from June but these were more common in gills examined from September onwards.

3.4.2 Summary of the variation in pathogen Ct values, epidemiology in the farms, gill score and temperatures.

A summary of the Ct values of the difference pathogens detected in the farms across the sampling points, together with the most relevant epidemiology data mentioned in Section 3.3.3, water temperature, and the gill scores for each of the fish analysed is presented in Figures 3.9 (Farm A) and 3.10 (Farm B).

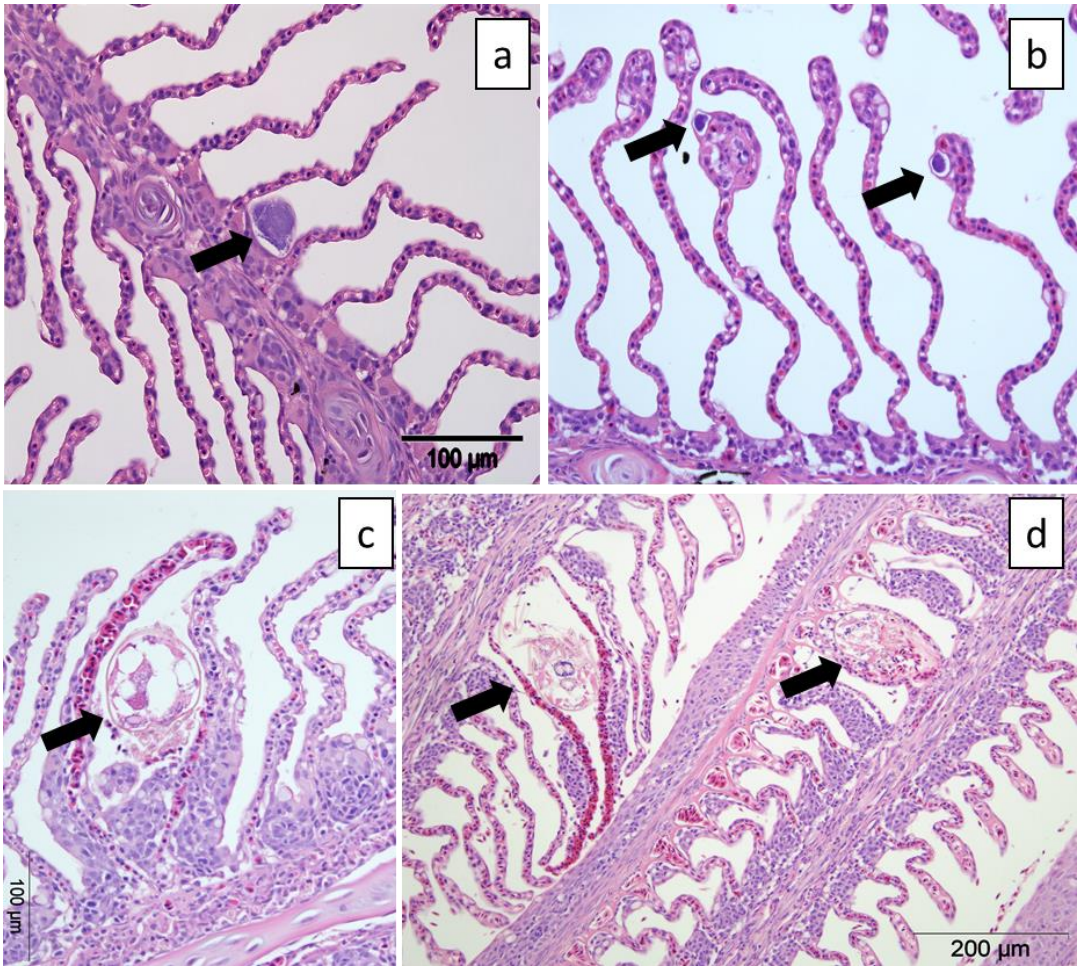

Figure 3.8. Histologic sections of gills from farmed Atlantic salmon stained with H&E. (a) Epitheliocyst in the base of the lamellae suggestive of *Ca.* Clavochlamydia salmonicola infection (arrow) (b) Epitheliocysts in the distal part of the lamellae suggestive of *Ca*. B. cysticola (arrows). (c & d) Unidentified metazoan organisms resembling copepods (arrows) between lamellae causing mild focal sloughing of tissue, lamellar epithelial hyperplasia and circulatory disturbances.

Table 3.10. Average and standard deviation (sd) of the environmental parameters measured 14 days before the sampling point.

	Oxygen Saturation (%)				Salinity (ppt)				Water Temperature (°C)			
	Farm A		Farm B		Farm A		Farm B		Farm A		Farm B	
Week	Average	sd	Average	sd	Average	sd	Average	sd	Average	sd	Average	sd
6	95.3	2.3	-	-	30.6	1.9	-	-	8.3	0.4	-	-
10	103.4	6.4	97.4	4.4	30.9	3.1	34.0	0.0	7.6	0.4	7.4	0.2
14	103.8	3.6	98.2	4.9	32.9	1.4	34.0	0.0	8.2	0.3	7.9	0.3
19	104.1	1.3	113.4	6.9	32.3	2.2	34.0	0.0	10.7	0.5	12.1	0.9
23	97.1	7.6	114.1	4.1	34.6	0.9	34.0	0.0	11.3	0.3	10.8	0.5
28	90.4	6.0	107.1	5.7	32.4	1.2	34.0	0.0	13.0	0.4	12.8	0.4
30	93.5	5.0	96.9	6.3	28.3	3.5	34.0	0.0	13.3	0.2	12.8	0.8
32	88.1	8.0	96.4	6.2	30.1	3.0	34.0	0.0	13.6	0.2	12.8	0.4
34	89.3	4.5	94.0	5.2	30.9	3.0	34.0	0.0	13.7	0.2	12.9	0.3
36	83.0	3.3	96.7	5.3	31.6	3.4	34.0	0.0	13.2	0.4	12.4	0.2
38	80.2	2.6	89.0	3.7	27.2	2.0	34.0	0.0	12.3	0.4	12.3	0.3
40	85.0	3.7	88.5	3.6	29.1	2.6	34.0	0.0	12.0	0.5	11.8	0.2
43	81.9	2.5	91.3	3.2	31.1	1.9	34.0	0.0	11.0	1.0	10.9	0.5
45	83.1	2.1	89.8	5.4	32.0	1.2	34.0	0.0	10.9	0.4	10.3	0.3
47	86.9	3.5	88.7	4.4	31.3	1.3	34.0	0.0	10.7	0.6	10.5	0.6
49	88.5	1.8	93.1	4.2	30.6	2.6	34.0	0.0	9.3	0.6	9.7	0.4
52	86.2	1.5	90.4	1.9	31.2	1.1	34.0	0.0	9.0	0.4	9.0	0.2
54	82.4	12.5	90.3	2.8	32.4	1.7	34.0	0.0	9.0	0.4	9.0	0.1
57	90.1	0.7	92.3	3.3	33.4	14.6	34.0	0.0	8.2	0.3	7.9	0.3

Table 3.11. Average histology, macroscopic AGD and PGD scores in each sampling timepoint of Farm A.

	Histology score				AGD score				PGD score			
	Farm A		Farm B		Farm A		Farm B		Farm A		Farm B	
Week	Average	sd	Average	sd	Average	sd	Average	sd	Average	sd	Average	sd
1	4.2	1.1	-	-	0.0	0.0	-	-	0.0	0.0	-	-
6	1.3	0.5	1.8	1.2	0.0	0.0	0.0	0.0	0.0	0.0	0.0	0.0
10	2.3	0.9	1.2	0.9	0.0	0.0	0.0	0.0	0.0	0.0	0.0	0.0
14	2.5	0.5	3.2	1.5	0.0	0.0	0.0	0.0	0.0	0.0	0.0	0.0
19	1.3	0.5	1.7	1.1	0.0	0.0	0.0	0.0	0.2	0.4	0.0	0.0
23	4.8	1.1	4.0	0.8	0.0	0.0	0.2	0.4	1.0	0.0	0.7	0.5
28	3.5	1.0	4.0	2.0	0.0	0.0	1.0	0.0	0.2	0.4	0.0	0.0
30	3.8	0.7	4.5	1.1	0.0	0.0	1.7	0.5	0.7	0.7	0.8	0.7
32	2.5	0.5	5.7	0.9	0.0	0.0	1.9	0.6	0.8	0.4	0.3	0.5
34	3.5	1.3	6.0	1.0	0.0	0.0	2.0	0.6	0.5	0.5	1.0	0.0
36	1.7	1.1	7.5	1.4	0.0	0.0	2.2	0.4	0.5	0.5	0.8	0.4
38	5.2	2.0	7.0	2.9	0.0	0.0	2.0	0.6	0.8	0.7	1.1	1.0
40	2.2	1.3	7.8	1.3	0.0	0.0	1.0	0.6	1.0	0.0	1.7	0.9
43	4.1	2.1	7.3	1.5	0.3	0.5	1.0	1.2	0.7	0.7	2.2	0.4
45	2.3	0.9	5.2	1.8	0.0	0.0	0.5	0.5	1.2	1.1	2.5	0.8
47	3.5	2.1	8.2	0.7	0.2	0.4	0.2	0.4	0.7	0.9	3.3	0.7
49	2.7	1.5	4.2	2.3	0.0	0.0	0.0	0.0	1.5	0.5	2.8	0.7
52	1.7	0.5	4.5	1.3	0.0	0.0	0.2	0.4	1.0	0.6	2.5	0.5
54	3.3	1.5	5.5	1.4	0.0	0.0	0.2	0.4	2.2	0.4	2.8	0.9
57	3.3	0.9	4.5	1.5	0.0	0.0	0.0	0.0	2.2	0.7	3.2	0.7

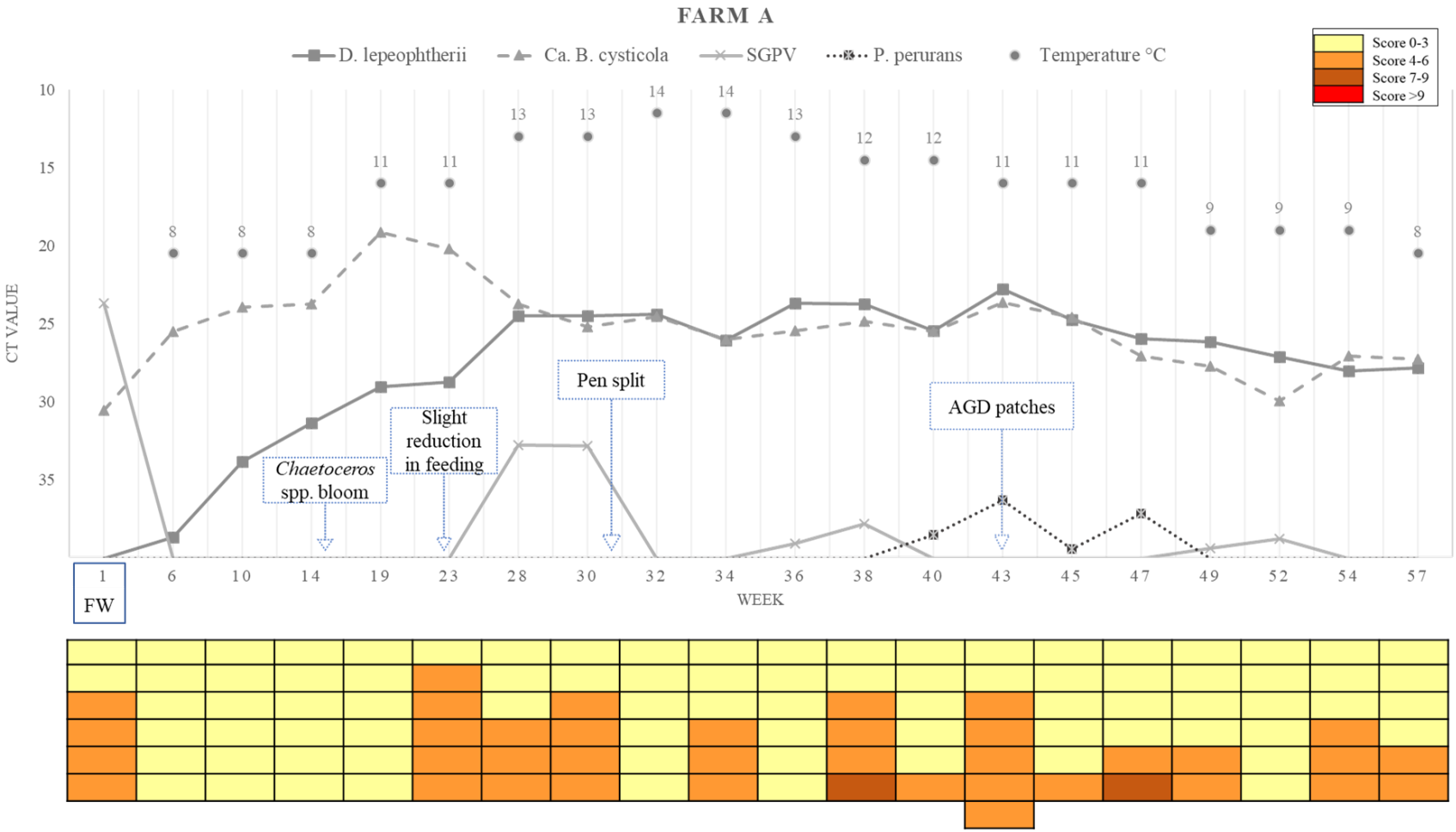

Figure 3.9. Pathogens Ct value variations, epidemiology, gill score and temperatures in each sampling week of Farm A. FW= Freshwater sampling point before transfer to Farm A.

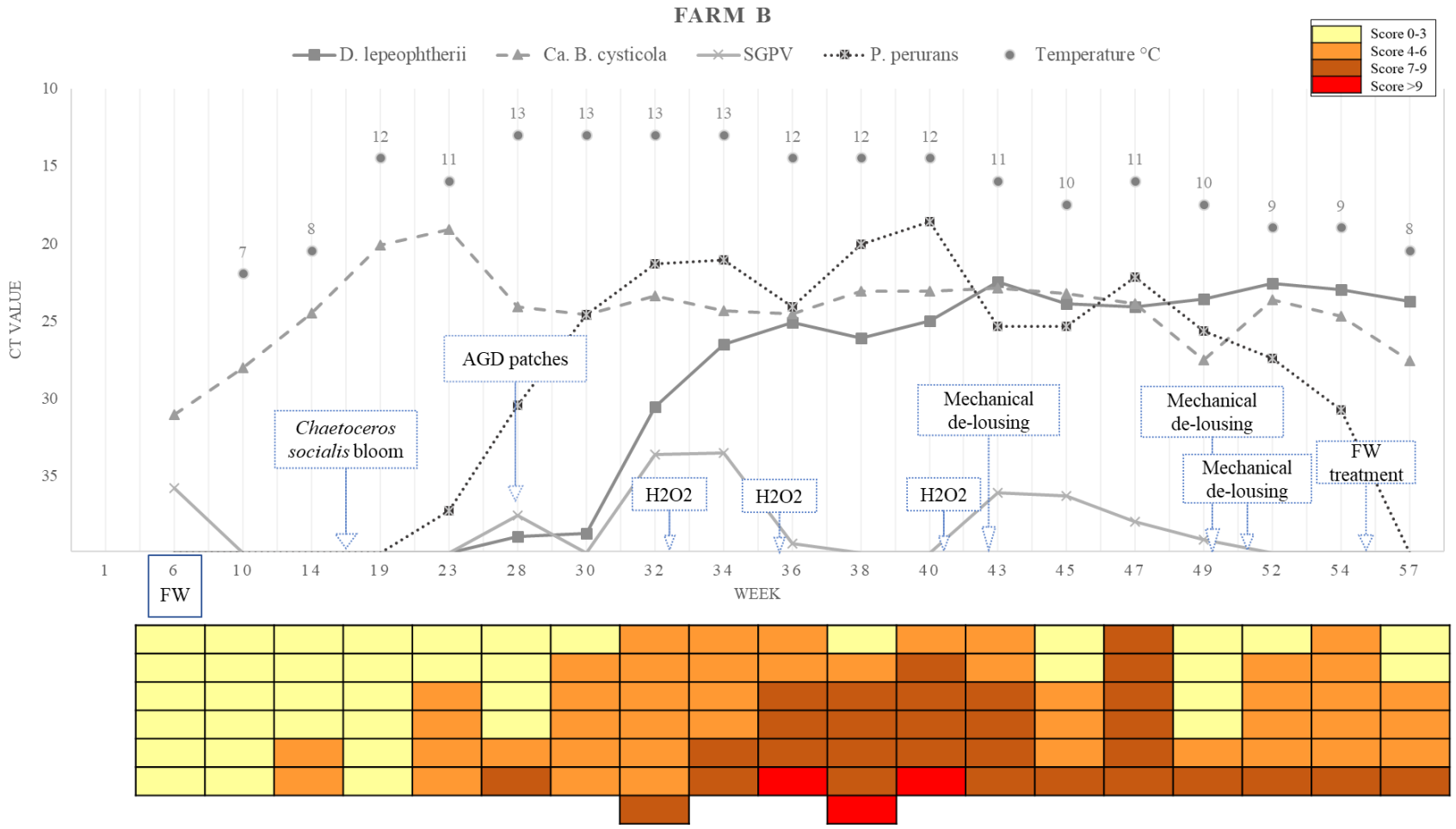

Figure 3.10. Pathogens Ct value variations, epidemiology, gill score and temperatures in each sampling week of Farm B. FW= Freshwater sampling point before transfer to Farm B.

3.4.3 Statistical analysis

3.4.3.1 Changes in the levels of the different pathogens across time

3.4.3.1.1 Comparison of GAMs for changes in levels of pathogens across time

Comparison of all GAMs for the prediction of the infectious dynamics in the gill infections by the four gill pathogens is shown in Table 3.12. Model 3, which used different smoothed data and intercepts in the two farms, always gave the lowest AIC results, which means that it provided the best fit to the data for each of the pathogens. The difference between model 2 and model 3 was <4 for SGPV and *Ca*. B. cysticola, and >10 for *D. lepeophtherii* and *P. perurans*. A lower AIC in a model indicates a better fit to the data for the future values (Ct of pathogens).

Table 3.12. Comparison of the GAMs for the prediction of Ct value for different pathogens (*D. lepeophtherii*, *P. perurans*, SGPV and *Ca*. B. cysticola) across weeks and between farms. Note that Model 3 always gave the lowest AIC results.

	AIC value of the model			
Pathogen	Model 0	Model 1	Model 2	Model 3
D. lepeophtherii	1470.037	1286.769	1166.898	1120.162
P. perurans	1463.528	1369.372	1464.715	1221.686
SGPV	1113.753	1067.951	1039.969	1038.828
Ca. B. cysticola	1189.390	1109.727	1103.921	1101.267

3.4.3.1.2 Variations of Ct values of *Desmozoon lepeophtherii*

Desmozoon lepeophtherii was first detected in the gills of one fish sampled in week 6 (10.03.2016) in Farm A (total 17% of the fish sampled). After week 14 (03.05.2020), *D. lepeophtherii* was detected in 100% of fish gills sampled throughout the rest of the year (Figure 3.11a). On Farm B, the first detection of *D. lepeophtherii* in the gills of salmon occurred in week 28 in 17% of the fish (11.08.2016). However, an increase in the percentage of positive fish to *D. lepeophtherii* was seen in week 32 (21.09.2020), with 100% of fish sampled positive. The presence of *D. lepeophtherii* was significantly associated with the seasons, and model estimates that higher percentage of positive fish were detected in summer compared with the first

sampling points in winter (estimate 2.240, SE 1.136, Z value, 1.97, p= 0.048). Presence of D. lepeophtherii was also sigfnificantly associated with the Farm ID, and estimates suggests that percentage of positive fish were significantly higher in Farm A compared with Farm B (estimate 1.974, SE 0.441, Z value -4.48, p < 0.001) (Figure 3.11b).

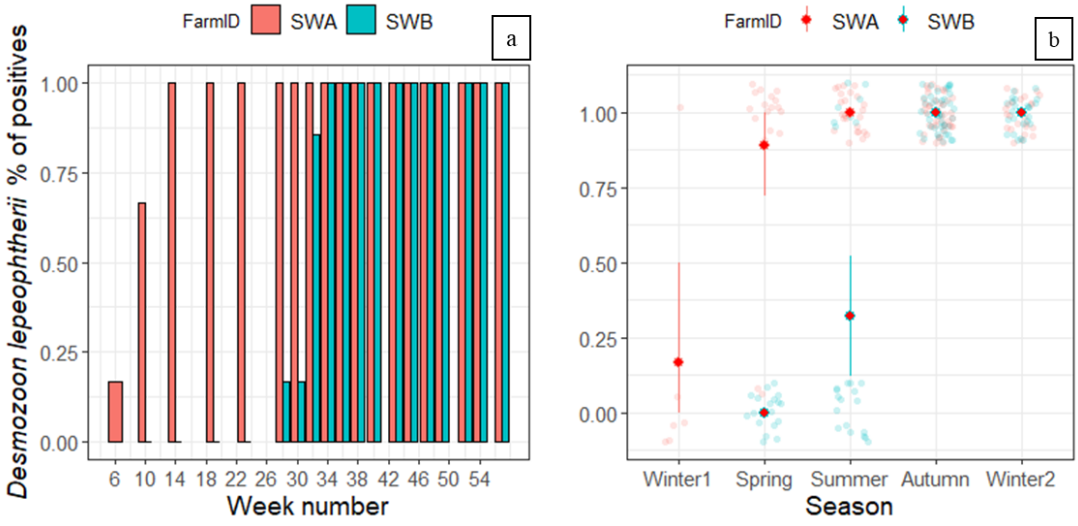

Figure 3.11. Percentage of fish positive for *D. lepeophtherii* in Farm A (SWA) and Farm B (SWB). (a) Percentage of fish positive for *D. lepeophtherii* across weeks. (b) Percentage of fish positive for *D. lepeophtherii* across seasons. In Farm A, the percentage of fish positive for *D. lepeophtherii* was significantly higher (p< 0.001) than in Farm B, and significantly higher (p< 0.001) in summer compared with the first sampling points in winter. The translucent points show the raw data, with random 'jitter' added to make the points easier to visualise, and the points with error bars show the mean for each farm and 95% CI.

The lowest Ct values, corresponding to the largest parasite load, were found between weeks 34-40 (06.09.2016- 01.11.2016) in Farm A and then the levels decreased after week 45 (07.12.2016) (Figure 3.12). In Farm B, the highest parasite load was detected in weeks 43 and 45 (sampling points in November). Contrary to Farm A, the levels of the parasite in Farm B remained high up to the last sampling points in weeks 54 and 57 (08.02.2017 and 28.02.2017) (Figure 3.12).

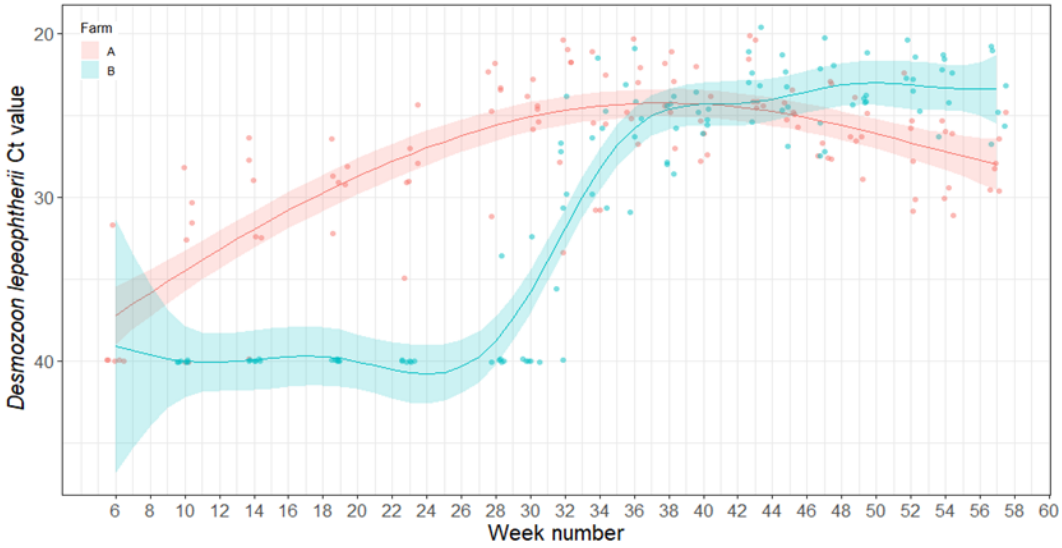

Figure 3.12. Variations of Ct values of *D. lepeophtherii* in the gills of salmon across weeks. First detection of *D. lepeophtherii* in Farm A occurred in week 6 and in Farm B in week 28. In Farm A, parasite load increased from week 10 to week 43, and then decreased from week 45 until week 57. In Farm B, parasite load increase from week 30 to week 40, and remained with high until week 57. Points show raw data and lines and shaded areas show estimates from GAM and 95% confidence interval.

3.4.3.1.3 Variations of Ct values of Ca. *Branchiomonas cysticola*

Candidatus B. cysticola was detected by RT-rtPCR in 99% of all gills examined (Figure 3.13a). Fish from both farms were positive for *Ca*. B. cysticola from the freshwater stage and remained positive throughout the marine stage. There were no statistically significant differences between the percentages of positive fish to *Ca*. B. cysticola between farms ($p \geq 0.05$) or seasons ($p \geq 0.05$) (Figure 3.13b).

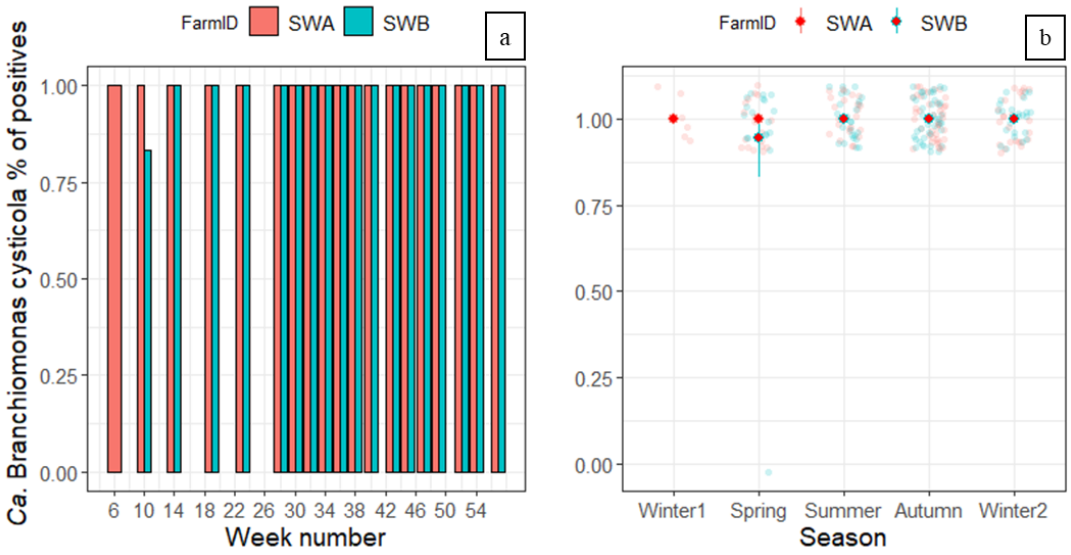

Figure 3.13. Percentage of fish positive for *Ca. B. cysticola* in Farm A (SWA) and Farm B (SWB). (a) Percentage of fish positive for *Ca. B. cysticola* across weeks. Note the high level of detection in both farms. (b) Percentage of fish positive for *Ca. B. cysticola* across seasons. Differences in percentage of fish positive for *Ca.* B. cysticola were not statistically significantly different between farms or seasons ($p \geq 0.05$). The translucent points show the raw data, with random 'jitter' added to make the points easier to visualise, and the points with error bars show the mean for each farm and 95% CI.

Levels of this bacterium increased after fish were transferred to the sea in both farms A and B, peaking in Weeks 19 and 23 in both farms (06 & 07.06.2016 and 07 & 08.07.2016) with Ct values between 16-29, and then maintaining relatively high levels during autumn (weeks 34 to 47, Ct values19-28) but decreasing after week 47 in Farm A (20.12.2016) and 49 in Farm B (05.01.2017) (Figure 3.14).

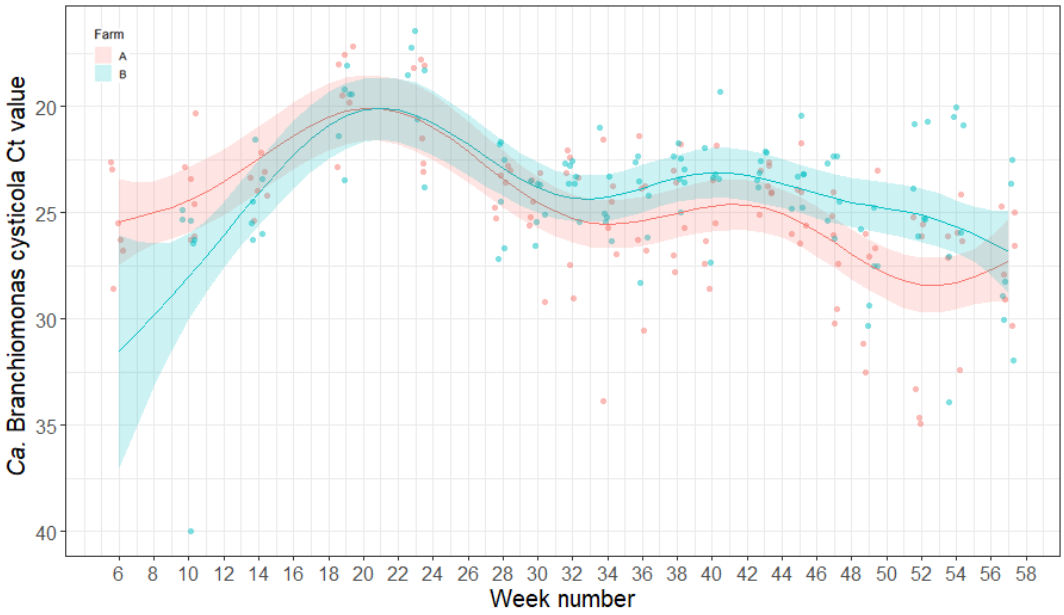

Figure 3.14. Variations of Ct values of *Ca.* B. cysticola across weeks. Note the presence of the bacterium throughout the sampling period. Levels peaked in week 19, decreased after week 24, and decreased further after week 48. Points show raw data and lines and shaded areas show estimates from GAM and 95% confidence interval.

3.4.3.1.4 Variations of Ct values of *Paramoeba perurans*

In Farm A, fish positive for *P. perurans* were detected in 17-42% of the fish sampled from week 40 to week 47 (01.11.2016-19.12.2020), respectively. In Farm B, *P. perurans* was first detected in week 23 (08.07.2016) in 33% of the fish sampled, and 100% were positive in the sampling point in week 28 (11.08.2016). All fish remained positive for *P. perurans* throughout the rest of the study until week 57 (01.03.2017), when it was no longer detected in the fish sampled (Figure 3.15a). The percentage of fish positive for *P. perurans* was significantly associated with the Farm ID, and estimates of the model suggest that numbers of positive fish were higher in Farm B compared to Farm A (estimate 3.974, SE 0.4730, Z value 8.40, $p < 0.001$) (Figure 3.15b). There were no significant differences in the percentage fish positive for *P. perurans* detected across seasons ($p \geq 0.05$).

Figure 3.15. Percentage of fish positive for *P. perurans* in Farm A (SWA) and Farm B (SWB). (a) Percentage of fish positive for *P. perurans* across weeks. (b) Percentage of fish positive for *P. perurans* across seasons. There were no significant differences between the number of positive fish detected across seasons (both farms were used in the model) ($p \geq 0.05$). The percentage of positive fish was significantly higher in Farm B compared to Farm A ($p < 0.001$). The translucent points show the raw data, with random 'jitter' added to make the points easier to visualise, and the points with error bars show the mean for each farm and 95% CI.

The number of positive fish detected in Farm A was very low (6 out of 120 fish sampled). Mean Ct value levels ranged from 31-36, with the lowest level (Ct 23) recorded on week 45 (07.12.2016). Amoeba levels in Farm B increased after week 28 (11.08.2016) then lower loads of the parasite (higher Ct values) were detected after week 43 (22.11.2016) (Figure 3.16).

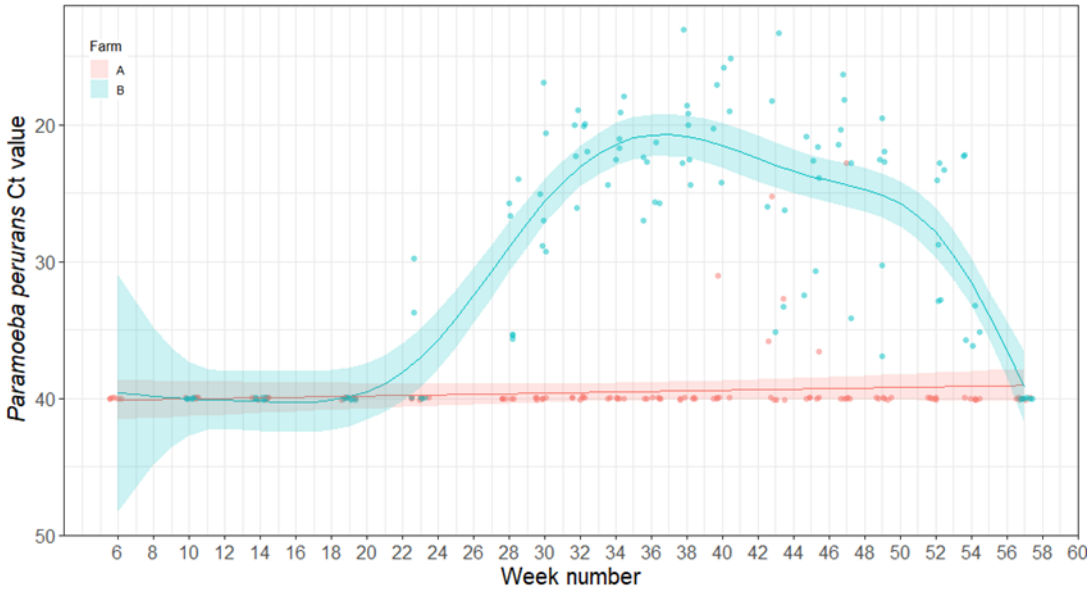

Figure 3.16. Variations of Ct values of *P. perurans* in the gills of salmon across weeks. Note how detection of *P. perurans* occurred in week 23 in a single fish, increased until week 43 and then decreased. *P. perurans* was detected in Farm B until week 57. Farm A had six positive fish between the weeks 40-47 but the rest of the fish examined were negative. Points show raw data and lines and shaded areas show estimates from GAM and 95% confidence interval.

3.4.3.1.5 Variations in Ct values for salmon gill poxvirus

All fish sampled at the freshwater stage of Farm A, before being transferred to sea, were positive for SGPV, and 67% of the fish sampled in the freshwater stage of Farm B were positive also. After transferred, the virus was detected sporadically in both farms throughout the year (Figure 3.17a). There were no statistically significant differences between the percentage of fish positive for SGPV across seasons or between farms ($p \geq 0.05$) (Figure 3.17b).

Figure 3.17. Percentage of fish positive for SGPV in Farm A (SWA) and Farm B (SWB). (a) Percentage of fish positive for SGPV across weeks. Presence of SGPV was first detected in Farm A in week 28 and then sporadically until week 52. In Farm B, SGPV was also first detected in week 28, and fish positive for the virus were found until week 49. Differences in the percentage of fish positive for SGPV were not statistically significantly different between farms or seasons ($p \geq 0.05$). The translucent points show the raw data, with random 'jitter' added to make the points easier to visualise, and the points with error bars show the mean for each farm and 95% CI.

Fish gill samples from Farm A had Ct values between 21-29 in samples taken during the freshwater stage (sampling week 1; 05.02.2016), whereas the gills of fish from the freshwater site of Farm B had higher Ct values (approximately 34) (sampling week 6; 10.03.2016). The pathogen was then sporadically detected throughout the year in both sea water farms, with the lowest Ct value being recorded in week 28 (10.08.2016) in Farm B (Ct 26), but Ct values of SGPV remained relatively high, between Ct values 28-39 in Farm A and in Farm B (Figure 3.18).

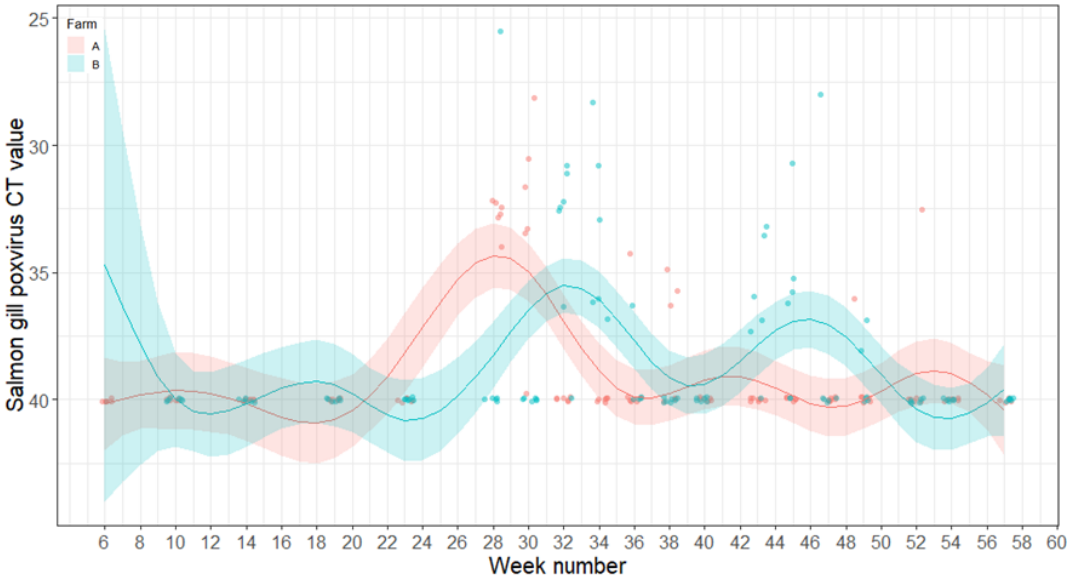

Figure 3.18. Variations of Ct values of SGPV. Sporadic detections of SGPV were detected from week 28 in both Farm A and Farm B but these did not follow a seasonal pattern and were not statistically significantly different between farms or seasons ($p < 0.01$). Fish from Farm A and Farm B were positive for the virus when tested in the freshwater stage of the cycle (data not shown). Points show raw data and lines and shaded areas show estimates from GAM and 95% confidence interval.

3.4.3.2 Linear regression models of the gill score

In LM1, the presence or absence of pathogens together with other parameters were studied as possible predictors for the increase in gill scores (Table 3.13). For this model, Farm B had a significantly higher gill score than Farm A ($p < 0.001$), the presence of *D. lepeophtherii* was significantly associated with an increase in the gill score ($p < 0.001$) and season was significantly associated with an increase in the gill score ($p < 0.001$) (Figure 3.19). Model estimates suggest that, in particular, gill score was significantly lower ($p < 0.001$) all seasons compared to autumn. For LM2 (Ct values were used instead of presence/absence of pathogens) the Farm ID was significantly associated with gill score, Farm B had a significantly greater score compared to Farm A ($p < 0.001$) (Table 3.14). Season was significantly associated with an increase in the gill score. Model estimates suggest that gill score was significantly lower ($p < 0.001$) in all seasons compared to autumn. An increase in *D. lepeophtherii* was associated with an increase in the gill score but only in Farm B, whilst in Farm A, the increase or decrease of *D. lepeophtherii* was not correlated

with any change in the gill scores (Figure 3.20a). Higher loads of *P. perurans* (lower Ct values) correlated with an increase in the gill score in both farms (Figure 3.20a).

Study of the potential predictors for changes in the gill score in Farm B (LM3 and LM4) showed only season as a significant predictor, and model estimates that gill score was significantly higher in autumn compared to other seasons (Tables 3.15 and 3.16) (Figure 3.21a). However, if season was substituted by temperature in LM5 (Table 3.17), then higher temperatures were significantly associated with the increase in gill score (Figure 3.21b). There was also a significant relationship between the increase of the score and fewer days since the last H_2O_2 treatment. LM 6 showed association between the detection of higher loads (lower Ct values) of *P. perurans* and *Ca*. B. cysticola, fewer days since net cleaning with high pressure, and fewer days since the last H_2O_2 treatment (Table 3.18).

General linear models revealed a significant positive association between the increase of *Ca*. B. cysticola loads and presence of epitheliocysts (estimate -0.138, SE 0.050, z value, -2.747, p 0.006). There was a significant association between increased gill scores in Farm A and Farm B and a reduced body condition (estimate -0.020, SE 0.007, t value -2.92, p = 0.003). However, there was no associated between the variations in the Ct values for *D. lepeophtherii* with the body condition of the fish (estimate -0.002, SE 0.003, t value -0.84, p = 0.401).

Table 3.13. Results of LM1. SE= standard error, FarmID:x pathogen = Interaction between FarmID and "x pathogen" presence, p = probability of no effect, (0) absence of the pathogen, (1) presence of the pathogen.

Variable	Estimate	SE	t value	Pr(>|t|)	F value	df	Pr(>F)
Rejected variables							
FarmID:*D. lepeophtherii* (0)	0.000	0.000	0.00	-	0.76	1	0.384
FarmID:*D. lepeophtherii* (1)	0.831	1.047	0.79	0.429			
FarmID:*P. perurans* (0)	0.000	0.000	0.00	-	3.29	1	0.071
FarmID:*P. perurans* (1)	1.571	0.865	1.82	0.071			
FarmID:SGPV (0)	0.000	0.000	0.00	-	1.94	1	0.166
FarmID:SGPV (1)	0.507	0.476	-1.39	0.166			
P. perurans (0)	0.000	0.000	0.00	-	1.49	1	0.224
P. perurans (1)	0.510	0.423	1.22	0.224			
SGPV (0)	0.000	0.000	0.00	-	0.01	1	0.935
SGPV (1)	0.027	0.328	0.08	0.935			
Oxygen	-0.012	0.028	-0.41	0.679	0.17	1	0.679
Salinity	0.116	0.106	1.09	0.277	1.19	1	0.277
Variables in final model							
Intercept	1.623	0.538	3.02	0.003			
Farm A	0.000	0.000	0.00	-	107.15	1	<0.001
Farm B	2.734	0.264	10.35	<0.001			
D. lepeophtherii (0)	0.000	0.000	0.00	-	24.66	1	<0.001
D. lepeophtherii (1)	2.126	0.428	4.97	<0.001			
Season (Autumn)	0.000	0.000	0.00	-			
Season (Spring)	-1.907	0.415	-4.60	<0.001			
Season (Summer)	-0.264	0.340	-0.78	0.439	10.09	4	<0.001
Season (Winter-1)	-0.644	0.844	-0.76	0.446			
Season (Winter-2)	-1.408	0.308	-4.57	<0.001			

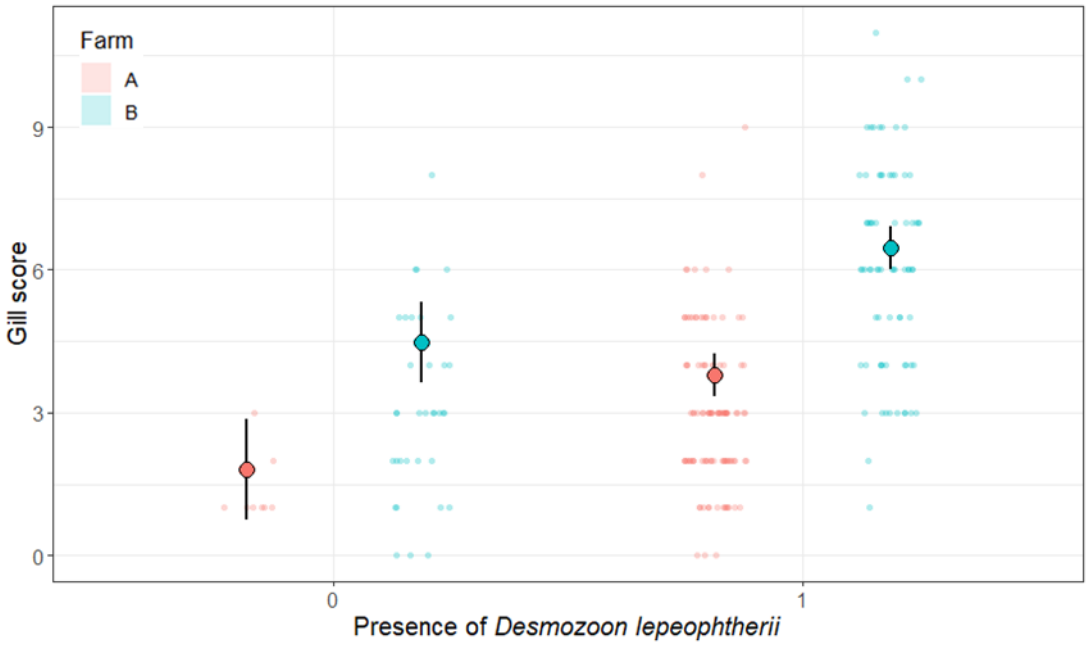

Figure 3.19. LM1 showed that both the presence of *D. lepeophtherii* and farm identity were significantly associated with gill scores (see Table 3.7 for details). Small points show the raw gill score data, while large points with error bars show predictions from LM1 and 95%CI.

Table 3.14. Results of LM2. SE= standard error, FarmID:x pathogen = Interaction between FarmID and "x pathogen" Ct value, p = probability of no effect.

Variable	Estimate	SE	t value	Pr(>|t|)	F value	df	Pr(>F)
Rejected variables							
FarmID:*Ca*. B. cysticola Ct	-0.059	0.074	-0.52	-0.793	0.43	1	0.429
FarmID:*P. perurans* Ct	-0.065	0.073	-0.88	0.380	0.77	1	0.380
FarmID:SGPV Ct	0.114	0.086	1.32	0.187	1.75	1	0.187
Ca. B. cysticola Ct	-0.071	0.037	-1.90	0.058	3.62	1	0.058
SGPV Ct	-0.005	0.045	-0.11	0.910	0.01	1	0.910
Oxygen	-0.017	0.028	-0.61	0.541	0.40	1	0.541
Salinity	0.083	0.112	0.75	0.456	0.56	1	0.456
Variables in final model							
Intercept	4.529	1.563	2.90	0.004	0.40	1	0.530
Farm A	0.000	0.000	0.00	-	-	1	<0.001
Farm B	5.931	1.545	3.84	<0.001			
Farm A:*D. lepeophtherii* Ct	0.040	0.046	0.86	0.390	8.67	1	0.004
Farm B: *D. lepeophtherii* Ct	-0.152	0.051	-2.95	0.004			
D. lepeophtherii Ct	0.040	0.046	0.86	0.390	-	1	-
P. perurans Ct	-0.049	0.024	-2.02	0.044	4.09	1	0.044
Season (Autumn)	0.000	0.000	0.00	-	7.11	4	<0.001
Season (Spring)	-1.913	0.473	-4.04	<0.001			
Season (Summer)	-0.162	0.354	-0.46	0.647			
Season (Winter-1)	-2.790	0.962	-2.90	0.004			
Season (Winter-2)	-1.307	0.339	-3.85	<0.001			

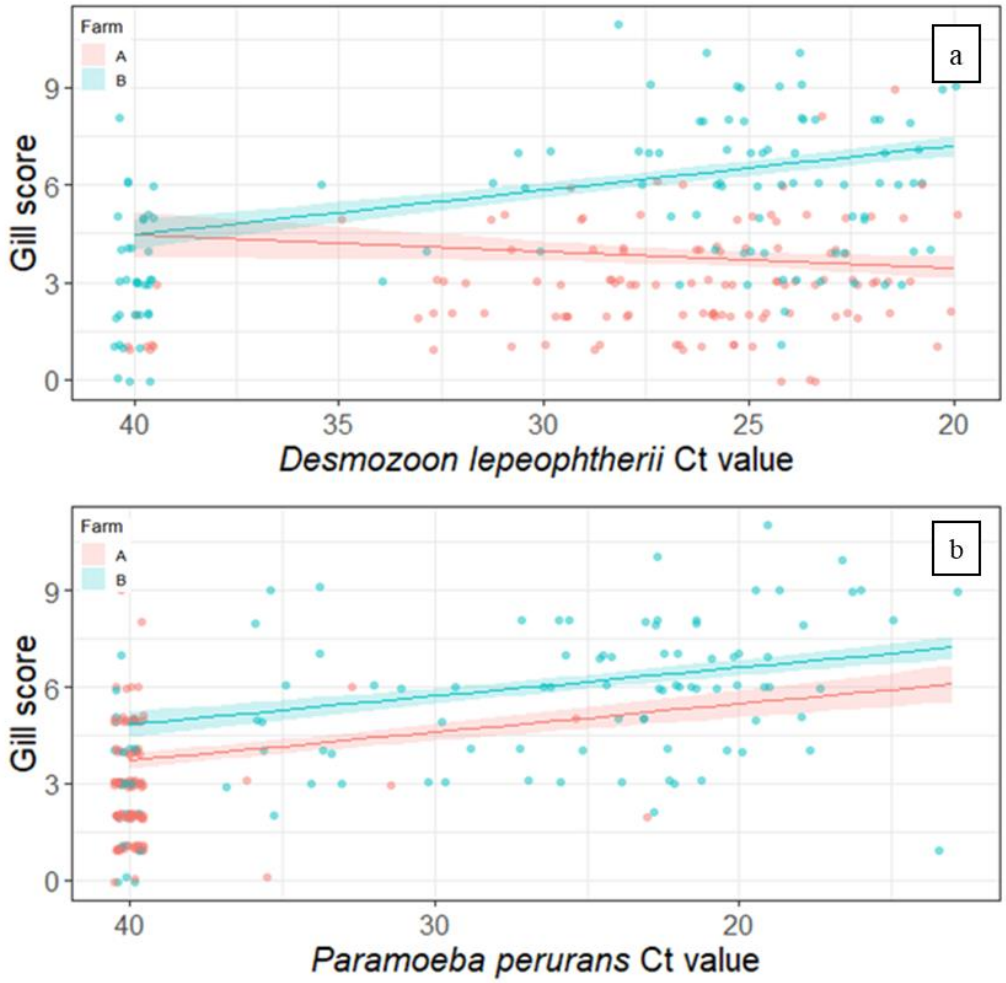

Figure 3.20.Representation of LM2. (a) The increase in the loads of *D. lepeophtherii* was significantly associated with the gill scores in Farm B but not in Farm A. (b) The increase in the loads of *P. perurans* was significantly associated with the increase of the gill scores in both Farm A and Farm B.

Table 3.15. Results of LM3. SE= standard error, p = probability of no effect, (0) absence of the pathogen, (1)= presence of the pathogen.

Variable	Estimate	SE	t value	Pr(>|t|)	F value	df	Pr(>F)
Rejected variables							
Ca. B. cysticola (0)	0.000	0.000	0.00	-	0.50	1	0.480
Ca. B. cysticola (1)	1.400	1.972	0.71	0.480			
D. lepeophtherii (0)	0.000	0.000	0.00	-	0.43	1	0.513
D. lepeophtherii (1)	0.538	0.820	0.66	0.513			
P. perurans (0)	0.000	0.000	0.00	-	0.10	1	0.748
P. perurans (1)	0.243	0.756	0.32	0.748			
SGPV (0)	0.000	0.000	0.00	-	0.11	1	0.748
SGPV (1)	-0.180	0.532	-0.34	0.736			
Days since H_2O_2 treatment	-0.009	0.012	-0.70	0.483	0.50	1	0.483
Days since mechanical treatment	-0.003	0.002	-1.45	0.764	2.12	1	0.149
Days since net cleaning	-0.002	0.002	-1.07	0.289	1.14	1	0.289
Variables in final model							
Season (Autumn)	7.000	0.268	26.12	<0.001	36.58	3	<0.001
Season (Spring)	-5.000	0.493	-10.14	<0.001			
Season (Summer)	-2.400	0.442	-5.43	<0.001			
Season (Winter-2)	-2.333	0.448	-5.21	<0.001			

.

Table 3.16. Results of LM4. SE= standard error, p = probability of no effect. Note that non-bold terms were removed from the model, and that the bold terms are the only variables in used in the final model.

Variable	Estimate	SE	t value	Pr(>|t|)	F value	df	Pr(>F)
Rejected variables							
D. lepeophtherii Ct	-0.015	0.060	-0.25	0.800	0.06	1	0.804
Ca. B. cysticola Ct	-0.068	0.053	-1.27	0.205	1.62	1	0.205
P. perurans Ct	-0.038	0.028	-1.35	0.180	1.82	1	0.180
SGPV Ct	0.010	0.071	0.14	0.888	0.02	1	0.888
Days since H_2O_2 treatment	-0.015	0.013	-1.17	0.246	1.36	1	0.246
Days since mechanical treatment	-0.003	0.002	-1.45	0.149	2.12	1	0.149
Days since net cleaning	-0.002	0.002	-0.91	0.363	0.83	1	0.363
Variables in final model							
Season (Autumn)	7.000	0.268	26.12	<0.001	36.58	3	<0.001
Season (Spring)	-5.000	0.493	-10.14	<0.001			
Season (Summer)	-2.400	0.442	-5.43	<0.001			
Season (Winter-2)	-2.333	0.448	-5.21	<0.001			

Table 3.17. Results of LM5. SE= standard error, p = probability of no effect, (0) absence of the pathogen, (1) presence of the pathogen.

Variable	Estimate	SE	t value	Pr(>|t|)	F value	df	Pr(>F)
Rejected variables							
D. lepeophtherii (0)	0.000	0.000	0.00	0.000	0.06	1	0.813
D. lepeophtherii (1)	0.205	0.863	0.24	0.813			
P. perurans (0)	0.000	0.000	0.00	0.000	1.81	1	0.181
P. perurans (1)	0.846	0.628	1.35	0.181			
SGPV (0)	0.000	0.000	0.00	0.000	0.57	1	0.451
SGPV (1)	0.382	0.505	0.76	0.451			
Days since mechanical treatment	-0.004	0.002	-1.80	0.074	3.25	1	0.074
Days since net cleaning	-0.001	0.002	-0.33	0.743	0.11	1	0.743
Variables in final model							
Water temperature	0.482	0.099	4.88	<0.001	23.78	1	<0.001
Days since H_2O_2 treatment	-0.008	0.001	-7.72	<0.001	59.62	1	<0.001

Table 3.18. Results of LM6. SE= standard error, p = probability of no effect.

Variable	Estimate	SE	t value	Pr(>|t|)	F value	df	Pr(>F)
Rejected variables							
D. lepeophtherii Ct	0.037	0.061	0.61	0.544	0.37	1	0.544
SGPV Ct	-0.050	0.071	-0.70	0.489	0.48	1	0.489
Days since mechanical treatment	-0.002	-0.002	0.00	-0.983	0.97	1	0.328
Water temperature	0.150	0.139	1.08	0.283	1.16	1	0.283
Variables in final model							
Ca. B. cysticola Ct	-0.154	0.056	-2.74	0.007	7.53	1	0.007
P. perurans Ct	-0.069	0.030	-2.33	0.022	5.42	1	0.022
Days since H2O2 treatment	-0.004	0.001	-3.27	0.001	10.71	1	0.001
Days since net cleaning	-0.004	0.002	-2.07	0.041	4.28	1	0.041

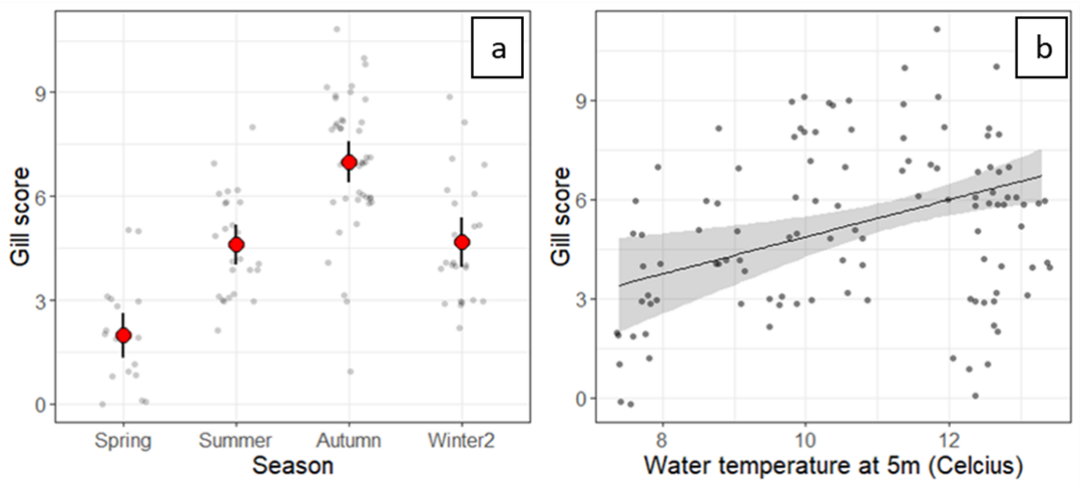

Figure 3.21. Representation of linear regression models with the gill score of Farm B. (a) Model LM3 & LM4, note the strong association between season and gill score in Farm B, the points show raw data; small points show the raw gill score data, while large points with error bars show predictions from models and 95%CI. (b) Model LM5, when temperature was used instead of season then temperature, the increase of temperature was significantly associated with the increase in the gill score line and shaded area show predicted gill score ± 95% confidence intervals

3.4.3.3 Effect of temperature on pathogens loads

A quadratic effect of temperature was significantly associated with the increase in loads of *D. lepeophtherii* ($p<0.001$) (Figure 3.22a), *P. perurans* ($p<0.001$) (Figure 3. 22b) and *Ca*. B. cysticola ($p<0.001$) (Figure 3.22c). No significant association was found between a non-linear (quadratic) effect of temperature with SGPV Ct values ($p>0.05$), but water temperature was significantly associated in linear terms ($p<0.001$) (Figure 3.22d).

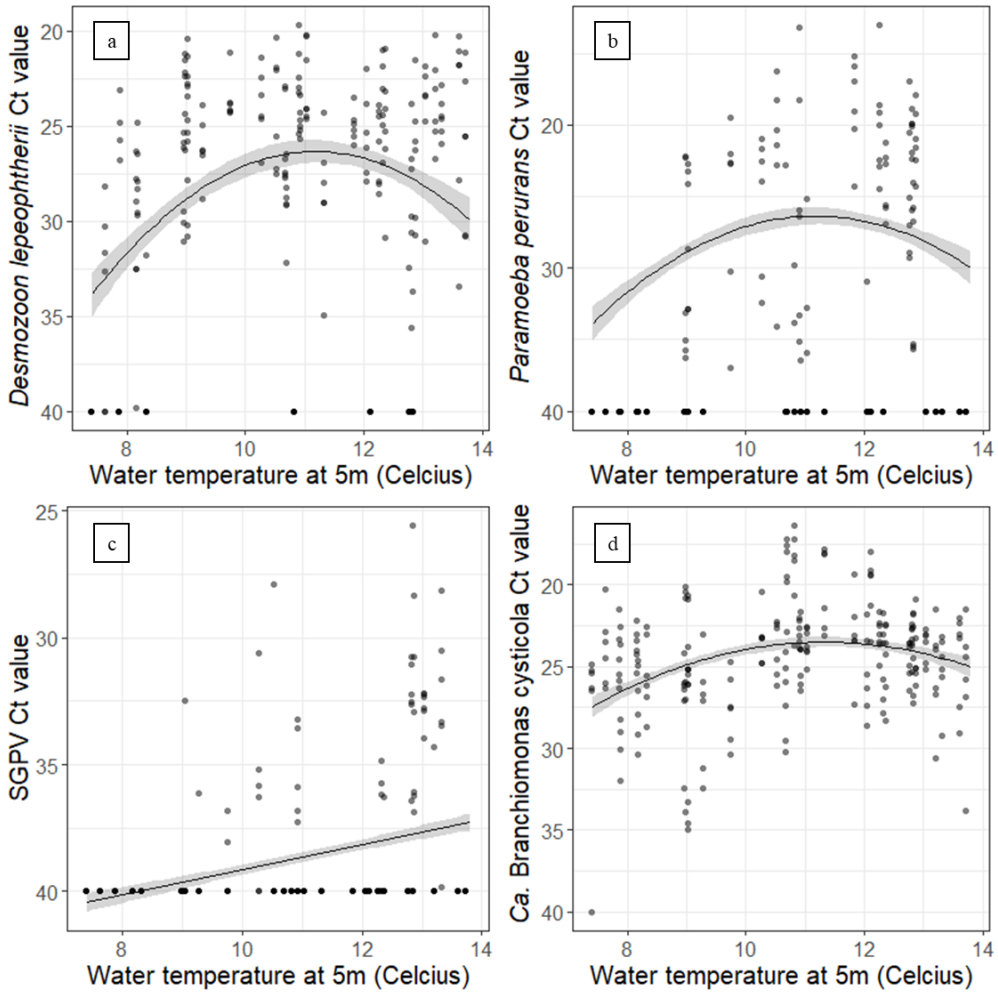

Figure 3.22.Graphs representating of the influence of water temperature on the Ct values of each pathogen. A linear and non-linear effect of water temperature was significantly associated with the loads of (a) *D. lepeophtherii*, (b) *P. perurans*, and (d) *Ca*. B. cysticola. A quadratic effect of temperature was not significantly associated with the Ct values of SGPV, although there was a linear effect of temperature in SGPV Ct values. The points show raw data; line and shaded area show predicted gill score ± 95% confidence intervals.

3.5 Discussion

Gill disease is an important challenge for salmonid aquaculture worldwide, due to the extent of the disease and the losses that result. The problem is compounded by the complex interactions between the multiple pathogens that can be present in the fish, environmental factors and the management practises used. The individual role and the possible interactions of the three principal putative pathogens associated with CGD (*D. lepeophtherii*, salmon gill poxvirus and *Ca*. B. cysticola) have not yet been fully elucidated. In the absence of *in vivo* or *in vitro* experimental models, prospective longitudinal studies help to clarify the associations that exist between exposure to a potential cause and the development of disease. When this project was initiated only a small number of prospective longitudinal studies assessing gill health had been published (Downes *et al*., 2015; Mitchell *et al*., 2012; Steinum *et al*., 2010). This is the first prospective longitudinal study examining the dynamics of the putative pathogens associated with CGD in Scotland and their relationship with gill disease. The study focused on the production cycle (the latter part of the freshwater stage and most of the marine phase) of two salmon pens, at two farm sites located on the West coast of Scotland.

Cumulative mortalities by the end of the study in the observational units of Farms A and B were 5% and 10%, respectively, and mostly of "unknown aetiology". Apart from the presence of salmon lice, no other diseases were reported as significant. Although the causes of mortalities in Farm A could not be determined, gill pathology was minimal in the fish examined throughout the study and was not considered to have had a major impact on the losses that occurred. Mortalities due to gill disease usually range between 5% and 20% (Downes *et al*., 2018; Nylund *et al*., 2008; Rodger 2007), although up to 80% has been reported (Stenium *et al*., 2009). In Farm B, gill disease occurred from the period of September to December (Week 30-47), which coincided with the period when the majority of mortalities were recorded. It is possible that gill disease was, at least in part, responsible for the deaths that occurred in Farm B, and gill damage due to "unknown" deaths was overlooked due to the rapid decomposition of gills *post mortem* (Wolf *et al*., 2015). There was a significant association between increased gill score and the reduced condition factor.

Gill disease is frequently associated with lethargy and anorexia (e.g. Steinum *et al*., 2008). However, this varies, and some dead fish can have food in their stomachs and appear to be in good condition (Munday *et al*., 1990). It has been shown that Atlantic salmon with AGD, exposed to high intensity exercise, had a significant reduction in oxygen uptake assessed using a swim tunnel respirometer, and their aerobic scope suggested that they had a compromised respiratory system as a result of AGD and this ultimately could affect the appetite of the fish, especially at high temperatures (Hvas *et al*., 2017). At temperatures of 15°C or above Atlantic salmon have reduced growth compared to fish at 13°C (Olsvik *et al*., 2013). Due to their ectothermic nature, fish have a higher metabolic rate at warmer environmental temperatures. This also increases when the respiratory surface area of the gill is reduced in events of gill disease, resulting in an increased ventilation rate and in turn reduced growth.

The load of *P. perurans* on gills had a significant association with a quadratic effect of water temperature, with higher *P. perurans* loads after 10 °C. Different environmental conditions have been reported during AGD outbreaks worldwide, with outbreaks recorded at water temperatures as low as 7°C and as high as 20°C (reviewed by Oldham *et al*. 2016). In Scotland, a threshold of 12°C is considered to be an important risk factor for the disease to develop by some salmon production companies (Benedicenti *et al*., 2019). Benedicenti *et al*., (2019) showed variations in severity of AGD when fish were infected *in vivo* at different water temperatures. Groups exposed to amoebae at 15°C developed severe lesions more rapidly than fish exposed to amoeba at 10°C. In the present study, the gills of fish from Farm B showed signs of *P. perurans* infection and AGD lesions over a range of water temperatures, from 9°C to 15°C. The increase in *P. perurans* load in the gills was significantly associated with increased gill scores. Amoebic gill disease is considered one of the biggest challenges occurring in salmon farming and is an important primary pathogen of gill disease (Oldham *et al*., 2016). The presence of *P. perurans* was initially detected at low levels (Ct values of 30 & 34) in two out of six fish sampled from farm B at week 23 (07.07.19), but gross and microscopic lesions consistent with AGD were only detected in the gills at sampling point Week 28 (11.08.19). Establishment of macroscopic and microscopic AGD lesions may be approximately one week to develop in gills after being experimentally challenged

with *P. perurans* (Marcos-López *et al*., 2018). Sporadic detection of *P. perurans* occurred in fish from Farm A in weeks 40 to 47 (01.11.2016-20.12.2016), but percentages of positive fish at the farm was very low. Low salinities is a known risk factor for the development of *P. perurans* infections (Clark & Nowak, 1999), and freshwater is the treatment of choice to reduce amoebae infections in salmon farming (Powell *et al*., 2015). In this study, the lower salinities reported in Farm A compared to Farm B (28-32 ppt and 34, respectively) may have been a limiting factor for the establishment of *P. perurans* infections. However, salinity levels reported in Farm A were still considered suitable for AGD to develop (Bustos *et al*., 2011), and therefore it could be that the incidence of infection by the amoeba was low and AGD did not cause an impact on the health of the fish population.

The two farms screened in this study were positive for the three main pathogens associated with CGD by RT-rtPCR, which suggests that the detection of *D. lepeophtherii*, *Ca*. B. cysticola, and SGPV is relatively common in marine Scottish salmon farms. Even though the presence of these pathogens is known to exist in the Scottish aquaculture industry (pers. comm. C. Matthews), public data about the prevalence and infection dynamics of these organisms is lacking.

Desmozoon lepeophtherii load was significantly associated with a quadratic effect of temperature (between 10-12 °C) (p value < 0.001) and this temperatures were commonly recorded during the autumn months. Gunnarson *et al*., (2017), showed that the microsporidian loads were significantly higher during the autumn months in the farms examined in Norway. Other studies have suggested that a higher prevalence of the parasite has been observed in marine farms in the Western part of Norway (Nylund *et al*., 2011), where temperatures are higher than northern Norway, and is the main region associated with PGI cases (Kvellestad *et al*., 2005; Nylund *et al*., 2011; Steinum *et al*., 2010). Sveen *et al*. (2012) compared the distribution of the parasite in the tissues of salmon transferred to sea at different times of the year using RT-rtPCR. The fish transferred in April, showed infection in the gills after transfer and, some weeks after, in the kidney. However, fish transferred to sea in November only showed infections in their gills, but not in kidneys. The authors hypothesised that the systemic development of the parasite was inhibited when water temperatures

were below 10°C in salmon farm site. Water temperature has been shown to affect the development of other microsporidians, for example *in vivo* experiments with the microsporidian *N. salmonis* showed an increase in mortalities of the chinook salmon when temperatures were shifted from 9ºC (10%) to 15ºC (60%) (Antonio & Hedrick, 1995). In this study, higher loads of *D. lepeophtherii* loads was associated with temperatures between 10 and 12 °C when both farms were used in the statistical model.

The percentage of fish positive for *D. lepeophtherii* was 93% and 68% in Farm A and B, respectively. The presence of *D. lepeophtherii* was initially detected in the gills of one fish in Farm A by RT-rtPCR in the first sampling point of the marine cycle, just one month after the fish were transferred to sea, and five months after the fish were transferred to Farm B. In Farm A, sea lice were not observed on the skin when *D. lepeophtherii* was first detected in the gills of fish, suggesting that infection occurred through the waterborne microsporidian spores present at the farm, in agreement with other studies (Sveen *et al*., 2012). There was a significant relationship between the presence of *D. lepeophtherii* and the increase in gill score in Farms A and B, but the increase in the parasite load (lower Ct value) was associated with the increase in the gill score in Farm B only. The pathology suggestive of *D. lepeophtherii* infections was minimal and not significant in the gills of fish examined from both farms, which suggests the significant associations are the result of the parasite developing in more affected gills (with higher gill score) rather than *D. lepeophtherii* being a causative agent of the gill pathology observed. It could also be that parasite development was favoured by the increase in water temperature, a factor that also influenced the gill score. However, the loads of *D. lepeophtherii* decreased in the gills of fish in Farm A after week 40 (02.11.2016), with the decline of temperature, but loads of *D. lepeophtherii* in Farm B increased despite the lower temperatures by the end of the sampling period (week 40-57), which suggests that fish with gill disease in Farm B provided a more suitable environment for the parasite to grow. Gunnarson *et al*. (2017) found similar associations between the increase in loads of *D. lepeophtherii* RNA and the presence of gill disease, unfortunately the authors did not describe the clinical signs or pathology related with these gill disease event and it is therefore unknown if the parasite was associated

with any of the lesions observed. Steinum *et al*. (2010) described higher loads of *D. lepeophtherii* in fish with PGI (statistical analysis was not performed) than fish without PGI. The authors did not mention if *D. lepeophtherii* was detected in tissue sections by histology, but most of the changes associated with PGI (epithelial cell necrosis, hyperplasia and gill inflammation) (Kvellestad *et al*., 2005), have been associated with the presence of *D. lepeophtherii* by light microscopy (Matthews *et al*., 2013; Weli *et al*., 2017) and therefore it is possible that the microsporidian was involved in the pathology observed. Contrary to this, Downes *et al*., (2018) did not find any association between the increase of *D. lepeophtherii* and the increase of severity of the gill disease during an outbreak of AGD in Ireland. *Desmozoon lepeophtherii* is very prevalent in salmon farms irrespective of the health status of the fish (Steinum *et al*., 2010). Farm A, which showed overall mild gill pathology, had a significantly higher percentage of fish positive for *D. lepeophtherii* compared to Farm B. There were no significant associations between the increase in parasite load in the fish with low condition factor, as shown in other studies (Gunnarson *et al*., 2017). However, in this study, fish were attracted to the surface with feed for sampling, which meant that the most active part of the population was caught, whilst the smaller fish (runts) were overlooked. Whether infestations with *D. lepeophtherii* can reduce the condition factor of salmon, or fish with low condition are more susceptible to *D. lepeophtherii*, remains to be elucidated. It may be that the conditions for the parasite to cause significant gill pathology were not present in this study and further studies are necessary to understand the conditions required for the parasite to cause disease.

Candidatus Branchiomonas cysticola was the most prevalent agent detected throughout this study (100% and 99% percentages of positive fish in Farm A and Farm B, respectively), in accordance with other observational studies (Gunnarson *et al*., 2017; Downes *et al*., 2018), and was first detected in the freshwater stage of Farm A and Farm B. It would appear that the fish carried the pathogen from their freshwater site to their seawater location. No significant differences were found in the percentages of fish positive for the bacterium across seasons or farms, but the increase in the bacterium load was associated with a quadratic effect of temperature. *Candidatus* B. cysticola was not associated with an increase in the gill score in the

most statistically powerful models used in this study (LM1 and LM2), in which both farms were assessed at the same time. However, an increase in the loads of *Ca*. B. cysticola were significantly associated with an increase in the gill score when only Farm B was assessed (LM6). *Ca.* B. cysticola is the most common epitheliocyst forming agent in Atlantic salmon (Mitchell *et al*., 2013). The presence of epitheliocysts have been recorded in at least 90 species of fish (Blandford *et al.*, 2018) and often in the presence of disease and mortalities (Katharios *et al.*, 2008). The loads of *Ca.* B. cysticola significantly increased with the presence of PGI (Mitchell *et al*., 2013). Further studies showed mild branchitis and lamellar epithelium proliferation when fish were infected with the bacterium in freshwater (Wiik-Nielsen *et al*., 2017). However, it seems that this agent is also highly prevalent and can be present in healthy fish without causing significant pathology (Downes *et al*., 2018). In this study, a few epitheliocysts consistent with *Ca.* B. cysticola detected in 30% of the fish gills. These appeared as basophilic cysts causing hypertrophy of the epithelial cells that were mostly located in the apical part of the lamellae, as described by Mitchell *et al*. (2013) when the cysts are found in low numbers. Presence of epitheliocysts suggestive of *Ca*. B. cysticola were significantly correlated with lower Ct values, which agrees with Mitchell *et al*. (2013) in *Ca*. B. cysticola being the most likely aetiology agent of the cysts observed. High numbers of *Ca.* B. cysticola and epitheliocysts have been observed in events of PGI, and its pathological effect may be load-dependant (Mitchell *et al*., 2013), but epitheliocysts numbers were low in this study. The inflammatory cell reaction in the gills was not marked in this study (one of the changes associated with *Ca.* B. cysticola (Wiik-Nielsen *et al*., 2017)) and the low level of epitheliocysts detected in the histopathology suggests the bacterium was not a major causative of the gill disease present in Farm B. Instead, the higher level of the bacterium seems to have increased when the gill score increased but only in Farm B. The various results obtained for this pathogen at Farms A and B, indicate that conditions required by the bacterium to cause disease were not suitable in these farms and the circumstances under which epitheliocysts replicate and are able to cause disease have yet to be understood. Another type of epitheliocyst was detected in Farm A during the first sampling point at sea (week 6). These were small basophilic cysts, with bacterial inclusions, present

at the base of the lamellae and were consistent with description for *Ca.* C. salmonicola. According to Mitchell *et al*. (2010), these agents are carried by salmon from the freshwater phase to the marine phase and disappear after 4-6 weeks post-transfer to sea. The agents were observed at only one sampling point and were assumed to have subsequently disappeared from fish after being moved to the seawater environment.

Salmon gill poxvirus was detected in both sets of fish in the freshwater stage of their production cycle prior to being moved onto both farms. The virus was only sporadically detected during the marine production phase during the study. Therefore, it appears that salmon carried the virus from the freshwater site to their sea location. Half of the fish in Farm A (3/6) sampled during the freshwater stage showed changes in their gills, suggestive of SGPV infection with the presence of moderate lamellar epithelium hyperplasia (although this pathology is not exclusive to viral infections of the gills), chromatin margination, apoptosis of epithelial cells, and cell budding. They also had the highest level of virus detected at any point throughout the study (Ct range 21-29). It is during the freshwater phase of farming when the most typical manifestation of clinical disease associated with the virus is observed (Gjessing *et al.*, 2016). In this study, mortalities in the freshwater stage were mainly attributed to *Saprolegnia* spp. infections, an oomycete that causes important economic losses to the salmon industry during freshwater rearing (Van West, 2006). Gjessing *et al.* (2017) speculated that SGPV infections could immunosuppress the fish and facilitate infections with *Saprolegnia* spp. Fish from Farm A (freshwater stage) had high loads of virus and presented pathology typical of SGPV infections, which have been reported to be associated with mortality events in other studies (Gjessing *et al.*, 2015). Therefore, it is possible that mortalities due to SGPV were masked by mortalities associated with the *Saprolegnia* spp infections (Gjessing *et al.*, 2017). In the case of fish from Farm B, SGPV was detected in most fish (4/6) during the freshwater rearing, but the loads of virus were lower compared to those measured in fish from Farm A (Ct range 32-36), and pathology in the gills was minimal and not suggestive of the disease associated with the virus. Similar to Farm A, mortalities of fish in the freshwater phase at Farm B were mostly attributed to *Saprolegnia* spp. infections, but it is unknown if the virus contributed to these

mortalities to some extent or if the virus load was too low and did not cause clinical disease. This has been reported in other studies in which infected fish transmitted the SGPV infection to naïve fish through the water but without physical contact, and where no pathology was associated to the infection (Wiik-Nielsen *et al.*, 2017).

In the marine phase, the percentage of fish positive for SGPV was not significantly different across seasons or between farms, but there was a positive association between the increase of water temperature and the increase in the virus load. In this study, there was not a significant association between SGPV and gill disease. The virus was detected by IHC and qPCR in the first case of AGD described in Norway, which was associated to 80% of mortalities (Gunnarson *et al.*, 2017) and the authors proposed SPGV to be a primary pathogen, capable of destroying the epithelial barrier and facilitating the entry of other pathogens. However, our findings are in agreement with the studies of Downes *et al*. (2018), in which SGPV was detected sporadically, and it was not significantly associated with the gill scores.

Potential factors that could affect the gill scores of fish sampled at Farms A and B were analysed using linear models (LM1 & LM2) and significant associations were found between different factors. There were significant differences in the severity of the gill score between farms. Farm A experienced mostly minimal to mild gill changes throughout the study, but Farm B suffered an outbreak of gill disease from late summer until early winter with the total gill scores reaching a moderate level during this period. Season was significantly associated with the gill score, and the model LM2 and LM1 estiamtes that autumn correlated with higher gill scores, in agreement with previous reports of gill disease in marine salmonids, which tend to be reported between the end of summer to early winter. Proliferative gill inflammation seems to be highly correlated with the autumn months in Norway (Kvellestad *et al*., 2005) and a similar pattern has been observed in Scotland (Matthews *et al*., 2013). Furthermore, the first outbreak in AGD in Norway occurred in autumn (Steinum *et al*., 2008), and Scotland was affected by AGD infections in several farms during late summer in 2017 (Roed, 2017). In addition, problems with algae blooms were recorded in late summer/autumn in Norway in 2018 (Hvas *et al*., 2017). The strong link with seasonality may indicate that water temperature is an important risk factor

in the development of gill disease, and in the present study when water temperature was used instead of season as a potential predictor of increased gill score in Farm B (LM3) there was a strong association between these. This is in agreement with the observation that, in Scotland, water temperatures reach their maximum in late August (~14°C) (The Scottish Government, 2011) and this is when the incidence of gill disease starts to peak. Pathogen infection rates are also influenced by the water temperature (Callaway *et al*., 2012), as is the abundance of non-infectious harmful organisms, such as gelatinous zooplankton (Kintner, 2016).

Blooms of *Chaetoceros* spp. were recorded in both farms by the end of May. In Farm A, *C. debilis* and *C. socialis* were detected, with maximum abundance of 1.8 x 10^5 algal cells L^{-1}, and in Farm B *C. socialis* was the predominant species with maximums of densities of 10^5 algal cells L^{-1}. *Chaetoceros* spp. is one of the most abundant diatoms in the ocean (Malviya *et al*., 2016) and blooms have been associated with fish kill events (reviewed by Rodger *et al*., 2011). *Chaetocerus debilis* was one of the predominant species found in an algae bloom together *Chaetoceros wighami*, associated with mortalities over 50% in a salmon farm in the Shetland Isles (Bruno, 1989). Unfortunately, the latter study was not accompanied with the exact densities of algal cells detected and it is unknown at which concentrations *C. debilis* can be deleterious to fish. During challenges of Atlantic salmon with *C. socialis in vivo* using concentrations of 4 x 10^6 algal cells L^{-1} (higher concentrations than those detected in this study) no mortalities resulted and no obvious effect were observed in the gills of fish after 24 h of exposure (Burridge *et al*., 2010). The authors of that study concluded that this species of algae is unlikely to be responsible for fish deaths at the concentrations tested. In this study, minimal to mild acute gill pathology was observed, consistent with that previously described resulting from exposure to harmful algae blooms (Bruno, 1989). Necrosis of the lamellar epithelium cells and tissue sloughing, was detected in fish from Farm A by the end of May in a mild extent but not in Farm B, when the *C. socialis* bloom occurred in the same period. The pathology observed in fish from Farm A was likely caused by direct contact with the algae or with the silicified setae, typical of *Chaetaceros* spp. (Malviya *et al*., 2016), resulting in small focal abrasions in the gill

epithelium. However, the impact of these changes on the gill health of the fish overall were low.

The hallmark of complex gill disorder, as recently defined by the presence of significant, non-specific, proliferative branchitis (Noguera *et al*., 2019), was not detected in any of the fish examined in the present study. The pathology observed in fish from Farm B was consistent with AGD but other non-AGD lesions were also seen, such as mild, occasionally moderate, multifocal lamellar vascular disturbances, including thrombi and haemorrhages, mild multifocal lamellar non-specific epithelium proliferation, and occasional lamellar tissue sloughing. These changes were mostly attributed to waterborne insults such as zooplankton or mechanical damage. Gelatinous zooplankton represents an important environmental challenge to gills, such as relatively large jellyfish, which are carried onto the outer surfaces of the fish cages by tides and currents, causing them to break up and pass through the mesh (Delannoy *et al.*, 2011). Pathology in the gills associated with the exposure to jellyfish include the presence of multifocal necrosis, haemorrhage and loss of tissue in the filaments and lamellae (Baxter *et al*., 2011; Marcos-López *et al*., 2016). Although similar lesions were seen in this study, zooplankton sampling was not carried out at the farm and the exact cause of the additional gill lesions remains unknown.

When using only Farm B in the linear model, the gill score significantly increased with the increase in days since the last net cleaning and the last H_2O_2 treatemnt. Although, as discussed previously, the statistical power of the models in which only Farm B was considered was low, it is still interesting that these two factors were shown to have a significant effect on the severity of the gill score. *In situ* net-pen pressure washing is a common strategy to clean the biofouling present on the fish cage nets (reviewed by Bannister *et al*., 2019) and was the strategy used in Farm B. Due to the release of fouling organisms such as hydroids and anemones, high pressure cleaning can cause lesions similar to those that occur in a jellyfish bloom, which also possess nematocysts (Baxter *et al.*, 2012). For instance, Atlantic salmon exposed to the hydroid *Ectopleura larynx*, a frequent fouling organism on cage nets, can cause epithelial sloughing, necrosis lamellar haemorrhages (Baxter *et*

al., 2012) and foci of lamellar thrombi. Farm A used a different type of net cleaning system termed the “environet”. The environet consists of a double net that can be rotated, maintaining the fish within the pen, and allowing half of the net to be hung up and air-dried to remove the waste accumulated (Fletcher, 2018). This system prevents the fouling and infectious organisms removed from entering the inside of the net pen. The overall gill health of Farm A was significantly better than in Farm B. Differences in net cleaning could have an impact on gill health and should be investigated further.

Regarding the use of H_2O_2 treatments, excessive exposure of fish to this chemical has been shown to have a negative impact on gill health, and the pathology is characterised by the lifting of the lamellar epithelium and epithelial cell necrosis (Rodger et al., 2011). However, lamellar epithelial lifting was not detected in the gills of fish from Farm B, and the occasional epithelial cell necrosis noted could have been caused by different reasons such as mechanical damage or contact with nematocysts. Therefore, excessive exposure to H_2O_2 is an unlikely explanation for the poorer gill health in Farm B. Handling of the fish during the administration of these treatments could have played a role in the increased gill score (i.e. mechanical damage to the fish gills during crowding) but, overall, this result should be interpreted with care. The significance of H_2O_2 treatments was measured in the model as "days since the last treatment". Only three H_2O_2 treatments were all performed in Farm B over the course of the study and these occurred between weeks 32-43 when the gill scores were increasing, mostly due to AGD. Therefore, it is not surprising there was a significant association between the increase in gill score and the lower number of days since H_2O_2 treatment. This result shows the importance of knowledge of all the parameters influencing the experimental system when interpreting the outputs from the statistical analyses, particularly in uncontrolled experiments undertaken in a commercial fish farm.

There were no statistically significant associations between the use of mechanical de-lousing treatments in this study and gill score. However, gill damage has been reported in Norway after thermal and mechanical de-loucing treatments, especially after testing during the developmental phase of the equipment (Grøntvedt

et al., 2015; Overton *et al*., 2018) but these procedures have now been widely adopted in the salmon farming industry (Overton *et al*., 2018). More studies are necessary to understand the potential damage that these methods can have on the fish.

In conclusion, statistical analysis of the data from the two farms showed that variations in SGPV and Ca. *B. cysticola* loads were not associated with an increase in the gill score in the marine stage, but *D. lepeophtherii* and *P. perurans* were. The absence of *D. lepeophtherii* associated pathology throughout the study suggests that the microsporidium does not play a significant role in the development of gill disease, but it was able to replicate more readily in compromised fish gills (i.e. those with a higher gill score). The presence of AGD in farm B during the months of July 2016 to January 2017, confirms *P. perurans* as one of the main causes of the gill disease observed.

4.5 Acknowledgments

Dr. Chris Cousens of Moredun Research Institute at Edinburgh (MRI) and Simon Rey of FVG Oslo, are thanked for their guidance with the validation of the RT-rtPCR assays. Dr Aaron Reeves of the Scottish Aquaculture Rural College in Inverness and Dr. Adam Hayward of MRI are thanked for their counsel in the analysis of the collected data and development of statistics. Dr. Mar Marcos-López of the FVG Inverness is thanked for her valuable advice in the analysis of the gill histopathology. The health professionals and fish farmers of the farms sampled in this study are hugely thanked for their assistance in the sampling and data collection.

Chapter 4 Development of a DNA-based *in situ* hybridization method to detect *Desmozoon lepeophtherii* in Atlantic salmon tissues

4.1 Introduction

4.1.1 Detection of *D. lepeophtherii* in tissue sections

Species diagnosis for Microsporidia has traditionally been carried out using transmission electron microscopy (TEM). Although it remains the gold standard for determining the species of these parasites, TEM is time-consuming and is not used for routine diagnostic investigations (Didier, 2005). At present, the most robust and widely practicable technique for the diagnosis of microsporidiosis in tissue sections is the detection of the spores using light microscopy (Garcia, 2002). However, microsporidia are not detected frequently in host tissue using the H&E, especially in cases where spores are small, widely distributed and occur either singly or in small aggregates rather than being present in large clusters or xenomas (Peterson *et al*., 2011). Hence, several other histological stains, such as Luna or Warthin-Starry, have been used to visualize the microsporidian spores (Peterson *et al*., 2011).

The small size of *D. lepeophtherii* spores, ranging from 1µm (auto-infective) to 2.5µm (environmental), and their presence singly or in small aggregates (Matthews *et al*., 2013; Nylund *et al*., 2010; Weli *et al*., 2017), makes detection of the parasite in histological tissue sections difficult (Herrero *et al*., 2020). Matthews *et al*. (2013) used Gram Twort staining to identify *D. lepeophtherii* auto-infective spores and, although this method is possibly sufficient for routine complex gill disorder diagnosis when the number of *D. lepeophtherii* spores is very high, it severely underestimates the number of spores present when compared to other, more sophisticated, techniques such as CW staining or immunohistochemistry (Herrero *et al*., 2020).

4.1.2 *Desmozoon lepeophtherii*-related pathology in the gills of Atlantic salmon

Due to the difficulty in detecting *D. lepeophtherii* in tissue sections, infections are normally diagnosed by molecular methods, routine H & E stained gill tissue sections and the use of other histochemical stains and labels to confirm the presence of spores (Herrero *et al*., 2020; Matthews *et al*., 2013). No successful *in vivo* or *in vitro* infection studies have been performed with *D. lepeophtherii* and its pathogenesis in salmon remains to be fully elucidated. However, several studies have associated high burdens of microsporidian spores with necrosis, hypertrophy and hyperplasia of the lamellar epithelial cells, and infiltration by inflammatory cells (Matthews *et al*., 2013; Nylund *et al*., 2010; Nylund *et al*., 2011; Weli *et al*., 2017). Matthews *et al*. (2013) described a case of *D. lepeophtherii* in a Scottish marine salmon farm in which, at the first sampling point, marked lamellar epithelial cell proliferation, spores and infiltration by large numbers of inflammatory cells into the necrotic and hypertrophied epithelial cells were present, although overall lamellar branchitis was mild. One week later, inflammation had decreased, the number of necrotic epithelial cells had reduced, and spores were rarely found such that only lamellar epithelial cell proliferation and hypertrophied cells were obvious. Sequential time-course observations on the disease were also made by Weli *et al*. (2017) on a Norwegian salmon farm in which *D. lepeophtherii* appeared to be the main pathogen causing the clinical signs. Necrotic lesions were more severe during the acute stage of the disease (during early sampling time points), while chronic pathology (present during later sampling time points) was characterised by a marked host response, including severe inflammatory cell infiltration and proliferation of the gill epithelium.

In outbreaks of gill disease caused by multiple aetiologies, lesions caused by individual agents can be difficult to discern, including those caused by *D. lepeophtherii*. Additionally, the high percentage of positive fish to the microsporidian in salmon populations, rapid change in the progression of the pathology (spores might be detected only for a short period of the infection), and the difficulty in detecting the parasite, makes the study of gill disease associated with this organism challenging. Other stains (*e.g*., CW) for microsporidians significantly

improve the detection of *D. lepeophtherii* but only detect the spore stage (Herrero *et al*., 2020). A more sensitive and specific method, capable of detecting all stages of the parasite's life cycle, would allow accurate detection of *D. lepeophtherii* and help gain insights into the development of the parasite infection and pathogenesis in CGD.

4.1.3 *In Situ* Hybridisation (ISH)

The underlying principle of ISH is to detect target DNA or RNA by application of the complementary strand of nucleic acid to which a reporter molecule has been attached (together referred to as the probe) (Jensen, 2014). Although conceptually simple, ISH procedures are usually lengthy and involve several steps (Palenzuela & Bartholomew, 2002). Sensitivity and specificity of ISH tends to be slightly lower when compared to quantitative polymerase chain reaction (RT-rtPCR) (Weli *et al*. 2017). However, in contrast to RT-rtPCR, the procedure has the ability to locate the parasite in counterstained tissue sections thereby showing its biological context and general morphological and spatial information (Holzer *et al*., 2003).

ISH studies on microsporidians have proven that the method is a powerful tool to visualise both the pre-sporogonic and sporogonic stages. The technique has been used previously with probes against the small subunit ribosomal RNA (SSU rRNA) or intergenic regions of fish microsporidian rRNA to detect *Enterospora nucleophila* and *N. salmonis* (Ahmed *et al*., 2019; Grésoviac *et al*., 2007). These methods were applied successfully to formalin fixed, paraffin-wax embedded (FFPE) tissue samples and detected more microsporidians and more infected cells when compared with histochemical stains.

Recently, an ISH method for the detection of *D. lepeophtherii* was developed based on a large, plasmid-encoded RNA probe (Weli *et al*., 2017). However, this procedure has notable practical difficulties with respect to the reproducibility of generating the probe and difficulties preserving tissue morphology versus adequate probe permeability. Additionally, the extremely labile nature of RNA probes demands the use of a scrupulously sterile technique and careful preparation of the tissue sections (Corthell, 2014). A more practical and robust ISH method based on

DNA oligonucleotide probes would be ideal for further research studies of *D. lepeophtherii* and would be suitable for diagnostic purposes.

4.1.4 Aims and Objectives

The aim of this work was to develop and optimise an *in situ* hybridisation protocol using oligonucleotide probes specifically designed for *D. lepeophtherii*. The sensitivity and specificity of the ISH technique were compared with other techniques currently used to detect the microsporidian in tissue sections. The distribution of the parasite, detected by ISH, was correlated with the histological lesions observed in tissue sections, and also compared with the results of reverse transcription PCR (RT-rtPCR).

4.2 Material and Methods

4.2.1 Development of the *in situ* hybridisation protocol for the detection of *D. lepeophtherii* in histological tissue sections

The developed protocol was based on the method described by Palenzuela & Bartholomew (2002), with modifications, and optimized for the probes and tissues used in the present study. Oligoprobes were synthesised and labelled with digoxigenin deoxyuridine triphosphate (DIG-dUTP) at the 5' and 3' end of the probes (Sigma-Aldrich, Dorset, UK).

The characteristic hypertrophied and necrotic epithelial cells associated with the presence of *D. lepeophtherii* spores in salmon gill tissues have been termed "microvesicles" (Weli *et al*., 2017). For the development and optimisation of the ISH technique, archived FFPE gills tissue from Atlantic salmon were used. These samples had large numbers of microvesicles, multifocal and widespread, in epithelial cells in the gill lamellae and were positive for *D. lepeophtherii* by specific RT-rtPCR previously performed by the Fish Vet Group (Oslo, Norway). Relative quantification of parasite specific RNA present in gill tissues (RT-rtPCR) was obtained from gill biopsies (20 fish) and gill swabs (8 fish) and expressed as Ct values. The negative control preparations were gills processed identically to the positive cases but negative for *D. lepeophtherii* by RT-rtPCR.

Table 4.1. Fish number with type of samples used in the RT-rtPCR study and Ct value result.

Fish no.	Type of sample	Ct value
1	Gill biopsy	Negative
2	Gill biopsy	Negative
3	Gill biopsy	Negative
4	Gill biopsy	13
5	Gill biopsy	15
6	Gill biopsy	15
7	Gill biopsy	16
8	Gill biopsy	17
9	Gill biopsy	17
10	Gill biopsy	17
11	Gill biopsy	17
12	Gill biopsy	18
13	Gill biopsy	18
14	Gill biopsy	20
15	Gill biopsy	20
16	Gill biopsy	20
17	Gill biopsy	21
18	Gill biopsy	22
19	Gill biopsy	28
20	Gill biopsy	32
21	Gill swab	17
22	Gill swab	17
23	Gill swab	19
24	Gill swab	20
25	Gill swab	20
26	Gill swab	23
27	Gill swab	24
28	Gill swab	29

4.2.1.1 Design of specific oligoprobes

Probe design was achieved by aligning all the sequences of *D. lepeophtherii* available within the SILVA database (Pruesse *et al.*, 2007, www.arb-silva.de), excluding variable regions. Most of the sequences analysed targeted the SSU rRNA region but some fragments from the internal transcribed spacer (ITS) and partial large subunit (LSU) region were also analysed. No RNA/DNA sequence divergences

were detected in the *D. lepeophtherii* sequences obtained from Atlantic salmon farmed in Scotland or Norway, or from different species of sea lice (*Caligus elongatus* and *Lepeophtheirus salmonis*), Ballan wrasse (*Labrus bergylta*) or rainbow trout (*Oncorhynchus mykiss*) (Table 4.1). Some variation was observed between the Canadian genotype of *D. lepeophtherii* and the sequence of European *D. lepeophtherii*, as reported previously by Jones *et al*. (2012).

To design the oligoprobes, sequences from closely related microsporidians belonging to the family Enterocytozoonidae were aligned (e.g. English Sole *Parophrys vetulus* unidentified microsporidian_AF201911.1; *Obruspora papernae*_H6005137; *N.a salmonis*_ NSU78176; *N. cyclopteri*_KC203457.1) with the longest sequences obtained for *D. lepeophtherii* (FJ594990; AJ431366.2; HM800847.2). In silico sequence analyses were performed using an NCBI BLAST search (http://blast.ncbi.nlm.nih.gov/Blast.cgi) to confirm their specificity and the software package OLIGO 7 (Rychlik, 2007). A total of five resultant antisense oligonucleotide probes targeting the regions SSU rRNA and ITS were designed for this study (Table 4.2).

4.2.1.2 Preparation of tissue sections

Formalin fixed, paraffin-wax embedded gill tissue samples were sectioned (4 µm) and mounted on Superfrost plus coated slides (Menzel-Gläser, Braunschweig, Germany) and incubated at 60°C for one hour. Sections were dewaxed in xylene, rehydrated through a descending ethanol series (100%, 95% and 70%), and equilibrated in Tris-$CaCl_2$ buffer (200mM Tris, 2mM $CaCl_2$ pH 7.2) for 10 min.

Table 4.2. Sequences of *D. lepeophtherii* recovered from different host species and countries of origin, aligned to exclude variable regions in the oligonucleotide probe design. 16S small subunit (SSU) and internal transcribed spacer (ITS), 23S large subunit (LSU).

Accession Number	Number of bp	Authors	Target Gene	Host species/ Country
FJ594990	1885	Nylund et al. (2008)	SSU (partial)	Female sea lice *L. salmonis* / Norway
FJ389667	1656	Nylund et al. (2008)	SSU and LSU (partial); ITS;(complete)	Farmed Atlantic salmon / Norway
HM800847.2	1826	Jones et al. (2012)	SSU (partial)	Farmed Atlantic salmon / Canada
AJ431366.2	1787	Freeman & Sommerville (2010)	SSU; ITS; LSU (partial)	*L. salmonis* / Scotland
KR187183	1584	Nylund & Plarre (2015)	SSU (partial)	Wild rock cook wrasse (*Centrolabrus exoletus*)/ Norway
FJ594979	1559	Nylund et al. (2010)	SSU (partial)	*Caligus elongatus*/ Norway
FJ594989	953	Nylund et al. (2008)	SSU (partial)	Farmed rainbow trout/ Norway
HM367691	685	Staveland & Nylund (2010)	SSU (partial)	Wild Atlantic salmon/ Norway

Table 4.2. Oligoprobe sequences designed for *in situ* hybridization. Small subunit ribosomal ribonucleic acid (SSU), internal transcribed spacer (ITS), melting temperature of the probes (Tm).

Name	Sequence 5'-3'	Region	Tm
1284L21	CAAATCTGAACGTGATGCTAT	ITS	62.5°C
16L21	CGTTCCCCATTCGGTTCACAG	SSU	69.8°C
819L25	TTGCCCCTCTCATGTCGCCAATCTA	SSU	74.4°C
1002L25	ATATTTATGTCGCTCAAACGGATA	SSU	64.5°C
1339L25	ACACACTCACTAAGCAGTCCTACTA	ITS	69.1°C

4.2.1.3 Permeabilisation of tissues

Desmozoon lepeophtherii is an intracellular pathogen and permeabilisation of the tissue was performed to allow intracellular penetration of the probe to improve binding to its target sequence. To optimise this procedure, serial sections were permeabilised with proteinase K (PK) (Roche, Welwyn, UK) at a concentration of 15 µg mL^{-1} in Tris-$CaCl_2$, for either 10 or 30 min at 37°C. Tissues which were not exposed to PK were also examined. Proteolysis was halted with two washes in 2x saline-sodium citrate buffer (SSC) for 10 min each.

4.2.1.4 Hybridisation Buffer

The slides were covered with 400 µL of freshly made hybridization mixture consisting of 112 µL nuclease-free water, 40 µL of 20x SSC buffer, 100 µL of deionized formamide (Sigma-Aldrich), 8 µl Denhardt's solution, 80 µl dextran sulphate (50%, w/v) (Sigma-Aldrich), 40 µL of 10x PBS, and 20 µL of DNA from fish sperm (MB-grade, Sigma-Aldrich).

Oligoprobes were adjusted to a concentration of 100mM with Tris-EDTA buffer (TE). Equal concentration of different probes were mixed together to make two cocktails. Cocktail 1 (C1) was made from probe 16L21, 819L25 & 1339L25. Cocktail 2 (C2) had 1284L21, 1002L25 & 1339L25. The different cocktails were prepared at different dilutions (1/1000, 1/500 and 1/200) in hybridization buffer.

Each oligonucleotide probe was tested individually on serial sections also at the 1/1000 dilution.

4.2.1.5 Hybridisation Procedure

Slides with the probes applied were placed on a heating block at 95ºC for 10 min. After two min at this temperature, slides were covered with Hybri-slips (Sigma-Aldrich) and incubated at 37˚C overnight to hybridize to complementary sequences.

4.2.1.6 Washing Steps

After overnight incubation slides were rinsed with 2x SSC buffer to remove the Hybri-slip. Stringency washes were then performed, to remove unbound probes, using 2x10 min washes in 2x SSC buffer at 37°C and 45°C, 2x10 min in 1x SSC buffer at 37°C, and finally in 0.25x SSC buffer at 37°C for C1. The same wash procedure was used for slides incubated with C2 except the last stringency wash, which was performed with 0.5x SSC buffer at 37°C and 45°C. During each wash step the slides were shaken slowly. Following the stringency washes, the tissue sections were transferred to wash buffer A (1M Tris base, 1.5M NaCl, pH 7.5) for 10 min at 24˚C.

4.2.1.7 Immunological detection

Subsequent to sections being washed in Buffer A they were incubated for 1h at 21°C with blocking solution (2% sheep serum, 0.1% Triton X-100 in wash buffer A) to prevent non-specific antibody binding. Bound probes were detected by covering the slides with anti-DIG Fab fragment antibody conjugated to alkaline phosphatase (AP) (Roche) at a dilution of 1:200 in blocking solution for 2h at 21°C. Unbound antibody was removed using wash buffer A for 2 x 10 min and then incubating in wash Buffer B (100 mM Tris, 100 mM, NaCl, 50 mM, $MgCl_2$ pH 9.5) for 10 min in a staining jar with agitation at 21°C. The signal was visualized by 3h or overnight incubation with AP enzyme substrate NBT/ BCIP (5-bromo-4-chloro-3-indolyl phosphate and 4-nitro-blue tetrazolium chloride) (Roche), diluted at 1:500 dilution with wash Buffer B, without $MgCl_2$. Incubation was undertaken at 21°C in darkness. The staining reaction was terminated by placing the slides in wash buffer A for 10 min.

Slides were counterstained with light green (1%) (AtomScientific, Manchester, UK) for 4 min, and transfered to an acetone solution with 0.05% of acetic acid for 1 min. Tissues were dipped 10 times in distilled water and then dehydrated through a series of rising concentrations of ethanol (96% and 100%), cleared in xylene and a coverslip applied using VectaMount (Vector Laboratories, Burlingame, CA, USA).

4.2.1.8 Specificity testing of the ISH method and analysis of other tissues

To test the specificity of the oligoprobes in the ISH protocol, sections from two closely related microsporidia from the Enterocytozonidae family, *Enterocytozoon hepatopenaei* in the hepatopancreas of the black tiger shrimp (*Penaeus monodon*) and *N. cyclopterii* in the kidney of the lumpfish (*Cyclopterus lumpus*), were subjected to the method to assess cross-reactivity.

Other tissue sections used to optimise the ISH protocol included tissues (heart, skin, muscle, intestine, pyloric caecae, stomach, liver, spleen, kidney and pancreas) from *D. lepeophtherii* positive Atlantic salmon, a sea louse (*L. salmonis*) (from a salmon farm in Scotland) that had xenomas under its cuticle suggestive of *D. lepeophtherii* infection, gills from a lumpfish (*Cyclopterus lumpus*) that had hypertrophic and necrotic gill epithelial cells typical of the lesions caused by *D. lepeophtherii* in salmon gills, and gill tissue from farmed Atlantic salmon in Canada suspected of being infected with *D. lepeophtherii* (which were positive for *D. lepeophtherii* by RT-rtPCR, kindly provided by Prof Simon Jones, Pacific Biological Station, Nanaimo, Canada).

4.2.2 Comparison of the ISH method with other techniques

4.2.2.1 Material

Archived FFPE gill samples (n=28) obtained from marine salmon farms located on the west coast of Scotland and collected between 2016 and 2017 were used. These tissues, previously subjected to RT-rtPCR for quantification of *D. lepeophtherii* using either gill biopsy or swabs, were provided by Fish Vet Group (Inverness, Scotland). Tissue sections from fish with different burdens of microsporidia, as represented by Ct value, were selected for this study.

4.2.2.2 Histology

Archived paraffin wax histology blocks were sectioned (4 μm) sequentially. All samples were stained with H&E according to Stevens & Wilson (1996). Calcofluor White (Fluka, Buchs, Switzerland) staining was performed as explained in Section 2.2.12). All sections were examined with an Olympus BX51 microscope and photomicrographs taken with an Olympus DP70 Digital Camera System using analySiS® software.

4.2.2.3 Quantification of microsporidia in tissue sections by ISH

Each gill section subjected to ISH was examined using 20x objective lens. A 10 mm^2 tissue area (Figure 4.1) was analysed to determine the number of *D. lepeophtherii* positive structures which labelled as an intense blue-purple signal (Ahmed *et al*., 2019).

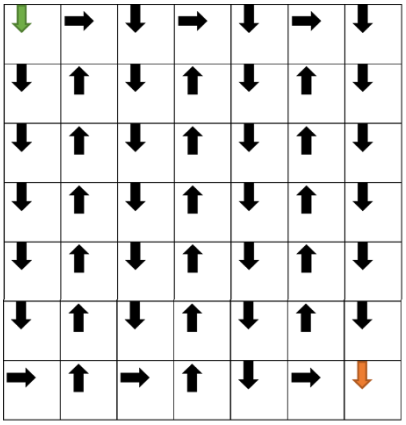

Figure 4.1. Schematic figure used to standardise the counting of ISH positively labelled structures in tissue sections. Each square represents the field observable under the microscope using 20x objective lens. A total of 49 areas were analysed per slide. The green arrow (top left) indicates the starting field; counting continues following the black arrows until the orange arrow (bottom right square).

4.2.2.4 Assessment of *D. lepeophtherii* presumptive pathology

The severity of pathology in gill tissue sections stained with H&E was scored from 0 to 3. A score of 0 was given in the absence of pathology suggestive of *D. lepeophtherii*; 1 for epithelial cell granular necrosis (Figure 4.2a) but no obvious *D. lepeophtherii* -related microvesicles; 2 for a small to medium number of *D. lepeophtherii*-related microvesicles; 3 when a large number of *D. lepeophtherii*-related microvesicles was present in the gill epithelial cells (Figure 4.2b).

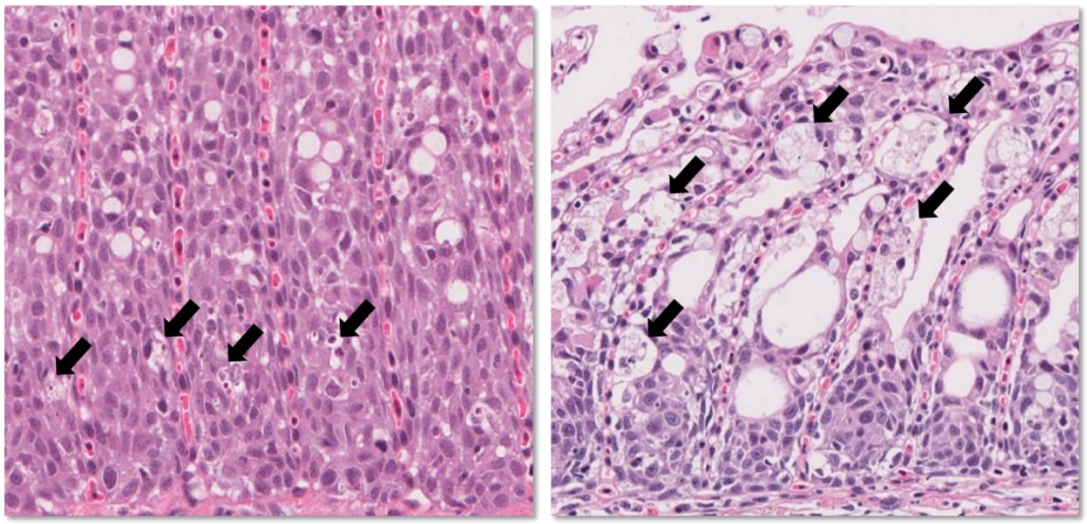

Figure 4.2. Examples of the different values ascribed by the scoring system used for Atlantic salmon gills (a) Epithelial cell granular necrosis (arrows) within areas of lamellar epithelial cell proliferation, this gill would receive a score of 1. (b) Multiple microvesicles within the epithelial cells of the lamellae (arrows). Depending on how extensive the lesions were, gills were ascribed a score of 2 for small to medium number of microvesicles and 3 when a large number of microvesicles was present.

4.2.2.5 Statistical analyses

Sensitivity, specificity, positive predictive value and negative predictive value were calculated as per the standard formula (Martin, 1977) (Table 4.3).

The data were not normally distributed (Shapiro-Wilk's test). Spearman rank correlation coefficient was calculated to determine the correlations between the level of severity of pathology in gill tissue stained with H&E (score) and the Ct values obtained by RT-rtPCR, and between the gill score and the total ISH counts observed in the gill tissue. Pearson's correlation coefficient test was used to examine correlations between the total ISH counts observed in the gill tissue with the Ct values obtained. $p \leq 0.05$ was considered to be statistically significant. All statistical analyses were performed using R software.

Table 4.3. Formulae used to calculate the sensitivity and specificity of the various *D. lepeophtherii* detection techniques.

Calculation	Formula
Sensitivity	∑true positive results/∑true positive samples *100
Specificity	∑true negative results/∑true negative samples*100
Positive predictive value	∑true positive results /∑ true and false positive results*100
Negative predictive value	∑true positive results /∑ true and false negative results*100

4.3 Results

4.3.1 Development and optimisation of the ISH technique

The influence of different concentrations of the reagents and the variation of incubation times on the success of the ISH protocol is summarised in Table 4.4. Permeabilization of the tissue with PK for 10 min compared to 30 min gave the same level of labelling of *D. lepeophtherii* but the tissue morphology was better with the 10 min PK incubation, so this was used. Furthermore, omission of the pre-hybridisation step did not affect the results. Cocktail 1 gave slightly more background signal compared to Cocktail 2, although this difference decreased upon increasing the stringency of the washing, i.e. using SSC buffer at 0.25x to remove unbound probes after using Cocktail 1. A 3h incubation time with the substrate was sufficient to produce an optimal signal, whereas the reaction with both probe cocktails was over developed when the substrate was applied overnight. The best dilution of the probes tested was 1/1000 for both Cocktail 1 and Cocktail 2, with higher concentrations giving no increased signal in the tissues. Optimisation of the protocol is summarised in Table 4.5. The probes were tested separately, using the final ISH protocol (Table 4.6), and the probes targeting the SSU rRNA (16L21, 819L25, and 1002L25) produced the best signal, with some background present when using probe 819L25. The probes targeting the ITS region gave a very weak signal with probe 1339L25 or no signal with probe1284L21.

Table 4.4. Results obtained by the variation of reagent concentrations and incubation times in the ISH protocol. +/- weak signal, + strong signal, BS background labelling, SBS strong background labelling. C1 cocktail 1, C2 cocktail 2.

Treatment	Concentration // Duration	Results
Proteinase K	15 µg mL^{-1} 10 min	C1: +, BS
		C2: +
	15 µg mL^{-1} 30 min	C1: +, BS
		C2: +
	No Proteinase K	C1: +/-, BS
		C2: +/-
Pre-hybridization	30 min	C1: +, BS
		C2: +
	None	C1: +, BS
		C2: +
Stringency washes	2x SSC, 10min 1x SSC, 10min 0.5x SSC	C1: +, SBS
		C2: +
	10min 2x SSC, 10min 1x SSC, 10min 0.25x SSC	C1: +, BS
		C2: +
Substrate incubation	3h	C1: +, BS
		C2: +
	Overnight	C1: SBS
		C2: SBS

Table 4.5. Summary of the ISH procedure optimised for *D. lepeophtherii*

Treatment	Duration
Dehydration through graded alcohols and equilibration in Tris-$CaCl_2$	50 min
Tissue permeabilization, PK 15 µg ml^{-1} in Tris-$CaCl_2$ at 37°C	10 min
2x SSC wash	10 min
Tissue denaturisation at 96°C	10 min
Incubation in hybridisation buffer at 37°C	Overnight
Stringency washes	60 min
Washing Buffer A (1M Tris Base, 1.5M NaCl, pH 7.5)	10 min
Incubation with blocking solution (2% sheep serum, 0.1% Triton X-100 in Washing Buffer A).	60 min
Immunological detection solution (AP-conjugated anti-DIG Fab fragments antibody in blocking solution)	120 min
Wash in Washing Buffer A	20 min
Wash in Washing Buffer B (100 mM Tris, 100 mM, NaCl, 50 mM, $MgCl_2$ pH 9.5).	10 min
Substrate reaction (with NBT/ BCIP in Washing Buffer B, without $MgCl_2$)	180 min
Wash slides in Washing Buffer A	10 min
Counterstaining (Light Green)	10 min
Xylene and mounting in VectaMount	15 min
Total time	23.6h (14h incubation overnight)

Table 4.6. Results using oligoprobes individually with their respective optimised protocol. - no signal, +/- weak signal, + strong signal, BS background staining.

Name	Sequence 5'-3'	Results
1284L21	CAAATCTGAACGTGATGCTAT	-
16L21	CGTTCCCCATTCGGTTCACAG	+
819L25	TTGCCCCTCTCATGTCGCCAATCTA	+, BS
1002L25	ATATTTATGTCGCTCAAACGGATA	+
1339L25	ACACACTCACTAAGCAGTCCTACTA	+

4.3.2 Detection *of D. lepeophtherii* in Atlantic salmon gills using ISH

Successful binding of the probes to the *D. lepeophtherii* target sequences, indicating the presence of the parasite, was denoted by a dark blue-purple signal against a light green counterstain (Figure 4.3 & 4.4). All negative control preparations were devoid of blue-purple signal (Figure 4.5a). Proliferative stages of *D. lepeophtherii*, *i.e.* pre-sporogonic structures and probably meronts, appeared as intensely blue-purple labelled round structures 4-6 µm in length (Figure 4.5b & c). They were present most frequently in the cytoplasm of gill epithelial and blood vessel endothelial cells. Sporont-like structures appeared as a vacuole containing multiple punctate blue-purple inclusions, which were considered to be immature spores (Figure 4.5d). Both types of spores, auto-infective and environmental, were less consistently labelled than the pre-sporogonic structures, but were still visible in the gills. Auto-infective spores were smaller, approximately 0.8-1 µm in diameter, and usually appeared in clusters in the cytoplasm of the gill epithelial cells. These spores did not always appear as a complete structure, but as small punctate labelling in degenerate tissue (Figure 4.6a). Environmental spores were larger (2-2.5µm) and present in the nucleus of gill epithelial cells or associated with degenerate epithelial cells (Figure 4.6b).

Spores were generally less intensely labelled than pre-sporogonic stages and variation in the intensity was noted (Figure 4.6c).

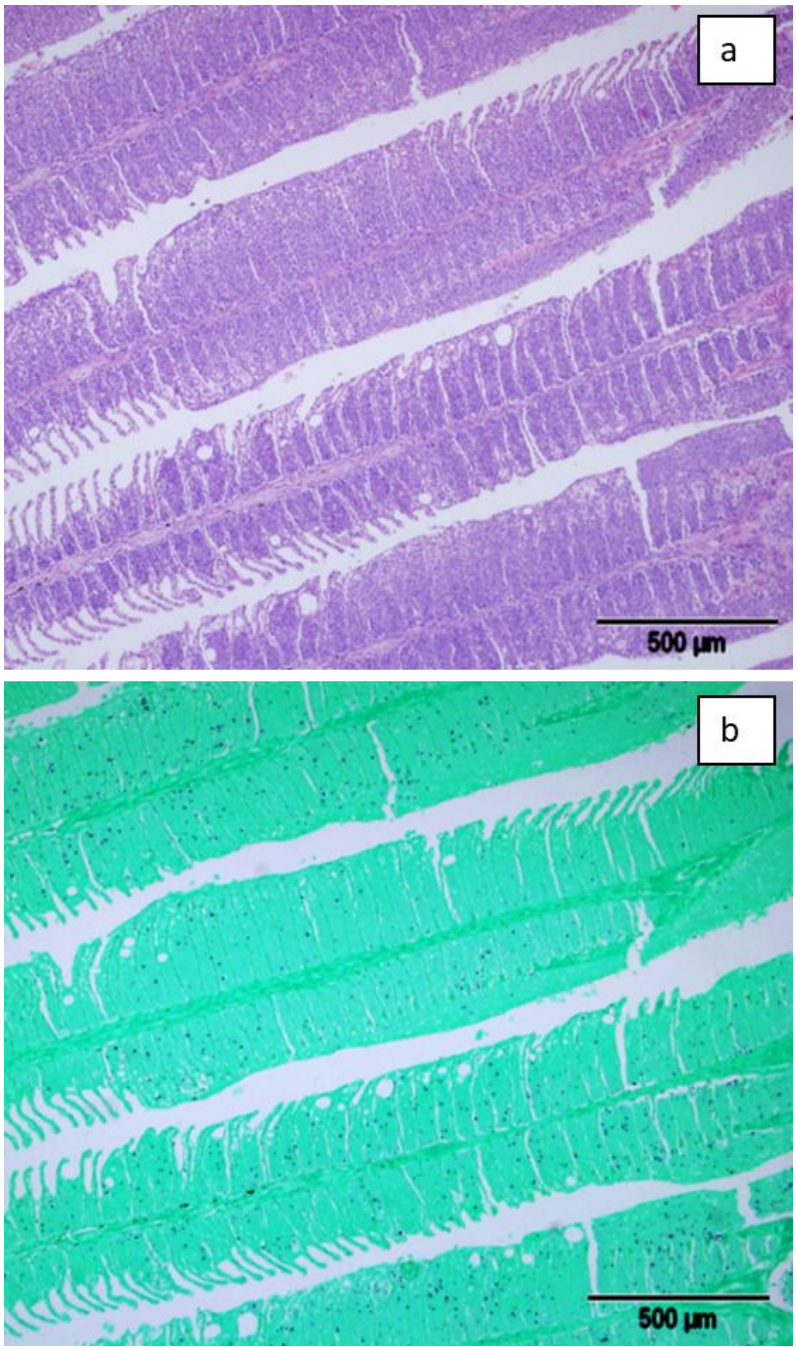

Figure 4.3. Semi-serial histological sections of gills of *Salmo salar* infected with *D. lepeophtherii*. (a) H&E stain and (b) ISH. Note the dark blue labelled structures present in the gill tissue subjected to ISH which are far more difficult to recognise in the corresponding H&E stained serial sections at identical magnifications.

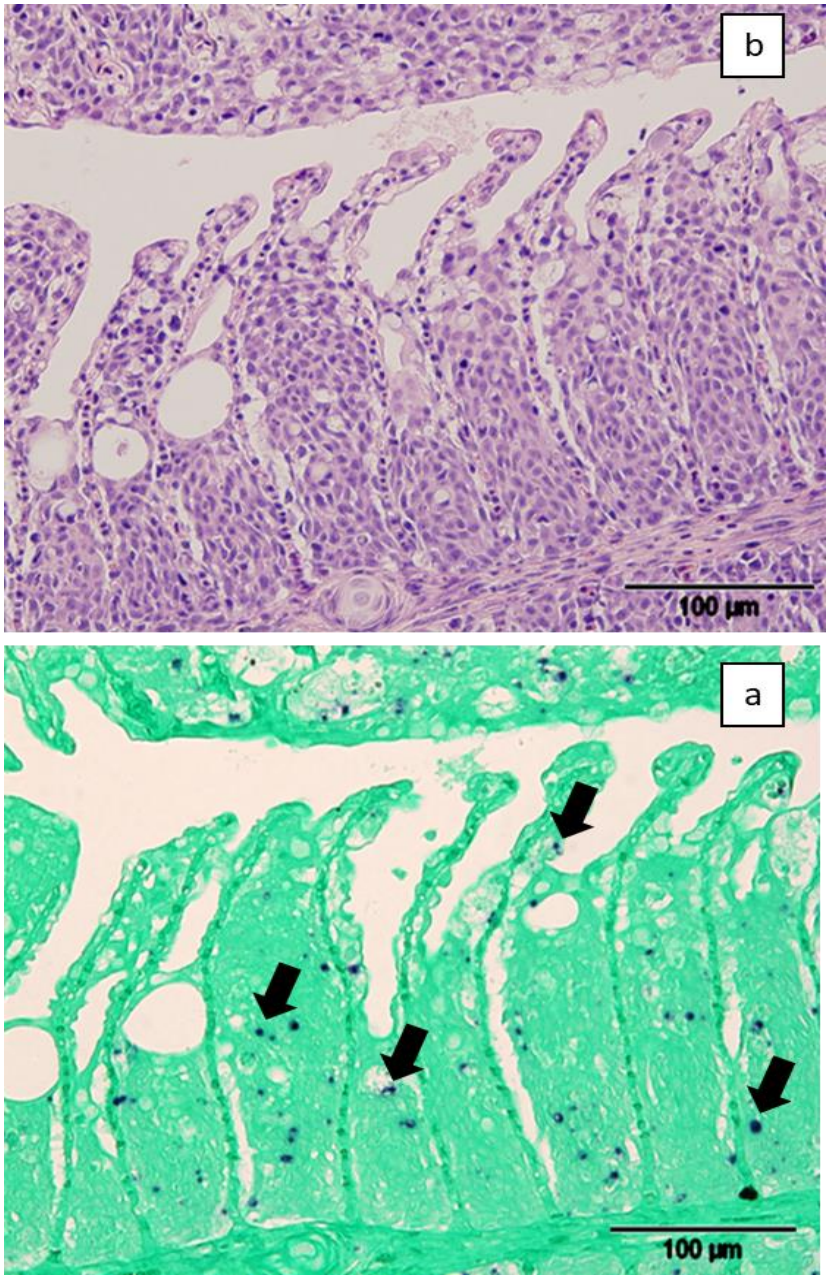

Figure 4.4. Semi-serial histological sections of gills of *Salmo salar* infected with *D. lepeophtherii*. (a) H&E stain and (b) ISH showing labelling of *D. lepeophtherii* (arrows) within the proliferated and degenerated epithelium of the gill lamellae.

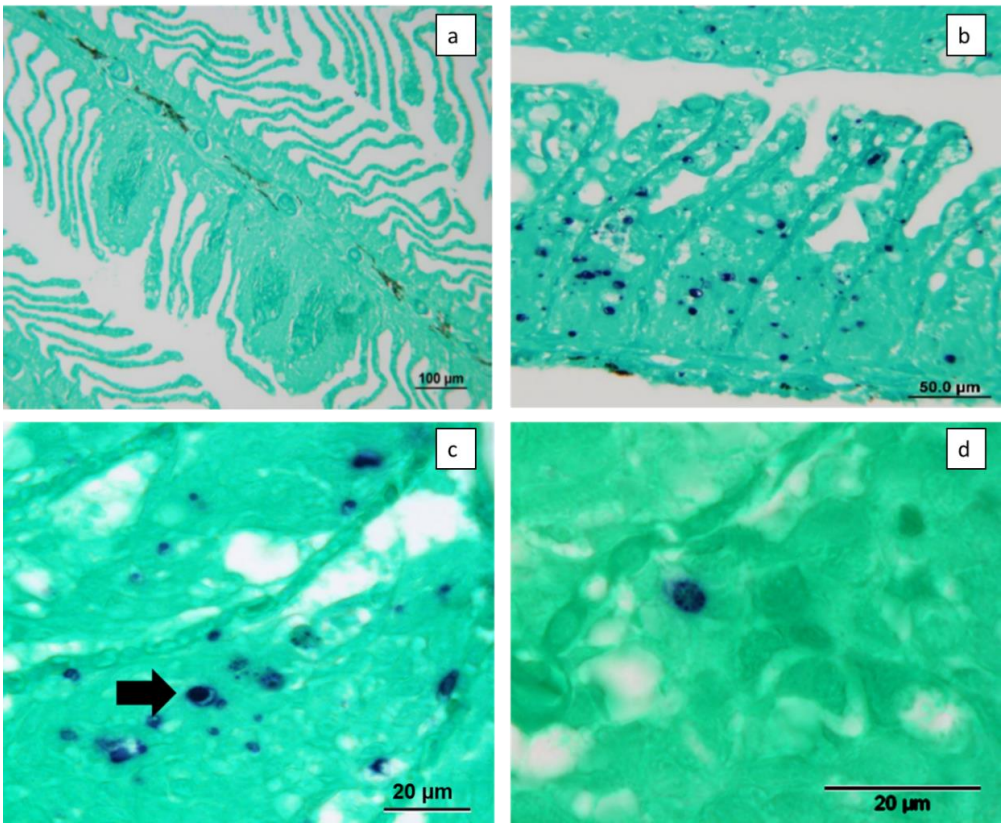

Figure 4.5. Atlantic salmon gill tissue subjected to *in situ* hybridisation specific for *Desmozoon lepeophtherii* (dark blue/purple pigment). (a) Gill of salmon negative to *D. lepeophtherii*. (b) Note pre-sporogonic stages present along the epithelial cells of the gill lamellae. (c) Example of a meront-like structure (arrow) approximately 4 µm in diameter (bar, 20 µm). (d) Note presence of a sporont-like structure and punctate labelling within a vacuole that corresponds to forming spores.

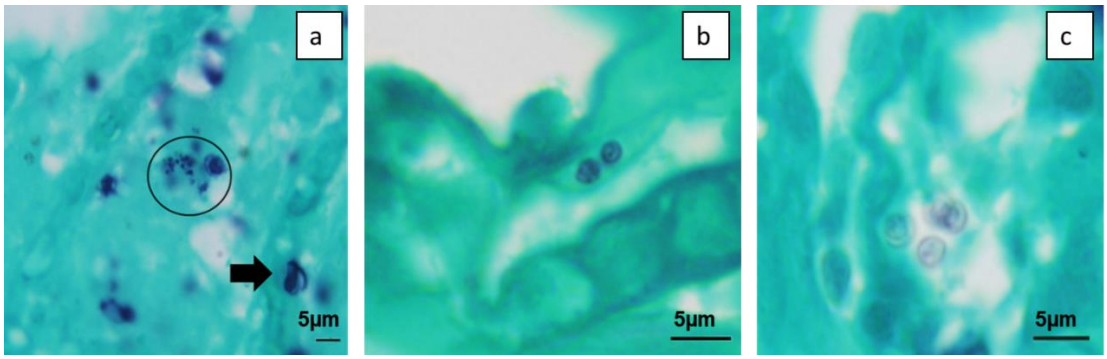

Figure 4.6. *In situ* hybridisation showing the presence of *Desmozoon lepeophtherii* in gills of Atlantic salmon (dark blue/purple pigment)*;* (a) Note proliferative stages (arrow) and a cluster of spore-like structures within the proliferated epithelium of the gill lamella (circle) (bar, 5µm); (b) Two labelled environmental spores; (c) A group of poorly labelled environmental spores of *D. lepeophtherii* measuring 2.5µm in diameter (bar, 5µm).

4.3.3 Detection of *D. lepeophtherii* in non-gill tissues and probe specificity

Tissues from the positive control fish also showed positive labelling for *D. lepeophtherii* by ISH in the interstitium of kidney (Figure 4.7a), spleen and liver parenchyma, *bulbus arteriosus* of the heart and *lamina propria* of the intestine (Figure 4.7b). Sections of sea lice (*Lepeophtheirus salmonis*) containing typical xenomas-like structures caused by *D. lepeophtherii* were ISH positive, with different foci of microsporidia labelled (Figure 4.8a). The gills from Atlantic salmon from Canadian farms showed similar labelling to salmon from Scottish farms using the probes targeting the SSU rRNA (Figure 4.8b) but were devoid of labelling when using the probes complementary to the ITS region. Examination by ISH of lumpfish gills with microvesicles, suggestive of *D. lepeophtherii* infection, did not label. Finally, the oligoprobes used in this study did not cross-react with any of closely related microsporidia species examined (*N. cyclopterii* and *E. hepatopenaei*) (Figure 4.9a & b).

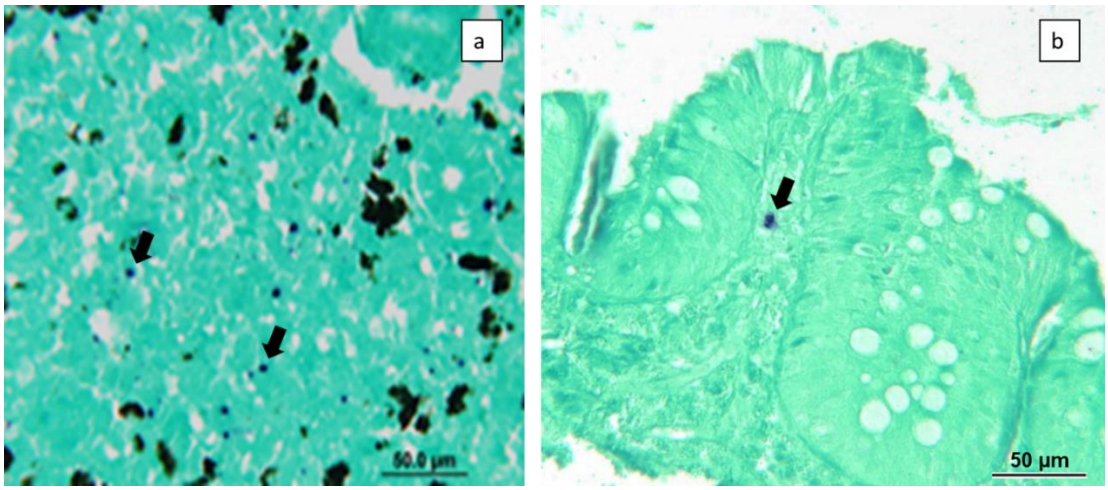

Figure 4.7. *In situ* hybridisation for *Desmozoon lepeophtherii* (dark blue/purple pigment) showing proliferative stages in (a) kidney interstitium (arrow) and (b) *lamina propria* (arrow) of the intestine of *Salmo salar*.

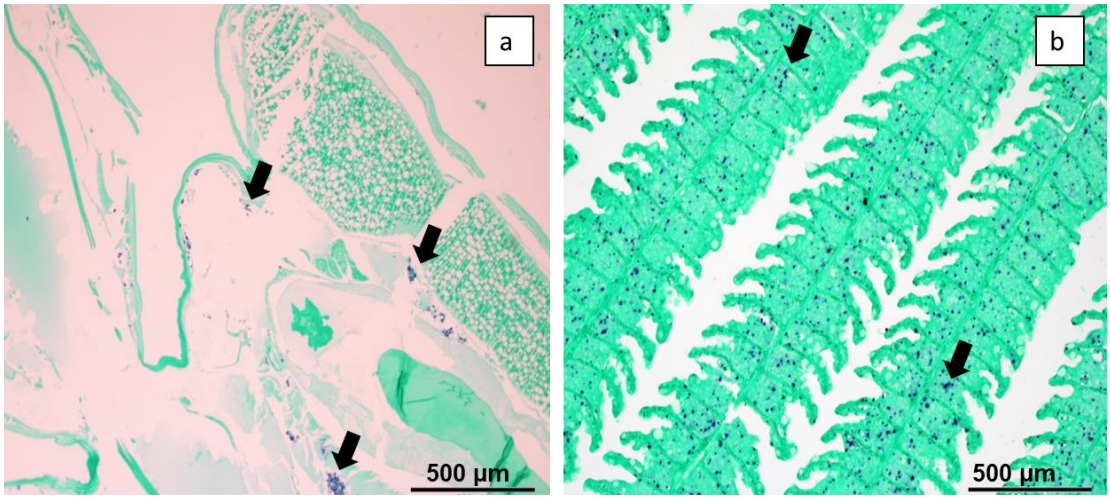

Figure 4.8. *In situ* hybridisation for *Desmozoon lepeophtherii* (dark blue/purple pigment) in sea lice (*Lepeophtheirus salmonis*) infected with the parasite and (b) gills collected from an Atlantic salmon from Canadian farms heavily infected with *D. lepeophtherii*.

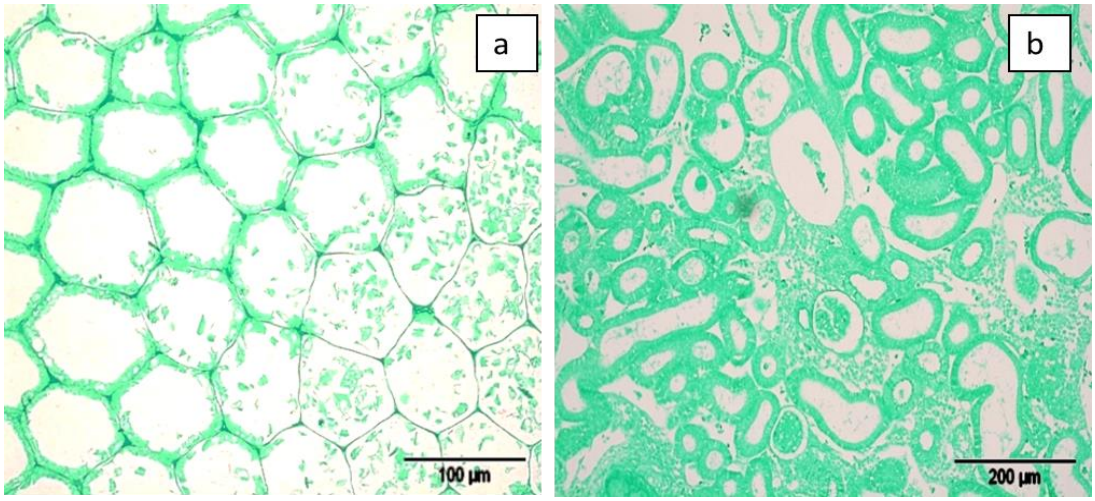

Figure 4.9. *In situ* hybridisation for *Desmozoon lepeophtherii* (dark blue/purple pigment) to test cross-reactions with closely related microsporidian species. (a) hepatopancreas of black tiger shrimp (*Penaeus monodon*) infected with *E. hepatopenaei;* and (b) *C. lumpus*) infected with *N. cyclopterii*. Note complete absence of labelling showing no cross reactivity with the probes used to detect *D. lepeophtherii.*

4.3.4 Comparison of ISH with other techniques used to identify *D. lepeophtherii*

Calcofluor White stained two different sizes of spores. One was smaller (1.1 μm length), ellipsoidal and present in the cytoplasm of cells along the lamellae but the specific cell types were difficult to identify due to the lack of preservation of tissue morphology. These smaller spores were present in aggregates of 3 to 20 and, when not in aggregates, 60x objective lens was required to identify them due to low levels of fluorescence (Figure 4.10). Larger, oval, spores were clearly visible under a 20x objective due to their stronger fluorescence signal and larger size (2.5 μm length).

These were present singularly or in pairs, typically within cells but it was unclear if they were located within the nucleus or the cytoplasm of the cells, again, due to the lack of preservation of tissue morphology with this technique. Spores were present in gills from all fish examined when stained with CW, including four of the fish which were devoid of staining by any other histological method, but only the larger spores were detected. Calcofluor White showed the presence of the large (environmental) spores in gill tissue even when parasite loads were low but the smaller autoinfective spores were only visible when total number of microsporidia labelled with ISH was high (≥150).

Results for the 28 gills sections analysed in this study using ISH, CW and H&E (based on the presence of micro-microvesicles), were compared with the results of the RT-rtPCR (Table 4.7). All methods appeared highly specific (100%) in their ability to detect *D. lepeophtherii*, but sensitivity was markedly higher using the ISH technique (92%), followed by CW (64%) and then H&E (52%). Positive and negative predictive values are shown in Table 4.7. Spearman rank correlation coefficient between the level of microvesicles in the gills stained with H&E and the total ISH counts observed in the gill tissue was significant (r_s= 0.89; 95% confidence interval; $p < 0.001$). There was significant correlation between the pathology score and Ct values obtained from gills biopsies (r_s= -0.92; 95% confidence interval; $p < 0.001$), but correlation between the score and the Ct results obtained from swabs was not significant (r_s= 0.69; 95% confidence interval; p= 0.056). When the total number of microsporidia labelled with ISH was compared with all RT-rtPCR results (from

gill biopsies and swabs), there was a significant correlation ($p \leq 0.03$), and also between the ISH and the gill biopsies Ct value results ($p \leq 0.03$). However, there was no correlation between the ISH results score and the gill swabs Ct results ($p = 0.22$).

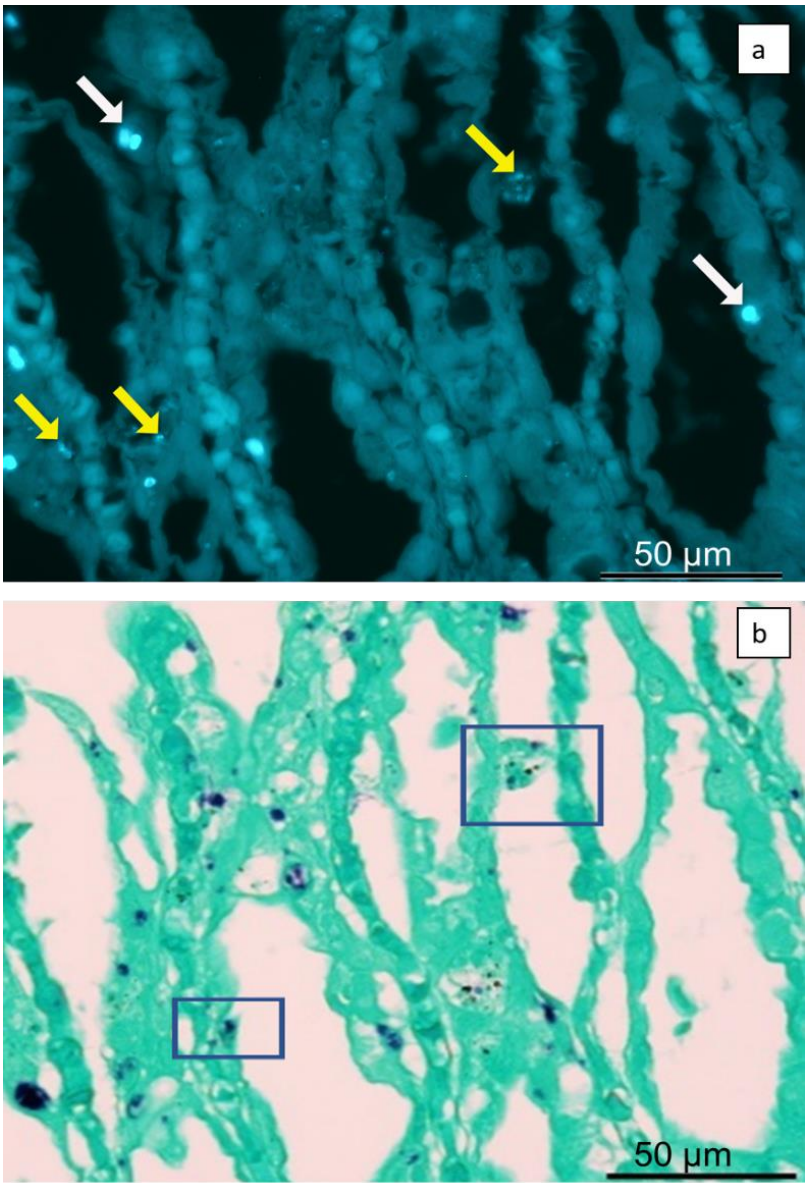

Figure 4.10. Semi-serial histological sections of gills of *Salmo salar* infected with *D. lepeophtherii*. (a) CW showing bright structures corresponding to large (white arrows) and small (yellow arrows) microsporidian spores, (b) note how the same structures label with ISH (boxes).

Table 4.7 Results of Sensitivity, Specificity, Positive Predictive Value (PPV) and Negative predictive value (NPV) on the techniques used when compared with the RT-rtPCR results for predicting the presence of *D. lepeophtherii* in salmon gills.

Method	Analysis	Result	Analysis	Result
In situ hybridization	Sensitivity	92.0%	PPV	100.0%
	Specificity	100.0%	NPV	60.0%
Calcofluor White	Sensitivity	64.0%	PPV	100.0%
	Specificity	100.0%	NPV	25.0%
Microvesicles (H&E)	Sensitivity	56.0%	PPV	100.0%
	Specificity	100.0%	NPV	21.4%

4.3.5 Gill *D. lepeophtherii* burden and the presence of microvesicles

Of the 28 fish examined, 9 did not show any pathology suggestive of *D. lepeophtherii*. Presence of mild to moderate, multifocal, lamellar epithelial cell granular necrosis (Figure 4.11) was present in 5 fish. Low numbers of microvesicles, suggestive of *D. lepeophtherii*, were present in 11 of the examined gills, and a large number were present in 3 fish. The presence of microvesicles was more obvious when the total number of *D. lepeophtherii* labelled with ISH was between 120-850 (in 10mm^2 area) in fish gills, although one fish had small numbers of microvesicles, and only 30 positive *D. lepeophtherii* structures labelled by ISH (Figure 4.12a). For the RT-rtPCR results obtained from gill biopsies, the presence of microvesicles was only observed when the *D. lepeophtherii* load was very high in the gill tissue, as determined by RT-rtPCR (Ct ≤19) (Figure 4.12b). However, gills that had been swabbed showed less consistent results with respect to the presence of necrosis. The swab from fish 23 showed a Ct of 19 but on HE, necrosis was not present in the tissue section from the gills. Conversely, fish 24 had a Ct value of 20 and had large numbers of microvesicles suggestive of *D. lepeophtherii*.

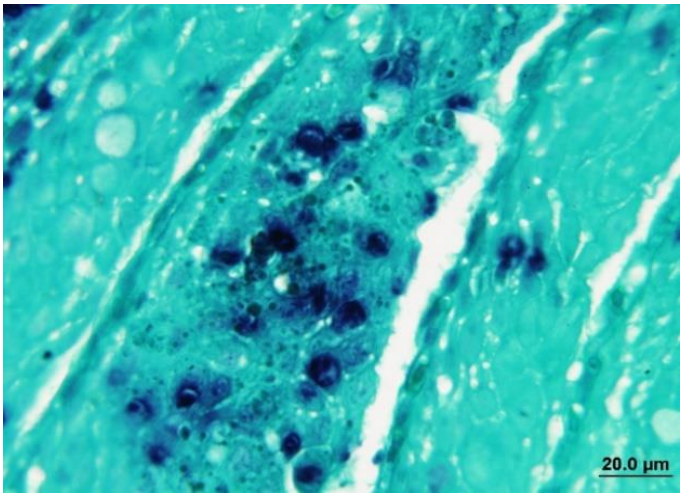

Figure 4.11. *In situ* hybridisation showing the presence of *Desmozoon lepeophtherii* in the gills of *Salmo salar* associated with a focal area of epithelial granular cell necrosis.

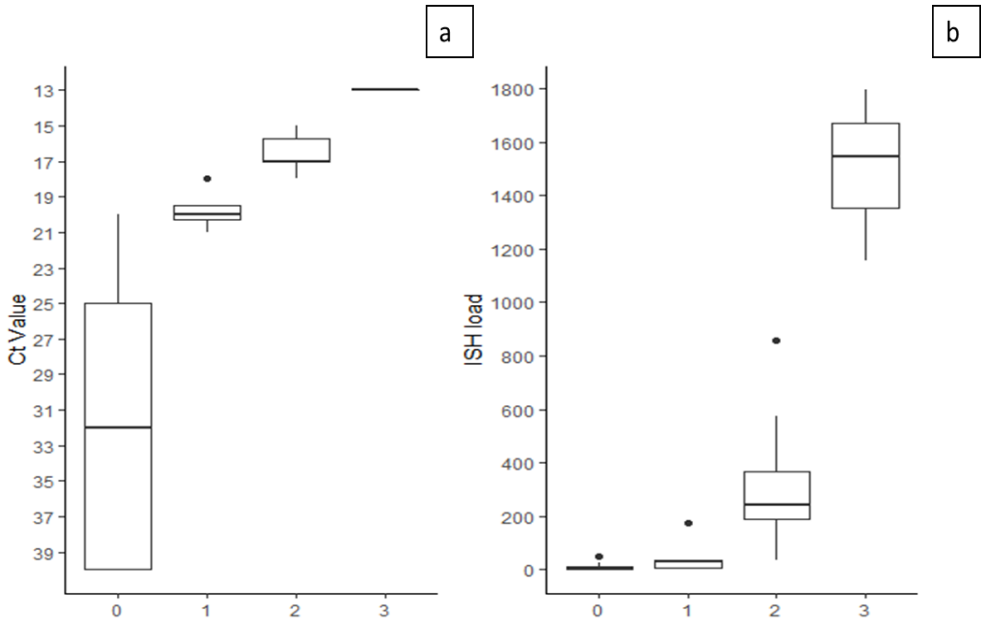

Figure 4.12. Boxplot of the pathology score in salmon gill tissue with different burdens of *D. lepeophtherii* represented as (a) RT-rtPCR Ct values and (b) ISH total counts in 10 mm² of gill tissue (ISH load). Pathology score (x- axis): 0 absence of necrosis, 1; epithelial granular cell necrosis but absence of microvesicles, 2; presence of small to medium numbers of microvesicles, 3; large numbers of microvesicles.

4.4 Discussion

Desmozoon lepeophtherii is one of the most prevalent putative disease-associated agents detected by molecular methods in the gills of farmed populations of Atlantic (Downes *et al*., 2018; Gunnarsson *et al*., 2017) and Pacific salmon (Laurin *et al*., 2019). In addition, the parasite has been detected in sea lice (*Lepeophtheirus salmonis* and *Caligus elongatus*) (Freeman & Sommerville, 2009; Nylund *et al*., 2010), which are themselves a parasite of salmon, various species of wrasse (Steigen *et al*., 2018) and trout (*Salmo trutta* and *Oncorhynchus mykiss*) (Nylund *et al*., 2010), and different species of wild Pacific salmon (ICES Working Group, 2018; Thakur *et al*., 2019). Although the microsporidian has been associated with gill disease (Matthews *et al*., 2013; Nylund *et al*., 2011; Weli *et al*., 2017) in farmed Atlantic salmon, the interaction between pathogen and hosts remains to be understood due to *D. lepeophtherii's* ubiquitous nature, difficulty of detection in tissue sections, and lack of *in vivo* and *in vitro* studies. Histopathological examination is critical to gaining an understanding of the association between the microsporidian and the pathology present in salmon affected by gill disease, but most of the techniques focus on the detection of the spores and do not clearly detect developmental stages (Herrero *et al*., 2020).

A total of five antisense oligonucleotides probes complementary to the positive strand were designed and subjected to the ISH method, three were complementary to the positive strand of the small subunit region (SSU) and two to the internal transcribed spacer (ITS) region of *D. lepeophtherii*. Four out of five probes (three complementary to the SSU and one to the ITS region) gave a strong positive signal but one, 819L25, gave a level of non-specific labelling that hindered the localisation of the parasite. Reduction of the excess non-specific labelling was achieved by increasing the stringency of washing steps (Wilcox, 1993) thereby removing unbound probe effectively. The four successful probes also detected *D. lepeophtherii* in the gill tissue of farmed salmon in Canada despite a presumably different *D. lepeophtherii* genotype (Jones *et al*., 2012) and despite two of the probes having one mismatch with the sequence described in Canada. Surprisingly, the only probe that did not work in any of the samples examined was probe 1284L21 which was the

oligonucleotide designed specifically to recognise the European *D. lepeophtherii* genotype (ITS region). Although oligonucleotide design or inadequate parameters in the ISH method need to be investigated first, there is a possibility that variations in the ITS region and also more diversity in the genotypes of *D. lepeophtherii* exist. In the fungal kingdom, the ITS region has been shown to be generally superior for inter- and intraspecific discrimination compared to the LSU or SSU (Schoch *et al*., 2012). For instance, more than 100 genotypes have been described for the microsporidian *Enterocytozoon bieneusi*, a microsporidian closely related to *D. lepeophtherii*, by sequence analysis of the ITS, and these have been associated with different host affinities and different levels of pathogenicity (Galván-Díaz *et al*., 2014). Further molecular characterization of intraspecies genetic diversity of *D. lepeophtherii* from different geographical areas and host species may help better understanding of the role of this microsporidian in gill disease.

The probes for the ISH appear to be specific for *Desmozoon* spp. in that they did not cross react with the two close related microsporidians examined (*E. hepatopenaei* and N. *cyclopterii*). In the sea louse with xenoma-like structures below the cuticle, which is highly suggestive of *D. lepeophtherii* infection (Freeman & Sommerville, 2009), an intense positive signal was present after application of the ISH method. This confirmation of the presence of *D. lepeophtherii* in the lice examined makes ISH a valuable tool for studying the various stages of *D. lepeophtherii* in this species (*i.e*. Økland, 2012). Although a description of the parasite's systemic distribution and associated pathology was not the aim of this study, fish with high burdens of *D. lepepophtherii* in the gills (by ISH signal or RT-PCR values) showed a positive ISH signal in other organs. The systemic distribution of the microsporidian has been commonly reported by other authors (Di Cicco *et al*., 2017; Matthews *et al*., 2013; Nylund *et al*., 2010) but typically has not been associated with major tissue damage with the exception of a case report by Weli *et al*. (2017) in which the presence of *D. lepeophtherii* was associated with severe pathology in the gills, peritoneal cavity and in the gastrointestinal tract. In our study, large numbers of *D. lepeophtherii* DNA were not detected in the gastrointestinal epithelium or pancreatic tissue. However, only single fish or small groups of fish from different clinical cases were selected for this study that may not necessarily have had the same clinical signs as the one

reported previously. Little is known about the effects of *D. lepeophtherii* in the other organs of fish and its systemic distribution is usually overlooked.

In the gill tissue, positive labelling, by ISH, of the parasite's developmental stages was present in the cytoplasm and nuclei of the gill lamellar epithelial cells and in the cytoplasm of endothelial cells of the blood vessels in the gills, which agrees with the described life cycle (Nylund *et al*., 2010) and previous studies (Weli *et al*., 2017). Auto-infective spores were labelled as small punctate foci, 0.6-1µm in size, present singly or in small aggregates and in direct contact with degenerate lamellar epithelial cells. Additionally, they were sometimes present within the cytoplasm of apparently normal gill lamellar epithelial cells. Larger environmental spores were observed occasionally by ISH, appearing as round to oval structures, 2.5µm in length, either singly, in pairs or, more rarely, in small aggregates of 5-6. These spores were present within the nucleus of the gill lamellar epithelial cells, or associated with degenerate epithelial cells, and had variable and less intense signal compared to the pre-sporogony stages. Limitations on ISH, due to low signal intensity, is reported frequently and is mainly associated with small numbers of the target or insufficient accessibility of the target sequence (Amann *et al*., 1995). The detection of microsporidia with ISH using antisense DNA oligonucleotides that target the SSU region may result in a poor spore signal due to reduced or absent protein synthesis during the spore stage and the highly condensed genome of some microsporidian species, which would reduce the availability of the regions of the parasite's genomic rDNA with which the probes could hybridize (Ahmed *et al*., 2019). This reduced intensity of the labelling in the spores by ISH has been reported for other microsporidian species including a recent RNA-based ISH method for detecting *D. lepeophtherii* (Weli *et al*., 2017). In our procedure, spores were identified mainly as punctate labelling and rarely as fully labelled oval structures. The increased intensity of ISH spore signal compared to other studies could be due to the use of the 5′-, 3′-doubly labelled probes instead of the more typical singly labelled probes, and this approach has proven successful in other studies (Stoecker *et al*., 2010).

An analysis of the sensitivity and specificity of the ISH method was undertaken to determine the usefulness of the technique compared to other detection methods.

However, complete validation of this ISH requires the analysis of samples from a large population of *D. lepeophtherii*-infected vs. non-infected fish (see Georgiadis *et al*., 1998). A sampling of this magnitude was outwith the scope of the present study. Additionally, the peak in incidence of clinical disease is usually seasonal and short (Matthews *et al*., 2013) and a large number of fish tissue samples with gross pathology would be difficult to collect. The ISH method was applied to gill samples from 28 fish to allow initial comparison with other histological methods (CW and HE) used commonly to detect *D. lepeophtherii* in gill tissue sections. To do this, tissue sections containing various parasite loads were selected based on RT-rtPCR results as a 'gold standard positive control', because of the specificity and sensitivity of the PCR technique to detect the parasite (Nylund *et al*., 2011). The sensitivity of the ISH was high (92%) and similar to that of the RT-rtPCR. As both techniques target the genome of the microsporidian, PCR and ISH are capable of detecting clinical and subclinical infections that can be missed by other, less sensitive, histological methods. Although quantitative PCR is more sensitive than ISH, because of the amplification of the original signal, RT-rtPCR is susceptible to false positive results due to contamination, and also there is no association with specific histological lesions. For a higher level of resolution, the ISH combines the high sensitivity and specificity of molecular detection with direct observation of the presence, subjective load and distribution of the parasite in the gill tissue. In addition, when gill biopsies where subjected to RT-rtPCR, the Ct values obtained correlated significantly with the total number of parasites observed in the gill tissue using ISH. However, no correlation was found between gill swab PCR Ct values and the ISH of the corresponding gill tissue. These results highlight the usefulness of ISH for quantifying both the level and associated pathology of the microsporidian in the gills. The ISH method can be used as a standalone procedure in the absence of RT-rtPCR results. Although using gill swabs to perform RT-rtPCR is a non-lethal option of assessing the presence of the microsporidian in fish gills, the results will be less reliable compared to those from RT-rtPCR of gill tissue biopsies or ISH because of the intracellular nature of the parasite.

Calcofluor White allowed the visualization of the two types of spores described for *D. lepeophtherii* (Nylund *et al*., 2010) in agreement with previous studies (Herero

et al., in press; Weli *et al*., 2017). This fluorochrome has been widely used to detect microsporidia (Didier *et al*., 1995; Khanaliha *et al*., 2014; Luna *et al*., 1995), due to its ability to bind to chitin, which is present on the inner layer of the spore wall (Franzen *et al*., 1995). Calcofluor White has been previously demonstrated to detect higher numbers of *D. lepeophtherii* spores in gill tissue compared with other routine histological techniques (Herrero *et al*., 2020). However, the sensitivity of CW was only 64% when compared to RT-PCR probably because the pre-sporogonic stages develop prior to the spores are not detected by the fluorochrome. Assessment of *D. lepeophtherii* based on the presence of microvesicles in gill tissue sections stained with H&E gave a sensitivity of 52%. Pathology caused by the microsporidian is probably the consequence of intense parasite proliferation and spore formation and only obvious in the advanced stages of the disease. Microvesicles were detected in 14 out of the 28 fish examined. Absence of necrosis suggestive of *D. lepeophtherii* was recorded in 8 fish. High burdens of *D. lepeophtherii* in tissue sections were significantly associated with the development of the microvesicles such that Ct values below 19 and/or ISH total counts of over 100 microsporidia seem to be necessary. The presence of necrosis of epithelial cells but absence of microvesicles, in this study denoted as epithelial granular cell necrosis, has been suspected to be an early stage of *D. lepeophtherii* infection. Nevertheless, this change is very non-specific and was not consistently associated with the presence of positive ISH signal. Although the presence of medium to high numbers of microvesicles are highly suggestive of *D. lepeophtherii* infections in Atlantic salmon gills, a positive result with RT-rtPCR or ISH is necessary to confirm the presence of the parasite in clinical cases. Gills of lumpfish that had microvesicles present were negative for *D. lepeophtherii* by ISH demonstrating that the presence of microvesicles is a non-specific change that can be associated with other disease processes.

In conclusion, the DNA based ISH method developed during this study effectively detects *D. lepeophtherii* in Atlantic salmon in FFPE tissue sections. The method enables assessment of the burden of *D. lepeophtherii* in tissues, and significantly correlates with the RT-rtPCR results. Although the presence of microvesicles was observed in histological sections only when the burdens of *D. lepeophtherii* in the gill tissue, as determined by PCR, were very high (Ct values ≤

19), the pathology associated with the presence of the parasite (necrosis, epithelial cell proliferation and inflammation in the gills) seems to change during the course of the disease (Matthews *et al*., 2013; Weli *et al*., 2017) and, unless severe, pathology caused by *D. lepeophtherii* is difficult to discern in a complex gill disease scenario. Under these circumstances the capacity of the developed ISH to detect the agent of interest, and the wider information provided when doing so is far superior compared to all other techniques. Routes of infection or spatio-temporal migration in different host tissues are mostly unknown for this species, mainly due to the lack of *in vitro* culture models of the parasite and, therefore, lack of *in vivo* experimental infection studies. A further use of this novel ISH method would be to study the progressive development and spread of the parasite after exposure via feeding of infected tissue or cohabitation studies of infected and naïve fish.

4.5 Acknowledgments

This work was financially supported by the European Commission under the TNA programme within AQUAEXCEL^{2020} project. I would like to thank Oswaldo Palenzuela at the Instituo de Acuicultura Torre de la Sal (Castellón, Spain), for his enormous help and guidance in the development of the ISH technique. I also thank Simon Jones for providing gill tissue from farmed Atlantic salmon from Canada infected with *D. lepeophtherii*.

Chapter 5 General Discussion

5.1 Complex gill disorder syndrome

Gill disease is an important cause of morbidity and mortality in the marine stage of Atlantic salmon farming, and a challenge for fish welfare (Gjessing *et al*., 2017; Rodger, 2014). The real cost of gill disease for the salmonid industry is not known, but it is one of the main causes of losses in production experienced by salmon producers worldwide (Mowi, 2019). In Scotland, salmon industry stakeholders have agreed to report their mortality events to the competent authority (Marine Scotland Fish Health Inspectorate) as detailed in the Industry Code of Good Practices (The Scottish Government, 2019). Analysis of mortality events recorded from 2015 until June 2019, including "*reason of death*" and "*total mortalities*", show gill diseases, such as AGD, proliferative gill disease (PGD) and complex gill disorder (alone or together with other non-gill diseases), as the "*explained reason*" for more than 60% of the total mortalities recorded. Although these mortality numbers have not been obtained from a comprehensive study of the disease situation, they still suggest gill disorders are one of the most important issues currently facing the industry. Additional economic costs of gill disease can be difficult to calculate, but include the cost of reduced productivity, treatments (Mitchell & Rodger, 2011; Shinn *et al.*, 2015) and increased susceptibility to other pathogens (Rodger, 2014).

In some gill diseases the relationship between the infectious agent and its host is clear (e.g. AGD). However, gill disease can often be the result of a combination of factors including infectious agents, environmental conditions and various husbandry practices (Mitchell & Rodger, 2011). In recent years, a recurrent pattern of gill disease of unknown aetiology has occurred in Norway, Scotland and Ireland (Kvellestad *et al*., 2005; Matthews *et al*., 2013; Mitchell & Rodger, 2011). Complex gill disorder (CGD, also known as complex gill disease) is a term being used by those working in fish health that encompasses previously defined gill diseases such as PGI and PGD. Complex gill disorder incorporates a range of clinical and pathological presentations of gill disease found in Atlantic salmon in seawater farms due to the resultant interactions between the environment,

management practices, pathogenic microorganisms and host factors. The histopathological criteria of CGD has recently been defined as a moderate to severe gill lamellar branchitis of unknown aetiology together with other histo-morphological changes (Noguera *et al*., 2019). The use of "disorder" instead of "disease" results from the lack of knowledge of the true aetiology of this syndrome. The term "disorder" refers to the disruption of the normal function of, in this case an organ, whilst a strict definition of "disease" involves a disorder attributable to a specific cause (Mosby, 2016).

Respiratory diseases of multifactorial aetiopathogeneses have also been described in farmed mammalian species. For instance, bovine respiratory disease complex is one of the main causes of loss in bovine production in North America and includes the interaction between stress, management practices and several viral and bacterial pathogens (Griffin *et al*., 2010). However, despite the obvious infectious nature of bovine respiratory disease, it has been difficult to reproduce the clinical signs of the disease *in vivo* when cattle have only been exposed to individual bacteria or viruses due to the disease's multicomponent aetiology (Lillie, 1974; Taylor *et al*., 2010). A similar situation appears to occur in CGD as when cohabitation challenges were performed with ASPV, a virus detected during PGI outbreaks, the virus was transmitted successfully to naïve fish from infected fish, but the former failed to develop clinical signs of the disease (Kvellestad *et al*., 2003). Wiik-Nielsen *et al*. (2017) exposed naïve fish to the same water (freshwater) in which fish infected with SGPV, *Ca*. B. cysticola, *Ca.* P. salmonis were held. Even though naïve fish became infected with all three agents, only mild lamellar epithelial hyperplasia and branchitis was observed in association with *Ca*. B. cysticola infections. It is possible that for experimental reproduction of the pathology and clinical signs associated with CGD, it may be necessary to expose fish to other stressors rather than just a single pathogen.

Studies on infectious gill disease agents in Scottish aquaculture, other than *P. perurans*, are scarce. Since PGI was defined in 2005 in Norway (Kvellestad *et al*., 2005) the only published article focusing on any CGD- related pathogen in Scotland was performed by Matthews *et al*. (2013) who reported a case of gill disease in

which *D. lepeophtherii* was involved. Additionally, Pflaum (2012) found a significant relationship between RT-rtPCR loads of *D. lepeophtherii* and gill pathology in cases of gill disease. Work investigating SGPV in Scotland has published recently (Gjessing *et al*., 2018) in which fish from a flow-through hatchery were positive for the virus by PCR and had lesions suggestive of SGPV. *Candidatus* B. cysticola is found in the gills of farmed salmon in Scotland (pers. comm. H. Rodger) but surprisingly, no public reports existed until now and only for epitheliocysts suggestive of *Ca*. B. cysticola (Herrero *et al*., 2020; Rodger & Mitchell, 2013). However, projects focusing on gills disease are currently underway (SRUC, 2019) which will help to address many of the knowledge gaps of this condition.

5.2 Status of CGD putative pathogens in Scotland

The dynamics of the putative pathogens associated with CGD in Scotland (*D. lepeophtherii*, *Ca.* B. cysticola and SGPV) as well as *P. perurans*, the aetiological agent of amoebic gill disease (AGD), was examined in Chapter 3. A longitudinal study was performed in two salmon farms in different locations in Scotland commencing with the sampling of fish from the later stage of the freshwater rearing and terminating after the fish had spent one year in their marine site. In the freshwater stage both farms were positive to *Ca*. B. cysticola and SGPV and their detection continued in the marine phase which suggests that the fish had carried the pathogens with them from their freshwater location to their marine site. The results showed that the two farms were RT-rtPCR positive for the four pathogens examined in the marine farm. *Ca.* B. cysticola and *D. lepeophtherii* were the most prevalent of the agents, in agreement with other studies in Ireland, Norway, and more recently, Canada (Downes *et al*., 2018; Gunnarson *et al*., 2017; Laurin *et al*., 2019), whilst SGPV was detected sporadically throughout the study, as also described in a salmon farm in Ireland (Downes *et al*., 2018). The loads of the screened pathogens were significantly associated with the water temperature, with higher loads when temepratures were above 10 °C. In addition, the increase in severity of gill disease was significantly associated with the season (autumn), and when season was removed from the statistical model for the farm showing gill disease, there was also a

significant association between gill disease and increasing water temperature. These findings suggest that temperature is not only a significant contributor for the increased pathogens load, but also for the development of gill disease. Further studies are necessary to determine the role of *Ca*. B. cysticola and SGPV as potential gill pathogens in the marine environment.

5.3 On-farm practices and CGD

The role that on-farm practices have in gill health deserves further investigation. In Chapter 3, the farms studied used different types of net cleaning and treatment methodologies, therefore it was not possible to account for these factors in models in which scores from both farms were used. However, the models in which only Farm B was analysed, net cleaning with high pressure water jet methods had a significant effect on the gill score. The effects of the high-pressure net cleaning in gill health (used in Farm B) have been discussed in previous sections. In this study, other factors, such as AGD infections, were considered to be more important causes of the higher gill disease scores seen in Farm B compared to Farm A. However, the difference in the net cleaning practices between farms could have contributed to the development of more severe overall gill disease in Farm B. It is therefore essential that future studies in CGD include the type and frequency in net cleaning as a factor affecting gill health.

The days since the last treatment with hydrogen peroxide was also significant in the model in which only Farm B was assessed. In Chapter 3, it was discussed why this result should be interpreted with care and how there was not enough evidence in the gill histopathology results to suggest that this factour would have been key in the development of gill disease. However, the excessive exposure to this chemical has shown to be detrimental to gill health (Rodger et al., 2011) and it should be considered when studying the effect development of gill disease in field studies. This result shows the importance of knowledge of all the parameters influencing the experimental system when interpreting the outputs from the statistical analyses, particularly in uncontrolled experiments undertaken in a commercial fish farm. The use mechanical methods to remove the sea lice from the fish was not associated with

the development of gill disease in this study. The use of non-medicinal de-lousing systems has increased in the recent years as a response to the increased resistance lice have developed to chemical treatments (Overton et al., 2018) and adverse effects, such as gill haemorrhages, have been reported in Norway when using these methods (Hjeltnes et al., 2018; Hjeltnes et al., 2019). The mechanical and thermal treatments need fish to be crowded in the net-pen and then transferred to the treatment boat. These handling events are stressful for the fish and increase the risk of physical damage to the skin, eyes and gills (Hjeltnes et al. 2018). Also, panic reactions due to exposure of warm water could cause collisions in the treatment chambers during the thermal treatment (Hjeltnes et al. 2018). Independent experimental studies investigating the effect of these two methods of treatment on gill health are very limited (Overton et al., 2018) which is surprising considering the increasing use of these technologies. The potential effect thermal and mechanical de-lousing methods could have on gill health and their impact on fish welfare requires urgent investigation.

5.4 Future studies on CGD

The presence of the most important pathogens associated with CGD was investigated in Chapter 3. The use of next-generation sequencing technologies should be considered for future studies to characterize the organisms present in the gills of salmon with CGD. Instead of targeting a single agent, metagenomic sequencing allows the analysis of any organism present, whose genomic sequence is available, within a single sequencing analysis (Van Dijk *et al*., 2014)

An important area for future research would be the role of the microbiome in CGD. The microbiome has been defined as “the ecological community of commensal, symbiotic, and pathogenic microorganisms” (Lederberg, 2001) that share a body space. In a similar way to mammals, teleost fish show varied microbial communities associated with different biogeographic locations such as gut, gills or skin (Merrifield & Rodilles, 2015). The microbial population is considered to be dynamic and is affected by several factors such as the life stage of the fish (Llewellyn et al., 2016), environment (Lokesh & Kiron, 2016), diet (Green et al.,

2013), diseases (Llewellyn et al., 2017) or the application of treatments (Navarrete et al., 2008). The microbiome has an intrinsic relationship with the host's immune system and certain changes can alter the microbiota-host immune system interaction affecting susceptibility to diseases (Pérez et al., 2010). Furthermore, alteration of the homeostasis of the microbial communities can lead to dysbiosis (imbalance in the microbial community) facilitating the proliferation of opportunistic pathogens present naturally in the microbiome of the fish. For instance, an increase in opportunistic pathogenic bacteria in the skin microbiome of farmed Atlantic salmon has been associated with elevated sea lice burdens (Llewellyn et al., 2017) and high-infection levels of salmon alphavirus (Reid et al., 2017).

The gills of fish are in direct contact with their aquatic environment and it is therefore a primary barrier of defence against pathogens. Although there are some studies on the gill microbiome in teleosts (e.g. Legrand *et al*., 2018), investigation of the resident microbiota present in the gills of farmed Atlantic salmon is at its early stage. Considering the various factors involved in the development of CGD, future studies should focus on characterising the composition of the gill microbiome and how it changes over time in the production cycle and during the pathogenesis of the disease.

5.5 Insight into the biology of *D. lepeophtherii*

Desmozoon lepeophtherii is a microsporidian parasite associated with CGD in salmon, but it is also known to infect the sea lice (Freeman 2002, Nylund *et al*., 2010). It is the first described microsporidian that alternates its development and sporogony between invertebrate and fish hosts (Kent *et al*., 2014) but the mode of transmission of the parasite is unknown. The sea louse has been suggested to be the definitive host of *D. lepeophtherii* due to the variation between mono- and diplokaryotic nuclei in the development of the microsporidian indicating the presence of sexual processes such as meiosis and karyogamy, which do not occur in salmon (Nylund *et al*., 2010; Økland, 2012). Salmon is thought be an alternate host, which becomes infected by spores released from the sea lice after their death (Sveen *et al*., 2012). In view of this theory, attempts were made in Chapter 2 to reproduce

the life cycle of the microsporidian *in vitro* using RTgill-W1 and SHK-1 cell lines. Chapter 2 represents the first documented experiment in which fish cell lines were exposed to *D. lepeophtherii* and the results obtained may provide valuable information for subsequent trials focusing on the culture of this microsporidian. These studies should include the use of insect cell lines and the Atlantic salmon gill cell line recently developed by Gjessing *et al*., (2018). Trials with spores isolated from salmon gills are recommended also, together with the use of more sophisticated techniques to assess the parasite development such as the ISH developed in Chapter 4. In addition, the results raise interesting questions. The conditions required for a parasite with a complex life cycle, such as *D. lepeophtherii*, to grow *in vitro* could be difficult to achieve. It is also possible that transmission from louse to salmon does not occur, or even that another intermediate host is necessary for the infection to occur in salmon. Future experimental models to investigate the transmission and infection routes of *D. lepeophtherii* in the lice and salmon and to better understand the parasite's biology, should include *in vivo* infections. Different routes of infection can be utilised to achieve the infections under experimental conditions such as bath exposure of Atlantic salmon and sea lice to spores of *D. lepeophtherii* derived from lice or salmon gills, feeding with infected tissue or isolated spores, direct gavage into the stomach of anaesthetized salmon, or through co-habitation studies between infected and naïve lice or between infected and naïve salmon. Using ISH method developed in this work would enable study of the sequential development and spread of the parasite in salmon after exposure to the microsporidian.

5.6 *Desmozoon lepeophtherii*: primary or opportunistic pathogen?

Microsporidia are generally considered to be opportunistic parasites but their ability to negatively affect the health of fish as primary pathogens has been demonstrated (Kent *et al*., 2014). For instance, *L. salmonae* is a well-studied microsporidian, the causative agent of microsporidial gill disease that affects different species of Pacific salmon and rainbow trout (Becker and Speare, 2007). Pathology associated with *L. salmonae* starts with the formation of xenomas in the pillar cells of the gills, followed by the rupture of this structure and formation of a marked granulomatous

inflammatory response (Sánchez *et al*., 2001). However, the role of *D. lepeophtherii* is controversial despite various studies linking the microsporidian with PGI (Stenium *et al*., 2010; Nylund *et al*., 2011; Weli *et al*., 2017) or similar necrotic and proliferative pathologies (Matthews *et al*., 2013). Proliferative gill inflammation is based on a criterion of four concurrent histomorphological changes in the gills which include epithelial cell necrosis, epithelial lamellar hyperplasia, infiltration by inflammatory cells and circulatory disturbances (Kvellestad *et al*., 2005). Interestingly, the pathology related with *D. lepeophtherii* is very similar to the changes described for PGI (with exception of circulatory disturbances). In acute stages of the infection, *D. lepeophtherii* has been associated with necrosis of the epithelial cells and formation of microvesicles, whilst in sub-acute and chronic stages a host response involving lamellar epithelial hyperplasia and infiltration of inflammatory cells has been described (Weli *et al*., 2017). Furthermore, *D. lepeophtherii* has been hypothesised to be a primary fish gill pathogen by some authors (Gunnarson *et al*., 2017; Nylund *et al*., 2010; Nylund *et al*., 2011;). Conversely, others suggest *D. lepeophtherii* is an opportunistic pathogen requiring an immunosuppressed host, similarly to microsporidiosis in humans (Freeman and Sommerville, 2009; Steinum *et al*., 2010). In Chapter, 3 the relationship between changes in the load of the four pathological agents associated with gill disease and their relationship with gill disease was examined over time. Statistical analysis of the data from the two farms showed that variations in in the RNA loads of SGPV and *Ca*. B. cysticola loads were not associated with the gill score ($p>0.05$), while increasing loads of *D. lepeophtherii* and *P. perurans* significantly correlated with an increased gill score in fish from the farm suffering from gill disease ($p< 0.001$). However, obvious pathology suggestive of *D. lepeophtherii* (microvesicles) was not observed, which suggests the significant associations are the result of the parasite developing in more disease affected gills (with higher gill score) rather than *D. lepeophtherii* being a causative agent of the gill pathology. In Chapter 4, a highly specific and sensitive ISH method was developed to detect *D. lepeophtherii* in tissue sections. In addition to this, the relationship between the loads of *D. lepeophtherii* (assessed by ISH counts and by RT-rtPCR Ct values) and the severity of *D. lepeophtherii* presumptive pathology was examined. The results showed a significant

association between gill pathology and high loads of *D. lepeophtherii,* but high burdens of *D. lepeophtherii* in tissue sections (i.e. Ct values below 19) were significantly associated with the development of *D. lepeophtherii* microvesicles. Therefore, pathology caused by the microsporidian was probably a consequence of intense parasite proliferation and spore formation and only obvious in the advanced stages of the disease.

It would seem that detection of *D. lepeophtherii* is common in farmed salmon gills and the microsporidian is rather an opportunistic pathogen that a contributor to the pathology present in CGD. Furthermore, chronic infections with *D. lepeophtherii* in farmed salmon present a risk for potential reactivation of latent microsporidiosis, although the factors for triggering this are unknown. Another possibility to consider is the existence of different genotypes of *D. lepeophtherii* with different levels of pathogenicity. The only different genotype described for *D. lepeophtherii* to the one reported in Europe was detected in Canada (Jones *et al*., 2012), but other species of Microsporidia show a high interspecies variability by sequence analysis of the ITS (Galván-Díaz *et al*. 2014). The ITS is the noncoding stretch of the ribosomal DNA located between the small and the large subunit genes, largely used to study differences in the genotypes within microsporidian species (Henriques-Gil *et al*., 2010). Approximately 470 different genotypes have been described for *E. bieneusi* by sequencing the ITS (Li *et al.*, 2019). *Enterocytozoon bieneusi* is one of the most frequent microsporidian found in humans with AIDS, and is able to infect a wide range of different animal species (Galván-Díaz *et al*. 2014). Studies of the *E. bieneusi* ITS have shown that some genotypes have only been isolated from a specific animal host, while others have zoonotic potential (Santin & Fayer, 2009). Variations in the pathogenicity of different *E. cuniculi* genotypes, another important microsporidian for humans, were demonstrated by infecting immunodeficient mice (Kotková *et al*., 2018). Immunodeficient mice infected with *E. cuniculi* genotype III survived longer than mice infected with *E. cuniculi* genotype II, despite having a higher parasitic burden. The experiment concluded that spore burden did not reliably reflect the pathogenicity and mortality associated with the microsporidian, but instead were related to differences in the genotype of *E. cunuculi*. Differences in the effect of Albendazole, a common drug used in humans to treat *Encephalitozoon* sp.

infection, were also detected between different genotypes of *E. cuniculi* (Kotková *et al*., 2017). While the therapy successfully inactivated genotype II, the effect was minimal in genotype III.

For the ISH method developed in Chapter 4, five different oligoprobes were designed. Four of these worked well, but one oligoprobe, specifically targeting the ITS of the available sequence of the European genotype, did not work in the salmon gill Scottish samples nor the Canadian samples infected with *D. lepeophtherii*. It is possible that the probe was complementary to an ITS nucleotide sequence not present in the range of samples used, and that a much higher variability of interspecies exist for *D. lepeophtherii*. Further molecular characterization of intraspecies genetic diversity of *D. lepeophtherii* from different geographical areas, host species and fish with different health status (fish presenting pathology associated with *D. lepeophtherii* vs. healthy fish) are necessary to better understand the pathogenicity and epidemiology of *D. lepeophtherii* and its role in CGD.

5.7 Final conclusion

Different aspects of *D. lepeophtherii* were studied in this thesis, with a particular focus on its role in CGD in Scotland. *Desmozoon lepeophtherii* is highly prevalent in healthy salmon farms as well as in fish with gill disease. An increase in parasite load was associated with gill disease in Chapter 3, but the presence of pathology was not noted. However, in Chapter 4 it was shown that very high loads of *D. lepeophtherii* were significantly associated with gill pathology. *Desmozoon lepeophtherii* is therefore considered to contribute to the pathology of CGD syndrome, but the results of this thesis, together with other research suggests that *D. lepeophtherii* is an opportunistic pathogen rather than a primary aetiological agent. The parasite seems to be endemic in farmed salmon worldwide. This also exposes the potential risk for reactivation of the parasite when conditions for its development are optimal. Another consideration is the possible existence of genotypes with differences in pathogenicity. Proposed experiments for future research should include feeding salmon infected sea lice or salmon tissue and further molecular characterization of intraspecies genetic diversity of *D. lepeophtherii*. The management of multifactorial

gill disease such as CGD is influenced by our knowledge in the risk factors and role of the pathogens involve. Insight into the role of *D. lepeophtherii* in CGD has been gained in this thesis, leading to a better understanding of how to prevent and control CGD.

References

Aaen, S. M., Helgesen, K. O., Bakke, M. J., Kaur, K., & Horsberg, T. E. (2015). Drug resistance in sea lice: a threat to salmonid aquaculture. *Trends in Parasitology*, *31*(2), 72-81.

Adams, M. B., Ellard, K., & Nowak, B. F. (2004). Gross pathology and its relationship with histopathology of amoebic gill disease (AGD) in farmed Atlantic salmon, *Salmo salar* L. *Journal of Fish Diseases*, *27*(3), 151-161.

Ahmed, N.H., Caffara, M., Sitjà-Bobadilla, A., Fioravanti, M.L., Mazzone, A., Aboulezz, A.S., Metwally, A.M., Omar, M.A.E. & Palenzuela, O.R. (2019). Detection of the intranuclear microsporidian *Enterospora nucleophila* in gilthead sea bream by *in situ* hybridization. *Journal of Fish Diseases*, *42*(6), 809-815.

Alarcón, M., Thoen, E., Poppe, T. T., Bornø, G., Mohammad, S. N., & Hansen, H. (2016). Co-infection of *Nucleospora cyclopteri* (Microsporidia) and *Kudoa islandica* (Myxozoa) in farmed lumpfish, *Cyclopterus lumpus* L., in Norway: a case report. *Journal of Fish Diseases*, *39*(4), 411-418.

Amann, R. I., Ludwig, W., & Schleifer, K. H. (1995). Phylogenetic identification and *in situ* detection of individual microbial cells without cultivation. *Microbiology and Molecular Biology Reviews*, *59*(1), 143-169.

Amigo, J. M., Gracia, M. P., Rius, M., Salvadó, H., Maillo, P. A., & Vivarés, C. P. (1996). Longevity and effects of temperature on the viability and polar-tube extrusion of spores of *Glugea stephani*, a microsporidian parasite of commercial flatfish. *Parasitology Research*, *82*(3), 211-214.

Antonio, D. B., & Hedrick, R. P. (1995). Effect of water temperature on infections with the microsporidian *Enterocytozoon salmonis* in chinook salmon. *Diseases of Aquatic Organisms*, *22*(3), 233-236.

AnvariFar, H., Amirkolaie, A. K., Miandare, H. K., Ouraji, H., Jalali, M. A., & Üçüncü, S. İ. (2017). Apoptosis in fish: environmental factors and programmed cell death. *Cell and Tissue Research*, *368*(3), 425-439.

Avendaño-Herrera, R., Toranzo, A. E., & Magariños, B. (2006). Tenacibaculosis infection in marine fish caused by *Tenacibaculum maritimum*: a review. *Diseases of Aquatic Organisms*, *71*(3), 255-266.

Bancroft, J. D., & Stevens, A. (1977). *Theory and practice of histological techniques* (p. 126). Philadelphia, USA: Churchill Livingstone, Elsevier.

Bannister, J., Sievers, M., Bush, F., & Bloecher, N. (2019). Biofouling in marine aquaculture: a review of recent research and developments. *Biofouling, 35*(6), 631-648.

Barker, D. E., Braden, L. M., Coombs, M. P., & Boyce, B. (2009). Preliminary studies on the isolation of bacteria from sea lice, *Lepeophtheirus salmonis*, infecting farmed salmon in British Columbia, Canada. *Parasitology Research, 105*(4), 1173-1177.

Baxter, E. J., Sturt, M. M., Ruane, N. M., Doyle, T. K., McAllen, R., Harman, L., & Rodger, H. D. (2011). Gill damage to Atlantic salmon (*Salmo salar*) caused by the common jellyfish (*Aurelia aurita*) under experimental challenge. *PLoS One, 6*(4), e18529.

Baxter, E. J., Sturt, M. M., Ruane, N. M., Doyle, T. K., McAllen, R., & Rodger, H. D. (2012). Biofouling of the hydroid *Ectopleura larynx* on aquaculture nets in Ireland: Implications for finfish health. *Fish Veterinary Journal, 13*, 18-30.

Beaman, H. J., Speare, D. J., & Brimacombe, M. (1999). Regulatory effects of water temperature on *Loma salmonae* (Microspora) development in rainbow trout. *Journal of Aquatic Animal Health, 11*(3), 237-245.

Becker, J. A., & Speare, D. J. (2007). Transmission of the microsporidian gill parasite, *Loma salmonae*. *Animal Health Research Reviews, 8*(1), 59-68.

Becnel, J. J., Takvorian, P. M., & Cali, A. (2014). Checklist of available generic names for microsporidia with type species and type hosts. In *Microsporidia: Pathogens of opportunity* (pp. 671-686). Oxford, UK: Wiley Blackwell.

Belkorchia, A., Biderre, C., Militon, C., Polonais, V., Wincker, P., Jubin, C., Delbac, F., Peyretaillade, E., & Peyret, P. (2008). *In vitro* propagation of the microsporidian pathogen *Brachiola algerae* and studies of its chromosome and ribosomal DNA organization in the context of the complete genome sequencing project. *Parasitology International, 57*(1), 62-71.

Bell, G. R. (1961). Penetration of spines from a marine diatom into the gill tissue of lingcod (*Ophiodon elongatus*). *Nature, 192*(4799), 279-280

Béné, C., Barange, M., Subasinghe, R., Pinstrup-Andersen, P., Merino, G., Hemre, G. I., & Williams, M. (2015). Feeding 9 billion by 2050–Putting fish back on the menu. *Food Security, 7*(2), 261-274.

Benedicenti, O., Pottinger, T. G., Collins, C., & Secombes, C. J. (2019). Effects of temperature on amoebic gill disease development: Does it play a role?. *Journal of Fish Diseases*, *42*(9), 1241-1258.

Beznoussenko, G. V., Dolgikh, V. V., Seliverstova, E. V., Semenov, P. B., Tokarev, Y. S., Trucco, A., Micaroni, M., Giandomenico, D. D., Auinger, P., Senderskiy, I. V., Skarlato, S. O., Snigirevskaya, E. S., Komissarchik, Y. Y., Pavelka, M., De Matteis, M. A., Luini, A., Sokolova, Y. Y., & Mironov, A. A. (2007). Analogs of the Golgi complex in microsporidia: structure and avesicular mechanisms of function. *Journal of Cell Science*, *120*(7), 1288-1298.

Bigliardi, E., & Sacchi, L. (2001). Cell biology and invasion of the microsporidia. *Microbes and Infection*, *3*(5), 373-379.

Blandford, M. I., Taylor-Brown, A., Schlacher, T. A., Nowak, B., & Polkinghorne, A. (2018). Epitheliocystis in fish: an emerging aquaculture disease with a global impact. *Transboundary and Emerging Diseases*, *65*(6), 1436-1446.

Bloecher, N., Powell, M., Hytterød, S., Gjessing, M., Wiik-Nielsen, J., Mohammad, S. N., Johansen, J., Hansen, H., Floerl, O., & Gjevre, A. G. (2018). Effects of cnidarian biofouling on salmon gill health and development of amoebic gill disease. *PloS One*, *13*(7), e0199842.

Bosch-Belmar, M., M'Rabet, C., Dhaouadi, R., Chalghaf, M., Yahia, M. N. D., Fuentes, V., Piraino, S., & Yahia, O. K. D. (2016). Jellyfish stings trigger gill disorders and increased mortality in farmed *Sparus aurata* (Linnaeus, 1758) in the Mediterranean Sea. *PloS One*, *11*(4), e0154239.

Bridges, C. R., Berenbrink, M., Müller, R., & Waser, W. (1998). Physiology and biochemistry of the pseudobranch: an unanswered question? *Comparative Biochemistry and Physiology Part A: Molecular & Integrative Physiology*, *119*(1), 67-77.

Brocklebank, J. R., Speare, D. J., & Kent, M. L. (1995). Microsporidian encephalitis of farmed Atlantic salmon (Salmo salar) in British Columbia. *The Canadian Veterinary Journal*, *36*(10), 631.

Bruno, D. W., & Ellis, A. E. (1988). Histopathological effects in Atlantic salmon, *Salmo salar* L., attributed to the use of tributyltin antifoulant. *Aquaculture*, *72*(1-2), 15-20.

Bruno, D. W., Dear, G., & Seaton, D. D. (1989). Mortality associated with phytoplankton blooms among farmed Atlantic salmon, *Salmo salar* L., in Scotland. *Aquaculture*, *78*(3-4), 217-222.

Bruno, D., Collet, B., Turnbull, A., Kilburn, R., Walker, A., Pendrey, D., McIntosh, A., Urquhart, K., & Taylor, G. (2007). Evaluation and development of diagnostic methods for *Renibacterium salmoninarum* causing bacterial kidney disease (BKD) in the UK. *Aquaculture*, *269*(1-4), 114-122.

Burridge, L. E., Martin, J. L., Lyons, M. C., & LeGresley, M. M. (2010). Lethality of microalgae to farmed Atlantic salmon (*Salmo salar*). *Aquaculture, 308*(3-4), 101-105.

Bustos, P. A., Young, N. D., Rozas, M. A., Bohle, H. M., Ildefonso, R. S., Morrison, R. N., & Nowak, B. F. (2011). Amoebic gill disease (AGD) in Atlantic salmon (*Salmo salar*) farmed in Chile. *Aquaculture, 310*(3-4), 281-288.

Cali, A., & Takvorian, P. M., (2014). Developmental morphology and life cycles of the microsporidia. In *Microsporidia: Pathogens of opportunity* (pp. 71-133). Oxford, UK: Wiley Blackwell.

Callaway, R., Shinn, A. P., Grenfell, S. E., Bron, J. E., Burnell, G., Cook, E. J., Crumlish, M., Culloty, S., Davidson, K., Ellis, R. P., Flynn, K. J., Fox, C., Green, D. M., Hays, G. C., Hughes, A. D., Johnston, E., Lowe, C. D., Lupatsch, I., Malham, S., Mendzil, A. F., Nickell, T., Pickerell, T., Rowley, A. F., Stanley, M. S., Tocher, D. R., Turnbull, J. F., Webb, G., Wooton, E., & Shields, R. J. (2012). Review of climate change impacts on marine aquaculture in the UK and Ireland. *Aquatic Conservation: Marine and Freshwater Ecosystems*, *22*(3), 389-421.

Canning, E. U., & Hazard, E. I., (1982). Genus *Pleistophora* Gurley, 1893: an assemblage of at least three genera. *The Journal of Protozoology*, *29*(1), 39-49.

Carter, C. (2002). Ecological Aquaculture: The Evolution of the Blue Revolution, BA Costa-Pierce (ed.). *Aquaculture International*, *10*(5), 443-445.

Cavalier-Smith, T. (1983). Endocytobiology II. In *Intracellular Space as Oligogenetic Ecosystem* (pp. 265-279). Berlin, Germany: De Gruyter.

Cengiz, E. I., & Unlu, E. (2006). Sublethal effects of commercial deltamethrin on the structure of the gill, liver and gut tissues of mosquitofish, *Gambusia affinis*: a microscopic study. *Environmental Toxicology and Pharmacology*, *21*(3), 246-253.

Chance, R. J., Cameron, G. A., Fordyce, M., Noguera, P., Wang, T., Collins, C., Secombes, C. J., & Collet, B. (2018). Effects of repeated anaesthesia on gill and general health of Atlantic salmon, *Salmo salar*. *Journal of Fish Biology, 93*(6), 1069-1081.

Claiborne, J. B., Edwards, S. L., & Morrison-Shetlar, A. I. (2002). Acid–base regulation in fishes: cellular and molecular mechanisms. *Journal of Experimental Zoology, 293*(3), 302-319.

Clark, A., & Nowak, B. F. (1999). Field investigations of amoebic gill disease in Atlantic salmon, *Salmo salar* L., in Tasmania. *Journal of Fish Diseases*, *22*(6), 433-443.

Collado, J. S., Higes, M., Barrio, L., & Martín-Hernández, R. (2014). Flow cytometry analysis of *Nosema* species to assess spore viability and longevity. *Parasitology Research*, *113*(5), 1695-1701.

Corthell, J. T. (2014). *In Situ* Hybridization. In *Basic Molecular Protocols in Neuroscience: Tips, Tricks, and Pitfalls* (pp. 105-111). San Diego, USA: Academic Press, Elsevier.

Couzinet, S., Cejas, E., Schittny, J., Deplazes, P., Weber, R., & Zimmerli, S. (2000). Phagocytic uptake of *Encephalitozoon cuniculi* by nonprofessional phagocytes. *Infection and Immunity*, *68*(12), 6939-6945.

Dall, D. J. (1983). A theory for the mechanism of polar filament extrusion in the Microspora. *Journal of Theoretical Biology*, *105*(4), 647-659.

Dang, Z., Lock, R. A., Flik, G., & Wendelaar Bonga, S. E. (2000). Na (+)/K (+)-ATPase immunoreactivity in branchial chloride cells of *Oreochromis mossambicus* exposed to copper. *The Journal of Experimental Biology*, *203*(2), 379.

Davis, J. C., & Cameron, J. N. (1971). Water flow and gas exchange at the gills of rainbow trout, *Salmo gairdneri*. *The Journal of Experimental Biology*, *54*(1), 1-18.

Deeds, J. R., Reimschuessel, R., & Place, A. R. (2006). Histopathological effects in fish exposed to the toxins from *Karlodinium micrum*. *Journal of Aquatic Animal Health*, *18*(2), 136-148.

Delannoy, C. M., Houghton, J. D., Fleming, N. E., & Ferguson, H. W. (2011). Mauve Stingers (*Pelagia noctiluca*) as carriers of the bacterial fish pathogen *Tenacibaculum maritimum*. *Aquaculture*, *311*(1-4), 255-257.

Desportes, I., Charpentier, Y. L., Galian, A., Bernard, F., Cochand-Priollet, B., Lavergne, A., Ravisse, P., & Modigliani, R. (1985). Occurrence of a New Microsporidan: *Enterocytozoon bieneusi* ng, n. sp., in the Enterocytes of a Human Patient with AIDS 1. *The Journal of Protozoology*, *32*(2), 250-254.

Desportes-Livage, I., Chilmonczyk, S., Hedrick, R., Ombrouck, C., Monge, D., Maiga, I., & Gentilini, M. (1996). Comparative development of two microsporidian species: *Enterocytozoon bieneusi* and *Enterocytozoon salmonis*, reported in AIDS patients and salmonid fish, respectively. *Journal of Eukaryotic Microbiology*, *43*(1), 49-60.

Dezfuli, B. S., Giari, L., Simoni, E., Menegatti, R., Shinn, A. P., & Manera, M. (2007). Gill histopathology of cultured European sea bass, *Dicentrarchus labrax* (L.), infected with *Diplectanum aequans* (Wagener 1857) Diesing 1958 (Diplectanidae: Monogenea). *Parasitology Research*, *100*(4), 707-713.

Di Cicco, E., Ferguson, H. W., Schulze, A. D., Kaukinen, K. H., Li, S., Vanderstichel, R., Wessel, Ø., Rimstad, E., Gardner, I.A., Hammell, K.L., & Miller, K. M. (2017). Heart and skeletal muscle inflammation (HSMI) disease diagnosed on a British Columbia salmon farm through a longitudinal farm study. *PLoS One*, *12*(2), e0171471.

Didier, E. S. (2005). Microsporidiosis: an emerging and opportunistic infection in humans and animals. *Acta Tropica*, *94*(1), 61-76.

Didier, E. S., Orenstein, J. M., Aldras, A., Bertucci, D., Rogers, L. B., & Janney, F. A. (1995). Comparison of three staining methods for detecting microsporidia in fluids. *Journal of Clinical Microbiology*, *33*(12), 3138-3145.

Draghi, A., Popov, V. L., Kahl, M. M., Stanton, J. B., Brown, C. C., Tsongalis, G. J., West, A. B., & Frasca, S. (2004). Characterization of "*Candidatus* piscichlamydia salmonis"(order *Chlamydiales*), a chlamydia-like bacterium associated with epitheliocystis in farmed Atlantic salmon (*Salmo salar*). *Journal of Clinical Microbiology*, *42*(11), 5286-5297.

Drinan, E. M., Rodger, H. D., & Palmer, R. (1992). Microsporidian infection in Atlantic salmon, *Salmo salar* L. *Journal of Fish Diseases*, *15*(2), 211-214.

Dos Santos, N. M., Taverne-Thiele, J. J., Barnes, A. C., van Muiswinkel, W. B., Ellis, A. E., & Rombout, J. H. (2001). The gill is a major organ for antibody secreting cell production following direct immersion of sea bass (*Dicentrarchus labrax*, L.) in a *Photobacterium damselae* ssp. piscicida bacterin: an ontogenetic study. *Fish & Shellfish Immunology*, *11*(1), 65-74.

Dos Santos, N. M. S., Vale, A. D., Reis, M. I. R., & Silva, M. T. (2008). Fish and apoptosis: molecules and pathways. *Current Pharmaceutical Design*, *14*(2), 148-169.

Downes, J. K., Yatabe, T., Marcos-Lopez, M., Rodger, H. D., MacCarthy, E., O'Connor, I., Collins, E., & Ruane, N. M. (2018). Investigation of co-infections with pathogens associated with gill disease in Atlantic salmon during an amoebic gill disease outbreak. *Journal of Fish Diseases*, *41*(8), 1217-1227.

Eddy, B. F., & Handy, R. D. (2012). General principles of fish physiology: living in water. In *Ecological and environmental physiology of fishes* (pp. 43-101). Oxford, UK: Oxford University Press.

Edinger, A. L., & Thompson, C. B. (2004). Death by design: apoptosis, necrosis and autophagy. *Current Opinion in Cell Biology*, *16*(6), 663-669.

El Alaoui, H., Grésoviac, S. J., & Vivarès, C. P. (2006). Occurrence of the microsporidian parasite *Nucleospora salmonis* in four species of salmonids from the Massif Central of France. *Folia Parasitologica*, *53*(1), 37.

Elmore, S. (2007). Apoptosis: a review of programmed cell death. *Toxicologic Pathology*, *35*(4), 495-516.

Estes, K. A., Szumowski, S. C., & Troemel, E. R. (2011). Non-lytic, actin-based exit of intracellular parasites from *C. elegans* intestinal cells. *PLoS Pathogens*, *7*(9), e1002227.

Evans, D. H., Piermarini, P. M., & Choe, K. P. (2005). The multifunctional fish gill: dominant site of gas exchange, osmoregulation, acid-base regulation, and excretion of nitrogenous waste. *Physiological Reviews*, *85*(1), 97-177.

Falk, K., Batts, W. N., Kvellestad, A., Kurath, G., Wiik-Nielsen, J., & Winton, J. R. (2008). Molecular characterisation of Atlantic salmon paramyxovirus (ASPV): a novel paramyxovirus associated with proliferative gill inflammation. *Virus Research*, *133*(2), 218-227.

FAO. (2018). *The State of World Fisheries and Aquaculture 2018 - Meeting the sustainable development goals*. Rome. Licence: CC BY-NC-SA 3.0 IGO.

Farmen, E., Mikkelsen, H. N., Evensen, Ø., Einset, J., Heier, L. S., Rosseland, B. O., Salbu, B., Tollefsen, K. E., & Oughton, D. H. (2012). Acute and sub-lethal effects in juvenile Atlantic salmon exposed to low µg/L concentrations of Ag nanoparticles. *Aquatic Toxicology*, *108*, 78-84.

Ferguson, H. W. (2006) Introduction. In *Systemic pathology of fish: a text and atlas of normal tissues reponses in teleosts, and their responses in disease* (pp. 10-23). London, UK: Scotian Press.

Figueiredo-Fernandes, A., Ferreira-Cardoso, J. V., Garcia-Santos, S., Monteiro, S. M., Carrola, J., Matos, P., & Fontaínhas-Fernandes, A. (2007). Histopathological changes in liver and gill epithelium of Nile tilapia, *Oreochromis niloticus*, exposed to waterborne copper. *Pesquisa Veterinária Brasileira*, *27*(3), 103-109.

Fischer, J., Suire, C., & Hale-Donze, H. (2008). Toll-like receptor 2 recognition of the microsporidia *Encephalitozoon* spp. induces nuclear translocation of NF-κB and subsequent inflammatory responses. *Infection and Immunity*, *76*(10), 4737-4744.

Fletcher, 2018. The Fish Site. Retrieved from: https://thefishsite.com/articles/recasting-the-net

Floerl, O., Sunde, L. M., & Bloecher, N. (2016). Potential environmental risks associated with biofouling management in salmon aquaculture. *Aquaculture Environment Interactions*, *8*, 407-417.

Franzen, C. (2004). Microsporidia: how can they invade other cells?. *Trends in Parasitology*, *20*(6), 275-279.

Franzen, C. (2008). Microsporidia: a review of 150 years of research. *The Open Parasitology Journal*, *2*(1), 1-34.

Franzen, C., Müller, A., Hegener, P., Salzberger, B., Hartmann, P., Fätkenheuer, G., Diehl, V., & Schrappe, M. (1995). Detection of microsporidia (*Enterocytozoon bieneusi*) in intestinal biopsy specimens from human immunodeficiency virus-infected patients by PCR. *Journal of Clinical Microbiology*, *33*(9), 2294-2296.

Franzen, C., Müller, A., Hartmann, P., & Salzberger, B. (2005). Cell invasion and intracellular fate of *Encephalitozoon cuniculi* (Microsporidia). *Parasitology*, *130*(3), 285-292.

Freeman, M. A. (2002). *Potential biological control agents for the salmon louse Lepeophtheirus salmonis* (Kroyer, 1837) (Doctoral dissertation). University of Stirling.

Freeman, M. A., Bell, A. S., & Sommerville, C. (2003). A hyperparasitic microsporidian infecting the salmon louse, *Lepeophtheirus salmonis*: an rDNA-based molecular phylogenetic study. *Journal of Fish Diseases*, *26*(11-12), 667-676.

Freeman, M. A., & Sommerville, C. (2009). *Desmozoon lepeophtherii* n. gen., n. sp., (Microsporidia: Enterocytozoonidae) infecting the salmon louse *Lepeophtheirus salmonis* (Copepoda: Caligidae). *Parasites & Vectors*, *2*(1), 1-15

Freeman, M. A., & Sommerville, C. (2011). Original observations of *Desmozoon lepeophtherii*, a microsporidian hyperparasite infecting the salmon louse *Lepeophtheirus salmonis*, and its subsequent detection by other researchers. *Parasites & Vectors*, *4*(1), 231.

Fridell, F., Devold, M., & Nylund, A. (2004). Phylogenetic position of a paramyxovirus from Atlantic salmon *Salmo salar*. *Diseases of Aquatic Organisms*, *59*(1), 11-15.

Fringuelli, E., Savage, P. D., Gordon, A., Baxter, E. J., Rodger, H. D., & Graham, D. A. (2012). Development of a quantitative real-time PCR for the detection of *Tenacibaculum maritimum* and its application to field samples. *Journal of Fish Diseases*, *35*(8), 579-590.

Frisch, K., Småge, S. B., Vallestad, C., Duesund, H., Brevik, Ø. J., Klevan, A., Olsen, R. H., Sjaatil, S. T., Gauthier, D., Brudeseth, B., & Nylund, A. (2018). Experimental induction of mouthrot in Atlantic salmon smolts using *Tenacibaculum maritimum* from Western Canada. *Journal of Fish Diseases*, *41*(8), 1247-1258.

Galván-Díaz, A. L., Magnet, A., Fenoy, S., Henriques-Gil, N., Haro, M., Gordo, F.P., Miró, G., del Águila, C., & Izquierdo, F. (2014). Microsporidia detection and genotyping study of human pathogenic *E. bieneusi* in animals from Spain. *PLoS One*, *9*(3), e92289.

Garcia, L. S. (2002). Laboratory identification of the microsporidia. *Journal of Clinical Microbiology*, *40*(6), 1892-1901.

Garseth, Å. H., Gjessing, M. C., Moldal, T., & Gjevre, A. G. (2018). A survey of salmon gill poxvirus (SGPV) in wild salmonids in Norway. *Journal of Fish Diseases*, *41*(1), 139-145.

Gatward, I., Parker, A., Billing, S-L., & Black, K. (2017). *Scottish aquaculture: a view towards 2030: An innovation roadmap and sector needs study conducted by Imani Development and SRSL, on behalf of the Scottish Aquaculture Innovation Centre and Highlands and Islands Enterprise.* Scotish Aquaculture Innovation Centre.

Georgiadis, M. P., Gardner, I. A., & Hedrick, R. P. (1998). Field evaluation of sensitivity and specificity of a polymerase chain reaction (PCR) for detection of *Nucleospora salmonis* in rainbow trout. *Journal of Aquatic Animal Health*, *10*(4), 372-380.

Gisder, S., Möckel, N., Linde, A., & Genersch, E. (2011). A cell culture model for *Nosema ceranae* and *Nosema apis* allows new insights into the life cycle of these important honey bee-pathogenic microsporidia. *Environmental Microbiology*, *13*(2), 404-413.Gjessing, M. C., Yutin, N., Tengs, T., Senkevich, T., Koonin, E., Rønning, H. P., Alarcon, M., Ylving, S., Lie, K., Saure, B., Tran, Linh, Moss, B., & Dale, O. B. (2015). Salmon gill poxvirus, the deepest representative of the *Chordopoxvirinae*. *Journal of Virology*, *89*(18), 9348-9367.

Gjessing, M. C., Weli, S. C., & Dale, O. B. (2016). Poxviruses of Fish. In *Aquaculture Virology* (pp. 119-125). Academic Press, Elsevier.

Gjessing, M. C., Thoen, E., Tengs, T., Skotheim, S. A., & Dale, O. B. (2017). Salmon gill poxvirus, a recently characterized infectious agent of multifactorial gill disease in freshwater-and seawater-reared Atlantic salmon. *Journal of Fish Diseases*, *40*(10), 1253-1265.

Gjessing, M. C., Aamelfot, M., Batts, W. N., Benestad, S. L., Dale, O. B., Thoen, E., Weli, S.C., & Winton, J. R. (2018). Development and characterization of two cell lines from gills of Atlantic salmon. *PloS One*, *13*(2), e0191792.

Gluge, G. (1838). Notice sur quelques points d'anatomie pathologique comparée, suivie de quelques observations sur la structure des branchies dans épinoches. *Bulletins de l'Académie royale des sciences, des lettres et des beaux-arts de Belgique.5*, 771-772.

Granzow, H., Fichtner, D., Schütze, H., Lenk, M., Dresenkamp, B., Nieper, H., & Mettenleiter, T. C. (2014). Isolation and partial characterization of a novel virus from different carp species suffering gill necrosis–ultrastructure and morphogenesis. *Journal of Fish Diseases*, *37*(6), 559-569.

Green, L. C., LeBlanc, P. J., & Didier, E. S. (2000). Discrimination between viable and dead *Encephalitozoon cuniculi* (microsporidian) spores by dual staining with Sytox Green and Calcofluor White M2R. *Journal of Clinical Microbiology*, *38*(10), 3811-3814.

Green, T. J., Smullen, R., & Barnes, A. C. (2013). Dietary soybean protein concentrate-induced intestinal disorder in marine farmed Atlantic salmon, Salmo salar is associated with alterations in gut microbiota. *Veterinary Microbiology*, *166*(1-2), 286-292.

Grésoviac, S. J., Baxa, D. V., Vivarès, C. P., & Hedrick, R. P. (2007). Detection of the intranuclear microsporidium *Nucleospora salmonis* in naturally and experimentally exposed Chinook salmon *Oncorhynchus tshawytscha* by *in situ* hybridization. *Parasitology Research*, *101*(5), 1257-1264.

Griffin, D., Chengappa, M. M., Kuszak, J., & McVey, D. S. (2010). Bacterial pathogens of the bovine respiratory disease complex. *Veterinary Clinics: Food Animal Practice*, *26*(2), 381-394.

Grøntvedt, R. N., Nerbøvik, I. K. G., Viljugrein, H., Lillehaug, A., Nilsen, H., & Gjevre, A. G. (2015). Thermal de-licing of salmonid fish–documentation of fish welfare and effect. *Norwegian Veterinary Institutes Report Series*, *13*, 2015.

Guevara Soto, M., Vaughan, L., Segner, H., Wahli, T., Vidondo, B., & Schmidt-Posthaus, H. (2016). Epitheliocystis distribution and characterization in brown trout (*Salmo trutta*) from the headwaters of two major European rivers, the Rhine and Rhone. *Frontiers in Physiology*, *7*, 131.

Gunnarsson, G. S., Blindheim, S., Karlsbakk, E., Plarre, H., Imsland, A. K., Handeland, S., Sveier, H., & Nylund, A. (2017). *Desmozoon lepeophtherii* (microsporidian) infections and pancreas disease (PD) outbreaks in farmed Atlantic salmon (*Salmo salar* L.). *Aquaculture*, *468*(1), 141-148.

Haley, A. J. (1954). Microsporidian parasite, *Glugea hertwigi*, in American smelt from the Great Bay region, New Hampshire. *Transactions of the American Fisheries Society*, *83*(1), 84-90.

Hanf, M., Guégan, J. F., Ahmed, I., & Nacher, M. (2014). Disentangling the complexity of infectious diseases: time is ripe to improve the first-line statistical toolbox for epidemiologists. *Infection, Genetics and Evolution*, *21*, 497-505.

Haugarvoll, E., Bjerkås, I., Nowak, B. F., Hordvik, I., & Koppang, E. O. (2008). Identification and characterization of a novel intraepithelial lymphoid tissue in the gills of Atlantic salmon. *Journal of Anatomy*, *213*(2), 202-209.

Hedrick, R. P., Groff, J. M., & Baxa, D. V. (1991). Experimental infections with *Enterocytozoon salmonis* Chilmonczyk, Cox, Hedrick (Microsporea): an intranuclear microsporidium from chinook salmon *Oncorhynchus tshawytscha*. *Diseases of Aquatic Organisms*, *10*(2), 103-108.

Henriques-Gil, N., Haro, M., Izquierdo, F., Fenoy, S., & del Águila, C. (2010). Phylogenetic approach to the variability of the microsporidian *Enterocytozoon bieneusi* and its implications for inter-and intrahost transmission. *Applied Environmental Microbiology*, *76*(10), 3333-3342.

Herrero, A., Padros, F., Pflaum, S., Mathews, C., Del-Pozo, J., Rodger, H., Dagleish, M. P., & Thompson, K. (2020). Comparison of histologic methods for the detection of *Desmozoon lepeophtherii* spores in gills of Atlantic salmon. *Journal of Veterinary Diagnostic Investigation, 32(1), 142-146.*

Hjeltnes, B., Bornø, G., Jansen, M. D., Haukaas, A., & Walde, C. (2017). The health situation in Norwegian aquaculture 2016. *Norwegian Veterinary Institute*.

Hjeltnes, B., Bang-Jensen, B., Bornø, G., Haukaas, A., & Walde, CS. (2018), The health situation in Norwegian aquaculture 2017. *Norwegian Veterinary Institute.*

Hoffman, G. L., Dunbar, C. E., Wolf, K., & Zwillenberg, L. O. (1969). Epitheliocystis, a new infectious disease of the bluegill (*Lepomis macrochirus*). *Antonie Van eeuwenhoek*, *35*(1), 146-158.

Holzer, A. S., Sommerville, C., & Wootten, R. (2003). Tracing the route of *Sphaerospora truttae* from the entry locus to the target organ of the host, *Salmo salar* L., using an optimized and specific *in situ* hybridization technique. *Journal of Fish Diseases*, *26*(11-12), 647-655.

Hughes, G. M. (1960). A comparative study of gill ventilation in marine teleosts. *Journal of Experimental Biology*, *37*(1), 28-45.

Hvas, M., Karlsbakk, E., Mæhle, S., Wright, D. W., & Oppedal, F. (2017). The gill parasite *Paramoeba perurans* compromises aerobic scope, swimming capacity and ion balance in Atlantic salmon. *Conservation Physiology*, *5*(1), cox066.

ICES Working Group. (2018). *Report of the Working Group on Pathology and Diseases of Marine Organisms* (WGPDMO), Riga, Latvia.

Jagoe, C. H., & Haines, T. A. (1997). Changes in gill morphology of Atlantic salmon (*Salmo salar*) smolts due to addition of acid and aluminum to stream water. *Environmental Pollution*, *97*(1-2), 137-146.

Jensen, E. (2014). Technical review: *In situ* hybridization. *The Anatomical Record*, *297*(8), 1349-1353.

Jones, M. A., Powell, M. D., Becker, J. A., & Carter, C. G. (2007). Effect of an acute necrotic bacterial gill infection and feed deprivation on the metabolic rate of Atlantic salmon *Salmo salar*. *Diseases of Aquatic Organisms*, *78*(1), 29-36.

Jones, S. R., Prosperi-Porta, G., & Kim, E. (2012). The Diversity of Microsporidia in Parasitic Copepods (Caligidae: Siphonostomatoida) in the Northeast Pacific Ocean with Description of *Facilispora margolisi* ng, n. sp. and a new Family Facilisporidae n. fam. *Journal of Eukaryotic Microbiology*, *59*(3), 206-217.

Karges, R. G., & Woodward, B. (1984). Development of lamellar epithelial hyperplasia in gills of pantothenic acid-deficient rainbow trout, *Salmo gairdneri* Richardson. *Journal of Fish Biology*, *25*(1), 57-62.

Karlsen, M., Nylund, A., Watanabe, K., Helvik, J. V., Nylund, S., & Plarre, H. (2008). Characterization of '*Candidatus* Clavochlamydia salmonicola': an intracellular bacterium infecting salmonid fish. *Environmental Microbiology*, *10*(1), 208-218.

Katharios, P., Papadaki, M., Papandroulakis, N., & Divanach, P. (2008). Severe mortality in mesocosm-reared sharpsnout sea bream *Diplodus puntazzo* larvae due to epitheliocystis infection. *Diseases of Aquatic Organisms*, *82*(1), 55-60.

Keeling, P. (2009). Five questions about microsporidia. *PLoS Pathogens*, *5*(9), e1000489.

Keeling, P. J., & Fast, N. M. (2002). Microsporidia: biology and evolution of highly reduced intracellular parasites. *Annual Reviews in Microbiology*, *56*(1), 93-116.

Keeling, P. J., Fast, N. M., & Corradi, N. (2014). Microsporidia genome structure and function. In *Microsporidia: Pathogens of opportunity* (pp. 221-229). Oxford, UK: Wiley Blackwell.

Keen, A. N., Fenna, A. J., McConnell, J. C., Sherratt, M. J., Gardner, P., & Shiels, H. A. (2016). The dynamic nature of hypertrophic and fibrotic remodeling of the fish ventricle. *Frontiers in Physiology*, *6*, 427.

Kenyon, W., & Davies, D. (2018). *Salmon Farming in Scotland*. The Information Centre (SPICe). The Scottish Parliament.

Kent, M. L., & Dawe, S. C. (1994). Efficacy of fumagillin DCH against experimentally induced *Loma salmonae* (Microsporea) infections in chinook salmon *Oncorhynchus tshawytscha*. *Diseases of Aquatic Organisms*, *20*, 231-231.

Kent, M. L., Whyte, J. N. C., & LaTrace, C. (1995). Gill lesions and mortality in seawater pen-reared Atlantic salmon *Salmo salar* associated with a dense bloom of *Skeletonema costatum* and *Thalassiosira* species. *Diseases of Aquatic Organisms*, *22*(1), 77-81.

Kent, M. L., & Speare, D. J. (2005). Review of the sequential development of *Loma salmonae* (Microsporidia) based on experimental infections of rainbow trout (*Oncorhynchus mykiss*) and Chinook salmon (*O. tshawytscha*). *Folia Parasitologica*, *52*(1/2), 63.

Kent, M. L., Shaw, R. W., & Sanders, J. L. (2014). Microsporidia in fish. In *Microsporidia: Pathogens of opportunity* (pp. 493-520). Oxford, UK: Wiley Blackwell.

Keohane, E. M., & Weiss, L. M. (1999). The structure, function, and composition of the microsporidian polar tube. In *The microsporidia and microsporidiosis* (pp. 196-224). American Society of Microbiology. Washington, USA: ASM Press.

Khanaliha, K., Mirjalali, H., Mohebali, M., Tarighi, F., & Rezaeian, M. (2014). Comparison of three staining methods for the detection of intestinal *Microspora* spp. *Iranian Journal of Parasitology*, *9*(4), 445.

Kiemer, M. C., & Black, K. D. (1997). The effects of hydrogen peroxide on the gill tissues of Atlantic salmon, *Salmo salar* L. *Aquaculture*, *153*(3-4), 181-189.

Kintner, A. H. (2016). *Hydrozoan jellyfish and their interactions with Scottish salmon aquaculture* (Doctoral dissertation). University of St Andrews.

Klopfleisch, R. (2013). Multiparametric and semiquantitative scoring systems for the evaluation of mouse model histopathology-a systematic review. *BMC Veterinary Research*, *9*(1), 123.

Knudsen, D., Jutfelt, F., Sundh, H., Sundell, K., Koppe, W., & Frøkiær, H. (2008). Dietary soya saponins increase gut permeability and play a key role in the onset of soyabean-induced enteritis in Atlantic salmon (*Salmo salar* L.). *British Journal of Nutrition*, *100*(1), 120-129.

Kotková, M., Sak, B., Hlásková, L., & Kváč, M. (2017). The course of infection caused by *Encephalitozoon cuniculi* genotype III in immunocompetent and immunodeficient mice. *Experimental Parasitology*, *182*, 16-21.

Kotková, M., Sak, B., & Kváč, M. (2018). Differences in the intensity of infection caused by *Encephalitozoon cuniculi* genotype II and III-Comparison using quantitative real-time PCR. *Experimental Parasitology*, *192*, 93-97.

Koppang, E. O., Kvellestad, A., & Fischer, U. (2015). Fish mucosal immunity: gill. In *Mucosal health in aquaculture* (pp. 93-133). Academic Press, Elsevier.

Kou, G. H., Wang, C. H., Hung, H. W., Jang, Y. S., Chou, C. M., & Lo, C. F. (1995). A cell line (EP-1 cell line) derived from "Beko disease" affected Japanese eel elver (*Anguilla japonica*) persistently infected with *Pleistophora anguillarum*. *Aquaculture*, *132*(1-2), 161-173.

Kroemer, G., Galluzzi, L., Vandenabeele, P., Abrams, J., Alnemri, E. S., Baehrecke, E. H., Blagosklonny, M. V., El-Deiry, W. S., Golstein, P., Green, D. R., Hengartner, M., Knight, R. A., Kumar, S., Lipton, S. A., Malorni, W., Nuñez, G., Peter, M. E., Tschopp, J., Yuan, J., Piacentini, Zhivotovsky, B., Melino, G., & Hengartner, M. (2009). Classification of cell death: recommendations of the

Nomenclature Committee on Cell Death 2009. *Cell Death and Differentiation*, *16*(1), 3.

Kumar, G., Saleh, M., Abdel-Baki, A. A., Al-Quraishy, S., & El-Matbouli, M. (2014). *In vitro* cultivation model for *Heterosporis saurida* (Microsporidia) isolated from lizardfish, *Saurida undosquamis* (Richardson). *Journal of Fish Diseases*, *37*(5), 443-449.

Kumar, V., Abbas, A. K., & Aster, J. C. (2017). Cell injury, Cell death and Adaptations. In *Robbins basic pathology e-book* (pp. 1-29). Philadelphia, USA: Elsevier Health Sciences.

Kvellestad, A., Dannevig, B. H., & Falk, K. (2003). Isolation and partial characterization of a novel paramyxovirus from the gills of diseased seawater-reared Atlantic salmon (*Salmo salar* L.). *Journal of General Virology*, *84*(8), 2179-2189.

Kvellestad, A., Falk, K., Nygaard, S. M., Flesjå, K., & Holm, J. A. (2005). Atlantic salmon paramyxovirus (ASPV) infection contributes to proliferative gill inflammation (PGI) in seawater-reared *Salmo salar*. *Diseases of Aquatic Organisms*, *67*(1-2), 47-54.

Lallo, M. A., Da Costa, L. F. V., Alvares-Saraiva, A. M., Rocha, P. R. D. A., Spadacci-Morena, D. D., de Camargo Konno, F. T., & Suffredini, I. B. (2016). Culture and propagation of microsporidia of veterinary interest. *Journal of Veterinary Medical Science*, *78*(2), 171-176.

Laurent, P., & Dunel, S. (1980). Morphology of gill epithelia in fish. *American Journal of Physiology-Regulatory, Integrative and Comparative Physiology*, *238*(3), 147-159.

Laurent, P., & Perry, S. F. (1991). Environmental effects on fish gill morphology. *Physiological Zoology*, *64*(1), 4-25.

Laurin, E., Jaramillo, D., Vanderstichel, R., Ferguson, H., Kaukinen, K. H., Schulze, A. D., Keith, I.R., Gardner, I.A., & Miller, K. M. (2019). Histopathological and novel high-throughput molecular monitoring data from farmed salmon (*Salmo salar* and *Oncorhynchus* spp.) in British Columbia, Canada, from 2011-2013. *Aquaculture*, *499*, 220-234.

LeBlanc, F., Ditlecadet, D., Arseneau, J. R., Steeves, R., Boston, L., Boudreau, P., & Gagné, N. (2019). Isolation and identification of a novel salmon gill poxvirus variant from Atlantic salmon in Eastern Canada. *Journal of Fish Diseases*, *42*(2), 315-318.

Lederberg, J., & McCray, A. T. (2001). Ome SweetOmics--A genealogical treasury of words. *The Scientist*, *15*(7), 8-8.

Leiro, J., Ortega, M., Estevez, J., Ubeira, F. M., & Sanmartin, M. L. (1996). The role of opsonization by antibody and complement in in vitro phagocytosis of microsporidian parasites by turbot spleen cells. *Veterinary Immunology and Immunopathology*, *51*(1-2), 201-210.

Li, D., Zhang, Y., Jiang, Y., Xing, J., Tao, D., Zhao, A., ... & Zhang, L. (2019). Genotyping and Zoonotic Potential of *Enterocytozoon bieneusi* in Pigs in Xinjiang, China. *Frontiers in Microbiology*, 10, 2401.

Lillie, L. E. (1974). The bovine respiratory disease complex. *The Canadian Veterinary Journal*, *15*(9), 233-242

Linden, S. K., Sutton, P., Karlsson, N. G., Korolik, V., & McGuckin, M. A. (2008). Mucins in the mucosal barrier to infection. *Mucosal Immunology*, *1*(3), 183.

Llewellyn, M. S., McGinnity, P., Dionne, M., Letourneau, J., Thonier, F., Carvalho, G. R., ... & Derome, N. (2016). The biogeography of the Atlantic salmon (*Salmo salar*) gut microbiome. *The ISME Journal*, *10*(5), 1280-1284.

Llewellyn, M. S., Leadbeater, S., Garcia, C., Sylvain, F. E., Custodio, M., Ang, K. P., ... & Derome, N. (2017). Parasitism perturbs the mucosal microbiome of Atlantic Salmon. *Scientific Reports*, *7*, 43465.

Lokesh, J., & Kiron, V. (2016). Transition from freshwater to seawater reshapes the skin-associated microbiota of Atlantic salmon. *Scientific Reports*, *6*, 19707.

Lom, J. (2002). A catalogue of described genera and species of microsporidians parasitic in fish. *Systematic Parasitology*, *53*(2), 81-99.

Lom, J., & Nilsen, F. (2003). Fish microsporidia: fine structural diversity and phylogeny. *International Journal for Parasitology*, *33*(2), 107-127.

Lores, B., Rosales, M. J., Mascaro, C., & Osuna, A. (2003). In vitro culture of *Glugea* sp. *Veterinary Parasitology*, *112*(3), 185-196.

Lovy, J., Wright, G. M., & Speare, D. J. (2007). Ultrastructural examination of the host inflammatory response within gills of netpen reared chinook salmon (*Oncorhynchus tshawytscha*) with Microsporidial Gill Disease. *Fish & Shellfish Immunology*, *22*(1-2), 131-149.

Luna, V. A., Stewart, B. K., Bergeron, D. L., Clausen, C. R., Plorde, J. J., & Fritsche, T. R. (1995). Use of the fluorochrome Calcofluor White in the screening of stool

specimens for spores of microsporidia. *American Journal of Clinical pathology*, *103*(5), 656-659.

MacLeod, M. J. (2012). *In vitro study of the microsporidian parasite Loma morhua, using cod-derived cells and novel culture techniques* (Master dissertation). Wilfrid Laurier University.

MacLeod, M. J., Vo, N. T., Mikhaeil, M. S., Monaghan, S. R., Alexander, J. A. N., Saran, M. K., & Lee, L. E. (2018). Development of a continuous cell line from larval Atlantic cod (*Gadus morhua*) and its use in the study of the microsporidian, *Loma morhua*. *Journal of Fish Diseases*, *41*(9), 1359-1372.

Mallatt, J. (1985). Fish gill structural changes induced by toxicants and other irritants: a statistical review. *Canadian Journal of Fisheries and Aquatic Sciences*, *42*(4), 630-648.

Malviya, S., Scalco, E., Audic, S., Vincent, F., Veluchamy, A., Poulain, J., Wincker, P., Iudicone, D., de Vargas, C., Bittner, L., Zingone, A., & Bowler, C. (2016). Insights into global diatom distribution and diversity in the world's ocean. *Proceedings of the National Academy of Sciences*, *113*(11), E1516-E1525.

Marcos-López, M., Espinosa, C. R., Rodger, H. D., O'Connor, I., MacCarthy, E., & Esteban, M. A. (2018). Oxidative stress is associated with late-stage amoebic gill disease in farmed Atlantic salmon (*Salmo salar* L.). *Journal of Fish Diseases*, *41*(2), 383-387.

Marcos-López, M., Mitchell, S. O., & Rodger, H. D. (2016). Pathology and mortality associated with the mauve stinger jellyfish *Pelagia noctiluca* in farmed Atlantic salmon *Salmo salar* L. *Journal of Fish Diseases*, *39*, 111-115.

Marcos-López, M. (2018). *Gill Disease in Ireland: 2017 Update*. Presented at the Gill Health Initiative. Galway, Ireland.

Mariottini, G. L., & Pane, L. (2010). Mediterranean jellyfish venoms: a review on scyphomedusae. *Marine Drugs*, *8*(4), 1122-1152.

Martin, S. W. (1977). The evaluation of tests. *Canadian Journal of Comparative Medicine*, *41*(1), 19.

Matthews, C. G. G., Richards, R. H., Shinn, A. P., & Cox, D. I. (2013). Gill pathology in Scottish farmed Atlantic salmon, *Salmo salar* L., associated with the microsporidian *Desmozoon lepeophtherii* Freeman et Sommerville, 2009. *Journal of Fish Diseases*, *36*(10), 861-869.

McConnachie, S. H., Sheppard, J., Wright, G. M., & Speare, D. J. (2015). Development of the microsporidian parasite, *Loma salmonae*, in a rainbow trout gill epithelial cell line (RTG-1): evidence of xenoma development in vitro. *Parasitology*, *142*(2), 326-331.

McPhee, Duhaime, J., Tuen, A., & Parsons, G. (2017). Canadian Aquaculture R&D Review 2017. *Aquaculture Association of Canada Special Publication. 25*.

Merrifield, D. L., & Rodiles, A. (2015). The fish microbiome and its interactions with mucosal tissues. In *Mucosal Health in Aquaculture* (pp. 273-295). Academic Press, Elsevier.

Meyers, T. R., & Batts, W. N. (2016). Paramyxoviruses of Fish. In *Aquaculture Virology* (pp. 259-265). Academic Press, Elsevier.

Mikheev, V. N., Pasternak, A. F., Valtonen, E. T., & Taskinen, J. (2014). Increased ventilation by fish leads to a higher risk of parasitism. *Parasites & Vectors*, *7*(1), 281.

Miller, M. A., & Zachary, J. F. (2017). Mechanisms and morphology of cellular injury, adaptation, and death. In *Pathologic Basis of Veterinary Disease* (pp. 2-43). St. Louis, USA: Elsevier.

Mitchell, S. O., Steinum, T., Rodger, H., Holland, C., Falk, K., & Colquhoun, D. J. (2010). Epitheliocystis in Atlantic salmon, *Salmo salar* L., farmed in fresh water in Ireland is associated with '*Candidatus* Clavochlamydia salmonicola'infection. *Journal of Fish Diseases*, *33*(8), 665-673.

Mitchell, S. O., & Rodger, H. D. (2011). A review of infectious gill disease in marine salmonid fish. *Journal of Fish Diseases*, *34*(6), 411-432.

Mitchell, S. O., Baxter, E. J., Holland, C., & Rodger, H. D. (2012). Development of a novel histopathological gill scoring protocol for assessment of gill health during a longitudinal study in marine-farmed Atlantic salmon (*Salmo salar*). *Aquaculture International*, *20*(5), 813-825.

Mitchell, S. O., Steinum, T. M., Toenshoff, E. R., Kvellestad, A., Falk, K., Horn, M., & Colquhoun, D. J. (2013). '*Candidatus* Branchiomonas cysticola'is a common agent of epitheliocysts in seawater-farmed Atlantic salmon *Salmo salar* in Norway and Ireland. *Diseases of Aquatic Organisms*, *103*(1), 35-43.

Molestina, R., Becnel, J. J. and Weiss, L. M. 2014. Culture and propagation of microsporidia. In *Microsporidi: Pathogens of Opportunity* (pp. 457–467). Oxford, UK: Willey Blackwell.

Mölich, A., Waser, W., & Heisler, N. (2009). The teleost pseudobranch: a role for preconditioning of ocular blood supply?. *Fish Physiology and Biochemistry*, *35*(2), 273-286.

Monaghan, S. R. (2011). Use of fish cell cultures for the study and cultivation of microsporidia. University of Waterloo. Doctor of Philosophy. Waterloo, Ontario, Canada, 2011.

Monaghan, S. R., Kent, M. L., Watral, V. G., Kaufman, R. J., Lee, L. E., & Bols, N. C. (2009). Animal cell cultures in microsporidial research: their general roles and their specific use for fish microsporidia. *In Vitro Cellular & Developmental Biology-Animal*, *45*(3-4), 135.

Monaghan, S. R., Rumney, R. L., Vo, N. T., Bols, N. C., & Lee, L. E. (2011). In vitro growth of microsporidia *Anncaliia algerae* in cell lines from warm water fish. *In Vitro Cellular & Developmental Biology-Animal*, *47*(2), 104-113.

Morrison, R. N., Cooper, G. A., Koop, B. F., Rise, M. L., Bridle, A. R., Adams, M. B., & Nowak, B. F. (2006). Transcriptome profiling the gills of amoebic gill disease (AGD)-affected Atlantic salmon (*Salmo salar* L.): a role for tumor suppressor p53 in AGD pathogenesis?. *Physiological Genomics*, *26*(1), 15-34.

Mosby. (2016). *Mosby's medical dictionary*. St. Louis, USA: Elsevier.

Mosier, D. A. (2017). Vascular disorders and thrombosis. In *Pathologic Basis of Veterinary Disease* (pp. 44-72). St. Louis, USA: Elsevier.

Mowi (2019). *Integrated Annual Report 2018*. Retrieved from: https://mowi.com/blog/2019/04/07/mowis-2018-annual-report

Munday, B. L., Foster, C. K., Roubal, F. R., & Lester, R. J. G. (1990). Paramoebic gill infection and associated pathology of Atlantic salmon, *Salmo salar*, and rainbow trout, *Salmo gairdneri*, in Tasmania. *Pathology in Marine Science*, 215-222.

Munday, B. L., Zilberg, D., & Findlay, V. (2001). Gill disease of marine fish caused by infection with *Neoparamoeba pemaquidensis*. *Journal of Fish Diseases*, *24*(9), 497-507.

Murray, A. G., Wardeh, M., & McIntyre, K. M. (2016). Using the H-index to assess disease priorities for salmon aquaculture. *Preventive Veterinary Medicine*, *126*, 199-207.

Nageli, C. (1857). Uber die neue Krankheit der Seidenraupe und verwandte Organismen. *Botanische Zeitung*, *15*, 760-761.

Navarrete, P., Mardones, P., Opazo, R., Espejo, R., & Romero, J. (2008). Oxytetracycline treatment reduces bacterial diversity of intestinal microbiota of Atlantic salmon. *Journal of Aquatic Animal Health*, *20*(3), 177-183.

Noguera, P., Olsen, A. B., Hoare, J., Lie, L. I., Marcos-López, M., Poppe, T. T., & Rodger, H. . Complex gill disorder (CGD): A histopathology workshop report. (2019). *Bulletin of European Association of Fish Pathologists*, *39*(4), 172-176.

Nowak, B. F., & LaPatra, S. E. (2006). Epitheliocystis in fish. *Journal of Fish Diseases*, *29*(10), 573-588.

Nylund, A., Kvenseth, A. M., & Isdal, E. (1998). A morphological study of the epitheliocystis agent in farmed Atlantic salmon. *Journal of Aquatic Animal Health*, *10*(1), 43-55.

Nylund, A., Watanabe, K., Nylund, S., Karlsen, M., Saether, P. A., Arnesen, C. E., & Karlsbakk, E. (2008). Morphogenesis of salmonid gill poxvirus associated with proliferative gill disease in farmed Atlantic salmon (*Salmo salar*) in Norway. *Archives of Virology*, *153*(7), 1299-1309.

Nylund, A., Watanabe, K., Nylund, S., Sævareid, I., Arnesen, C. E., & Karlsbakk, E. (2009). Salmon louse: A biological vector for a salmonid parasite. *Naturen*, *133*, 217-222.

Nylund, S., Nylund, A. R. E., Watanabe, K., Arnesen, C. E., & Karlsbakk, E. (2010). *Paranucleospora theridion* n. gen., n. sp. (Microsporidia, Enterocytozoonidae) with a life cycle in the salmon louse (*Lepeophtheirus salmonis*, Copepoda) and Atlantic salmon (*Salmo salar*). *Journal of Eukaryotic Microbiology*, *57*(2), 95-114.

Nylund, S., Andersen, L., Sævareid, I., Plarre, H., Watanabe, K., Arnesen, C.E., Karlsbakk, E. & Nylund, A. (2011). Diseases of farmed Atlantic salmon *Salmo salar* associated with infections by the microsporidian *Paranucleospora theridion*. *Diseases of Aquatic Organisms*, *94*(1), 41-57.

Nylund S., Steigen A., Karlsbakk E., Plarre H., Andersen L., Karlsen M., Watanabe K. & Nylund A. (2015). Characterization of '*Candidatus* Syngnamydia salmonis' (Chlamydiales, Simkaniaceae), a bacterium associated with epitheliocystis in Atlantic salmon (*Salmo salar* L.). *Archives of Microbiology*, *197*(1), 17-25.

Okabe, M., & Graham, A. (2004). The origin of the parathyroid gland. *Proceedings of the National Academy of Sciences*, *101*(51), 17716-17719.

Økland, A. L. (2012). *The occurrence, pathology and morphological development of Paranucleospora theridion in salmon louse (Lepeophtheirus salmonis)* (Master dissertation). The University of Bergen.

Oldham, T., Rodger, H., & Nowak, B. F. (2016). Incidence and distribution of amoebic gill disease (AGD) - an epidemiological review. *Aquaculture, 457*, 35-42.

Olson, K. R. (1998). Hormone metabolism by the fish gill. *Comparative Biochemistry and Physiology Part A: Molecular & Integrative Physiology*, *119*(1), 55-65.

Olsvik, P. A., Vikeså, V., Lie, K. K., & Hevrøy, E. M. (2013). Transcriptional responses to temperature and low oxygen stress in Atlantic salmon studied with next-generation sequencing technology. *BMC Genomics*, *14*(1), 817.

Ong, K. J., Stevens, E. D., & Wright, P. A. (2007). Gill morphology of the mangrove killifish (*Kryptolebias marmoratus*) is plastic and changes in response to terrestrial air exposure. *Journal of Experimental Biology*, *210*(7), 1109-1115.

Ostland, V. E., Byrne, P. J., Lumsden, J. S., MacPhee, D. D., Derksen, J. A., Haulena, M., Skar, K., Myhr, E., & Ferguson, H. W. (1999). Atypical bacterial gill disease: a new form of bacterial gill disease affecting intensively reared salmonids. *Journal of Fish Diseases*, *22*(5), 351-358.

Overton, K., Dempster, T., Oppedal, F., Kristiansen, T. S., Gismervik, K., & Stien, L. H. (2019). Salmon lice treatments and salmon mortality in Norwegian aquaculture: a review. *Reviews in Aquaculture*, *11*(4), 1398-1417.

Palenzuela, O., & Bartholomew, J. L. (2002). Molecular tools for the diagnosis of *Ceratomyxa shasta* (Myxozoa). In *Molecular diagnosis of salmonid diseases* (pp. 285-298). Dordrecht, Netherlands: Springer

Palenzuela, O., Redondo, M. J., Cali, A., Takvorian, P. M., Alonso-Naveiro, M., Alvarez-Pellitero, P., & Sitjà-Bobadilla, A. (2014). A new intranuclear microsporidium, *Enterospora nucleophila* n. sp., causing an emaciative syndrome in a piscine host (*Sparus aurata*), prompts the redescription of the family Enterocytozoonidae. *International Journal for Parasitology*, *44*(3-4), 189-203.

Panek, J., Alaoui, H. El, Mone, A., Urbach, S., Demettre, E., Texier, C., Brun, C., Zanzoni, A., Peyretaillade, E., Parisot, Lerat, E., Peyret, P., Delbac, F., & Biron, D. G. (2018). Hijacking of host cellular functions by an intracellular parasite, the microsporidian *Anncaliia algerae*. *PLoS One*, *9*(6), e100791.

Park, K., Kim, W., & Kim, H. Y. (2014). Optimal lamellar arrangement in fish gills. *Proceedings of the National Academy of Sciences*, *111*(22), 8067-8070.

Pérez, T., Balcázar, J. L., Ruiz-Zarzuela, I., Halaihel, N., Vendrell, D., De Blas, I., & Múzquiz, J. L. (2010). Host–microbiota interactions within the fish intestinal ecosystem. *Mucosal Immunology*, *3*(4), 355-360.

Perry, S. F., Jonz, M. G., & Gilmour, K. M. (2009). Oxygen sensing and the hypoxic ventilator response. In *Fish Physiology* (pp. 193–253). Academic Press, Elsevier.

Peterson, T. S., Spitsbergen, J. M., Feist, S. W., & Kent, M. L. (2011). Luna stain, an improved selective stain for detection of microsporidian spores in histologic sections. *Diseases of Aquatic Organisms*, *95*(2), 175-180.

Pflaum, S. (2012). *Investigations of Desmozoon lepeophtherii (syn. Paranucleospora theridion) and gill disease in Atlantic salmon (Salmo salar)* (Master Thesis). University of Stirling.

Pote, L. M., Hanson, L. A., & Shivaji, R. (2000). Small subunit ribosomal RNA sequences link the cause of proliferative gill disease in channel catfish to *Henneguya* n. sp. (Myxozoa: Myxosporea). *Journal of Aquatic Animal Health*, *12*(3), 230-240.

Poppe, T. T., & Ferguson, H. W. (2006). Cardiovascular system. In *Systemic pathology of fish: a text and atlas of normal tissues reponses in teleosts, and their responses in disease* (pp. 140-167). London, UK: Scotian Press.

Powell, M., Carson, J., & van Gelderen, R. (2004). Experimental induction of gill disease in Atlantic salmon *Salmo salar* smolts with *Tenacibaculum maritimum*. *Diseases of Aquatic Organisms*, *61*(3), 179-185.

Powell, M. D., Reynolds, P., & Kristensen, T. (2015). Freshwater treatment of amoebic gill disease and sea-lice in seawater salmon production: Considerations of water chemistry and fish welfare in Norway. *Aquaculture*, *448*, 18-28.

Pruesse, E., Quast, C., Knittel, K., Fuchs, B. M., Ludwig, W., Peplies, J., & Glöckner, F. O. (2007). SILVA: a comprehensive online resource for quality checked and aligned ribosomal RNA sequence data compatible with ARB. *Nucleic Acids Research*, *35*(21), 7188-7196.

Pulkkinen, K., Suomalainen, L. R., Read, A. F., Ebert, D., Rintamäki, P., & Valtonen, E. T. (2009). Intensive fish farming and the evolution of pathogen virulence: the case of columnaris disease in Finland. *Proceedings of the Royal Society B: Biological Sciences*, *277*(1681), 593-600.

Randall, D. (2014). Hughes and Shelton: the fathers of fish respiration. *Journal of Experimental Biology*, *217*(18), 3191-3192.

Rašković, B., Jarić, I., Koko, V., Spasić, M., Dulić, Z., Marković, Z., & Poleksić, V. (2013). Histopathological indicators: a useful fish health monitoring tool in common carp (*Cyprinus carpio* Linnaeus, 1758) culture. *Open Life Sciences*, *8*(10), 975-985.

Reabel, S. (2012). *Molecular diagnostic methods for Detection of Encephalitozoon cuniculi in pet rabbits* (Master thesis). The University of Gelph.

Reid, K. M., Patel, S., Robinson, A. J., Bu, L., Jarungsriapisit, J., Moore, L. J., & Salinas, I. (2017). Salmonid alphavirus infection causes skin dysbiosis in Atlantic salmon (*Salmo salar* L.) post-smolts. *PloS One*, *12*(3).

Reite, O. B. (1997). Mast cells/eosinophilic granule cells of salmonids: staining properties and responses to noxious agents. *Fish and Shellfish Immunology*, *7*(8), 567-584.

Roberts, R. J., & Rodger, H. D. (2012). The pathophysiology and systematic pathology of teleosts. In *Fish Pathology* (pp. 62-143). Hoboken, USA: Wiley-Blackwell.

Roed, M. (2017). *Gill Health in Scotland 2016-2017*. Presented at the International Gill Health Initiative 2017. University of Bergen, Norway.Rodger, H. D., Turnbull, T., Edwards, C., & Codd, G. A. (1994). Cyanobacterial (blue-green algal) bloom associated pathology in brown trout, *Salmo trutta* L., in Loch Leven, Scotland. *Journal of Fish Diseases*, *17*(2), 177-181.

Rodger, H. D., & McArdle, J. F. (1996). An outbreak of amoebic gill disease in Ireland. *Veterinary Record*, *139*, 348-348.

Rodger, H. D. (2007). Gill disorders: an emerging problem for farmed Atlantic salmon (*Salmo salar*) in the marine environment. *Fish Veterinary Journal*, *9*, 38-48.

Rodger, H. D., Henry, L., & Mitchell, S. O. (2011). Non-infectious gill disorders of marine salmonid fish. *Reviews in Fish Biology and Fisheries*, *21*(3), 423-440.

Rodger, H. D., & Mitchell, S. O. (2013). Marine Gill Histopathology Workshop. *Bulletin of the European Association of Fish Pathology*, *33*(2), 35.

Rodger, H. D. (2014). Amoebic gill disease (AGD) in farmed salmon (*Salmo salar*) in Europe. *Fish Veterinary Journal*, (14), 16-27.

Rodger, H. D. (2016). UK-Ireland EAFP meeting (Stirling) keynote presentation (15th-16th September).

Rodrigues, S., Antunes, S. C., Nunes, B., & Correia, A. T. (2019). Histopathological effects of the antibiotic erythromycin on the freshwater fish species *Oncorhynchus mykiss*. *Ecotoxicology and Environmental Safety*, *181*, 1-10.

Rodriguez-Tovar, L. E., Speare, D. J., & Markham, R. F. (2011). Fish microsporidia: immune response, immunomodulation and vaccination. *Fish & Shellfish Immunology*, *30*(4-5), 999-1006.

Rosety-Rodrıguez, M., Ordoñez, F. J., Rosety, M., Rosety, J. M., Rosety, I., Ribelles, A., & Carrasco, C. (2002). Morpho-histochemical changes in the gills of turbot, *Scophthalmus maximus* L., induced by sodium dodecyl sulfate. *Ecotoxicology and Environmental Safety, 51*(3), 223-228.

Rychlik, W. (2007). OLIGO 7 primer analysis software. In *PCR primer design* (pp. 35-59). New York, USA: Humana Press.

Saleh, M., Kumar, G., Abdel-Baki, A. A., El-Matbouli, M., & Al-Quraishy, S. (2014). In vitro growth of the microsporidian *Heterosporis saurida* in the eel kidney EK-1 cell line. *Diseases of Aquatic Organisms*, *108*(1), 37-44.

Sanchez, J. G., Speare, D. J., Markham, R. J. F., & Jones, S. R. M. (2001). Experimental vaccination of rainbow trout against *Loma salmonae* using a live low-virulence variant of *L. salmonae*. *Journal of Fish Biology*, *59*(2), 442-448.

Santana, J. (2018, April). *Gill Disease in Chile*. Industry Updates presented at the 6th Gill Health Initiative, Galway, Ireland.

Santiana, M., Takvorian, P. M., Altan-Bonnet, N., & Cali, A. (2016). A Novel Fluorescent Labeling Method Enables Monitoring of Spatio-Temporal Dynamics of Developing Microsporidia. *Journal of Eukaryotic Microbiology*, *63*(3), 318-325.

Santin, M., & Fayer, R. (2009). *Enterocytozoon bieneusi* genotype nomenclature based on the internal transcribed spacer sequence: a consensus. *Journal of Eukaryotic Microbiology*, *56*(1), 34-38.

Schaeck, M., Van den Broeck, W., Hermans, K., & Decostere, A. (2013). Fish as research tools: alternatives to in vivo experiments. *Alternatives to Laboratory Animals*, *41*(3), 219-229.

Schoch, C. L., Seifert, K. A., Huhndorf, S., Robert, V., Spouge, J. L., Levesque, C. A., Chen, W. & Fungal Barcoding Consortium. (2012). Nuclear ribosomal internal transcribed spacer (ITS) region as a universal DNA barcode marker for Fungi. *Proceedings of the National Academy of Sciences*, *109*(16), 6241-6246.

Secombes, C. J. (1990). Isolation of salmonid macrophages and analysis of their killing activity. *Techniques in Fish Immunology.*, 137-154.

Shaw, R. W., Kent, M. L., & Adamson, M. L. (2000). Viability of *Loma salmonae* (Microsporidia) under laboratory conditions. *Parasitology Research*, *86*(12), 978-981.

Shaw, R. W., Kent, M. L., & Adamson, M. L. (2001). Phagocytosis of *Loma salmonae* (Microsporidia) spores in Atlantic salmon (*Salmo salar*), a resistant host, and chinook salmon (*Oncorhynchus tshawytscha*), a susceptible host. *Fish &Shellfish Immunology*, *11*(1), 91-100.

Shinn, A. P., Pratoomyot, J., Bron, J. E., Paladini, G., Brooker, E. E., & Brooker, A. J. (2015). Economic costs of protistan and metazoan parasites to global mariculture. *Parasitology*, *142*(1), 196-270.

Sitjà-Bobadilla, A., & Alvarez-Pellitero, P. (2009). Experimental transmission of *Sparicotyle chrysophrii* (Monogenea: Polyopisthocotylea) to gilthead seabream (*Sparus aurata*) and histopathology of the infection. *Folia Parasitologica*, *56*(2), 143.

Småge, S. B., Brevik, Ø. J., Duesund, H., Ottem, K. F., Watanabe, K., & Nylund, A. (2016). *Tenacibaculum finnmarkense* sp. nov., a fish pathogenic bacterium of the family Flavobacteriaceae isolated from Atlantic salmon. *Antonie Van Leeuwenhoek*, *109*(2), 273-285.

Småge, S. B., Frisch, K., Vold, V., Duesund, H., Brevik, Ø. J., Olsen, R. H., Sjaatil, S. T., Klevan, A., Brudeseth, B., Watanabe, K., & Nylund, A. (2018). Induction of tenacibaculosis in Atlantic salmon smolts using *Tenacibaculum finnmarkense* and the evaluation of a whole cell inactivated vaccine. *Aquaculture*, *495*, 858-864.

Speare, D. J., Ferguson, H. W., Beamish, F. W. M., Yager, J. A., & Yamashiro, S. (1991). Pathology of bacterial gill disease: sequential development of lesions during natural outbreaks of disease. *Journal of Fish Diseases*, *14*(1), 21-32.

Speare, D.J. & Ferguson, H. W. (2006), Gills and pseudobranchs. In *Systemic pathology of fish: a text and atlas of normal tissues in teleosts and their responses in disease* (pp. 25-62). London, UK: Scotian Press.

SRUC. (2019). Gill health in Scottish Farmed Salmon. Retrieved from: https://epidemiology.sruc.ac.uk/projects/gillhealth

Steigen, A., Nylund, A., Plarre, H., Watanabe, K., Karlsbakk, E., & Brevik, Ø. (2018). Presence of selected pathogens on the gills of five wrasse species in western Norway. *Diseases of Aquatic Organisms, 128*(1), 21-35.

Steinum, T., Kvellestad, A., Rønneberg, L. B., Nilsen, H., Asheim, A., Fjell, K., Nygård, S. M. R., Olsen, A. B., & Dale, O. B. (2008). First cases of amoebic gill disease (AGD) in Norwegian seawater farmed Atlantic salmon, *Salmo salar* L., and phylogeny of the causative amoeba using 18S cDNA sequences. *Journal of Fish Diseases, 31*(3), 205-214.

Steinum, T., Sjåstad, K., Falk, K., Kvellestad, A., & Colquhoun, D. J. (2009). An RT PCR-DGGE survey of gill-associated bacteria in Norwegian seawater-reared Atlantic salmon suffering proliferative gill inflammation. *Aquaculture, 293*(3-4), 172-179.

Steinum, T., Kvellestad, A., Colquhoun, D. J., Heum, M., Mohammad, S., Grøntvedt, R. N., & Falk, K. (2010). Microbial and pathological findings in farmed Atlantic salmon *Salmo salar* with proliferative gill inflammation. *Diseases of Aquatic Organisms, 91*(3), 201-211.

Stentiford, G. D., Feist, S. W., Stone, D. M., Bateman, K. S., & Dunn, A. M. (2013). Microsporidia: diverse, dynamic, and emergent pathogens in aquatic systems. *Trends in Parasitology, 29*(11), 567-578.

Stentiford, G. D., & Dunn, A. M. (2014). Microsporidia in aquatic invertebrates. In *Microsporidia: Pathogens of Opportunity* (pp.579-604). Oxford, UK: Wiley Blackwell.

Stevens A. & Wilson I.G. (1996). The haematoxylins and eosin. In *Theory and Practice of Histological Techniques* (p.99-112). Edinburgh, UK: Churchill Livingstone.

Stoecker, K., Dorninger, C., Daims, H., & Wagner, M. (2010). Double labeling of oligonucleotide probes for fluorescence *in situ* hybridization (DOPE-FISH) improves signal intensity and increases rRNA accessibility. *Applied Environmental Microbiology, 76*(3), 922-926.

Sveen, S., Øverland, H., Karlsbakk, E., & Nylund, A. (2012). *Paranucleospora theridion* (Microsporidia) infection dynamics in farmed Atlantic salmon *Salmo salar* put to sea in spring and autumn. *Diseases of Aquatic Organisms, 101*(1), 43-49.

Szumowski, S. C., & Troemel, E. R. (2015). Microsporidia–host interactions. *Current Opinion in Microbiology, 26*, 10-16.

Takvorian, P. M., Buttle, K. F., Mankus, D., Mannella, C. A., Weiss, L. M., & Cali, A. (2013). The Multilayered Interlaced Network (MIN) in the sporoplasm of the Microsporidium *Anncaliia algerae* is derived from Golgi. *Journal of Eukaryotic Microbiology*, *60*(2), 166-178.

Tang, K. F., Pantoja, C. R., Redman, R. M., Han, J. E., Tran, L. H., & Lightner, D. V. (2015). Development of in situ hybridization and PCR assays for the detection of *Enterocytozoon hepatopenaei* (EHP), a microsporidian parasite infecting penaeid shrimp. *Journal of Invertebrate Pathology, 130*, 37-41.

Taylor, J. D., Fulton, R. W., Lehenbauer, T. W., Step, D. L., & Confer, A. W. (2010). The epidemiology of bovine respiratory disease: What is the evidence for predisposing factors?. *The Canadian Veterinary Journal*, *51*(10), 1095-1102

Temmink, J. H. M., Bouwmeister, P. J., De Jong, P., & Van Den Berg, J. H. J. (1983). An ultrastructural study of chromate-induced hyperplasia in the gill of rainbow trout (*Salmo gairdneri*). *Aquatic Toxicology*, *4*(2), 165-179.

Thakur, K. K., Vanderstichel, R., Kaukinen, K., Nekouei, O., Laurin, E., & Miller, K. M. (2019). Infectious agent detections in archived Sockeye salmon (*Oncorhynchus nerka)* samples from British Columbia, Canada (1985–94). *Journal of Fish Diseases*, *42*(4), 533-547.

The Scottish Government (2011). Temperature, salinity and ocean acidification. Retrieved from: https://www2.gov.scot/Publications/2011/03/16182005/26

The Scottish Government (2019). Mortality information. Retrieved from: https://www2.gov.scot/Topics/marine/FishShellfish/FHI/CaseInformation/MortalityinformationToenshoff, E. R., Kvellestad, A., Mitchell, S. O., Steinum, T., Falk, K., Colquhoun, D. J., & Horn, M. (2012). A novel betaproteobacterial agent of gill epitheliocystis in seawater farmed Atlantic salmon (*Salmo salar*). *PLoS One*, *7*(3), e32696.

Toranzo, A. E., Magariños, B., & Romalde, J. L. (2005). A review of the main bacterial fish diseases in mariculture systems. *Aquaculture, 246*(1-4), 37-61.

Tort, M. J., Pasnik, D. J., Fernandez-Cobas, C., Wooster, G. A., & Bowser, P. R. (2002). Quantitative scoring of gill pathology of walleyes exposed to hydrogen peroxide. *Journal of Aquatic Animal Health*, *14*(2), 154-159.

Trager, W. (1937). The hatching of spores of Nosema bombycis Nägeli and the partial development of the organism in tissue cultures. *The Journal of Parasitology*, 226-227.

Undeen, A. H. (1990). A proposed mechanism for the germination of microsporidian (Protozoa: Microspora) spores. *Journal of Theoretical Biology*, *142*(2), 223-235.

Van Dijk, E. L., Auger, H., Jaszczyszyn, Y., & Thermes, C. (2014). Ten years of next-generation sequencing technology. *Trends in Genetics*, *30*(9), 418-426.

Van Gelderen, R., Carson, J., & Nowak, B. (2009). Effect of extracellular products of *Tenacibaculum maritimum* in Atlantic salmon, *Salmo salar* L. *Journal of Fish Diseases*, *32*(8), 727-731.

Van West, P. (2006). *Saprolegnia parasitica*, an oomycete pathogen with a fishy appetite: new challenges for an old problem. *Mycologist*, *20*(3), 99-104.

Vávra, J., & Lukeš, J. (2013). Microsporidia and 'The Art of Living Together'. In *Advances in Parasitology* (pp. 253–320). London, UK: Academic Press.

Vávra, J., & Larsson, J. R. (2014). Structure of microsporidia. In *Microsporidia: pathogens of opportunity* (pp. 1-70). Oxford, UK: Wiley Blackwell.

Visvesvara, G. S. (2002). In vitro cultivation of microsporidia of clinical importance. *Clinical Microbiology Reviews*, *15*(3), 401-413.

Wallig, M. A., & Janovitz, E. B. (2013). Morphologic manifestations of toxic cell injury. In *Haschek and Rousseaux's Handbook of Toxicologic Pathology* (pp. 77-105). Amsterdam, Netherlands: Academic Press.

Weiss, L. M. (2001). Microsporidia: emerging pathogenic protists. *Acta Tropica*, *78*(2), 89-102.

Welch, M. D. (2015). Why should cell biologists study microbial pathogens?. *Molecular Biology of the Cell*, 26(24), 4295-4301.

Weli, S. C., Dale, O. B., Hansen, H., Gjessing, M. C., Rønneberg, L. B., & Falk, K. (2017). A case study of *Desmozoon lepeophtherii* infection in farmed Atlantic salmon associated with gill disease, peritonitis, intestinal infection, stunted growth, and increased mortality. *Parasites & Vectors*, *10*(1), 370.

Wiik-Nielsen, J., Gjessing, M., Solheim, H. T., Litlabø, A., Gjevre, A. G., Kristoffersen, A. B., Powell, M. D., & Colquhoun, D. J. (2017). *Ca. B. cysticola*, *Ca.* Piscichlamydia salmonis and Salmon Gill Pox Virus transmit horizontally in Atlantic salmon held in fresh water. *Journal of Fish Diseases*, *40*(10), 1387-1394.

Wilcox, J. N. (1993). Fundamental principles of in situ hybridization. *Journal of Histochemistry & Cytochemistry*, *41*(12), 1725-1733.

Williams, B. A. (2009). Unique physiology of host - parasite interactions in microsporidia infections. *Cellular Microbiology*, *11*(11), 1551-1560.

Williams, B. A., Hirt, R. P., Lucocq, J. M., & Embley, T. M. (2002). A mitochondrial remnant in the microsporidian *Trachipleistophora hominis*. *Nature*, *418*(6900), 865.

Williams, B. A., Dolgikh, V. V., & Sokolova, Y. Y. (2014). Microsporidian Biochemistry and Physiology. In *Microsporidia: Pathogens of opportunity* (pp. 245-260). Oxford, UK: Wiley Blackwell.

Wilson, J. M., & Laurent, P. (2002). Fish gill morphology: inside out. *Journal of Experimental Zoology*, 293(3), 192-213.

Wittner, M. (1999). Historic perspective on the microsporidia: expanding horizons. In *The Microsporidia and Microsporidiosis* (pp. 1-6). Washington, USA: American Society of Microbiology.

Wolf, J. C., Baumgartner, W. A., Blazer, V. S., Camus, A. C., Engelhardt, J. A., Fournie, J. W., Frasca, S., Groman, D. B., Kent, M. L., Khoo, L. H., Law, J. M., Lombardini, E. D., Ruehl-Fehlert, C., Segner, H. E., Smith, S. A., Spitsbergen, J. M., Weber, K., & Wolfe, M. J (2015). Nonlesions, misdiagnoses, missed diagnoses, and other interpretive challenges in fish histopathology studies: a guide for investigators, authors, reviewers, and readers. *Toxicologic Pathology*, *43*(3), 297-325.

Wongtavatchai, J., Conrad, P. A., & Hedrick, R. P. (1994). In vitro cultivation of the microsporidian: *Enterocytozoon salmonis* using a newly developed medium for salmonid lymphocytes. *Journal of Tissue Culture Methods*, *16*(2), 125-131.

Wongtavachai, J., Conrad, P. A., & Hedrick, R. P. (1995). In vitro characteristics of the microsporidian: *Enterocytozoon salmonis*. *Journal of Eukaryotic Microbiology*, *42*(4), 401-405.

Wood, E. M., & Yasutake, W. T. (1957). Histopathology of Fish: V. Gill Disease. *The Progressive Fish-Culturist*, *19*(1), 7-13.

Xu, Y., & Weiss, L. M. (2005). The microsporidian polar tube: a highly specialised invasion organelle. *International Journal for Parasitology*, *35*(9), 941-953.

Yang, C. Z., & Albright, L. J. (1992). Effects of the harmful diatom *Chaetoceros concavicornis* on respiration of rainbow trout *Oncorhynchus mykiss*. *Diseases of Aquatic Organisms*, *14*(2), 105-114.

Yang, D., Pan, L., Chen, Z., Du, H., Luo, B., Luo, J., & Pan, G. (2018). The roles of microsporidia spore wall proteins in the spore wall formation and polar tube anchorage to spore wall during development and infection processes. *Experimental Parasitology*, *187*, 93-100.